



Virginia Commonwealth University
VCU Scholars Compass

Theses and Dissertations

Graduate School

2020

The Effects of GSPT1 Degradation on Serum Calcium, Parathyroid Hormone, and Fibroblast Growth Factor 23 Concentrations in Human Cereblon Knock-in Mice

Kamran Ghoreishi
Virginia Commonwealth University

Follow this and additional works at: <https://scholarscompass.vcu.edu/etd>



Part of the [Other Medicine and Health Sciences Commons](#)

© The Author

Downloaded from

<https://scholarscompass.vcu.edu/etd/6490>

This Dissertation is brought to you for free and open access by the Graduate School at VCU Scholars Compass. It has been accepted for inclusion in Theses and Dissertations by an authorized administrator of VCU Scholars Compass. For more information, please contact libcompass@vcu.edu.

The Effects of GSPT1 Degradation on Serum Calcium, Parathyroid Hormone, and Fibroblast
Growth Factor 23 Concentrations in Human Cereblon Knock-in Mice

by

Kamran Ghoreishi

Bachelor of Science in Microbiology and Clinical Laboratory Sciences, San Diego State
University, 1995

Master of Science in Public Health (Toxicology), San Diego State University, 2003

Master of Science in Regulatory Affairs, San Diego State University, 2013

A dissertation submitted in the partial fulfillment of the requirements for the degree of Doctor of
Philosophy at Virginia Commonwealth University.

Virginia Commonwealth University, 2020

Advisor: William J. Korzun, Ph.D.

Associate Professor

Department of Clinical Laboratory Sciences Virginia Commonwealth University
Richmond, Virginia

November 19, 2020

ACKNOWLEDGEMENT

Firstly, I would like to express my sincere gratitude to my advisor Dr. William Korzun for the continuous support and guidance of my research, which incited me to widen my research from various perspectives.

My sincere thanks also go to Dr. Joseph Piccotti who provided me an opportunity to conduct this research, without his endless support it would not be possible to conduct this research. I am also thankful for his patience, thoughtful support, and immense knowledge of the field. His guidance helped me in all aspects of my research and writing of this thesis. I could not have imagined having a better counselor and mentor for my PhD study.

Besides my advisor, I would like to thank the rest of my thesis committee: Dr. Teresa Nadder and Dr. Melissa Jamerson for their insightful comments and encouragement.

I thank my colleagues for their support and contribution to this research, their skills, expertise, knowledge, and most importantly, their willingness to push the boundaries in the laboratory techniques, produced valuable data for this thesis. I like to thank Mr. Luis Alvarado, Mr. Ayan Alavi, Ms. Yan Ren, Ms. Tatiana Galvez, Ms. Kelsie Smith, Ms. Yang Tang, and Dr. Roberto Guzman for their contributions.

Finally, but most importantly, I would like to thank my family: my parents, my wife Sahar, my daughter Parisa, and my son Parsa for their emotional support and encouragement, which made this journey so much more pleasant. I am forever grateful for their patience and understanding, they have earned this degree right along with me.

TABLE OF CONTENTS

TABLE OF CONTENTS.....	I
LIST OF FIGURES	V
LIST OF TABLES	VII
GLOSSARY OF ABBREVIATIONS AND DEFINITIONS OF TERMS	IX
Abstract	1
CHAPTER 1: INTRODUCTION	3
Purpose of this Study and Research Questions.....	10
Hypotheses	11
Summary	13
CHAPTER 2: LITERATURE REVIEW	14
Calcium	14
Phosphate	15
Magnesium.....	16
Calcium Homeostasis.....	20
Hypocalcemia	21
Drug-Induced Hypocalcemia	24
Vitamin D.....	26
The Fibroblast Growth Factor 23.....	28
The Parathyroid Glands	30
Rodent Parathyroid	31
Parathyroid Hormone.....	31
Calcium Sensing Receptor	34
Hypoparathyroidism	41
Allosteric Modulators of The Calcium Sensing Receptor	45
Positive allosteric modulator of CaSR NPS R-568.....	45
Negative Allosteric Modulator of CaSR NPS 2143	47
Translation Termination Factor G1 to S phase Transition 1 (GSPT1) Degradation and.....	48
Hypocalcemia	49
Parathyroid Hormone mRNA	50
Cereblon Modulators and Hypocalcemia.....	51

Human Cereblon Knock-in Mice Use in Research.....	52
Summary	52
Significance of This Research	53
CHAPTER THREE: METHODS	54
Hypotheses	55
Pilot Study Design	58
Main Study Design	59
Experimental Animals	59
Test Substances 1	59
Test Substances 2.....	60
Dose Selection Criteria	61
Dose Preparation and Administration	62
CC-325	62
NPS 2143	64
Formulation Analysis.....	65
Experimental Groups	66
Treatment Descriptions.....	68
Measurement Procedures	69
Clinical observations.....	69
Body weights	69
Clinical laboratory tests	69
Serum Chemistry	70
Serum Chemistry Panel (Axcel Analyzer).....	71
Toxicokinetics.....	71
Preparation of Sorenson's buffer:	73
Euthanasia	74
Pathology	74
Histopathology	74
Hematoxylin & Eosin (H&E) Staining	74
Immunohistochemistry	75
<i>In Situ</i> hybridization.....	75
Statistical Analysis.....	76
ANALYTICAL METHODS AND INSTRUMENTATION.....	76

Image analysis:.....	77
Protocol Deviation:	77
CHAPTER FOUR: RESULTS	79
Interference studies for further assay validation.....	83
ELISA kits	83
Sample preparation	84
PTH assay	85
FGF23 assay.....	88
Main Study Results	91
Clinical Observations.....	91
Toxicokinetic Data.....	92
Blood collection for endpoints measurements	94
Serum Chemistry (Axcel analyzer).....	95
Serum Chemistry (Stat Profile Prime)	104
Serum PTH (ELISA Assay).....	109
Serum FGF23 (ELISA assay)	112
Histopathology evaluation	114
Immunohistochemistry	115
GSPT1	120
In Situ Hybridization:	123
Summary	138
CHAPTER FIVE: DISUSSION	140
Overview of the Problem	140
Discussion of the Studies	141
Pilot Study.....	141
Interference studies	143
Main Study.....	144
Clinical findings.....	144
Exposure of CC-325 and NPS 2143 in mice	144
Accuracy of total calcium measurement.....	145
The impact of protocol deviation on study integrity.....	147
The impact of parathyroid necrosis on PTH production.....	147
Hypotheses.....	147

Effects on PTH.....	147
Effects on FGF23	151
Conclusion	151
Limitation of the Study	152
Recommendation for Future Studies	153
APPENDIX A.	156
APPENDIX B.	160
APPENDIX C.	168
APPENDIX D.	170
APPENDIX E.	172
APPENDIX F.....	180
APPENDIX G.	186
APPENDIX H.	193
APPENDIX I.	201
REFERENCES	215
VITA.....	225

LIST OF FIGURES

Figure 1.	21
Figure 2.	27
Figure 3.	34
Figure 4.	35
Figure 5.	37
Figure 6:	41
Figure 7.	80
Figure 8.	81
Figure 9.	81
Figure 10:	86
Figure 11:	87
Figure 12.	88
Figure 13:	90
Figure 14:	91
Figure 15.	96
Figure 16.	97
Figure 17.	98
Figure 18.	99
Figure 19.	100
Figure 20.	101
Figure 21.	102
Figure 22.	103
Figure 23.	105
Figure 24.	105
Figure 25.	106
Figure 26.	107
Figure 27.	108
Figure 28.	108
Figure 29.	110
Figure 30:	111
Figure 31:	113

Figure 32:	114
Figure 33:	117
Figure 34:	118
Figure 35:	119
Figure 36:	120
Figure 37:	122
Figure 38:	123
Figure 39:	124
Figure 40:	126
Figure 41:	127
Figure 42:	129
Figure 43:	129
Figure 44:	130
Figure 45:	131
Figure 46:	132
Figure 47:	133
Figure 48:	134
Figure 49:	136
Figure 50:	137
Figure 51:	138

LIST OF TABLES

Table 1.	19
Table 2.	20
Table 3.	22
Table 4.	23
Table 5.	25
Table 6.	38
Table 7.	45
Table 8:	58
Table 9.	65
Table 10:	68
Table 11.	69
Table 12:	70
Table 13:	71
Table 14:	72
Table 15:	72
Table 16:	74
Table 17:	77
Table 18:	78
Table 19:	82
Table 20:	83
Table 21:	84
Table 22:	85
Table 23:	86
Table 24:	88
Table 25:	89
Table 26:	92
Table 27.	92
Table 28:	93
Table 29:	94
Table 30:	95
Table 31:	97

Table 32.	98
Table 33:	99
Table 34:	100
Table 35:	102
Table 36:	103
Table 37:	106
Table 38:	107
Table 39:	109
Table 40:	111
Table 41:	113
Table 42:	115
Table 43:	117
Table 44:	121
Table 45:	125
Table 46:	134
Table 47:	136

GLOSSARY OF ABBREVIATIONS AND DEFINITIONS OF TERMS

ACRDYS	Acrodysostosis
ADH	Autosomal Dominant Hypocalcemia
ADIS	Agonist-driven insertional signaling (ADIS)
AHO	Albright hereditary osteodystrophy
AML	Acute Myeloid Leukemia
AMP	Adenosine monophosphate
APS	Autoimmune Polyglandular Syndrome Type I
ASH	American Society of Hematology
AU	Adenosine-uridine
AUF1	Adenosine-uridine binding factor 1 (AUF1)
BCG	Bromcresol green
BDMR	Brachydactyly mental retardation syndrome
BID	Bis in die
Ca	Calcium
cAMP	Cyclic adenosine monophosphate
CaSR	Calcium sensing receptor
CELMoD	Cereblon Modulators
CKD	chronic kidney disease
Cl	Chloride
C _{max}	Maximum concentration
CMC	Carboxy methycellulose
CRBN	Cereblon
Cu	Copper
CV	Coefficient of variation
CYP27B1	Cytochrome P450 family 27 subfamily B member 1
DBP	Vitamin D binding protein
DMR	Differentially methylated region
EARD	Endoplasmic reticulum-associated degradation
EDTA	Ethylenediamine tetraacetic acid
EGTA	Ethylene glycol tertaacetic acid
ELISA	Enzyme-linked immunosorbent assay
ER	Endoplasmic reticulum

eRF3a	Gene name for G1 to S phase transition 1
ERK	Extracellular-signal-regulated kinase
Eya1	EYA Transcriptional Coactivator And Phosphatase 1
FGF23	Fibroblast growth factor 23
FGF23	Fibroblast growth factor 23
FGFR	Fibroblast growth factor receptor
GATA3	GATA Binding Protein 3
Gcm2	Glial cells missing 2
GCMB	Glial cells missing gene, also known as GCMB.
GNA11	Guanine nucleotide-binding protein alpha 11
GPCR	G protein-coupled receptor
GSPT1	G1 to S Phase Transition 1
Gs α	Alpha subunit of the stimulatory G protein
H&E	Haemotoxylin & Eosin
HCl	Hydrochloride
HDR	Deafness, and renal dysplasia
Hoxa3	Homeobox A3
HPLC	High pressure liquid chromatography
HP β CD	Aqueous 15% (2-Hydroxypropyl)- β -cyclodextrin (HP β CD)
HRP	Horse Radish Peroxidase
huCRBN	Human Cereblon
iCa	Ionized Calcium
iFGF23	Intact fibroblast growth factor 23
IHC	immune histo-chemistry
iMg	Ionized magnesium
IP	Intraperitoneal
IP3	Inositol triphosphate
iPPSD	Inactivating PTH/PTH related protein
ISH	In-situ hybridization
IV	Intravenous
K	Potassium
KSPR	K-homology splicing regulatory protein
LoB	Limit of blank
LoD	Limit of detection

LoQ	Limit of quantitation
MafB	musculoaponeurotic fibrosarcoma oncogene homologue B
MAPK	mitogen-activated protein kinases
MAPK	Mitogen-activated protein kinases
MEK	Mitogen-activated protein kinases
Mg	Magnesium
mg	Miligram
MIM	Mendelian inheritance in man
miRNA	Micro ribonucleic acid
MLPA	Multiplex ligand-dependent probe amplification
MOA	Mechanism of Action
mRNA	Messenger ribonucleic acid
MS-MLPA	Methylation sensitive multiplex ligand-dependent probe amplification
Na	Sodium
ng	Nanogram
Pax1	Paired Box 1
Pax9	Paired Box 9
Pg	Picogram
PHP	pseudohypoparathyroidism
PHP	Pseudohypoparathyroidism
PHP-1A	Pseudohypoparathyroidism type 1A
PHP-1B	Pseudohypoparathyroidism type 1B
PHP-1C	Pseudohypoparathyroidism type 1C
PHP-2	Pseudohypoparathyroidism type 2
PKA	Protein kinase A
PKC	Protein kinase C
PLC β	phospholipase β
PPHP	Pseudopseudohypoparathyroidism
PTH	Parathyroid Hormone
PTH	Parathyroid hormone
QC	Quality Control

Abstract

The Effects of GSPT1 Degradation on Serum Calcium, Parathyroid Hormone, and Fibroblast Growth Factor 23 Concentrations in Human Cereblon Knock-in Mice

By Kamran Ghoreishi, M.S.

Dissertation Chair: William J. Korzun, Ph.D.

Associate Professor

Department of Clinical Laboratory Sciences

Test article CC-325 is a potent oral cereblon (CRBN) modulator that has shown potent G1 to S phase transition 1 (GSPT1) degradation and anti-tumor activity in pre-clinical models. One of the adverse effects associated with CC-325 was dose dependent hypocalcemia, which was determined to be an on-target toxicity.

To investigate the mechanism of hypocalcemia, we conducted a toxicity study in human cereblon (huCRBN) knock-in (KI) mice with CC-325. The huCRBN KI mice are transgenic mice engineered to express human cereblon that is capable of binding to CRBN and degrading GSPT1. Four groups of mice were treated with vehicle (0 mg/kg), CC-325 (50 mg/kg BID), NPS 2143 (120 mg/kg), or CC-325 + NPS 2143. The NPS 2143 is an oral negative allosteric modulator of calcium sensing receptor (CaSR), which upon administration to mice significantly increased plasma ionized calcium (iCa^{2+}) and parathyroid hormone (PTH). Mice treated with CC-325 alone had significant decreases in serum iCa^{2+} and PTH, while mice treated with NPS 2143 alone as expected had significant increases in serum iCa^{2+} and PTH. Treatment of mice with CC-325 + NPS 2143 did not reverse the decreases in serum iCa^{2+} and PTH caused by CC-325, indicating that CC-325 prevents the increase of PTH. To investigate the mechanism of

hypocalcemia, we stained parathyroid gland for PTH by immunohistochemistry (IHC) and showed significantly lower PTH in parathyroid with CC-325 treated mice compared to vehicle or NPS 2143 treated mice. To further investigate the cause of low PTH in parathyroid gland in mice treated with CC-325, we stained parathyroid with in-situ hybridization (ISH) probes for PTH mRNA. Results from this analysis showed significantly lower PTH mRNA in parathyroid of CC-325 mice compare to vehicle or NPS 2143 mice, indicating that lower serum PTH in CC-325 treated mice were due to decreased PTH mRNA in Chief cells.

These data collectively indicate that hypocalcemia caused by CC-325 is due to reduction in PTH, which leads to hypocalcemia. Additionally, mice treated with CC-325 are unable to restore normocalcemia because their parathyroid gland did not synthesize sufficient PTH for release into blood stream. Lack of PTH synthesis is caused by diminished level of PTH mRNA in parathyroid gland.

We also measured the level of FGF23 in mice treated with CC-325. Our data indicated that decrease in PTH significantly decreased FGF23 levels even in presence of hyperphosphatemia, indicating that PTH plays a big role in controlling FGF23 during hypoparathyroidism. The cause of decrease in PTH mRNA in parathyroid, whether it is related to lower transcription of PTH mRNA or lack of stability of PTH mRNA, remains to be determined.

CHAPTER 1: INTRODUCTION

Calcium (Ca^{2+}) is the most abundant mineral in the bone, and has several short- and long-term physiological functions in the body including mediation of cell proliferation or apoptosis, exocytosis, muscle contraction, and neurotransmitter release (Diaz-Soto, Rocher, Garcia-Rodriguez, Nunez, & Villalobos, 2016). The mediation of these functions and several intracellular signaling pathways is critically dependent upon the intracellular and extracellular concentrations. In human plasma, 35-40% of the calcium is bound to proteins, mostly to albumin. Approximately 10-15% of calcium is complexed with bicarbonate, phosphate, lactate and citrate, while 50% of calcium is “free”, also known as “ionized calcium” (iCa^{2+}) (Glendenning, 2013). The concentration of total calcium in serum ranges from 2.10-2.60 mmol/l (8.5-10.5 mg/dL), while the iCa^{2+} concentration is 1.16-1.31 mmol/l (4.65-5.25 mg/dl) and is tightly controlled by the action of parathyroid hormone (PTH) (Cooper & Gittoes, 2008). In humans, a decrease in total serum calcium below 2.1 mmol/L (8.5 mg/dl), or ionized calcium lower than 1.1 mmol/L (4.6 mg/dl), is considered hypocalcemia (Liamis, Milionis, & Elisaf, 2009).

Hypocalcemia can be asymptomatic in mild cases, but potentially life-threatening in severe cases. The clinical manifestations of hypocalcemia associated with decrease in PTH, known as hypoparathyroidism, vary with the severity of hypoparathyroidism, which ranges from mild hypocalcemia with few symptoms, such as numbness and tingling in the face and hands, to severe and life-threatening symptoms including seizures, congestive heart failure, and bronchospasm (Hakami & Khan, 2019)

Hypocalcemia occurs in about 18% of all patients in the hospital, and 85% of patients in intensive care units. The most common cause of hypocalcemia in patients in the hospital is

vitamin D deficiency (Cooper & Gittoes, 2008). Hypoparathyroidism, is another cause for hypocalcemia (Hakami & Khan, 2019). Clinical manifestation of hypoparathyroidism is driven by hypocalcemia, which has an impact on a large number of tissues and organs including muscle, heart, brain, kidney, gastrointestinal tract, and skin (Giusti & Brandi, 2019). Hypocalcemia has also been associated with many drugs, including cisplatin, antiepileptics, bisphosphonates, aminoglycosides, diuretics, loop diuretics estrogens, and drugs that can cause vitamin D deficiency or resistance (Fong & Khan, 2012; Liamis et al., 2009).

Calcium homeostasis is maintained by the parathyroid gland, kidney, bone, and intestine, with multiple points of regulation. The parathyroid gland responds to changes in iCa^{2+} concentration in the extracellular space and alters the secretion of PTH. The concentration of PTH in plasma regulates calcium resorption from bone, calcium reabsorption by the renal tubules, and vitamin D activation in the kidney, which promotes calcium and phosphate absorption in the intestines. Fibroblast growth factor 23 (FGF23), and α klotho, either in blood or as a transmembrane protein, mediate calcium homeostasis by binding to its receptor in the parathyroid gland and kidney (Moe, 2016). PTH-stimulated 1- α hydroxylase (CYP27B1) activity in the kidney results in increased level of activated vitamin D ($1,25(OH)_2D$) in plasma, which feeds back on the parathyroid to suppress PTH secretion and decrease calcium. An increase in the serum $1,25(OH)_2D$ also stimulates FGF23 synthesis in the bone and membrane-bound α Klotho in the kidney. Increased FGF23 production in the bone inhibits the activity of the CYP27B1 in the kidney, leading to $1,25(OH)_2D$ reduction and subsequently a drop in plasma calcium (Hu, Shi, & Moe, 2019). Fibroblast growth factor 23 suppresses PTH secretion in the short term but increases secretion in the long term (Kawakami et al., 2017). In acute hypocalcemia, when increased PTH secretion is needed to restore the calcium homeostasis, the

FGF23 inhibitory effect is diminished. However, to date, there is no published data on the effects and concentrations of FGF23 under hypoparathyroidism conditions with suppressed plasma calcium concentration.

PTH is a peptide hormone comprising 84 amino acids, encoded by a gene on chromosome 11 in humans. It is synthesized by Chief cells in the parathyroid gland as a larger precursor called PreproPTH, which moves through the cell from the endoplasmic reticulum and Golgi body, until it reaches the secretory vesicles where the final processing takes place (Hinson et al., 2016). PTH works with the other calcium-regulating hormones, such as $1,25(\text{OH})_2\text{D}$ and calcitonin, to control the expression of parathyroid transcription factors and the calcium sensing receptor (CaSR) (Hakami & Khan, 2019). The release of PTH stored in secretory granules within the parathyroid gland and the synthesis of new PTH impact plasma PTH concentrations and therefore calcium concentration in the plasma (Kumar & Thompson, 2011). A decrease in extracellular iCa^{2+} concentration induces PTH secretion but is promptly inhibited by G Protein i (Gi)-dependent inhibition of adenylate cyclase in the presence of high iCa^{2+} concentration. An increase in PTH production results in increased resorption of calcium from the bones, increased reabsorption of filtered calcium by the renal tubules, and increased production of $1,25(\text{OH})_2\text{D}$ in the kidney. This increase in $1,25(\text{OH})_2\text{D}$ subsequently increases the calcium absorption by the small intestine (Diaz-Soto et al., 2016). An increase in PTH secretion by the parathyroid gland elevates plasma iCa^{2+} concentration; high levels of iCa^{2+} in turn promote the thyroid gland to release calcitonin. Calcitonin slows down the activity of the osteoclasts in bone, which decreases serum iCa^{2+} levels. (E. M. Brown & MacLeod, 2001; Ma et al., 2011).

PTH synthesis is modulated by several transcription factors, including GATA binding protein 3 (GATA3), Glial cells missing-2 (Gcm2), which is a zinc finger-type transcription

factor, and v-maf musculoaponeurotic fibrosarcoma oncogene homologue B (MafB). These proteins are essential for normal parathyroid gland development, and interact with each other to activate the PTH gene promoter (T. Naveh-Many & Silver, 2018). GATA3 recognizes G-A-T-A nucleotide sequences in targeted gene promoters and activates or represses those genes. The genes that regulate GATA3 in the parathyroid gland remain unknown, despite its role in regulation and development of the parathyroid gland (Han, Tsunekage, & Kataoka, 2015). In humans, GATA3 haplo-insufficiency is associated with hypoparathyroidism, deafness, and renal dysplasia (HDR) syndrome (Irina V. Grigorieva & Thakker, 2011). GATA3 expression has been detected in the human thymus, inner ear, central nervous system, kidney and parathyroid gland (Muroya et al., 2001; Van Esch et al., 2000).

The transcription factor Gcm2 is a known regulator for embryonic development of the parathyroid glands and is involved in adult parathyroid cell proliferation and cell death. Reduction of Gcm2 in the adult parathyroid gland causes changes in cell death patterns and reduced cell proliferation (Yamada et al., 2019). Parathyroid cell differentiation and survival also require Gcm2 (Liu, Yu, & Manley, 2007); Gcm2 knockout mice have been shown to have lower serum PTH levels by six months of age (Morito et al., 2018; Yuan, Opas, Vrikshajanani, Libutti, & Levine, 2014).

Downstream of Gcm2 is another transcription factor known as MafB, which is a critical transcription factor for development and differentiation of the parathyroid gland. In MafB-deficient (MafB^{-/-}) mice, the separation of parathyroid glands from the thymus during the embryological development does not occur; subsequently, the expression of PTH is severely reduced in the parathyroid gland of neonates (Morito et al., 2018). The MafB protein directly regulates PTH synthesis by binding to the promoter of the PTH gene (Morito et al., 2018).

However, the role of MafB in other tissues is not well understood, because MafB^{-/-} mice display other developmental anomalies.

A ubiquitous transcription factor specificity protein 1 (SP1), which is a known GC box-binding protein, physically interacts with GATA3, Gcm2, and MafB (Han et al., 2015). Furthermore, evidence suggests that GATA3, Gcm2, and MafB and SP1 interact with each other when two of them are co-expressed. It is believed that these transcription factors synergistically activate PTH gene transcription (Irina V. Grigorieva & Thakker, 2011; Han et al., 2015). Of these three transcription factors, GATA3 is the most upstream, followed by Gcm2, and then MafB in parathyroid development (T. Naveh-Many & Silver, 2018).

MafB is involved in PTH expression; however, it has a more important role in development and differentiation of the parathyroid gland. Hypocalcemia induced by ethylenediamine tetraacetic acid (EDTA) or adenine-induced renal failure model in MafB wild-type mice have shown that reduction in extracellular calcium concentration regulated MafB through CaSR. In MafB^{+/-} mice, plasma PTH is similar to wild-type under normal conditions; however, hypocalcemia induced by ethylene glycol tertaacetic acid (EGTA) in MafB^{+/-} mice resulted in impaired increase in serum PTH, PTH mRNA, parathyroid cell proliferation, and serum calcium (Morito et al., 2018; T. Naveh-Many & Silver, 2018).

The modulation of PTH secretion by iCa^{2+} in blood is accomplished via the extracellular calcium-sensing receptor (CaSR). This transmembrane protein is a G protein-coupled receptor (GPCR) activated by extracellular iCa^{2+} and by other physiological cations including ionized magnesium (iMg^{2+}), amino acids, and polyamines. The CaSR is an important controller of extracellular calcium homeostasis. It is expressed at high levels in the parathyroid gland, kidney, bone and intestine (Diaz-Soto et al., 2016). The CaSR regulates PTH gene expression by a

post-transcriptional mechanism (Edward M. Brown, 2013; Levi et al., 2006). Activation of the CaSR enhances the expression of vitamin D receptor (VDR) (Edward M. Brown, 2013; Rodriguez et al., 2007). It also mediates intracellular degradation of PTH that occurs during hypercalcemia (Edward M. Brown, 2013; Morrissey, Hamilton, MacGregor, & Cohn, 1980).

The VDR expressed in the parathyroid gland is also increased after administration of 1,25(OH)₂D (Calcitriol) (Justin Silver & Naveh-Many, 2018). Binding of 1,25(OH)₂D to the VDR decreases PTH mRNA and gene expression, parathyroid cell proliferation, and serum PTH concentration (Justin Silver & Naveh-Many, 2018; J. Silver, Naveh-Many, Mayer, Schmelzer, & Popovtzer, 1986; J. Silver, Russell, & Sherwood, 1985). Administration of 1,25(OH)₂D in rats increases VDR mRNA and decreases PTH mRNA in the parathyroid gland (T. Naveh-Many, Marx, Keshet, Pike, & Silver, 1990). An increase in 1,25(OH)₂D level reduces PTH gene expression and parathyroid cell proliferation; while activation of CaSR by hypercalcemia suppresses PTH production, secretion, parathyroid cellular proliferation, and PTH gene expression; as well as decrease 1,25(OH)₂D production. This is a feedback loops in that PTH synthesis and secretion, and 1,25(OH)₂D production, initially stimulated by reductions in circulating iCa^{2+} and 1,25(OH)₂D levels are subsequently shut off as iCa^{2+} and 1,25(OH)₂D concentrations return to normal.

In patients with chronic kidney disease (CKD), administration of calcimimetics such as NPS Pharmaceuticals molecule *N*-(3-[2-chlorophenyl]propyl)-(R)- α -methyl-3-methoxybenzylamine (NPS R-568) significantly decreases serum PTH levels, leading to reduction in plasma calcium, and calcium-phosphorus products in patients on hemodialysis (Levi et al., 2006; Lindberg, 2005). Binding of calcimimetics such as NPS R-568 to CaSR cause decreases in PTH secretion (Nemeth et al., 1998), parathyroid cell proliferation

(Colloton et al., 2005; Wada et al., 1997) and gene expression (Levi et al., 2006). The mechanisms by which calcimimetics regulate PTH secretion or affect PTH mRNA stability or cell proliferation have not been elucidated. Experiments to elucidate the mechanisms involved in the regulation of $i\text{Ca}^{2+}$ concentration in the plasma or serum have been facilitated by using synthetic molecules that are either calcimimetic or calcilytic, which are positive, and negative allosteric modulators of CaSR, respectively. Some calcimimetics, such as NPS R-568, enhance the sensitivity of the CaSR for extracellular $i\text{Ca}^{2+}$, leading to inhibition of parathyroid hormone secretion *in vitro*. Administration of NPS R-568 to rats decreased serum PTH level, followed by a decrease in serum calcium (Fox, Lowe, Petty, & Nemeth, 1999), but did not affect CaSR in the kidney (E. M. Brown & Hebert, 1997; Riccardi et al., 1996).

A calcilytic compound, such as 2-Chloro-6-[(2R)-3-[[1,1-dimethyl-2-(2-naphthalenyl)ethyl] amino]-2-hydroxypropoxy]-benzonitrile (NPS 2143), is a selective positive allosteric modulator of CaSR that stimulate secretion of parathyroid hormone. *In vitro* treatment of bovine parathyroid hormone cells with NPS 2143 stimulated the secretion of parathyroid hormone over a range of extracellular calcium concentrations and reversed the effects of calcimimetic compound NPS R-467 (analog of NPS R-568) on calcium concentration and secretion of PTH (Nemeth et al., 2001). Administration of NPS 2143 to normal rats caused a four-fold increase in plasma PTH approximately 15 minutes post-dose, which remained elevated up to 6 hours post-dose. Following increased plasma PTH, serum calcium concentration increased about 90 minutes post-dose, peaked at 3 hours, and returned to baseline by 6 hours post-dose (Gowen et al., 2000). The NPS 2143 molecule lowers the sensitivity of the CaSR to $i\text{Ca}^{2+}$ concentration, which induces adenylate cyclase and promotes phospholipase C activation—a signal transduction that results in increased serum PTH (Letz et al., 2010). Whether the increase

in PTH is due to increased cell proliferation, increased stability of PTH mRNA, or increased expression of mRNA remains to be studied.

Recently, a pharmaceutical compound, CC-325, was synthesized for the treatment of Acute Myeloid Leukemia (AML). Preliminary studies have shown anti-proliferative effects in tumor cell lines, which are the result of cereblon-dependent ubiquitination and subsequent proteasomal degradation of GSPT1. This protein, also known as eRF3a, is a translation termination factor that binds eRF1 to mediate stop codon recognition and nascent protein release from the ribosome (Matyskiela et al., 2016). In-house (Bristol Myers Squibb Corporation) pilot studies in huCRBN KI mice and cynomolgus monkeys have revealed development of hypocalcemia as a side effect of the drug, that if left untreated could be life threatening. Analysis of the samples from huCRBN KI mice studies has revealed a decrease in parathyroid hormone. This suggests that the hypocalcemia associated with the administration of CC-325 may be due to an effect of the compound on the parathyroid gland and may impact circulating PTH concentration. Elucidating the mechanism of this drug-induced hypocalcemia will be important for design and development of future drugs in this class of compounds.

Purpose of this Study and Research Questions

The purpose of this research is to investigate the effects of CC-325, a GSPT1 protein degrader, on parathyroid hormone synthesis and release and on iCa^{2+} concentration in the plasma. Additionally, this research is designed to investigate the effect of CC-325 on FGF23 plasma concentration and its impact on plasma calcium concentration.

The research questions that guide this study are:

- 1- What is the mechanism that leads to drop in PTH after treatment with CC-325?

- a. Does it affect secretion of PTH?
 - b. Does it affect transcription?
 - c. Does it affect translation?
- 2- What is the effect of CC-325 on FGF23 plasma concentration and how does it impact plasma calcium concentration?

To date, there are no published data associating degradation of GSPT1 with hypocalcemia. This research is the first to explore part of this mechanism in a preclinical setting.

Hypotheses

The objectives of this research are summarized in the four hypotheses listed below. The focus of this research is to investigate the effects of GSPT1 degradation on transcription, translation and secretion of PTH. Testing these hypotheses will provide information about the impact of GSPT-1 degradation on PTH mRNA, PTH synthesis, and PTH release from parathyroid and its impact on plasma calcium concentration. This study will also investigate the impact of GSPT1 degradation on serum FGF23 concentration and its effect on serum calcium concentration.

As described earlier, CC-325 administration to mice results in decrease in serum PTH and then calcium, while treatment of mice with a single dose of NPS 2143 results in significant increase in serum PTH and calcium. In this study, after subacute dosing of CC-325 to huCRBN KI mice, followed by a single dose of NPS 2143 on the last day of study, we will collect samples to test the following hypotheses. The details and procedures for testing these hypotheses are described in method section.

Hypothesis 1: Treatment of huCRBN KI mice with CC-325 will inhibit the synthesis of Parathyroid Hormone.

H₀1: After 5 days of treatment with CC-325, a single dose administration of NPS 2143 will not be able to increase the serum parathyroid hormone and iCa²⁺.

H_A1: After 5 days of treatment with CC-325, a single dose administration of NPS 2143 will increase serum parathyroid hormone and iCa²⁺.

Hypothesis 2: Treatment of huCRBN KI mice with CC-325 does not affect the secretion of parathyroid hormone from the parathyroid gland.

H₀2: After 5 days of treatment with CC-325, with or without a single dose administration of NPS 2143, extracellular parathyroid hormone level (in serum) correlate with the intracellular parathyroid hormone level in parathyroid.

H_A2: After 5 days of treatment with CC-325, with or without a single dose administration of NPS 2143, intracellular parathyroid hormone level in parathyroid will be higher than serum parathyroid hormone level suggesting sequestration in parathyroid.

Hypothesis 3: Treatment of huCRBN KI mice with CC-325 regulates parathyroid hormone production at transcription level.

After treatment of mice with CC-325 for 5 days, followed by a single dose administration of either vehicle or NPS 2143, we will measure the level of PTH mRNA in the parathyroid. The data will be used to test this hypothesis.

H₀3: Treatment with CC-325 has no effect on parathyroid hormone mRNA.

H_A3: Treatment with CC-325 decreases parathyroid hormone mRNA

Hypothesis 4: After treatment with CC-325, serum FGF23 decreases.

Since FGF23 suppresses PTH when elevated, we are hypothesizing that when PTH is low the FGF23 concentration in serum will decrease.

H₀4: After 5 days of treatment with CC-325, serum FGF23 concentration does not change.

H_A4: After 5 days of treatment with CC-325, serum FGF23 concentration decreases.

Summary

Hypocalcemia is a potentially life-threatening condition if left untreated. Several organs including, thyroid, parathyroid, kidney, bone and gastrointestinal (GI) tract are involved in maintaining the calcium homeostasis. Any injury or toxicity to any of these organs can disrupt this homeostasis. Recently, we have discovered the impact of some pharmaceuticals, known as GSPT1 degraders, on parathyroid gland. It has been shown that degradation of GSPT1 can reduce calcium level in the plasma. Currently there is no published data regarding the mechanism of GSPT1 induced hypocalcemia in preclinical species. In-house pilot studies have shown that huCRBN KI mice treated with CC-325 have low levels of parathyroid hormone in circulation. The proposed study is designed to investigate the mechanism by which the GSPT1 degrader, CC-325, causes hypocalcemia.

CHAPTER 2: LITERATURE REVIEW

Calcium

Calcium is the fifth most prevalent cation and the fifth most common element in the body. The body of an average person contains about 1 kg of calcium, which is mainly found in the skeleton (99%) as well as the soft tissue (1%), and to a lesser degree in extracellular fluids (<0.2%). In the blood, almost all of the calcium is in the plasma portion with a mean concentration of 2.38 mmol/L (9.5 mg/dL) in humans (Burtis, Ashwood, Bruns, & Tietz, 2013). In plasma, calcium is present in three physiological states; free or ionized calcium (iCa^{2+}), bound to plasma proteins, and complexed with small anions. The biologically active calcium is the iCa^{2+} , which is tightly controlled by PTH and $1,25(OH)_2D$ (Glendenning, 2013). Roughly half of calcium in plasma is free, the remaining is either bound to albumin or globulin or complexed with bicarbonate, phosphate, lactate or citrate. About 70-80% of the protein bound fraction is bound to albumin and lesser degree to globulin. The complexed fraction is about 10-15% of total plasma calcium. The free fraction, also referred to as ionized calcium, is the diffusible fraction that is biologically important and is often measured for accurate diagnosis. Because calcium binds to the negatively charged sites of proteins, its binding is pH dependent (Fogh-Andersen, Bjerrum, & Siggaard-Andersen, 1993; Kragh-Hansen & Vorum, 1993). Albumin has about 30 binding sites for calcium; increases in pH increase the albumin-bound calcium (Fogh-Andersen et al., 1993). Acidosis leads to a decrease in binding, resulting in increased iCa^{2+} , whereas alkalosis increases binding and results in decreased iCa^{2+} . *In vitro* data has shown that for every 0.1 unit change in pH, the iCa^{2+} changes by approximately 0.05 mmol/L (0.2 mg/dL) (Burtis et al., 2013; Fogh-Andersen et al., 1993).

Calcium can be either intracellular or extracellular, and the skeleton serves as a reservoir for both, Table 1 shows the percent distribution of calcium, phosphate, and magnesium in the body. Intracellular calcium plays an important role in many physiological functions, including hormone secretion, glycogen metabolism, muscle contraction, and cell division. Extracellular calcium provides calcium ion for the maintenance of intracellular calcium, blood coagulation, bone mineralization, and plasma membrane potential. The intracellular concentration of calcium in the cytosol is between 10^{-7} and 10^{-6} mol/L which is about 1000 fold less than the extracellular fluid, which is 10^{-3} mol/L (Burtis et al., 2013; Pozzan, Rizzuto, Volpe, & Meldolesi, 1994). Calcium homeostasis is discussed in detail further in this literature review.

Phosphate

Inorganic and organic phosphate (collectively referred to as phosphorus) are present in plasma; however, only inorganic phosphate is measured in the plasma or serum. An adult human body has about 600g of phosphorus; about 85% of the phosphorus is in the skeleton, and the rest in the soft tissue (Burtis et al., 2013). Roughly 10% of the phosphate in the plasma is protein bound, 35% complexed with sodium, calcium, or magnesium, and 55% is free. The ratio of monovalent phosphate to divalent phosphate changes with blood pH. At pH 7.4, the ratio of monovalent phosphate to divalent phosphate is 1:4 which decreases in acidosis and increases in alkalosis (Burtis et al., 2013; Yu & Lee, 1987). The organic phosphate esters are primarily intracellular, whereas inorganic phosphate is in bone and extracellular fluid. In cells, both organic and inorganic phosphate are present; however, most organic phosphate is in the nucleic acids, phospholipids, phosphoproteins and high-energy compounds involved in metabolism (Yu & Lee, 1987). Plasma phosphate levels are coupled to calcium homeostasis through the actions of PTH. In primary and secondary hyperparathyroidism, a decrease in plasma phosphate

(hypophosphatemia) is observed. In hypoparathyroidism or pseudohypoparathyroidism, phosphate renal tubular reabsorption is increased and plasma phosphates are elevated (Burtis et al., 2013). In vitro studies have suggested that phosphate could directly affect PTH secretion. Intravenous infusion of phosphate to dogs, and simultaneous infusion of calcium to prevent hypocalcemia, resulted in a delayed and transient increase in PTH only at very high concentration of phosphate (4-5 mM) in plasma (Estepa et al., 1999). However, this study suggests that PTH stimulation by phosphate can be calcium independent. Serum phosphate directly affects PTH synthesis by promoting the stability of PTH mRNA (Kawakami et al., 2017; Moallem, Kilav, Silver, & Naveh-Many, 1998).

Magnesium

Magnesium is the second most abundant intracellular cation and the fourth most prevalent cation in the body. Of the total magnesium in the body, 53% is in the skeleton, 27% is intracellular compartments of muscle, and 19% in soft tissue. Plasma contains about 0.3% of the total body magnesium (Fawcett, Haxby, & Male, 1999). Similar to calcium, magnesium in plasma is present in three different forms, ionized or diffusible, protein bound, and complexed with anions such as phosphate (Fawcett et al., 1999; Rude & Singer, 1981). It is involved in several processes such as: gating of transmembrane calcium channels, hormone receptor binding, transmembrane ion flux and regulation of adenylate cyclase, neuronal activity, cardiac excitability, muscle contraction, and neurotransmitter release (Fawcett et al., 1999).

Intracellularly, the majority of the magnesium is bound to negatively charged molecules and proteins; in the cytosol, 80% of the magnesium is bound to ATP, which is a substrate for many enzymes (Burtis et al., 2013; Rude & Singer, 1981; Saris, Mervaala, Karppanen, Khawaja, & Lewenstam, 2000). Intracellular magnesium concentrations range from 5-20 mmol/L, with 1-5%

ionized. The concentration increases as the metabolic activity of the cell increases (Elin, 2010; Jahnhen-Dechent & Ketteler, 2012). Extracellular magnesium is about 1% of the total body magnesium, which is primarily found in plasma. Free or ionized magnesium accounts for about 55% of the total plasma magnesium, while 30% is bound to protein, mainly albumin, and 15% is complexed with phosphate, bicarbonate, citrate, sulphate, and other anions (Burtis et al., 2013; Fawcett et al., 1999; Jahnhen-Dechent & Ketteler, 2012). Table 2 provides details of different physiological states of calcium, phosphate, and magnesium in plasma.

Magnesium deficiency has been reported in 7-11% of the hospitalized patients, and in many cases it co-exists with other electrolyte abnormalities such as hypocalcemia and hypophosphatemia (Fawcett et al., 1999; Jahnhen-Dechent & Ketteler, 2012). Similar to calcium, magnesium is absorbed in the gut and stored in bone minerals; excess magnesium is excreted by the kidney and in the feces. A common cause of magnesium deficiency is renal loss (Fawcett et al., 1999; Swaminathan, 2003). Magnesium and calcium are in competition for the same binding sites on plasma protein molecules (Swaminathan, 2003). Similar to calcium, magnesium measurement in serum does not accurately reflect the total body content of magnesium because only 1% of total body magnesium is present in extracellular fluids and only 0.3% of the total magnesium is found in plasma; therefore, serum magnesium concentrations are poor predictors of intracellular or total body magnesium (Jahnhen-Dechent & Ketteler, 2012; Swaminathan, 2003).

Magnesium reabsorption in the kidneys can range from 0.5-70% of the filtered load, which is mainly dependent on the concentration of the magnesium in plasma, and to a lesser degree dependent on the concentration of hormones such as: parathyroid hormone, anti-diuretic hormone, and calcitonin (Jahnhen-Dechent & Ketteler, 2012). Other hormones that can influence

the magnesium balance in the body include 1,25(OH)₂D, glucagon, aldosterone, and insulin. Extracellular magnesium directly inhibits PTH release by stimulating the CaSR. Magnesium is two-to-threefold less potent than calcium in activating the CaSR (Vetter & Lohse, 2002). In parathyroid, the intracellular events that are stimulated by CaSR activation include transient increase in intracellular calcium, stimulation of Phospholipase A2 activity and inhibition of cyclic adenosine monophosphate (cAMP) accumulation. These effects are mediated via G protein Gi and Gq classes and are detailed in the Calcium Sensing Receptor section and explained in Figure 5 (page 37). PTH stimulates magnesium reabsorption in the Loop of Henley and in the distal tubule by activation of adenylate cyclase (AC) and cAMP production. This stimulates the paracellular uptake of magnesium and calcium reabsorption by stimulating the Na⁺, K⁺ and 2Cl⁻ and the K⁺ channels in cortical thick ascending limb of the Loop of Henle (de Rouffignac & Quamme, 1994; Morel, 1981; Vetter & Lohse, 2002). In the convoluted tubule PTH can enhance absorption of magnesium via AC activation, although the exact mechanism has not been elucidated (Vetter & Lohse, 2002).

Hypomagnesemia is a term used when there is a magnesium deficiency in the blood. Some of the causes of hypomagnesemia include reduced intake, reduced intestinal absorption, increase renal loss, increased gastrointestinal loss, hyperparathyroidism and drugs such as cisplatin, carboplatin, and gallium nitrate (Swaminathan, 2003). Hypocalcemia can occur when there is a magnesium deficiency. One of the important factors that results in hypocalcemia during the hypomagnesemia is impaired release of PTH (Liamis et al., 2009; Swaminathan, 2003). The acute effects of extracellular magnesium on PTH release is similar to calcium; however, in hypomagnesemia, there is a diminished release of PTH. In addition to diminished levels of PTH, end-organ resistance to PTH and an increase in PTH catabolism

occurs (Jahnen-Dechent & Ketteler, 2012; Swaminathan, 2003). The evidence suggesting that in hypomagnesemia there is an end-organ resistance to PTH based on the occurrence of hypocalcemia in the presence of normal or elevated serum PTH levels. Administration of PTH to patients with hypocalcemia due to magnesium deficiency does not normalize calcium levels or increase the urinary excretion of phosphate or cAMP (Swaminathan, 2003). In hypomagnesemia, there is also a diminished level of $1,25(\text{OH})_2\text{D}$ due to a decrease in conversion of $25(\text{OH})_2\text{D}$ to $1,25(\text{OH})_2\text{D}$. There is also evidence of increased clearance of $1,25(\text{OH})_2\text{D}$ and end-organ resistance in hypomagnesemia (Risco, Traba, & de la Piedra, 1995; Swaminathan, 2003).

Hypermagnesemia occurs when there is excessive administration of magnesium salts or magnesium-containing drugs, which has a high prevalence in patients with reduced renal function. Some other causes of hypermagnesemia include lithium therapy, hypothyroidism, Addison's disease, milk alkali syndrome and familial hypocalciuric hypercalcemia (Marcucci & Brandi, 2019; Swaminathan, 2003).

Table 1.

Distribution of Calcium, Phosphate, and Magnesium in The Body as a Percentage.

Tissue	Calcium	Phosphate	Magnesium
Skeleton	99%	85%	55%
Soft tissues	1%	15%	45%
Extracellular fluid	<0.2%	<0.1%	1%
Total	1000 g (25 mol)	600 g (19.4 mol)	25 g (1.0 mol)

Note. Source: (Burtis et al., 2013)

Table 2.

Physiochemical States of Calcium, Phosphate, and Magnesium in Normal Plasma.

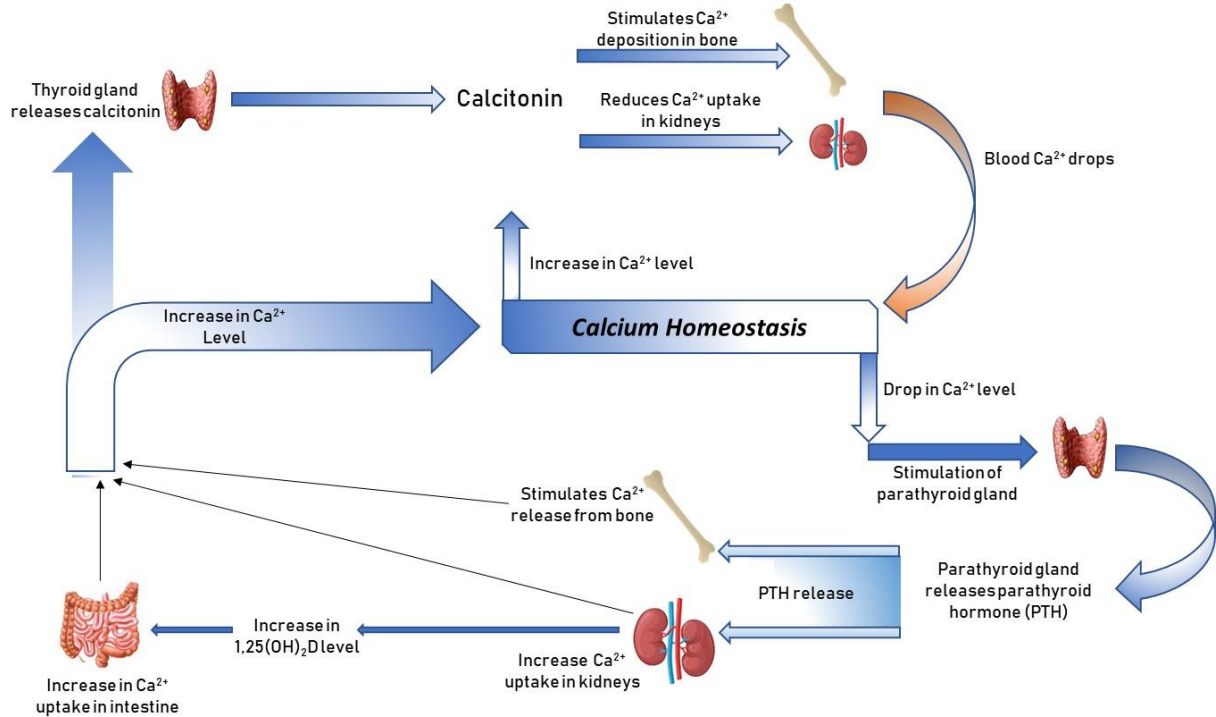
State	Approximate Percent of Total		
	Calcium	Phosphate	Magnesium
Free (ionized)	50%	55%	55%
Protein-bound	40%	10%	30%
Complexed	10%	35%	15%
Total (mg/dL)	8.6-10.3	2.5-4.5	1.7-2.4
(mmol/L)	2.15-2.57	0.81-1.45	0.70-0.99

Note. Source: (Burtis et al., 2013)**Calcium Homeostasis**

Regulation of extracellular and intracellular ionized calcium is essential to life. Plasma iCa^{2+} concentration, phosphate concentration, as well as the concentrations of PTH, calcitonin, and $1,25(OH)_2D$ (calcitriol) all contribute to the regulation of calcium homeostasis. The synthesis and secretion of the three hormones is regulated in part by the plasma concentrations of calcium and phosphate. A decrease in calcium or an increase in phosphate will stimulate the parathyroid gland to secrete PTH. Parathyroid hormone acts directly on the kidney to increase renal tubular reabsorption of calcium from the glomerular filtrate, and activates vitamin D, which increases intestinal absorption of calcium. Parathyroid hormone also acts directly on bones to stimulate the release of calcium. An increase in plasma calcium concentration will result in a drop in PTH secretion, which then results in a drop in plasma calcium levels. Upon a decrease in the plasma iCa^{2+} concentration and a decrease in plasma levels of $1,25(OH)_2D$, the cascade of signaling to increase PTH synthesis and secretion initiates, as illustrated in Figure 1. Calcitonin is produced in parafollicular cells of the thyroid and inhibits bone resorption and reduce calcium reabsorption by the kidney; an increase in plasma calcium levels stimulate calcitonin release.

Figure 1.

Multiorgan Mechanisms for The Regulation of Calcium Homeostasis.



Note. Decrease in plasma calcium concentration results in release of PTH from parathyroid gland. Release of PTH stimulates the release of calcium from bone and uptake of calcium by the kidney. Additionally, PTH stimulates the activation of vitamin D in kidney, resulting in increased calcium uptake in the intestine. Collectively, these mechanisms result in increase in plasma concentration to normal level. Increase in plasma calcium stimulates the release of calcitonin from thyroid gland, inducing calcium uptake by bone and increasing renal secretion of calcium to reduce plasma calcium to normal level.

Hypocalcemia

Hypocalcemia is a potentially life-threatening condition that is defined in humans as a drop in total plasma calcium level below 2.12 mmol/L (8.5 mg/dl), or ionized calcium level below 1.17 mmol/L (4.7 mg/dl) (Liamis et al., 2009). It is a common electrolyte imbalance in patients that manifests in a wide range of clinical symptoms including dyspnea, dysrhythmia, circumoral numbness and paresthesia spasms. The symptoms associated with hypocalcemia are listed in Table 3 (Michels & Kelly, 2013). The most common causes of hypocalcemia include: Vitamin D deficiency, hypoparathyroidism, resistance to calcitriol or PTH, and kidney disease

(Fong & Khan, 2012). Hypocalcemia has also been associated with many drugs including biphosphonates, cisplatin, antiepileptics, aminoglycosides, diuretics, and protein pump inhibitors as well as several other classes of drugs (Fong & Khan, 2012; Liamis et al., 2009). Conditions that can lead to hypocalcemia are listed in Table 4.

Table 3.

Symptoms Associated with Hypocalcemia.

Organ System	Most common symptoms and possible diagnosis
Cardiovascular	Dyspnea, edema, palpitations, syncope Dysrhythmia, prolonged corrected QT interval, systolic dysfunction
Neurologic	Headache, impaired vision, neuropsychiatric symptoms Premature cataracts, pseudotumor cerebri
Neuromuscular	Circumoral numbness and paresthesias; cramping, muscle twitching, spasms; seizures Carpopedal spasm

Note. Source: (Michels & Kelly, 2013)

Table 4.

Conditions and Causes of Hypocalcemia.

Hypoparathyroidism (low or inappropriately normal PTH)
• Post thyroid or parathyroid surgery
• Autoimmune – isolated or autoimmune polyglandular syndrome I
• Chronic magnesium deficiency or acute hypermagnesemia
• Developmental disorders associated with genetic variants
• Parathyroid gland destruction (e.g., radiation, infiltration, iron or copper, metastatic disease, granulomatous disease)
• Other causes (such as mitochondrial disease and maternal hyperparathyroidism)
Vitamin D inadequacy (high PTH and low vitamin D)
• Nutritional deficiency
• Lack of sunlight exposure
• Malabsorption, including celiac disease
• Gastric bypass surgery
• Extensive bowel surgery
• Pancreatic insufficiency
• Chronic kidney disease
• End-stage liver disease and cirrhosis
Resistance to PTH (high PTH and normal vitamin D)
• Pseudohypoparathyroidism type 1
• Pseudohypoparathyroidism type 2
• Other forms of PTH resistance
Miscellaneous
• Drugs (e.g., bisphosphonates, denosumab, cinacalcet, cisplatin, foscarnet, anticonvulsants)
• Hungry bone syndrome
• Osteoblastic metastases
• Osteopetrosis
• Sepsis and acute and critical illnesses
• Acute pancreatitis
• Spurious hypocalcemia

Note. Source: (Hakami & Khan, 2019)

Vitamin D in activated form and PTH play an important role in calcium homeostasis.

Inadequate 1,25(OH)₂D levels can cause up to a 50% reduction in absorption of calcium from the intestinal tract. Low PTH levels in the blood reduce the extracellular calcium concentration by causing excessive urinary calcium excretion, a reduction in bone remodeling, and decreased activation of vitamin D. Although uncommon, resistance to PTH can occur, which results in an increase in plasma PTH concentration without an increase in calcium concentration, a condition called pseudohypoparathyroidism (Cooper & Gittoes, 2008; Fong & Khan, 2012).

Drug-Induced Hypocalcemia

Drug-related hypocalcemia is often mild and asymptomatic; however, severe hypocalcemia could result in adverse clinical effects. Several medications have been associated with hypocalcemia; however, diagnosis of drug-induced hypocalcemia can often be missed because of other existing clinical conditions in the patient (Liamis et al., 2009). Iron overload due to long-term blood transfusion or misuse of iron supplements can infiltrate and destroy the parathyroid gland, which would result in low PTH and hypocalcemia (Angelopoulos et al., 2006; Liamis et al., 2009). Cisplatin, aminoglycosides, and amphotericin are known to cause hypocalcemia secondary to hypomagnesemia. Cisplatin treatment results in dose-dependent hypocalcemia. In fact, hypocalcemia is a common toxic side effect of high-dose cisplatin chemotherapy, while low dose cisplatin treatment has rarely been associated with severe hypocalcemia (Arany & Safirstein, 2003). Cinacalcet, a calcimimetic drug used in patients with renal failure to control secondary hyperparathyroidism (SHP), has been associated with hypocalcemia due to its ability to inhibit PTH release (Dong, 2005; I. V. Grigorieva et al., 2010). Secondary hyperparathyroidism occurs in renal failure when parathyroid glands become enlarged

and release too much PTH into plasma in response to hypocalcemia. The list of drugs or treatments and their associated with hypocalcemia are shown in Table 5.

Table 5.

Principal Causes and Underlying Mechanisms of Drug Induced Hypocalcemia.

Drug or Treatment	Mechanism
Gadolinium-based contrast agents: gadodiamide and gadoversetamide	Pseudohypocalcemia
Infiltration of the parathyroid gland (iron overload): long-term blood transfusion therapy, inappropriate use of iron	Low PTH levels (hypoparathyroidism)
Neck radiation	Damage to parathyroid gland
Cisplatin, diuretics, aminoglycosides, amphotericin	Drug-induced hypomagnesemia
Magnesium-containing antacids and laxatives, magnesium sulfate tocolytic therapy	Drug-induced hypermagnesemia
Cinacalcet	Reduce PTH
Alcohol	Reduce PTH
Calcium chelators: ethylenediaminetetraacetic acid (EDTA), citrate, foscarnet, hydrofluoric acid	High PTH levels (secondary hyperparathyroidism)
Phenytoin, phenobarbital, carbamazepine, isoniazid, theophylline, glutethimide, and rifampin	Causing vitamin D deficiency or resistance
Bisphosphonates, plicamycin, estrogens, calcitonin, colchicine overdose	Inhibitors of bone resorption
Loop diuretics	Excess calcium excretion
PTH resistance	Drug-related hypomagnesemia
Phosphate-containing enemas, drugs that cause tumor lysis syndrome (e.g., anticancer agents)	Drug-induced hyperphosphatemia
Proton pump inhibitors (PPIs) and H2-blockers	Diminished calcium absorption caused by reduced gastric acid production
Glucocorticoids, Strontium-89, deferasirox, electroconvulsive therapy, bicarbonates, propylthiouracil, dobutamine, calcium channel blockers	Other mechanisms not fully elucidated

Source: (Liamis et al., 2009)

Vitamin D

Vitamin D is a fat-soluble vitamin that can be obtained from natural food intake, food supplements, or from 7-dehydrocholesterol in the epidermal layer of the skin when it is exposed to ultraviolet rays from sunlight. The vitamin D produced from sun exposure, or obtained from food and supplements is biologically inert and must undergo two enzymatic hydroxylation in the body to form $1,25(\text{OH})_2\text{D}$, which is referred to as calcitriol or activated vitamin D (Bikle, 2018). The three main steps in vitamin D metabolism include: 25-hydroxylation, 1α -hydroxylation, and 24-hydroxylation that are all performed by cytochrome P450 mixed function oxidases (Bikle, 2018).

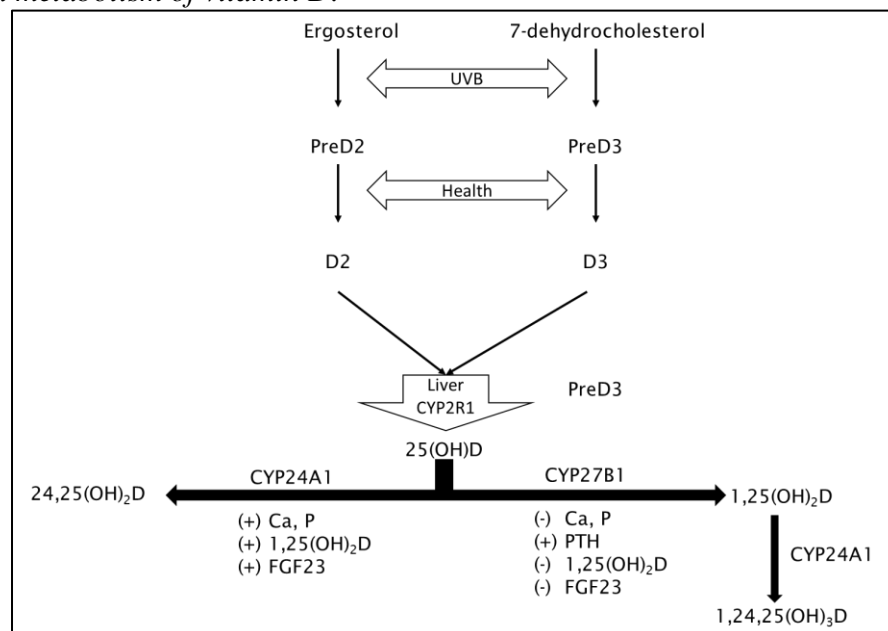
In the first step, the liver converts 25-hydroxyvitamin D [$25(\text{OH})\text{D}$], also known as calcidiol, from both cholecalciferol (vitamin D from the skin) and ergocalciferol (vitamin D from plants and supplements). Several cytochrome P450 enzymes such as CYP27A1, CYP2R1, and CYP3A4 have 25-hydroxylase activity (Bikle, 2018; David Goltzman, Hendy, Karaplis, Kremer, & Miao, 2018).

The second step, which forms the physiologically active $1,25$ -dihydroxyvitamin D [$1,25(\text{OH})_2\text{D}$], is mediated by a 1α -Hydroxylase (CYP27B1). Although other tissues and cells of the immune system express CYP27B1, the kidneys are the main source of this enzyme (Bikle, 2018; Bikle, Patzek, & Wang, 2018; David Goltzman et al., 2018). A third hydroxylation is mediated by CYP24A1, which is 24-hydroxylase, Figure 2. The 24-hydroxylase reaction generates biologically inactive calcitroic acid. Another hydroxylase reaction can generate biologically active $25(\text{OH})\text{D}$ -26, 23-lactone and $1,25(\text{OH})_2\text{D}$ -26, 23 lactone (Bikle, 2018). $1,25(\text{OH})_2\text{D}$ is the preferred substrate for CYP24A1, producing $1,24,25(\text{OH})_3\text{D}$, which has high affinity for VDR and is biologically active. In the kidney, PTH inhibits expression of CYP24A1

while it induces CYP27B1 expression (Bikle, 2018; D. Goltzman, Mannstadt, & Marcocci, 2018; Tebben & Kumar, 2018). An increase in PTH stimulates the renal conversion of 25-hydroxyvitamin D (25(OH)D to 1,25(OH)₂D, which then increases intestinal calcium absorption. This process is believed to take several hours. Sustained hypocalcemia and elevated plasma PTH also result in 1,25(OH)₂D mediated release of phosphate, calcium, and FGF23 release from bones. Fibroblast growth factor 23 causes a reduction in 1,25(OH)₂D concentration and decreases PTH production (D. Goltzman et al., 2018). In plasma, vitamin D and its metabolites are bound to a vitamin D binding protein (DBP), which is a member of the albumin family of proteins (D. Goltzman et al., 2018). The synthesis and metabolism of vitamin D are shown in Figure 2.

Figure 2.

Synthesis and metabolism of vitamin D.



Note. UVB light from sun exposure and intake of vitamin D are the sources of vitamin D in the body. The first step of liver metabolism is by CYP2R1 in the liver, and subsequently by CYP27B1 in the kidney. Stimulating (+) and inhibitory (-) factors are shown for each enzyme and pathway. Stimulation of CYP24A1 enzyme take the 25(OH)D away from the CYP27B1 and Vitamin D3 pathway. Modified from (D. Goltzman et al., 2018).

The Fibroblast Growth Factor 23

Fibroblast growth factor 23 (FGF23) is an osteogenic phosphaturic hormone secreted from bone; it is a member of the FGF family of 22 genes and proteins. Fibroblast growth factor 23 is a phosphatonin that is secreted by osteocytes and osteoblasts in response to hyperphosphatemia and $1,25(\text{OH})_2\text{D}$ (J. Silver & Naveh-Many, 2010). Alpha-Klotho (αKlotho) is a single-pass transmembrane protein, which also circulates in the blood. αKlotho is predominantly expressed in renal distal convoluted tubules with less expression in proximal convoluted tubules, as well as in osteocytes and osteoblasts and in the parathyroid gland (Ben-Dov et al., 2007; Hu et al., 2010), therefore, making parathyroid gland and kidney the primary FGF23 target organs for calcium and phosphorus homeostasis. Fibroblast growth factor receptor (FGFR) is a single-pass receptor tyrosine kinase transmembrane protein. There are four isoforms, FGFR1-4, and although they are ubiquitously expressed, they are differentially activated by different FGF ligands in complexes with heparan sulfate proteoglycan and with Klotho (α and β). Since FGFR is ubiquitously expressed, the effect of FGF23 on specific tissue is based on the presence of αKlotho and the tertiary complex formation of FGF23/ αKlotho /FGFR (Chen et al., 2018; Hu et al., 2019). FGF23 binding to FGFR and αKlotho in parathyroid glands leads to decrease of PTH gene expression and PTH secretion through activation of the MAPK pathway (J. Silver & Naveh-Many, 2010). FGF23 suppresses the production of $1,25(\text{OH})_2\text{D}$ from the kidney as it reduces the 1α hydroxylation (Kawakami et al., 2017) and reduce the intestinal Pi absorption (Hu et al., 2019). PTH reduces renal tubular phosphate reabsorption by inducing the endocytosis of NaPi-2a and NaPi-2c in the proximal tubule, resulting in increase of urinary phosphate excretion (Bourgeois et al., 2013; Chen et al., 2018; Gattineni & Baum, 2012). High levels of PTH can stimulate FGF23 and $1,25-(\text{OH})_2\text{D}$ secretion, increase in $1,25-(\text{OH})_2\text{D}$ increases intestinal phosphate absorption. In a feedback loop mechanism, PTH stimulates

FGF23 production in the bone, whereas FGF23 inhibits the production of PTH (Chen et al., 2018; Quarles, 2012). Inhibition of PTH production and secretion by FGF23 in parathyroid gland is mediated by phosphorylation of ERK1/2 as an indication of activation of MAPK pathway (Ben-Dov et al., 2007).

Fibroblast growth factor 23 suppresses PTH secretion in the short term but increases secretion in the long term (Kawakami et al., 2017). This contrasts with calcium, which stimulates PTH secretion in acute and chronic hypocalcemia. Intravenous (iv) administration of FGF23 to rats decreases the serum PTH level at 10- and 30-minute post administration; but when given intraperitoneally (ip), serum PTH levels decrease at 40 minutes and 24 h post administration. FGF23 decreased PTH mRNA levels at 40 min following ip administration (J. Silver & Naveh-Many, 2010).

In a chronic kidney disease (CKD) mouse model, plasma FGF23 increases and causes parathyroid cells to proliferate, leading to increase in PTH (Kawakami et al., 2017). Rats treated with intravenous injection of a recombinant FGF23 and FGFR inhibitor (FGFRi) (PD173074) under normal- and hypocalcemic condition had significant decrease in plasma intact FGF23 (iFGF23) and increase in PTH, revealing that FGF23 binding to its receptor, FGFR has an inhibitory effect on PTH secretion (Mace, Gravesen, Nordholm, Olgaard, & Lewin, 2018). In the absence of FGFRi inhibitor, FGF23 quickly inhibited the PTH secretion, however treatment with FGFRi inhibited the PTH reduction. It was also shown that, inhibition of the FGFR by itself significantly increased PTH levels, indicating that FGF23 play a key role in the parathyroid gland's PTH secretion. When hypocalcemia with high plasma PTH was induced in rats by EGTA administration, injection with recombinant FGF23, with or without FGFRi, had no effect on serum PTH (Mace et al., 2018). In acute hypocalcemia, when increased PTH secretion is

needed to restore the calcium homeostasis, the FGF23 inhibitory effect is diminished. The FGF23 also effects CYP27B1, which is responsible for transforming 25OHD to 1,25(OH)₂D. The FGF23 and 1,25(OH)₂D inhibit CYP27B1, whereas PTH stimulate this enzyme. Elevated calcium suppresses CYP27B1 primarily via suppression of PTH; elevated phosphate suppresses CYP27B1 primarily by stimulating FGF23 (Bikle, 2014).

However, to date, there is no published data on the effects and concentrations of FGF23 in hypoparathyroidism where the plasma calcium level is also low.

The Parathyroid Glands

In humans, the parathyroid glands comprise four small glands located on the posterior part of the thyroid gland, located bilaterally or near the thyroid gland capsule. The parathyroid glands consist of two main cell types, chief cells, and oxyphil cells. The chief cells synthesize, store and secrete PTH (Burtis et al., 2013). The CaSR located on the surface of the chief cells responds to low serum calcium and activates translation and secretion of PTH. Oxyphil cells, also known as oxyntic cells, have no recognized function. The proportion of oxyphil cells in the parathyroid glands increases with age (Lofrese et al., 2019) (Fong & Khan, 2012).

The parathyroid glands develop with the thymus from a shared organ primordium. Both organs arise from the third pharyngeal pouch endoderm and surrounding neural crest cells.

Transcriptional processes that are key to early pouch pattern and development of the parathyroid and thymus organ primordium are: Hoxa3, Pax1/Pax9, Eya1, Tbx1, Sox3, and Six1/Six4 (Han et al., 2015; Tally Naveh-Many, Silver, & Kronenberg, 2020). The parathyroid-destined domain can be distinguished from E10.5 (embryonic day 10.5) by the expression of the transcription factor Gcm2, which is necessary for parathyroid differentiation and survival (Liu et al., 2007). Superior and inferior parathyroid glands develop from the endoderm of the

third and fourth pharyngeal pouches around the sixth week of gestation in humans. Parathyroid glands are functional during gestation, acting to control calcium balance in the fetus (Lefrese et al., 2019). The secretory product PTH is released by exocytosis at the apicolateral domain of the plasma membrane into the intercellular space (Quinn, Kifor, Kifor, Butters, & Brown, 2007).

Rodent Parathyroid

Mouse and rat parathyroid glands are derived from the third pharyngeal pouch. The fourth pharyngeal pouch does not develop in these species, and as a result only one pair of glands is present. Because of the close embryological relationship between the thymus and parathyroid, ectopic parathyroid tissue can develop in the thymus or vice-versa. Parathyroid glands are located at the anteriolateral position of the thyroid and are separated by a delicate strand of connective tissue from the thyroid gland. In the mouse parathyroid glands only chief cells are present (Kittel et al., 1996). The closely packed chief cells possess a smooth plasma membrane. The cytoplasm contains abundant mitochondria, free ribosomes, a well-developed Golgi apparatus and a rough endoplasmic reticulum. There are small and large secretory granules present in mouse parathyroid cells. The diameter of the small secretory granules is 150-200 nm, while the large secretory granules are about 300-600 nm in diameter. The large secretory granules are believed to serve as storage granules, but there is no evidence suggesting that the small secretory granules have similar capability (Isono et al., 1983; Isono et al., 1985)

Parathyroid Hormone

Parathyroid hormone is produced by parathyroid glands and binds to its receptor in two main target organs, kidney and bone. The main function of the PTH is to tightly control the iCa^{2+} concentration in the plasma, and calcium homeostasis throughout the body. In parathyroid chief cells, transcription and translation of the PTH gene generates a PreproPTH, a 115- amino

acid peptide. This is processed to ProPTH, a 90 amino acid peptide, and then to PTH, which is 84 amino acids. The intact PTH with 84 amino acids is required for biological activity, while truncated forms (amino acids 34-84 and 37-84) are not active and cannot bind to the PTH receptor. These fragments can be produced while PTH awaits secretion by the parathyroid gland, and to a lesser degree by proteolytic cleavage of intact PTH by Kupffer cells. The serum half-life of PTH is just a few minutes and under normocalcemic conditions only 20% of the circulating PTH is active (D. Goltzman et al., 2018; Hinson, Raven, & Chew, 2010). Parathyroid hormone and vitamin D are the primary hormones that regulate bone and mineral metabolism as well.

The transcription factors, GATA3, Gcm2, and MafB are transcription factors that regulate parathyroid development and parathyroid hormone expression. In humans, conditions such as congenital hypoparathyroidism, deafness, and renal dysplasia syndrome are associated with GATA3 haploinsufficiency (Han et al., 2015; Tally Naveh-Many et al., 2020). The GATA3^{+/-} mice are viable and develop a normal parathyroid gland; however, hypocalcemia induced by a low calcium and vitamin D diet does not increase PTH and calcium levels as in WT mice, indicating that GATA3 plays an important role in PTH production (I. V. Grigorieva et al., 2010).

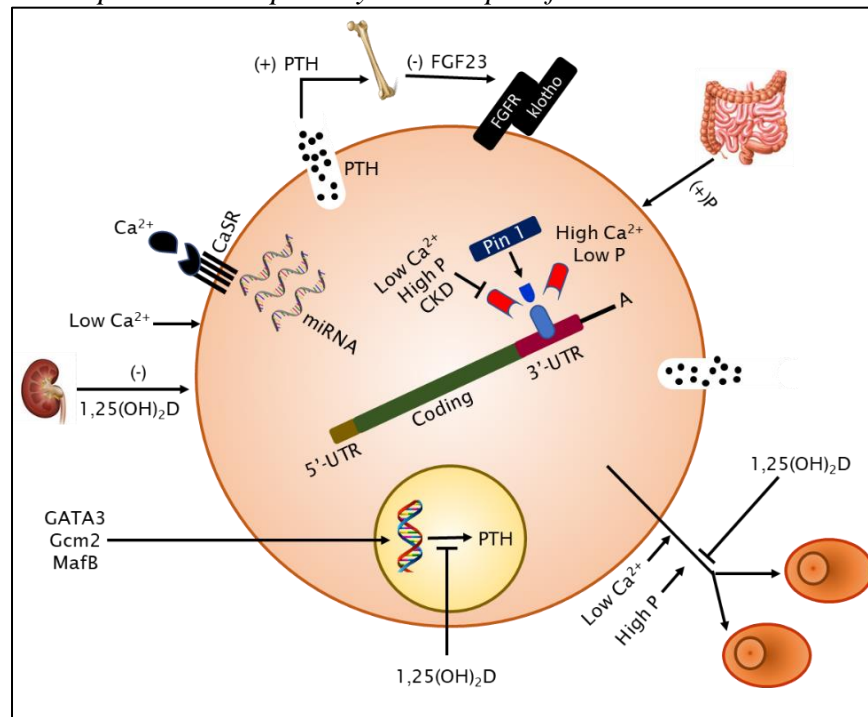
GATA3 directly binds to Gcm2 to regulate its expression. Upregulation of Gcm2 is essential for parathyroid differentiation and survival. Mutation in the Gcm2 gene is associated with familial isolated hypoparathyroidism (Yamada et al., 2019). In Gcm2 knockout mice, the plasma PTH concentration was too low to be detectable, indicating that Gcm2 continues to play an important role in parathyroid function post-development (Liu et al., 2007; T. Naveh-Many & Silver, 2018).

MafB is a leucine zinc finger transcription factor expressed in the developing parathyroid after E11.5 and postnatally in mice. In Gcm2 null mice, the expression of MafB in parathyroid primordium is absent. MafB has a critical role in parathyroid development, which involves separation from thymus and migration toward the thyroid (Morito et al., 2018). In MafB^{+/-} mice, the response to induced hypocalcemia was impaired, resulting in a minimal increase in serum PTH, PTH mRNA, and parathyroid cell proliferation (Kamitani-Kawamoto et al., 2011).

In the complex of GATA3, Gcm2 and MafB, GATA3 is the most upstream, followed by Gcm2 then MafB, which is the most downstream. Studies have shown that these transcription factors are critical for parathyroid development and function and PTH gene expression (Han et al., 2015; Yamada et al., 2019; Yuan et al., 2014). Figure 3 shows the cascade of PTH production in parathyroid chief cells. In parathyroid gland, GATA3 binds to the double-GATA-motif within the Gcm2 promotor, activating the Gcm2 gene. GATA3, Gcm2, and MafB synergistically activate PTH gene expression by interacting with the ubiquitous SP1 transcription factor regulating PTH gene expression in the parathyroid (Han et al., 2015; Hendy & Canaff, 2016).

Figure 3.

Regulators of PTH expression and parathyroid cell proliferation.



Note. Calcium, $1,25(\text{OH})_2\text{D}$, the high phosphate of uremia, and FGF23 all regulate PTH secretion, parathyroid cell proliferation, and PTH gene expression through transcriptional and post-transcriptional mechanisms. GATA3, Gcm2, and MafB form a transcriptional complex that mediates parathyroid specific PTH expression. Of the PTH transcription factors, GATA3 is the most upstream, followed by Gcm2, and then MafB. miRNAs are necessary for the activation of the parathyroid gland in secondary hyperparathyroidism. FGF23: Fibroblast growth factor 23, FGFR: Fibroblast growth factor receptor, 5'-UT: 5' untranslated region, $1,25(\text{OH})_2\text{D}$: 1,25-dihydroxyvitamin D₃, CaSR: Calcium sensing receptor, CKD: Chronic kidney disease, miRNA: Micro RNA. Modified from (T. Naveh-Many & Silver, 2018).

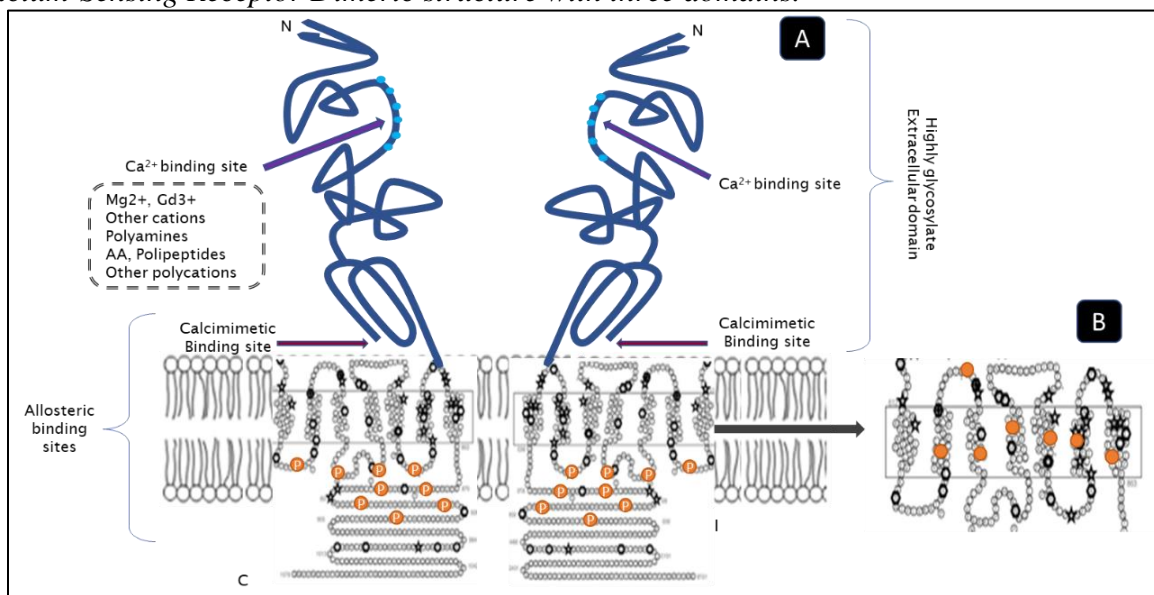
Calcium Sensing Receptor

In humans, the CaSR gene resides on chromosome 3 and at the band 3q13.3-21. In the mouse and rat, the CaSR gene resides on chromosomes 11 and 16, respectively (Janicic et al., 1995). The CaSR protein has been classified as a member of group II G protein couple receptors. The human CaSR consists of 1078 amino acid residues with 3 different structural regions. The regions include: an extreme N-terminus, which binds Ca^{2+} ; the

transmembrane domain consisting of seven helices (typical of the superfamily of GPCRs); and a large carboxyl terminal cytosolic domain that contains many phosphorylation consensus sequences to protein kinases type A (PKA), and C (PKC), as illustrated in Figure 4. The carboxyl terminal domain is capable of binding to filamin A and activating mitogen-activated protein kinases (MAPK) (Bai, 2004; Diaz-Soto et al., 2016).

Figure 4.

Calcium-Sensing Receptor Dimeric structure with three domains.



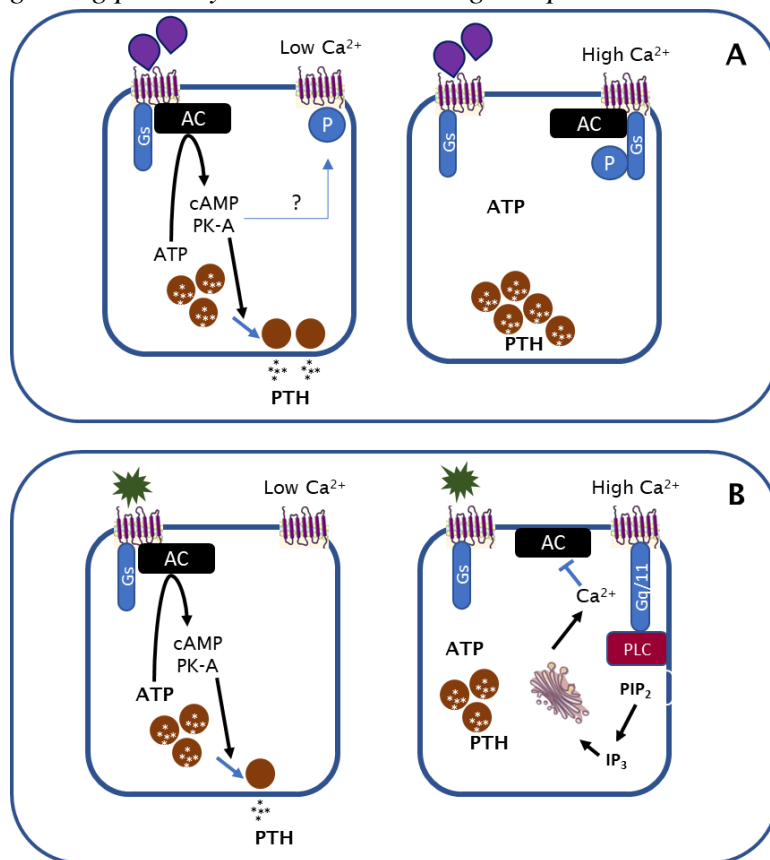
Note. Negatively charged binding site for Ca^{2+} and the calcimimetic binding sites are marked (A). Residues involved in both calcimimetic and calcilytic binding are shown in black. Residues described play a part in calcilytic binding only are shown in orange (B). Modified from (Diaz-Soto et al., 2016; Saidak, Brazier, Kamel, & Mentaverri, 2009).

Binding of calcium to the CaSR results in its activation and a decrease in plasma PTH. CaSR interaction with several heterotrimeric G proteins such as $\text{G}_{q/11}$, $\text{G}_{12/13}$, and G_i controls the activity of several downstream signaling pathways. Activation of $\text{G}_{q/11}$ by CaSR activates phospholipase β ($\text{PLC}\beta$), releasing inositol triphosphate (IP_3) from membrane phosphoglycerides, which mediates the release of Ca^{2+} from the intracellular stores. This creates a transient increase in cytosolic Ca^{2+} , which is followed by an influx of Ca^{2+} through activated plasma membrane

Ca^{2+} channels (Diaz-Soto et al., 2016; Kifor, Diaz, Butters, & Brown, 1997). In the parathyroid gland, CaSR responds to an increase of extracellular iCa^{2+} , by inhibiting cAMP synthesis via a pertussis toxin-insensitive mechanism that involves inhibition of a calcium-sensitive adenylate cyclase (de Jesus Ferreira et al., 1998; Diaz-Soto et al., 2016), as illustrated in Figure 5. The CaSR also mediates migration, RhoA activation, and Rho kinase-dependent formation of actin stress fibers through $\text{G}_{12/13}$ in CaSR expressing cells (Conigrave & Ward, 2013; Diaz-Soto et al., 2016). Inhibition of PTH synthesis due to a high concentration of Ca^{2+} is mediated by MAPK pathway activation and cAMP decreased by inhibition of adenyl cyclase. Although *in vitro* studies using a bovine parathyroid pseudogland system have shown that calcium can activate the MAP kinase pathway, the inhibition of adenylate cyclase, MEK pathway, p38 or addition of exogenous dibutyl-cyclic AMP had no effect on PTH mRNA (Ritter, Pande, Krits, Slatopolsky, & Brown, 2008).

Figure 5.

Intracellular signaling pathways in calcium-sensing receptor.



Note. Two mechanisms are shown; one is stimulated and the other is spontaneous, which result in either secretion or inhibition of PTH based on the Ca²⁺ concentration. Exogenous agonists, including neurotransmitters or hormones, can activate Gs-coupled GPCRs (A). PTH secretion continues when the Ca²⁺ concentration remains low but is promptly inhibited by Gi-dependent inhibition of adenylate cyclase in the presence of high Ca²⁺ concentration. The mechanism by which CaSR, preferentially binds to Gi is unknown but might depend on local protein kinase-A (PK-A) activation. The second mechanism (B), which is spontaneous, involves constitutive Gs-coupled GPCR activity and/or by autocrine/paracrine production of receptor activators. PTH secretion continues when the Ca²⁺ is low but is inhibited by high Ca²⁺ concentration. Source: Modified from (Conigrave, 2016; Diaz-Soto et al., 2016).

In addition to calcium and magnesium, other physiological cations (e.g. spermine, b-amyloid peptides, cationic amino acids) and pharmacological agents (e.g. aminoglycosides) act as CaSR receptor agonists (Vetter & Lohse, 2002). There are two types of CaSR ligands, type I and type II. Type I are orthosteric agonists and type II are allosteric modulators, which could be positive or negative modulators. Orthosteric agonists activate CaSR on their own, however

allosteric modulators bind to allosteric binding sites on the CaSR (Figure 5 (B), page 37), and increase the sensitivity of the CaSR to orthosteric agonists (Quinn et al., 2007). Calcium is the main orthosteric agonist of CaSR with the most impactful physiological effect on CaSR; however, there are other divalent and trivalent cations that display CaSR agonism with various affinities. In general, the agonist with the higher positive charge density tends to have higher potency (Cheng, Geibel, & Hebert, 2004; McGehee et al., 1997). Table 6 lists the known orthosteric agonists and allosteric modulators of CaSR. To date, no orthosteric antagonist of CaSR has been identified.

Table 6.

Different types of CaSR ligands.

Agonists	
Cations	High affinity: Gd^{3+} , La^{3+} , Eu^{3+} , Tb^{3+}
	Medium affinity: Zn^{2+} , Ni^{2+} , Cd^{2+} , Pb^{2+} , Cu^{2+} , Fe^{2+}
	Low affinity: Ca^{2+} , Mg^{2+} , Ba^{2+} , Mn^{2+} , Sr^{2+}
Polyamines	Spermine, spermidine, putrescine
Aminoglycosides	Neomycin, paromomycin, tobramycin, gentamicin, kanamycin
Positive Allosteric Modulators	
Endogenous: L-amino acids Phe, Trp, Tyr, His	
Basic polipeptides: poly-L-arginine, poly-lysine, protamine, amyloid β peptide	
Synthetic phenylalkylamines calcimimetics: NPS R467, NPS R568 (cinacalcet), AMG416	
Negative Allosteric Modulators	
Endogenous: none	
Synthetic phenylalkylamines calcilytics: NPS 2143, Calbex 231	

Note. Sources: (Cheng et al., 2004; Diaz-Soto et al., 2016; McGehee et al., 1997; Ward, McLarnon, & Riccardi, 2002)

Calcimimetic drugs such as NPS R568 amplify the sensitivity of the CaSR to extracellular iCa^{2+} concentration (shift the concentration-response curve of Ca^{2+} to the left) and decrease PTH synthesis and secretion in a dose-dependent manner, resulting in a decrease in

blood iCa^{2+} concentration. Calcilytics drugs such as NPS 2143, shift the concentration-response curve of Ca^{2+} to the right, and increase PTH secretion, raising plasma iCa^{2+} concentrations and urinary phosphate excretion (Arey et al., 2005; Saidak et al., 2009).

Extracellular concentration of iCa^{2+} does not affect the CaSR gene expression in parathyroid gland or kidney. Treatment of mice with an allosteric modulator of CaSR suppressed plasma PTH and iCa^{2+} and parathyroid cell proliferation, but had no effect on the levels of parathyroid CaSR mRNA (Imanishi et al., 2011). However, GATA3, Gcm2, and MafB transcription factors play a key role in CaSR and PTH expression (Han et al., 2015; Hendy & Canaff, 2016). Downregulation or absence of Gcm2, a transcription factor for parathyroid development and PTH production, can cause a decrease in expression of CaSR in parathyroid cells (Hendy & Canaff, 2016; Mizobuchi et al., 2009). In the parathyroid gland, GATA3 transactivates the Gcm2 gene by binding specifically to double-GATA-motif within the Gcm2 promotor, and consequently, the GATA3 knockout mouse embryos lack Gcm2.

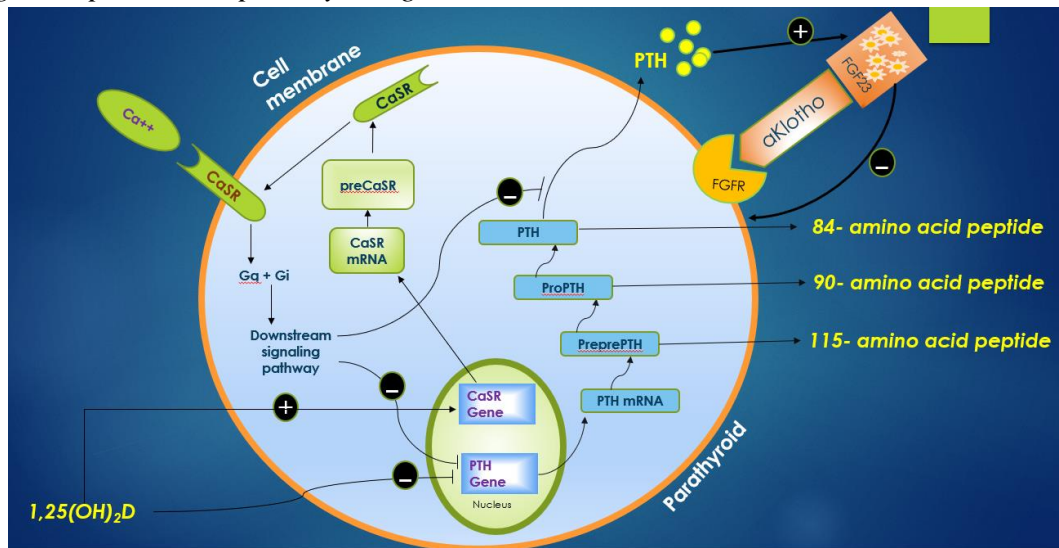
In the thyroid, activation of CaSR by iCa^{2+} has a stimulatory effect on calcitonin secretion from C cells of the thyroid, resulting in inhibition of bone resorption and increase in plasma iCa^{2+} levels (Garrett et al., 1995). This contrasts with the action of iCa^{2+} on parathyroid hormone secretion. The CaSR plays a critical role in maintaining calcium homeostasis by precise regulation of PTH and calcitonin release in response change in iCa^{2+} levels.

G protein-coupled receptors are synthesized and exported along the secretory pathway from the endoplasmic reticulum (ER) to the plasma membrane immediately after cellular quality control check is complete. However, CaSR, a GPCR, predominantly localizes in intracellular compartments and is not transferred to the cell surface immediately after the quality check is complete (Breitwieser, 2013, 2014; Cavanaugh, Huang, & Breitwieser, 2012; Huang,

Cavanaugh, & Breitwieser, 2011). Activation of CaSR in the cell membrane by calcium or orthosteric agonists recruits additional CaSR to the cell surface from intracellular stores. Molecules including brefeldin A (blocking ER-Golgi trafficking) or tunicamycin (blocking glycosylation of newly synthesized CaSR) can acutely block the intracellular localization of CaSR (Grant, Stepanchick, Cavanaugh, & Breitwieser, 2011). Intracellular calcium is increased by CaSR activation, which increases the plasma membrane CaSR for only a short time; additional signaling outputs are required to maintain this increased level of CaSR in the plasma membrane (Breitwieser, 2014). The proteins and signaling that contribute to the regulation and release of CaSR to the secretory pathway have not been identified. However, it has been shown that the carboxyl terminus of CaSR contains binding site(s) that mediates ER retention (Breitwieser, 2014; Cavanaugh, McKenna, Stepanchick, & Breitwieser, 2010). The evolving model, agonist-driven insertional signaling (ADIS), describes the transverse of CaSR in the cell membrane. This model suggests that the CaSR is only weakly expressed at the plasma membrane at low extracellular calcium. Increasing extracellular calcium and/or addition of orthosteric agonists leads to an increase in anterograde trafficking through the secretory pathway from all compartments including the ER, with no change in the constitutive endocytosis rate (Breitwieser, 2012, 2013; Grant et al., 2011). This is illustrated in Figure 6.

Figure 6:

Diagram showing the effect Ca^{2+} binding to CaSR, PTH gene expression, PTH release, and CaSR gene expression in parathyroid gland.



Note. Increase in plasma calcium concentration inhibit PTH production and release by parathyroid cells. Increase in plasma PTH results in increase of plasma $1,25(\text{OH})_2\text{D}$, which has an inhibitory effect on PTH production but stimulated calcium sensing receptor expression on parathyroid cells.

Hypoparathyroidism

Hypoparathyroidism is a disorder in which either the parathyroid glands fail to secrete enough biologically active PTH, or the PTH is incapable of stimulating a biological response in its target organ. In both conditions, hypocalcemia and hyperphosphatemia occurs.

Hypoparathyroidism results in a decrease in active transport of calcium from glomerular filtrate in the distal renal tubules. Patients with hypoparathyroidism also have low plasma $1,25(\text{OH})_2\text{D}$ concentrations (Conigrave, 2016).

Hypoparathyroidism occurs when there is an abnormality in parathyroid gland development, a decrease in PTH production or its action, or damage to the parathyroid gland. Damage to the parathyroid gland or its blood supply may occur during thyroid or neck surgery, an autoimmune condition targeting the parathyroid gland, or radiation therapy to the neck area.

Other causes that could lead to abnormal development of parathyroid and hypoparathyroidism include: metabolic disorders, mineral deposition, magnesium abnormalities, or developing resistance to PTH action (Bandeira, Rubin, Cusano, & Bilezikian, 2018). Persistent hypocalcemia with low or inappropriately normal PTH levels and hyperphosphatemia is diagnostic of hypoparathyroidism (Hakami & Khan, 2019). In the United States there are an estimated 60,000-115,000 cases of hypoparathyroidism (Powers, Joy, Ruscio, & Lagast, 2013). Below is the summary of the disorders causing hypoparathyroidism.

PTH Gene Mutations: The parathyroid gene mutations have been associated with impaired synthesis and secretion of parathyroid gland (Arnold et al., 1990).

Hypoparathyroidism, Sensorineural Deafness, and Renal Dysplasia Syndrome (HDR Syndrome): HDR syndrome results from mutations in the GATA-binding protein 3 gene (GATA3) causing inadequate production of PTH (Muroya et al., 2001).

Sanjad-Sakati Syndrome and Kenny-Caffey Type 1 Syndrome: This is caused by mutations in the tubulin-specific chaperone E (TBCE) gene on chromosome 1q42–q43, which encodes a protein involved in tubulin binding. Clinical manifestation includes congenital hypoparathyroidism (Sanjad, Sakati, Abu-Osba, Kaddoura, & Milner, 1991).

Isolated Hypoparathyroidism conditions: Autosomal recessive hypoparathyroidism and X-linked are such disorders. In an autosomal recessive condition, the leading cause of autosomal recessive isolated hypoparathyroidism is the loss of function of the glial cells missing (Gcm2) gene, also known as GCMB. Gcm2 is expressed predominantly in the developing parathyroid gland (Ding, Buckingham, & Levine, 2001). In X-Linked hypoparathyroidism disorder, patients could have defect in the development of the parathyroid gland (Bowl et al., 2005).

Reduced Synthesis or Secretion of PTH: Autosomal Dominant Hypocalcemia (ADH):

ADH causes reduction in PTH synthesis or secretion.

- Type I: It is caused by an activating mutation in the *CaSR* gene, increasing the sensitivity of the receptor to calcium leading to decrease in PTH. Renal calcium reabsorption is low because of mutant CaSRs in the kidney.
- Type II: It is caused by an activating mutation in the guanine nucleotide-binding protein alpha 11 (*GNA11*) gene that encodes the alpha subunit of the G protein G11, which is a key mediator of CaSR signaling leading to increased suppression of PTH release at even lower serum calcium levels., thus producing relative hypercalciuria, Renal calcium reabsorption is not affected (Lienhardt et al., 2001; Nesbit et al., 2013).

DiGeorge Syndrome: DiGeorge syndrome results from the abnormal development of the third and fourth pharyngeal pouches resulting in parathyroid aplasia or hypoplasia. DiGeorge syndrome is the leading cause of persistent hypocalcemia in newborns. Hypoparathyroidism is present in up to 60% of patients with DiGeorge Syndrome (Kobrynski & Sullivan, 2007).

Autoimmune Disorder: A condition where patients develop an anti-CaSR antibody, and hypoparathyroidism can develop (Li et al., 1996).

Autoimmune Polyglandular Syndrome Type I (APS I): Autoimmune damage of the parathyroid glands leading to hypoparathyroidism. This syndrome results from mutations in the autoimmune regulator gene, which is expressed in other tissues including the thymus, pancreas, adrenal cortex, and lymph nodes. Approximately 50% of APS I patients with hypoparathyroidism have antibodies that react with the NACHT leucine-rich-repeat protein 5

(NALP5), which is expressed predominantly in the cytoplasm of parathyroid chief cells (Alimohammadi et al., 2008)

PTH resistance: Target organ resistance to parathyroid hormone is referred to as pseudohypoparathyroidism (PHP). In these patients, the target organ does not produce a biological response to PTH. Table 7 provides the description and classification of PHP.

- PHP Type 1: It is caused by mutations in *GNAS1*, which is a gene encoding the alpha subunit of the stimulatory G protein coupled to the PTH receptor. These mutations lead to inability of this G protein to activate adenylate cyclase after binding to its receptor on PTH, leading to failure of signal transduction to produce an end-organ response to PTH. It is characterized by a series of clinical syndromes known as Albright's hereditary osteodystrophy (AHO), which include subcutaneous calcifications among other conditions. Biochemical findings include hypocalcemia in association with hyperphosphatemia, as a result of renal tubular resistance to PTH, and secondary hyperparathyroidism (Nakamoto, Sandstrom, Brickman, Christenson, & Van Dop, 1998). Related PHP disorders are: pseudo-PHP, progressive osseous heteroplasia, PHP type 1b, PHP type 1c (Hakami & Khan, 2019). Pseudo-PHP patients have normal serum levels of calcium, phosphate, and PTH (Mantovani & Elli, 2019). PHP 1b, also referred to as inactivating PTH/PTH-related protein signaling disorder 3 (iPPSD3), is characterized by renal resistance to PTH associated with resistance to the action thyroid stimulating hormone (TSH), in the absence of other physical abnormalities (Elli et al., 2019; Mantovani & Elli, 2019).
- PHP1C/PHP1A, PPHP, and POH are all referred to as iPPSD2, they all have similar clinical manifestations deriving from inactivating mutations affecting $G\alpha$ coding exons

and include: AHO features, resistance to PTH, TSH, gonadotropins, and growth hormone-releasing hormone (GHRH) (Mantovani & Elli, 2019).

- **PHP Type 2:** PHP type 2 cases are rare and the molecular defects that leads to this disease has not been fully elucidated. Some researchers have hypothesized that PHP type 2 maybe an acquired defect secondary to vitamin D deficiency (Mantovani, 2011). Patients with PHP type 2 is characterized by resistance to PTH, which manifests as high levels of PTH, hypocalcemia, hyperphosphatemia but absence of Albright's hereditary osteodystrophy.

Table 7.
Description and Classification of Pseudohypoparathyroidism.

Type	Hormone Resistance	Clinical Presentation	Genetic Cause
PHP1A	PTHm TSH, gonadotropins, GHRH	AHO, superficial HO	Maternal LOFBNAS genetic variants
PPHP	No	AHO, superficial HO	Paternal LOF GNA genetic variants
PHP1C	PTH, TSH, gonadotropins, GHRH	AHO, superficial HO	Few LOF GNAS genetic variants in exon 13 reported
PHP1B	PTH, TSH	No	Primary or secondary (UPD (20) pat; deletions within STX16 and /or NESP) GNAS epigenetic defects

Note. Other Forms of PTH Resistance. PTH resistance has also been associated with recessive missense mutations in the mature PTH(1–84) sequence, resulting in resistance to PTH because of reduced PTH binding to its receptor (S. Lee et al., 2015).

Allosteric Modulators of The Calcium Sensing Receptor

Positive allosteric modulator of CaSR NPS R-568

The small molecule, NPS R-568, is a phenylalkylamine compound that acts as positive allosteric modulator of CaSR (calcimimetic) and moves iCa^{2+} concentration-response curve to the right. NPS R-568 potentiates the effect of circulating iCa^{2+} on CaSR on the parathyroid,

leading to decreased PTH synthesis and secretion. The hypocalcemia response to NPS R-568 is rapid and dose-dependent. The site of action for NPS R-568 is parathyroid CaSR, because total nephrectomy did not have any effect on magnitude or kinetics of hypocalcemia in rats (Fox et al., 1999). In a rat model of chronic renal insufficiency, a uremic condition results in an increase in PTH levels and parathyroid cell proliferation. Treatment of uremic rats with NPS R-568 inhibited parathyroid cell proliferation (Wada et al., 1997). It has been shown that an increase in PTH mRNA in hypocalcemic rats is due to stabilization of PTH mRNA in parathyroid cells. Parathyroid cytosolic proteins bind to discrete elements in the rat PTH 3'-untranslated (UTR) region and stabilize PTH transcription. Control of PTH mRNA by iCa^{2+} does not involve an increase in the rate of PTH gene transcription. A decrease in extracellular iCa^{2+} stabilizes the PTH mRNA, resulting in an increase in PTH synthesis and secretion, and subsequently an increase in extracellular calcium. An increase in extracellular calcium will increase degradation of PTH mRNA in parathyroid cells (Moallem et al., 1998; Ritter et al., 2008). The effect of NPS R-568 on PTH levels is mediated by transcriptional and post-transcriptional degradation of PTH mRNA, however, maximal reduction of PTH mRNA by NPS R-568 involves gene transcription. This was shown in parathyroid cell cultures by inhibiting gene transcription with actinomycin D treatment prior to treatment with NPS R-568, which only partially decreased PTH mRNA reduction after treatment with NPS R-568. (Ritter et al., 2008).

In a uremic rat model developed by treating rats with an adenine high-phosphorus diet for either 7 or 21 days, PTH mRNA levels in the parathyroid gland and PTH concentration in serum increase. In rodent models, animals treated with adenine high-phosphorus diet exhibit chronic kidney disease with hyperphosphatemia and elevated plasma PTH levels (Levi et al., 2006). In

the adenine high-phosphorus CKD model, rats that were treated for 21 days had high serum phosphate, PTH, PTH mRNA, and decreased in calcium and 1,25(OH)₂D on Day 21. In that study, rats that were treated for either 4 or 7 days with NPS R-568 orally prior to Day 21, had decreases in both serum PTH and PTH mRNA when compared to a control group. Further in vitro studies confirmed that the effects of NPS R-568 on PTH gene expression was posttranscriptional and correlated with differences in protein-RNA binding and posttranscriptional modification of the trans acting factor AUF1 in the parathyroid cells (Levi et al., 2006).

Negative Allosteric Modulator of CaSR NPS 2143

Inhibitors of the CaSR, termed calcilytics, do not activate the wild-type CaSR directly; instead they shift the concentration-response curve of iCa^{2+} and other orthosteric agonists to the right (Ferry et al., 1997). As described earlier, the pharmacologic modulators of CaSR, including NPS 2143, target overlapping allosteric sites within the heptahelical transmembrane domain of CaSR (Nemeth et al., 2001; Saidak et al., 2009). Calcilytics and calcimimetics have a limited range of targets therefore they are preferred as therapy over other natural CaSR ligands.

Calcilytics, such as NPS 2143, cause increased PTH secretion, therefore causing an increase in plasma iCa^{2+} levels and urinary phosphate excretion. The ability of calcilytics to increase plasma PTH concentrations has made them a potential therapy for hypoparathyroidism, which is common in patients with an under reactive parathyroid gland or in ADH (Saidak et al., 2009). The mechanism of action of calcilytics drugs, including NPS 2143, involves binding to plasma membrane CaSRs and reducing its signaling capability in response to orthosteric agonists (Hannan et al., 2015). The CaSR undergoes dofin-mediated ubiquitination and degradation by endoplasmic reticulum-associated degradation (ERAD) during biogenesis.

Loss of function by mutations or the allosteric antagonist NPS 2143 destabilize CasR and increase degradation by endoplasmic reticulum-associated degradation (ERAD) (Huang & Breitwieser, 2007). Pharmacological agonists and antagonists contribute to G protein coupled receptor folding, which causes an increase in expression and plasma membrane localization of the CaSR. Changes in CaSR sensitivity influences its susceptibility to proteasomal degradation (Breitwieser, 2014; Huang & Breitwieser, 2007).

The inhibitory potency of NPS 2143 is dependent on the extracellular calcium concentration; NPS 2143 decreases the sensitivity of the CaSR activation to extracellular Ca^{2+} (Nemeth et al., 2001). Sprague Dawley (SD) rats that were subjected to a two-hour infusion of NPS 2143 at the rate of 1 mg/kg/min experienced a rapid increase in plasma PTH levels that peaked four- to five-fold over baseline about 30 minutes post-start of infusion, and stayed high for the duration of infusion. The increase in plasma PTH was associated with increased plasma iCa^{2+} levels, which increased about 90 minutes after the start of the infusion. Both PTH and iCa^{2+} returned to baseline after an hour after the end of the infusion. It is important to note that the change in plasma PTH preceded the change in plasma iCa^{2+} (Nemeth et al., 2001). Similar results were seen after intraperitoneal (ip) administration of 30 mg/kg NPS 2143 to mice, while oral administration of NPS 2143 prolonged the duration of PTH increase to approximately four hours (Gowen et al., 2000; Hannan et al., 2015).

Translation Termination Factor G1 to S phase Transition 1 (GSPT1) Degradation and Hypocalcemia

Translation termination factor G1 to S phase transition 1 (GSPT1, also known as eRF3a) is a translation termination factor that binds eRF1 to mediate stop codon recognition and nascent protein release from the ribosome (Matyskiela et al., 2016). Degradation of GSPT-1 has been

associated with an anti-proliferative phenotype in tumor cell lines, which is the result of cereblon-dependent ubiquitination and subsequent proteosomal degradation of GSPT1 (Matyskiela et al., 2016).

In the recent annual meeting of American Society of Hematology (ASH, December 7, 2019), preclinical and clinical data for CC-90009, a GSPT1 degrader, was shared. The presentation titled “Clinical Activity of CC-90009, a Cereblon E3 Ligase Modulator and First-in-Class GSPT1 Degradation, As a Single Agent in Patients with Relapsed or Refractory Acute Myeloid Leukemia (R/R AML): Initial Results from a Phase I Dose-Finding Study” highlighted the efficacy of the CC-90009 as well as the observed adverse effects including hypocalcemia. Based on the presentation, observed hypocalcemia was an on-target toxicity, which was reversible, manageable and did not lead to any treatment discontinuations. The preclinical data points to a decrease in PTH as the most probable cause of the hypocalcemia.

Treatment of mice and non-human primates with known GSPT1 degraders such as CC-325 have resulted in decreases in serum calcium (unpublished data). Evaluation of parathyroid tissue by immunohistochemistry (IHC) for presence of PTH in these animals showed decreased levels of PTH in parathyroid tissue. Similar decreases were observed in GATA3 and Gcm2 levels in parathyroid tissue when evaluated by IHC. Although the exact mechanism of the hypocalcemia in GSPT1 degrader treated animals is unknown, the data from the in-house studies point to a decrease in PTH in the parathyroid gland as the likely cause of hypocalcemia.

In order to explore the mechanism of hypocalcemia observed after treatment with GSPT1 degraders, the exploratory toxicology group at Bristol Myers Squibb conducted a series of studies to further investigate the mechanism of cereblon modulators induce hypocalcemia.

Parathyroid Hormone mRNA

Secondary hyperparathyroidism (SHP) is characterized by increased parathyroid hormone mRNA stability that leads to increased PTH mRNA and elevated plasma PTH levels. Changes in the stabilization or destabilization factors in the *cis* element in the PTH mRNA 3'-untranslated region (UTR) are key to controlling PTH synthesis. Two factors play a role in PTH mRNA stabilization or destabilization. Adenosine-uridine (AU) binding factor 1 (AUF1) is a PTH mRNA stabilizing protein, and K-homology splicing regulatory protein (KSPR) is a destabilizing protein that targets mRNAs, including PTH mRNA. The KSPR recruits the ribonuclease complex, the exosome, to target mRNAs including PTH mRNA for degradation (Nechama, Ben-Dov, Silver, & Naveh-Many, 2009). Rats fed an adenine and high-phosphorus diet developed uremic CKD, causing an increase in PTH mRNA and an increase in plasma iCa^{2+} . Treatment with calcimimetic NPS R-568 decreased the PTH mRNA levels and plasma iCa^{2+} in rats with CKD. Despite a decrease in PTH mRNA levels, there was no change in the PTH gene transcription rate between uremic rats and uremic rats treated with NPS R-568. This result indicates that the decrease in PTH gene expression in uremic rats treated with NPS R-568 is posttranscriptional (Levi et al., 2006). Calcimimetics have been shown to decrease serum PTH levels by a decrease in PTH secretion (immediate response), and PTH cell proliferation (intermediate effect). This suggests that calcimimetics could control serum PTH through decrease in gene expression. Treatment with NPS R-568 increased VDR mRNA levels in the normal rat parathyroid gland in vivo and in human parathyroid glands with diffuse hyperplasia (Nechama et al., 2009), which corroborates that the effect of vitamin D on PTH gene expression is transcriptional (J. Silver et al., 1986).

Better understanding of the calcimimetic-mediated decrease in PTH mRNA levels can provide relevant information for future clinical treatment. Parathyroid gland storage of PTH is very limited and can only sustain plasma PTH levels for a short time; a prolonged increase in plasma PTH requires PTH synthesis and parathyroid cell proliferation. Understanding the mechanism of action of different drugs on PTH levels has significant importance in future drug development or mitigation of toxicities.

Cereblon Modulators and Hypocalcemia

Cereblon E3 ligase modulators (CELMoDs), such as CC-325, bind to CRBN, an E3 ligase protein, which is a direct molecular target of compounds with anti-proliferative effects such as thalidomide. CRBN is a highly conserved from plants to mammals and the mRNA for human, rat, and mouse is ubiquitously expressed (Lopez-Girona et al., 2012). Mutations in CRBN in different species affect the efficacy, safety and sensitivity of these CELMoDs in commonly used animal models. Thalidomide and several of its analogs can bind to human, monkey, and rabbit CRBN to exert their efficacy and toxicity in these species. However, thalidomide cannot modulate mouse, rat, and hamsters cereblon. Analysis of the structure and mode of binding of thalidomide and its analogs revealed that lack of activity in rodents was caused by two amino acid differences proximal to the thalidomide binding pocket (Matyskiela et al., 2018). The cereblon surface around the substrate-binding site is the same in monkeys as in humans, therefore efficacy and safety of cereblon modulators are often investigated in monkeys.

The Bristol Myers Squibb has constructed a transgenic mouse engineered to express human cereblon. The huCRBN KI mouse has cereblon carrying a single amino acid change at position 391 (CRBNI391V), where isoleucine was replaced with the valine amino acid

counterpart of human CRBN. Homozygous huCRBN KI mice appeared normal in comparison to their wild-life littermates with no apparent differences in body weight or behavior. In vivo data with selected CELMoDs have shown similar findings in huCRBN KI mice and monkeys; however, mice appear to be less sensitive to effects of CELMoDs. Therefore, higher doses of these compounds are needed to mimic the finding in non-human primates.

Human Cereblon Knock-in Mice Use in Research

Data from in-house pilot studies support the conclusion that the administration of CC-325 to huCRBN KI but not WT mice can cause hypocalcemia. Data from these studies also supports the hypothesis that hypocalcemia is driven by decrease in PTH level in parathyroid gland. Preliminary data suggests that the decrease in PTH level is associated with degradation of GSPT1. In this research, we are investigating the mechanism by which GSPT1 degrader molecule (CC-325) affects PTH synthesis and secretion in parathyroid.

Summary

Hypocalcemia is a life-threatening condition that if not corrected can be fatal. The potential causes of hypocalcemia have been discussed in this section, and regardless of the cause of hypocalcemia, PTH, $1,25(\text{OH})_2\text{D}$, and calcitonin are important factors in maintaining normal physiological calcium concentration. Hypocalcemia occurs in patients with impaired parathyroid function.

The clinical manifestation of hypocalcemia vary by the severity of the hypoparathyroidism, which ranges from mild hypocalcemia with few symptoms, such as numbness and tingling in the face and hands, to severe and life-threatening symptoms including seizures, congestive heart failure, and bronchospasm (Hakami & Khan, 2019)

A decrease in PTH causes excessive renal calcium loss (and reabsorption of phosphate) and decreases in intestinal absorption of calcium due to reduced activation of vitamin D in the kidney. PTH stimulates the renal conversion of 1, 25(OH)D to 1,25(OH)₂D, which will result in increased intestinal calcium absorption. Prolonged hypocalcemia will result in sustained increase in PTH and increases in circulating 1, 25(OH)₂D mediated calcium and phosphorus release from the bone. As a result, the extra cellular fluid concentration of calcium increases and in turn decreases the release of PTH to normal levels. In addition, 1, 25(OH)₂D can cause release of FGF23 from the bone, which causes the decrease production of PTH and 1,25(OH)₂D (D. Goltzman et al., 2018). Calcimimetics on the other hand mediate reduction in serum PTH levels by decreasing PTH gene expression (Levi et al., 2006).

Many causes of hypocalcemia have been discussed here, including abnormal parathyroid gland development or PTH production, autoimmune causes, radiation damage to parathyroid gland, mineral deposition, magnesium abnormalities and more. However, as of this proposal defense, there has been no published data associating GSPT1 degradation with hypocalcemia.

The goal of this research is to explore the cause of hypocalcemia associated treatment with GSPT1 degraders. To investigate the cause of hypocalcemia, the impact of GSPT1 degradation of PTH, FGF23, Ca²⁺, Mg²⁺, and phosphorus concentrations was first investigated. These experiments were followed by assessment of the effect of GSPT1 degradation on PTH production and release.

Significance of This Research

Understanding the mechanism of action of drugs is important in several aspects. First, it will provide better understanding or the adverse effects, which could help with mitigation. Second, it will help with development of the next generation of drugs that could be safer and

more efficacious. Finally, as is the case for this research, it will help investigate the adverse effects of other drugs with similar clinical outcome.

A disturbance of this complex regulatory system of calcium homeostasis can result in a series of compensatory changes that could lead to clinical manifestations. One of the objectives of this study is to better understand the mechanism of action (MOA) of CC-325 on PTH production and calcium homeostasis. A better understanding of the MOA of this complex system will allow further investigation of the etiology and treatment of the various diseases associated with Ca^{2+} imbalance.

This study is designed to further investigate the mechanism of hypocalcemia observed after administration of a selected GSPT1 degrader in huCRBN KI mice. To date, there is little information about the exact mechanism of hypocalcemia observed with this class of compounds. In this study, we propose to test several hypotheses to elucidate the mechanism of hypocalcemia. Based on our initial data, development of hypocalcemia in mice treated with CC-325 is associated with a decrease in PTH. Therefore, the objectives of this study are to answer important questions. Does treatment of mice with CC-325 inhibits the synthesis of parathyroid hormone? Does it affect the release of parathyroid hormone from parathyroid? Testing of these hypotheses will provide further understanding of mechanism of hypocalcemia associated with CC-325.

CHAPTER THREE: METHODS

This chapter describes the research design, methodology, and analyses that will be used to investigate the mechanism of GSPT1 associated hypocalcemia, utilizing CC-325. This study will test the following hypotheses.

Hypotheses

Hypothesis 1: Treatment of huCRBN KI mice with CC-325 will inhibit the synthesis of Parathyroid Hormone

H₀1: After 5 days of treatment with CC-325, a single dose administration of NPS 2143 will not increase the serum parathyroid hormone and serum iCa^{2+} .

We have shown that treatment of mice with CC-325 for 5 days reduces serum calcium and PTH. We have also shown that a negative allosteric modulator of CaSR, NPS 2143, can significantly increase serum PTH and calcium after a single dose administration in mice. If parathyroid Chief cells in mice treated with CC-325 are still capable of synthesizing PTH, we should see an increase in PTH and subsequently calcium after single dose treatment with NPS 2143. However, if these cells are incapable of making PTH, we will not see any response to NPS 2143 administration following 5-day treatment of CC-325. Lack of response to NPS 2143 treatment further confirms that the mechanism of hypocalcemia in CC-325 treated animals is caused by decreased PTH levels.

H_A1: After 5 days of treatment with CC-325, a single dose administration of NPS 2143 will increase serum parathyroid hormone and iCa^{2+} .

If administration of single dose of NPS 2143 following 5-days of treatment with CC-325 can increase serum PTH and subsequently the serum calcium, we can infer that mechanism of hypocalcemia in CC-325 treated animals may not be directly caused by decrease in PTH, since PTH can be stimulated and serum PTH can be increased.

Hypothesis 2: Treatment of huCRBN KI mice with CC-325 does not affect the secretion of parathyroid hormone from the parathyroid gland.

H₀2: After 5 days of treatment with CC-325, with or without a single dose administration of NPS 2143, serum parathyroid hormone level correlate with the intracellular parathyroid hormone level in parathyroid gland measured by IHC.

When hypocalcemia occurs, parathyroid gland responds by releasing PTH into blood stream. If the stored parathyroid hormone in parathyroid chief cells is insufficient to maintain the normal plasma calcium level, these cells start synthesizing more PTH. This hypothesis test whether the decrease or increase in PTH in parathyroid cells is consistent with plasma PTH concentrations. If the level of PTH in parathyroid chief cells, which is measure semi-quantitatively, correlate with serum PTH, we can infer that chief cells are releasing PTH.

H_A2: After 5 days of treatment with CC-325, with or without a single dose administration of NPS 2143, intracellular parathyroid hormone level is higher than serum parathyroid hormone level.

If there is a normal or increased level of PTH in parathyroid cells (normal is considered at the level of vehicle control group) but low levels in plasma, we can infer that the parathyroid is producing PTH but it is not being released into the blood stream.

Hypothesis 3: Treatment of huCRBN KI mice with CC-325 regulates parathyroid hormone production at transcription level.

After 5-days of treatment with CC-325, we will collect parathyroid and stain it for PTH mRNA (ISH staining).

H₀3: Treatment with CC-325 has no effect on PTH mRNA.

If there is no decrease in PTH mRNA staining in parathyroid, we can infer that there is no change in transcription of PTH after treatment with CC-325.

H_A3: Treatment with CC-325 decreases PTH mRNA

Decrease in PTH mRNA indicates that decrease in serum and parathyroid PTH levels is due to decrease synthesis of PTH mRNA.

Hypothesis 4: After treatment with CC-325, serum FGF23 concentration decreases.

Fibroblast growth factor 23 production is stimulated by calcium, 1,25(OH)₂D, and phosphorus intake. Increase in PTH causes increase in FGF23; subsequent increase in FGF23 leads to decrease in PTH and 1,25(OH)₂D and calcium. Increase in 1,25(OH)₂D level is necessary to correct hypocalcemia and increase FGF23. Fibroblast growth factor 23 acts on its receptor, the klotho–FGFR1c receptor, to decrease PTH mRNA levels and secretion. Treatment with CC-325 will results in drop in PTH and plasma calcium, therefore we are hypothesizing that after subacute treatment with CC-325, FGF23 will decrease.

H₀4: After 5 days of treatment with CC-325, serum FGF23 concentration doesn't change, indicating the FGF23 does not respond to low serum PTH and iCa²⁺ concentration.

After treatment of mice with CC-325 for 5 days, serum FGF23 were measured. The absence of a decrease in plasma FGF23 will indicate that FGF23 is not responding to a decrease in serum PTH and iCa²⁺.

H_A4: After 5 days of treatment with CC-325, serum FGF23 concentration decreases, indicating that FGF23 is responding to low serum PTH and iCa²⁺ concentration.

After treatment of mice with CC-325 for 5 days, serum FGF23 were measured. A decrease in plasma FGF23 will indicate that decrease in PTH is directly and indirectly causing decrease in serum FGF23 level.

Pilot Study Design

In brief, three groups of male huCRBN KI mice were treated with a single dose of test article as follow, Group 1: Vehicle, Group 2: NPS R-568, and Group 3: NPS 2143. Each group of mice were bled at 0.5, 1, 2, and 4 hours postdose. Table 8 describes the details about each treatment group. Each group had two cohorts; cohort 1, which were bled at 0.5 and 2 hours postdose, and Cohort 2, which were bled at 1 and 4 hours postdose. The measurements at 0.5, 1, 2, and 4-hr postdose included iCa^{2+} , PTH, Na^+ , K^+ , Cl^- , which were measure using the Stat Prime Profile analyzer. At terminal times points, 2 and 4-hr postdose, additional blood was collected and albumin, Mg^{2+} , phosphate, and total protein were analyzed by Axcel clinical chemistry analyzer. The abbreviated protocol for pilot study is listed in Appendix E.

Table 8.

Pilot Study Groups and Endpoints.

Group	Treatment	Dose mg/kg	n/timepoint	Measurements at 0.5, 1, 2, and 4-hr postdose	Additional Measurements at 2 and 4-hr postdose (Terminal)
1	Vehicle	0	5	iCa^{2+} , PTH, Na^+ , K^+ , Cl^-	Albumin, Mg^{2+} , Phosphate, Total Protein
2	NPS R-568	50	5		
3	NPS 2143	200	5		

Main Study Design

Experimental Animals

Male huCRBN KI homozygous knock-in (KI) mice were obtained from Taconic and were randomly assigned to one of several toxicologic (Tox) assessment and Toxicokinetics (TK) groups. Animals were be approximately 10-12 weeks old and weigh approximately 19 to 27 grams at the time of group assignment. Animals were be allowed to acclimate to the laboratory environment for a minimum of 5 days. Animals were fed with Harlan Teklad diet and water ad libitum and housed with a 12-hour light/dark cycle. Mice were manually randomized and assigned to each treatment group using strata-based method for weight. Each group was identified with a cage card bearing the study identification number and dosing group. Assigned animal numbers were written on tails using an indelible marker. Mice assigned to each treatment groups were group housed up to 5 animals per cage. Animal(s) were housed individually if there is sign of fighting or injury. Mice were not fasted prior to necropsy.

Test Substances 1

Identity:	CC-325 [Free base]
Batch/Lot No.:	0000076909/S00L04
Supplier or Source:	Bristol Myers Squibb
Formulation:	0.5% CMC/0.25% Tween-80 in 50 mM citrate buffer pH 3
Molecular Weight:	423.42

Formula Weight:	423.42
Purity (%):	100
Storage Conditions:	The bulk powder will be stored at room temperature (17-27°C) protected from light. The formulated material was stored refrigerated protected from light.
Handling Precautions:	Per standard laboratory precautions for biologically active compounds and according to SDS.
Supplier/Manufacturer:	Bristol Myers Squibb
Certificate of Analysis:	A certificate of analysis or equivalent, if available, describing the test article characterization will be placed in the study file.

Test Substances 2

Identity:	NPS2143
Batch/Lot No.:	0000049663
Supplier or Source:	Sigma-Aldrich INC.
Formulation:	Aqueous 15% (2-Hydroxypropyl)- β -cyclodextrin (HP β CD)
Molecular Weight:	445.38
Formula Weight:	408.9

Correction Factor:	1.04
Purity (%):	≥95% (HPLC)
Storage Conditions:	Per standard laboratory precautions for biologically active compounds and according to SDS.
Handling Precautions:	Sigma-Aldrich INC. A certificate of analysis or equivalent describing the test article characterization were placed in the study file and information included in the study report.

Dose Selection Criteria

There are no published data on the effects of NPS 2143 in huCRBN KI mice. In our in-house pilot study (internal data), a single dose of 50 or 200 mg/kg was well tolerated for up to 6 hours; no clinical sign of toxicity was observed in these animals. Data from this pilot study was the first results of the effect of NPS 2143 in huCRBN KI mice. Our data shows that the NPS 2143 can increase PTH and iCa^{2+} in these mice. The dose of 50 mg/kg results in a 7% increase in iCa^{2+} from 0.5 to 2 hours post dose. The dose of 200 mg/kg resulted in a 15% increase in iCa^{2+} from 0.5-4 hours postdose. At 200 mg/kg, the increase in PTH was 48-, 18- and 8-fold over vehicle control group at 0.5, 2, and 4 hours postdose. An increase in phosphorus at 2-h postdose was seen, but phosphorus was decreased by 4-h postdose. Similarly, an increase in Mg^{2+} was observed at 2-h postdose but returned to vehicle control level by 4-h postdose. No change in albumin or electrolytes was observed at the measured timepoints of 2- and 4-h postdose. Therefore, the dose of 200 mg/kg was selected for this study; however, on dosing day,

an error in calculation resulted a dose of 120 mg/kg instead of 200 mg/kg. All tables and graphs have been corrected to reflect the actual dose that was administered.

CC-325 has been tested in male huCRBN KI mice in repeat-dose exploratory toxicity studies. In another internal study mice were dosed at 15 mg/kg BID (30 mg/kg/day) or 30 mg/kg QD for up to 7 Days. Both doses were tolerated up to Day 5, however, by Day 6, mild decreases in body weight was observed. On Day 7, clinical signs of toxicity included hunch posture and pilo-erection observed in both treatment groups, therefore a dose of 30 mg/kg for longer than 5 Days may not be tolerable. Some animals in 30 mg/kg also had decreased activity by Day 7. There was no mortality in the toxicological assessment groups.

In the current study, male huCRBN KI mice were dosed with CC-325 at 15 mg/kg BID (30 mg/kg total daily dose). Total daily doses of 30 mg/kg/day for up to 5 days are expected to be tolerated based on the timing of clinical signs of toxicity observed previously. This study will focus on the mechanisms leading to hypocalcemia and hypoparathyroidism in mice treated with CC-325.

Dose Preparation and Administration

CC-325

The oral route of administration was chosen because it is the intended human therapeutic route. Dosing formulations of CC-325 was prepared from the bulk powder by mixing with the vehicle according to the procedure below. Based on in-house stability data, CC-325 was stable in 0.5% CMC/0.25% Tween-80 in 50 mM citrate buffer pH 3 up to eight days at 4° - 8°C. Formulations were prepared once on Day -1 for the duration of the study. Formulations were aliquoted to 9 equal volumes for 5 days of daily twice daily (BID) dosing, except Day 5, which was once a day (QD) in the morning. The vehicle or test article formulation was given orally

BID (eight hours apart) daily for up to 5 consecutive days in a dose volume of 10 mL/kg.

Formulation was removed from refrigerator and placed at room temperature approximately 30 minutes prior to dosing. The required volume of vehicle or drug suspension for each animal was based on the most recent individual body weight.

The vehicle and CC-325 formulation was prepared according to the instructions below.

Preparation of 1 liter of 50 mM, pH 3.0 citrate buffer water solution:

1. Weighed out 0.88 g of sodium hydroxide
2. Weighed out 9.605 g of citric acid
3. Dissolved in 1L of HPLC grade water
4. Stir to mixed thoroughly until final solution forms.

Vehicle 1 (0.5% CMC/0.25% Tween-80 in 50 mM citrate buffer pH 3)

1. Placed 300 mL of 50 mM citrate buffer pH 3.0 in a 1 L beaker.
2. Measured out 2.5 g of CMC.
3. Slowly added CMC into 50 mM citrate buffer pH 3.0 while stirring.
4. Added 1.25 mL of Tween-80 into the mixture while stirring.
5. Adjusted the volume to 500 mL
6. Stirred the vehicle very slowly overnight at room temperature until homogeneous.
7. Adjusted the pH to 3.0 with NaOH or HCl.

CC-325 in 0.5% CMC/0.25% Tween-80 in 50 mM citrate buffer pH 3

1. Added 324.69 mg of CC-325 to a homogenizing tube.

2. Added 216.4 mL of 0.5% CMC/0.25% Tween-80 in 50 mM citrate buffer pH 3.0 vehicle to homogenizing tube while vortexing.
3. Homogenized the formulation using a Teflon pestle and mortar (Potter-Elvehjem tissue grinder).
4. Sonicated the formulations for 1 minute.
5. Final pH was recorded
6. Vortexed the formulations prior to dosing each animal.

NPS 2143

The oral route of administration was chosen because in published studies (Fox et al., 1999; Gowen et al., 2000; Hannan et al., 2015; Nemeth et al., 2001). Formulations of NPS 2143 will be prepared from the bulk powder by mixing with the vehicle according to the procedure below. Formulations was prepared on dosing day. The vehicle or test article formulation was given orally a dose volume of 5 mL/kg. The required volume of vehicle or drug solution for each animal was based on the most recent individual body weight.

The vehicle and NPS 2143 formulations were prepared according to the instructions below.

Vehicle 2: Aqueous 15% HP β CD (100 mL preparation)

1. Placed 15 g of HP β CD in a glass screw cap bottle.
2. Added 90 mL of HPLC grade water.
3. Stirred to mix thoroughly until final solution forms.
4. QS to 100 mL

NPS 2143 in 15% HP β CD

1. Added 75.00 mg of NPS 2143 to a small glass screw cap bottle.
2. Added 3 mL of 15% HP β CD vehicle to the bottle.
3. Vortexed for 1 minutes.
4. Sonicated the formulations for 1 minute.
5. Vortexed the formulations prior to dosing each animal.

Dose levels and dose concentrations are listed in Table 9.

Table 9.

Drug Preparation Concentrations and Administered Doses.

For Testing Hypothesis	Group	Treatment	Dose Level (mg/kg)	Total daily Dose (mg/kg)	Target Drug Concentration Free Base (mg/mL)	Formulation Concentration Salt Form (mg/mL)
Toxicological Assessment Groups (Tox)						
Control Group	1	Vehicle 1	0	0	0	0
		Vehicle 2	0	0	0	0
2,3	2	CC-325	15	30	1.5	1.5
		Vehicle 2	0	0	0	0
Baseline assessment	3	Vehicle 1	0	0	0	0
		NPS 2143	120	120	24	24.96
1,2,3,4	4	CC-325	15	30	1.5	1.5
		NPS 2143	120	120	24	24.96
Toxicokinetics Groups (TK)						
TK assessment only	5	CC-325	15	30	1.5	1.5
		Vehicle 2	0	0	0	0
TK assessment only	6	Vehicle 1	0	0	0	0
		NPS 2143	120	120	24	24.96
TK assessment only	7	CC-325	15	30	1.5	1.5
		NPS 2143	120	120	24	24.96

Note. Vehicle 1 = 0.5% CMC/0.25% Tween-80 in 50 mM citrate buffer pH 3

Vehicle 2 = Aqueous 15% (2-Hydroxypropyl)- β -cyclodextrin (HP β CD)

Formulation Analysis

Before dosing the toxicological assessment and TK animals on Day 5, two (2) aliquot of 200 μ L were taken from the middle portion of CC-325 and NPS 2143 formulations using positive displacement pipetting for accurate volume. Bubbles adhering to the side of the tip were wiped off prior to dispensing to the tubes. The aliquots were stored at -80° C, however the formulation analysis was not performed for this study because adequate exposures were achieved.

Experimental Groups

Male huCRBN KI mice were assigned to experimental groups as shown in Table 10, and were treated according to the schedule below. There were seven treatment groups in this experiment. In previous in-house studies, treatment with test article CC-325 resulted in serum calcium decrease at different dose concentrations and duration, including 15 mg/kg BID for 5 consecutive days of doing. In this experiment, the dose of 15 mg/kg BID for 5 days has been selected; this dose is expected to induce hypocalcemia without overt toxicity.

The test article, NPS 2143 dose was selected based on the in-house pilot study with NPS 2143. In that study, we dose NPS 2143 at 50 mg/kg, however, the decrease in serum calcium was minimal; therefore, the dose of 200 mg/kg was selected for this study. However due to a calculation error during formulation preparation, the formulation was prepared at 24 mg/mL or 120 mg/kg.

Pharmacokinetic measurement when performed in the context of toxicology study is referred to as Toxicokinetic. Toxicokinetic Groups (Groups 5-7) were included in this experiment to measure the concentration of each test article in respective treatment groups.

Group 1: Animals in Group 1 were dosed with vehicle 1, 0.5% CMC/0.25% Tween-80 in 50 mM citrate buffer pH 3, for 5 days. On the morning of Day 5, these animals also were treated with vehicle 2, Aqueous 15% (2-Hydroxypropyl)- β -cyclodextrin (HP β CD). This Group represented the control group for Groups, 2-4.

Group 2: The animals were treated with CC-325 for 5 days. This Group was designed to measure the effect of CC-325 in serum calcium concentration as a single agent. On the morning of Day 5, the animals were also dosed with a single vehicle 2 (NPS 2143 vehicle), to account for any effect vehicle 2 might have in mice.

Group 3: The animals in Group 3 were treated with NPS 2143 once. On Day 5, mice were treated with vehicle 1 and one hour later with NPS 2143. The single dose of NPS 2143 was dosed on Day 5 to keep the sample collection and analysis consistent. Group 3 was designed to measure the effects of NPS 2143 as a single agent in this experiment.

Since CC-325 and NPS 2143 had never been dosed as a combination, it is important to measure the effects of each test article as a single agent to compare with combination treatment.

Group 4: Combination treatment, test article CC-325 was dosed for 4 consecutive days at 15 mg/kg BID, and on Day 5, CC-325 was dosed in the morning followed by a single dose of 120 mg/kg of NPS 2143. CC-325 was expected to decrease serum calcium, while NPS 2143 was expected to increase the serum calcium by stimulating PTH production. This group was designed to test hypotheses 1-4, while Group 1 was serving as the vehicle control and Groups 2-3 were to evaluate the single agent effects.

Table 10:

Details of Experimental Groups.

Group	Animal Numbers	Treatment	Dose Level (mg /kg)	Total Daily Dose (mg/kg)	Dosing Day(s)
Group 1	1001-1025	Vehicle 1	0	0	1-5
		Vehicle 2	0	0	5
Group 2	2001-2025	CC-325	15	30	1-5
		Vehicle 2	0	0	5
Group 3	3001-3025	Vehicle 1	0	0	5
		NPS 2143	120	120	5
Group 4	4001-4025	CC-325	15	30	1-5
		NPS 2143	120	120	5
Group 5	5001-5006	CC-325	15	30	1-5
		Vehicle 2	0	0	5
Group 6	6001-6006	Vehicle 1	0	0	5
		NPS 2143	120	120	5
Group 7	7001-7006	CC-325	15	30	1-5
		NPS 2143	120	120	5

Note. Vehicle 1 = 0.5% CMC/0.25% Tween-80 in 50 mM citrate buffer pH 3

Vehicle 2 = Aqueous 15% (2-Hydroxypropyl)- β -cyclodextrin (HP β CD)

Treatment Descriptions

Group 1: Animals were dosed Days 1-4 BID and in the morning of Day 5 with vehicle 1; one hour after vehicle 1 dose administration, vehicle 2 was dosed.

Groups 2 and 5: Animals were dosed Days 1-4 BID and in the morning of Day 5 with CC-325; one hour after CC-325 dose administration, vehicle 2 was dosed.

Groups 3 and 6: Animals were dosed with vehicle 1 on Day 5; one hour after vehicle 1 administration, NPS 2143 was dosed.

Groups 4 and 7: Animals were dosed Days 1-4 BID and in the morning of Day 5 with CC-325; one hour after CC-325 administration, NPS 2143 was dosed. Predose collection was prior to CC-325 administration for Group 7.

Table 11 below provides the schedule of treatment and collection time; all samples were collected at necropsy.

Table 11.

Schedule of Blood and Tissue Collection from Toxicological Assessment Groups.

Treatment Group	0-hr* Day 5	2-hr postdose Day 5**	4-hr postdose Day 5**	6-hr postdose Day 5**	24-hr postdose Day 5**
Group 1	1001-1005	1006-1010	1011-1015	1016-1020	1021-1025
Group 2	2001-2005	2006-2010	2011-2015	2016-2020	2021-2025
Group 3	3001-3005	3006-3010	3011-3015	3016-3020	3021-3025
Group 4	4001-4005	4006-4010	4011-4015	4016-4020	4021-4025
n	20	20	20	20	20

Note. All timepoints were terminal, thyroid/parathyroid and kidney were collected from all animals. *= Post CC-325 dose and pre NPS 2143 dose on Day 5; **= Post NPS 2143 dose.

Measurement Procedures

Clinical observations

All animals were observed for clinical signs pre-dose and approximately 1 hour after the end of each oral administration on dosing day and prior to necropsy. All observations were recorded directly into electronic data capturing system.

Body weights

Body weights of all animals were recorded once prior to initial dosing and daily during the dosing days.

Clinical laboratory tests

Serum chemistry parameters were evaluated in all surviving animals on scheduled and unscheduled necropsy. The method for each blood or serum analysis is described in Table 12.

Serum Chemistry

At necropsy, 100 μL of whole blood was collected via retro-orbital bleeding into a capillary tube containing Li-heparin for iCa^{2+} , Na^+ , K^+ , pH and Cl^- measurement.

At necropsy, additional 600 μL of blood was collected in a gold top tube with serum separator. Serum was separated within 60 minutes of collection and aliquoted as described below detail of each methodology is described in Appendices A and B.

Aliquot 1: 75 μL of serum for PTH

Aliquot 2: 75 μL of serum for FGF23

Aliquot 3: 100 μL for serum chemistry panel

Aliquot 4: Backup sample

Table 12:

Blood/Serum Chemical Analyses Performed and Methods of Each Analysis.

Analyte	Analytical Method	Full Detail in Appendix
iCa^{2+} Na^+ K^+ Cl^- pH	Ion-Selective Electrode (ISE)	A
Ca^{2+} Mg^{2+} Phosphate Albumin Total Protein	Colorimetric	B
FGF23	ELISA	C
Parathyroid Hormone	ELISA	D

Serum Chemistry Panel (Axcel Analyzer)

On sample analysis day, all samples were thawed on wet ice and transferred to prelabeled sample cup for analysis. Calibration and quality control were performed for the assays on the Axcel clinical chemistry analyzer. Upon verification and acceptance of control results, serum samples were loaded and run for the selected analytes listed in Table 13. All serum chemistry samples were analyzed in the same run and on the same day.

Table 13:

Serum Chemistry Panel on Axcel Analyzer.

Serum Samples	Analyzer	Parameters
All samples from Groups 1-4	Axcel	Albumin, Calcium, Phosphate, Magnesium, Total protein, Globulin1

Note. 1 = Calculated

Toxicokinetics

Toxicokinetics provided the data related to exposure of mice to each test article. There were 3 toxicokinetic groups in this study. Toxicokinetic Groups 5, 6, and 7 were designed to measure the concentration of CC-325, NPS 2143, and combination of CC-325 and NPS 2143 in mice, respectively. It was important to evaluate whether the concentration of CC-325 had an effect on concentration of NPS 2143 or vice versa. Toxicokinetic measurements were also important, particularly when there was unexpected pharmacokinetics effects, which could be due to drug-drug interaction.

Blood samples (approximately 0.15 mL) were collected manually by retro-orbital bleeding from TK animals at 0, 1.5, 3, 5, 9, and 24 hours post CC-325 treatment in Groups 5 and 7, the same timepoints were collected from NPS 2143 only treatment group, Group 6 on Day 5.

Dosing the CC-325 on the morning of Day 5 triggered the timepoints for all TK groups. The NPS 2143 was dosed exactly 1-hr post CC-325 dose. Table 14 below shows the bleeding assignment for each TK animal.

Table 14:

Assigned Timepoints for Toxicokinetic Assessment Animals.

TK Day 5			Time Points (hour)					
Group	Treatment	Animal #	0	1.5	3	5	9	24
5	CC-325 15 mg/kg	5001-5003	√		√		Terminal	
		5004-5006		√		√		Terminal
6	NPS 2143 200 mg/kg	6001-6003	√		√		Terminal	
		6004-6006		√		√		Terminal
7	CC-325 15 mg/kg NPS 2143 200 mg/kg	7001-7003	√		√		Terminal	
		7004-7006		√		√		Terminal

Blood samples were collected into a chilled tube containing K₂EDTA as an anticoagulant. Samples were placed on wet ice and were protected from light until they were spun down at 3000 rpm for 8 minutes to separate plasma. Within 0.5-hr of whole blood collection, plasma was separated by centrifugation at 2-8°C. The TK samples for each timepoint were aliquoted according to Table 15.

Table 15.

Serum Aliquoting For Toxicokinetics Analysis.

Group	Test Article	Aliquot 1	Aliquot 2
5	CC-325	A	A
6	NPS 2143	B	B
7	CC-325	A	----
	NPS 2143	----	B

Note. A: Stabilized with Sorenson's buffer. B: Neat plasma

To stabilize with Sorenson's buffer after plasma separation, an accurate volume of plasma was transferred to a cryovial and stabilized with an equal volume (1:1) of 25 mM Sorenson's buffer (pH 1.5) and were mixed by vortexing.

All sample were frozen within 1 hour of whole blood collection in a freezer set to maintain -80°C . Plasma samples were stored frozen at $\leq -80^{\circ}\text{C}$ until submitted to the drug metabolism and pharmacokinetics (DMPK) Department, Bristol Myers Squibb, San Diego, CA. Plasma samples were analyzed for concentration of CC-325 and NPS 2143 by an LC-MS/MS method. Maximum concentration (C_{max}), Time of maximum concentration (T_{max}) and area under the concentration-time curve (AUC) were calculated.

Preparation of Sorenson's buffer:

Buffer A: 2 M Citric Acid in H_2O

To prepare 25 mL of 2 M citric acid solution in H_2O , dissolve 10.5 g of citric acid monohydrate (MW: 210.14) into 25 mL of purified H_2O . Mixed well and sonicated for approximately 5 minutes and stored solution at $2-8^{\circ}\text{C}$.

Buffer B: 0.1 M Sodium Citrate Tribasic Dihydrate

Exactly 1.47 g of sodium citrate tribasic dihydrate (MW: 294.0) was dissolved into 50 mL of deionized H_2O . Sonicated for 1 minute and stored at room temperature.

Preparation of Sorenson's Citrate Buffer pH 1.5

Exactly 580 mL of deionized H_2O was added to 7.0 mL of Buffer A, 10.5 mL of Buffer B, and 2.1 mL of concentrated hydrochloric acid (12 M). The pH was adjusted to 1.5 with HCl. Mixed well and stored at $2-8^{\circ}\text{C}$

Euthanasia

All animals were anesthetized with isoflurane, blood was collected and then mice were sacrificed via cervical dislocation.

Pathology

Pathology evaluation consisting of gross findings and tissue collections were performed at scheduled necropsy.

Histopathology

The list of tissues that were collected at necropsy for microscopic, IHC, and ISH examination are listed in Table 16.

Table 16.

Necropsy Tissue Collection List

Thyroid/parathyroid
Kidneys

Tissues were fixed in 10% buffered formalin. Thyroid/parathyroid gland was sectioned and stained with hematoxylin and eosin and examined microscopically. Kidneys were blocked and save for possible future analysis; however, no analysis was performed on the kidneys.

Hematoxylin & Eosin (H&E) Staining

Collected wet tissues were fixed in 10% neutral buffered formalin (NBF) and shipped to Experimental Pathology Laboratory (EPL). At EPL, the fixed wet tissues were either trimmed to < 0.5 cm or submitted whole as received (e.g., thyroid/parathyroid) into embedding cassettes and then transferred to 10% NBF until processing. All tissues were placed on a Tissue-Tek VIP processor and processed to paraffin using EPL's standard program for small animal tissues. Tissues were embedded into paraffin blocks using the Tissue-Tek embedding center. Tissues then were sectioned at 4 microns and mounted onto C&A Scientific Premiere slides in a water

(tap) bath. H&E staining was performed using a Hacker Linear Stainer, and slides were coverslipped using a Hacker Coverslipper.

Immunohistochemistry

Immunohistochemistry analysis of GSTP1 and PTH in the parathyroid glands were performed on the tissues collected at scheduled necropsy.

Immunohistochemistry (IHC) was performed on the Bond-III automated slide Stainer (Leica Microsystems, Buffalo Grove, Illinois) using the Bond Polymer Refine Detection system (Leica Microsystems, DS9800). Formalin fixed paraffin embedded (FFPE) tissues were sectioned at four-micron thickness and deparaffinized at 72°C on the Bond instrument. Antigen retrieval was performed with Epitope Retrieval 2 (ER2, pH 9.0) for 20 min at 100°C. Besides antigen pretreatment, all other staining procedures were conducted at room temperature. The slides were first blocked with Peroxide Block for 5 minutes, and then incubated with primary antibodies for 15 min. Post Primary and horseradish peroxidase (HRP) labeled Polymer were incubated at the instrument's default conditions using the Refine Detection System. Antigen-antibody complex was visualized with hydrogen peroxide substrate and diaminobenzidine tetrahydrochloride (DAB) chromogen for 10 min. Slides were then counterstained with hematoxylin for 5 min, dehydrated and coverslipped by the Tissue-Tek Film Automated Coverslipper.

***In Situ* hybridization**

In situ hybridization was performed for PTH mRNA in parathyroid gland. A fully automated ISH assay was performed on Leica BOND RX IHC & ISH Stainer with the RNAscope® 2.5 LSx Reagent Kit-RED (ACD, cat# 322750). Formalin fixed paraffin embedded (FFPE) rabbit embryos were sectioned at four micron thickness, baked at 60°C for 1 hour and

then deparaffinized in Dewax solution at 72°C. Antigen retrieval was performed in RNAscope 2.5 LSx Target Retrieval for 15 min at 95°C, followed by RNAscope 2.5 LSx Enzyme treatment for 15 min at room temperature. Custom-designed target probes was applied on the slides and hybridized at 42°C for 2 hours. Specific signals were then amplified using the default procedures of ACD ISH protocol. Slides were then rinsed in tap water and baked at 60°C oven for 20 min or until dry, and coverslipped using Tissue-Tek Film Automated Coverslipper.

Statistical Analysis

Statistical analysis of quantitative clinical laboratory data was conducted by data capturing and analysis system. In this experiment, for analysis of variance, a Two-way ANOVA was performed followed by Dunnett's multiple comparison test with a single pooled variance as post hoc analysis. Cochran and Cox Test was performed for nonparametric data.

Analytical Methods and Instrumentation

Table 17 lists the analytical method and the analyzer for each analyte measured in this experiment.

Table 17.

Description of Each Analytical Method and Corresponding Analyzer.

Analyte	Analytical Method	Analyzer	Manufacturer
iCa ²⁺ Na ⁺ K ⁺ Cl ⁻ pH	Ion-Selective Electrode (ISE)	Stat Profile PRIME CCS Analyzer	Nova biomedical
Ca ²⁺ Mg ²⁺ Phosphate Albumin Total Protein	Colorimetric	Axcel	Alfa Wassermann
Parathyroid Hormone	ELISA	N/A	Quidel Biomedical
FGF23			Quidel Biomedical

Image analysis:

After pathologist review and QC, slides were scanned using Aperio AT2 scanner (Leica Microsystems) at 20x for IHC stained slides or 40x for ISH stained slides. Images were sorted in Halolink and parathyroid of each sample was manually annotated with exclusion of the folding regions. Total area measurement and number of positive cells for each marker were digitally analyzed and H-scores were calculated using HALO software (Indica Lab). Final scores range for IHC was from 0 to 300, and for ISH from 0 to 400. H-scores were the sum of the products of percent of positively stained cells and intensity of staining to account for 100% of the cells analyzed [H-score = (% at 1+) X 1 + (% at 2+) X 2 + (% at 3+) X 3].

Protocol Deviation:

This experiment was conducted according to the method described above, however, there was one deviation in this experiment, which was the unintentional change in NPS 2143 dose from 200 mg/kg to 120 mg/kg. This deviation was due to miscalculation during the formulation

preparation; the actual administered dose was 120 mg/kg. The impact of this deviation was minimal because the elevation in serum PTH in mice in this experiment was even higher than the increase in serum PTH in mice in the pilot study, which used the dose of 200 mg/kg.

A detailed schedule of dose administration for all treatment groups is listed in Table 18. The vehicle and test article CC-325 were administered for four consecutive days, on Day 5, CC-325 was administered first (Group 2 and 4) and exactly 1 hour later NPS 2143 was administered (Group 3 and 4).

Table 18.

Schedule of Dosing for All Treatment Groups.

		Group 1	Group 2	Group 3	Group 4
Treatment	Time*	Vehicle	CC-325	NPS 2143	CC-325 + NPS 2143
Dose mg/mL		0	30 mg/kg/day	120 mg/kg/day	30 mg/kg/day CC-325 120 mg/kg/day NPS 2143
Treatment	Day 1	QD am	BID	ND	BID CC-325
	Day 2	QD am	BID	ND	BID CC-325
	Day 3	QD am	BID	ND	BID CC-325
	Day 4	QD am	BID	ND	BID CC-325
	Day 5	QD am	QD am only	QD am	QD am CC-325 One hour later NPS 2143 was dosed.

Note. * = Time is based on the NPS 2143 dose, QD = Once a day; am = morning; BID = twice a day; ND = Not Dosed

CHAPTER FOUR: RESULTS

Prior to conducting the main study to test the hypotheses, a pilot study was conducted. The purpose of the pilot study was twofold, first to select the appropriate dose of NPS 2143 for the main study and second, measure the range of iCa^{2+} and PTH response to a potent positive (NPS 2143) and negative (NPS R-568) allosteric modulator of CaSR. The abbreviated protocol for the pilot study is listed in Appendix E. Only the pilot data relevant to this dissertation is discussed in this section.

In Group 2, treatment with NPS R-568 resulted in significant decrease in iCa^{2+} and PTH during the 1-, 2- and 4-hr time points. Changes in electrolytes and total protein were minimal and not biologically relevant. At 4-hr postdose, minimal decrease in magnesium and moderate increase in phosphate were observed, which were consistent with moderate decrease in iCa^{2+} (Figure 7, Table 19 and Table 20).

In Group 3, treatment with NPS 2143 resulted in significant increase in iCa^{2+} and PTH, which started at 1-hr postdose and lasted until the last collection at 4-hr postdose. At 2-hr postdose, a minimal increase in magnesium was observed, a decrease in phosphate was observed at 4-hr post dose. These changes were consistent with moderate increase in iCa^{2+} during this period (Figure 7 & Figure 8, Table 19 and Table 20).

As detailed in Chapter 2, treatment with NPS 2143 causes a decrease in sensitivity of CaSR, which results in increase of serum calcium by increasing PTH. In Group 3, NPS 2143 treatment caused significant increases in PTH and iCa^{2+} at 1-, 2-, and 4-hr postdose when compared with vehicle control (Figure 7, Figure 8, Table 19 and Table 20). In this group, PTH peaked at 2-hr postdose while iCa^{2+} peaked at 4-hr postdose, indicating that an increase in PTH caused an increase in iCa^{2+} and a decrease in PTH at 4-hr will likely result in decrease in iCa^{2+} at

timepoints beyond 4 hours. The concentrations of iCa^{2+} and its corresponding serum PTH for each timepoint is shown in Figure 9. Based on these data, the dose of 200 mg/kg and timepoints of 0, 2, 4, 6, and 24-hr postdose were selected for the main study.

Figure 7.

Mean (\pm SD) iCa^{2+} in huCRBN KI mice treated with vehicle, NPS R-568, or NPS 2143.

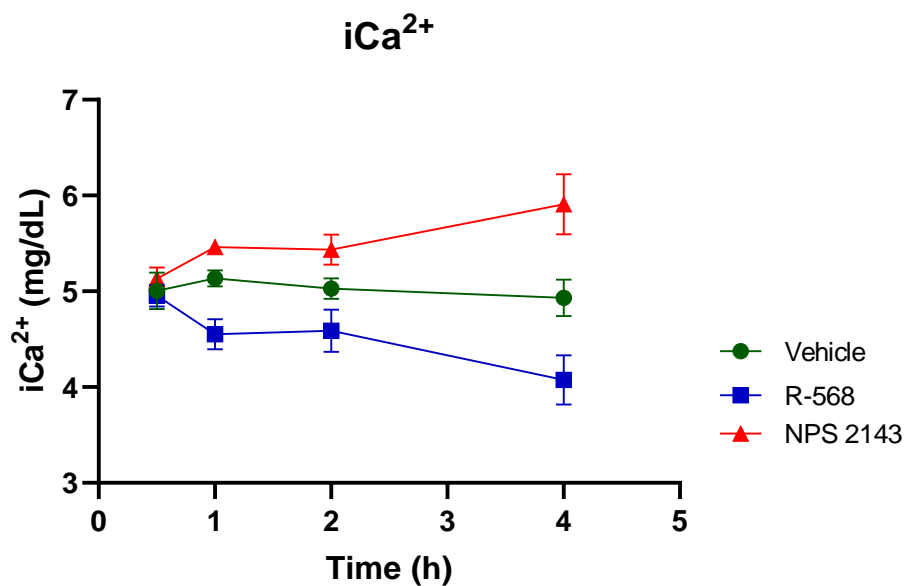


Figure 8.

Mean (\pm SD) PTH in huCRBN KI mice treated with vehicle, NPS R-568, or NPS 2143.

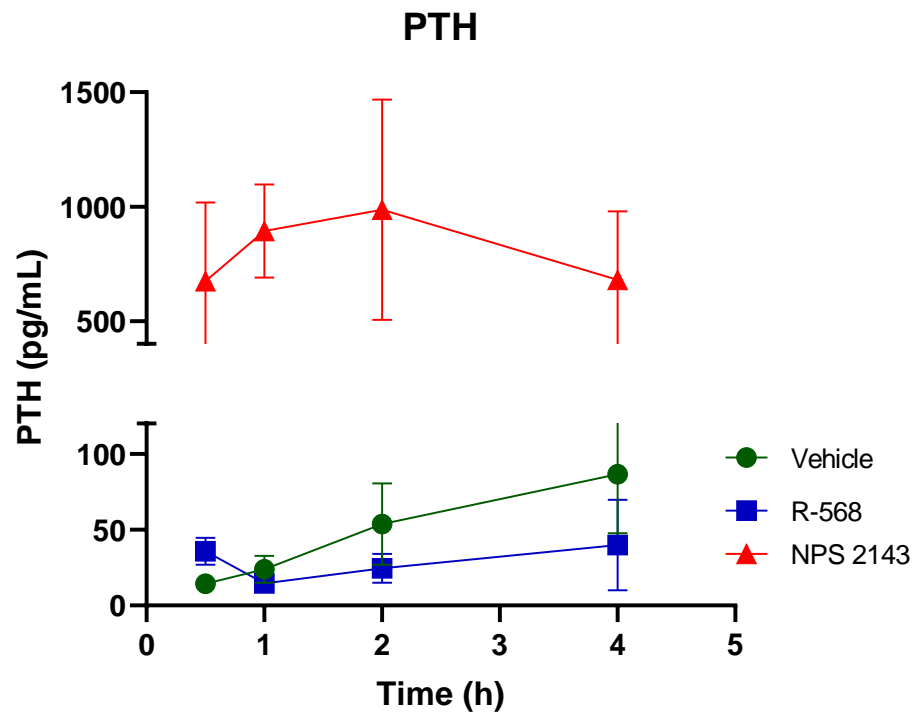


Figure 9.

Mean (\pm SD) iCa^{2+} in relation to PTH in huCRBN KI mice treated with vehicle, NPS R-568, or NPS 2143.

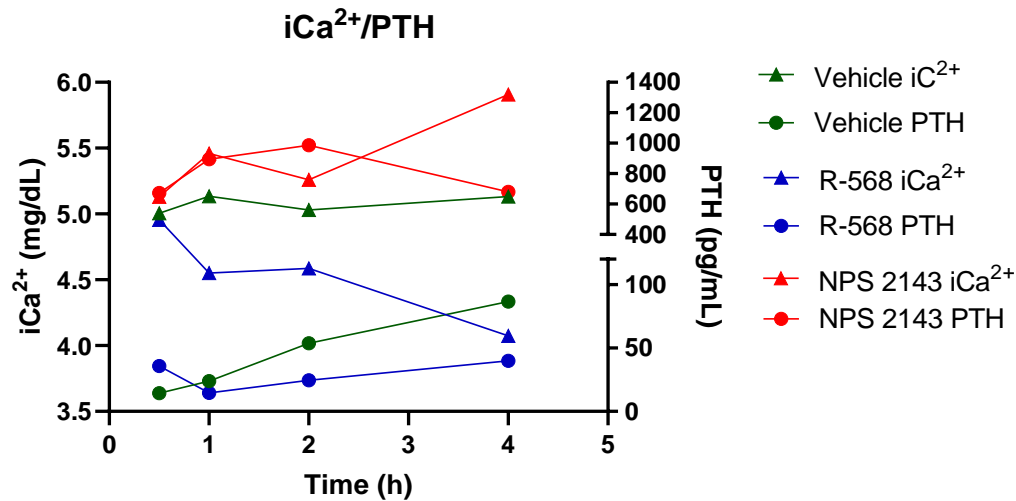


Table 19.

Serum Chemistry Results from Stat Prime Profile for All Treatment Groups.

Analyte	Time	Group 1	Group 2	Group 3
		Vehicle	NPS R-568	NPS 2143
iCa ²⁺ (mg/dL)	0.5-hr	5.01	4.96	5.13
	1-hr	5.14	4.55****	5.46*
	2-hr	5.03	4.58**	5.44**
	4-hr	4.94	4.07****	5.91****
PTH (pg/mL)	0.5-hr	14.34	35.74	673.80****
	1-hr	23.84	14.66	894.10****
	2-hr	53.81	24.51	985.90****
	4-hr	86.55	39.92	679.80***
Na ⁺ (mmol/L)	0.5-hr	143.4	145.8**	145.2*
	1-hr	142.8	144.2	145.5**
	2-hr	142.2	141.3	143.6
	4-hr	146.4	141.8****	146.2
K ⁺ (mmol/L)	0.5-hr	4.77	3.92**	4.53
	1-hr	4.71	4.60	4.50
	2-hr	4.54	4.52	4.77
	4-hr	4.80	5.14	4.83
Cl ⁻ (mmol/L)	0.5-hr	110.4	112.0*	110.8
	1-hr	112.2	111.4	110.4*
	2-hr	110.6	109.2*	109.6
	4-hr	112.0	110.2	110.8

Note. * = p≤ 0.05; ** = p≤ 0.01; *** = p≤ 0.001; **** = p≤ 0.0001

Table 20.

Whole Blood Chemistry Data from Stat Profile Prime for All Treatment Groups.

Analyte	Time	Group 1	Group 2	Group 3
		Vehicle	CC-325	NPS 2143
Albumin (g/dL)	2-hr	2.92	2.96	2.80
	4-hr	2.98	2.96	2.90
Mg ²⁺ (mg/dL)	2-hr	2.82	2.92	3.28*
	4-hr	2.90	2.42*	2.88
Phosphate (mg/dL)	2-hr	7.56	8.04	11.24****
	4-hr	9.24	12.16***	7.72
Total Protein (g/dL)	2-hr	4.36	4.68*	4.46
	4-hr	4.64	4.60	4.50

Note. * = $p \leq 0.05$; ** = $p \leq 0.01$; *** = $p \leq 0.001$; **** = $p \leq 0.0001$

Interference studies for further assay validation

In order to evaluate the effect of CC-325 and NPS 2143 on the quantification of PTH and FGF23 by ELISA assays, each ELISA assay was evaluated for such interference. Serum from naïve mice was pooled and spiked with different concentration of CC-325 or NPS 2143. An ELISA run for each analyte was performed. The detail of this interference study is described below.

ELISA kits

The lot and expiration date for PTH and FGF23 ELISA kits are listed in Table 21 below, and these lots were used for all PTH and FGF23 sample analysis in this dissertation. Since the control values for each kit were lot specific, the lot numbers were recorded carefully. The manufacturer of both kits was Quidel Corporation.

Table 21.

Control Values for PTH and FGF23 ELISA kits.

	PTH	FGF23
Reference No.	60-2305	60-6800
Lot No.	161535	163846
Expiration Date	09/30/2020	11/11/2020
Control I Range	46-76	58-97
Control II Range	140-234	166-277

Sample preparation

Blood from naïve huCRBN KI mice was collected and serum was separated and pooled. Since the maximum concentration (C_{\max}) of test articles in huCRBN KI mice was not known, the highest concentration of 20 μM was selected for each test article. To prepare the highest concentration of CC-325 stock solution, 1.693 mg of CC-325 was spiked into 5 mL of DMSO, and then vortexed for 3 minutes to dissolve the compound. To prepare the highest concentration of NPS 2143 stock solution, 1.709 mg of NPS 2143 was spiked into 5 mL of DMSO, and then also vortexed for 3 minutes to dissolve the compound. To prepare the serial dilutions for the interference assay, 1 μL of stock solution was added to 39 μL of naïve mouse serum, which resulted in 8468.4 ng/mL of CC-325 (20 μM) or 8547.6 ng/mL of NPS 2143 (20 μM) in respective vials. A 1:2 serial dilution of DMSO stock was performed and 1 μL of each dilution was added to 39 μL of the naïve mouse serum to obtain the concentrations listed in Table 22, below.

Table 22.

Parathyroid Hormone ELISA Plate Format for CC-325 and NPS 2143 Interference Testing.

	Column 1 & 2	Column 3 & 4	Column 5 & 6
A	Blank	N-serum	N-serum
B	Standard 1	N-serum + DMSO	N-serum + DMSO
C	Standard 2	N-serum 20 μ M CC-325	N-serum 20 μ M NPS 2143
D	Standard 3	N-serum 10 μ M CC-325	N-serum 10 μ M NPS 2143
E	Standard 4	N-serum 5 μ M CC-325	N-serum 5 μ M NPS 2143
F	standard 5	N-serum 2.5 μ M CC-325	N-serum 2.5 μ M NPS 2143
G	Control 1	N-serum 1.25 μ M CC-325	N-serum 1.25 μ M NPS 2143
H	Control 2	N-serum 0.6125 μ M CC-325	N-serum 0.6125 μ M NPS 2143

Note. N-serum = naïve serum.

PTH assay

Plate setup and PTH assay data are shown in Table 22 and Table 23, respectively. A standard curve was prepared to measure the controls and unknown values, Figure 10.

Both control I and II were within the manufacturer established range. To measure the impact of DMSO on the PTH assay, data from wells with naïve serum + DMSO (B3-4) were compared with wells with naïve serum only in A3-4. Similar calculation was done for FGF23 column. (B5-6 and A5-6). The DMSO had a negative effect on the concentration of PTH and FGF23 of above 12-14%, as shown in Table 23. To further measure the impact of test articles on PTH assay, the results from each well was compared with the naïve serum + DMSO well. Percent changes for each concentration are listed in Table 23.

Figure 10.

Standard curve for PTH assay

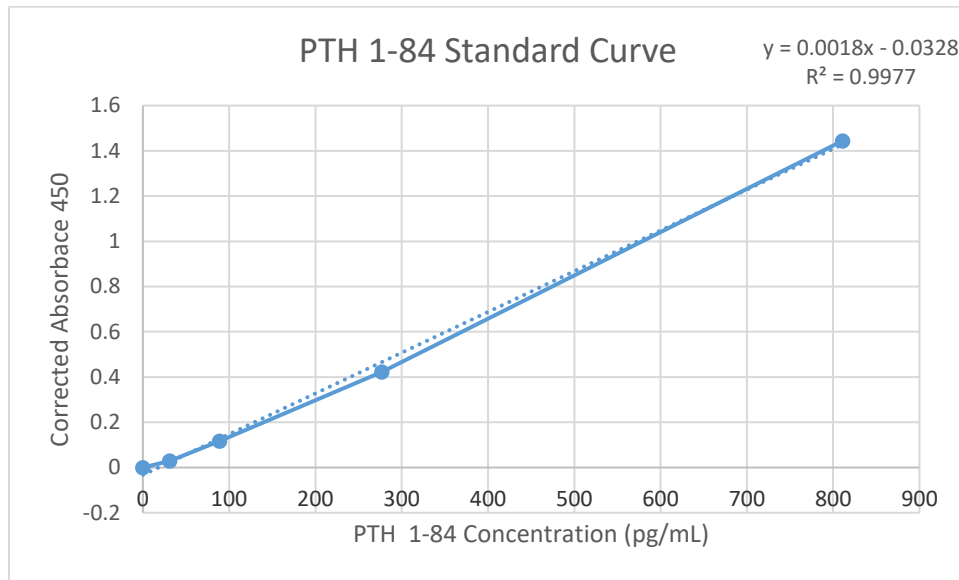


Table 23.

The PTH ELISA Results for CC-325 and NPS 2143 Interference Testing.

	Mean Value Well 1 & 2	Mean Value Well 3 & 4	Mean Value Well 5 & 6
A	Blank	46	41.778
B	Standard	40 (-13.6)1	37 (-12.2)1
C	Standard	36 (-8.5)2	35 (-4.9)2
D	Standard	37 (-6.6)2	35 (-4.4)2
E	Standard	37 (-5.5)2	35 (-4.9)2
F	Standard	38 (-3.1)2	36 (-1.1)2
G	66	42(7.1)2	39 (5.1)2
H	175	39 (-2.2)2	35 (-4.6)2

Note. () indicates percent change; 1= percent change from N-serum; 2 = percent change from N-serum + DMSO.
Control I range: 46-76; Control range II: 140-234.

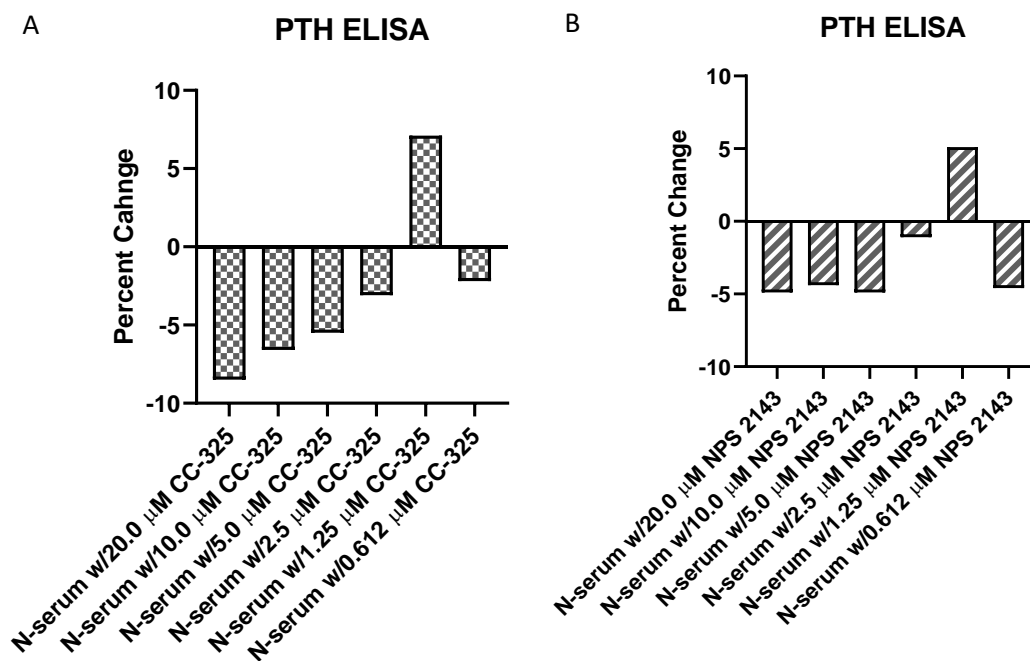
The effect of CC-325 on PTH assay was dose dependent, with the maximum and minimum decreases in PTH concentrations observed at the highest and lowest concentration of CC-325, respectively, Figure 11. The 1.25 μ M concentration of CC-325 caused an increase of 5% in

PTH, and overall, the concentrations of $\leq 2.5 \mu\text{M}$ had minimal impact on measuring serum PTH measurement. Based on the information in package insert the inter-assay coefficient of variation is 5.7% for low concentrations (60 pg/mL) and 5.4% for high concentrations (209 pg/mL).

The effect of NPS 2143 on PTH assay was not dose dependent and maximum decrease in PTH concentration was limited to $< 5\%$, which was measured at 0.612, 5.0, 10, and 20.0 pg/mL. An increase of 5% in concentration of PTH was observed at 1.25 μM , Figure 11. The inconsistency in direction and magnitude of change at concentrations of $\leq 2.5 \mu\text{M}$ made it difficult to assess the impact of NPS 2143 on PTH measurement at these low concentrations. However, the overall data suggests the impact of NPS 2143 in PTH concentration is within the established coefficient of variation.

Figure 11.

Percent change in serum PTH measurement from target value (naïve serum) due to CC-325 (A) and NPS 2143 (B) concentrations in serum.



FGF23 assay

Plate setup for FGF23 assay is shown in Table 24. A standard curve was made to measure the controls and unknown values, Figure 12.

Table 24.

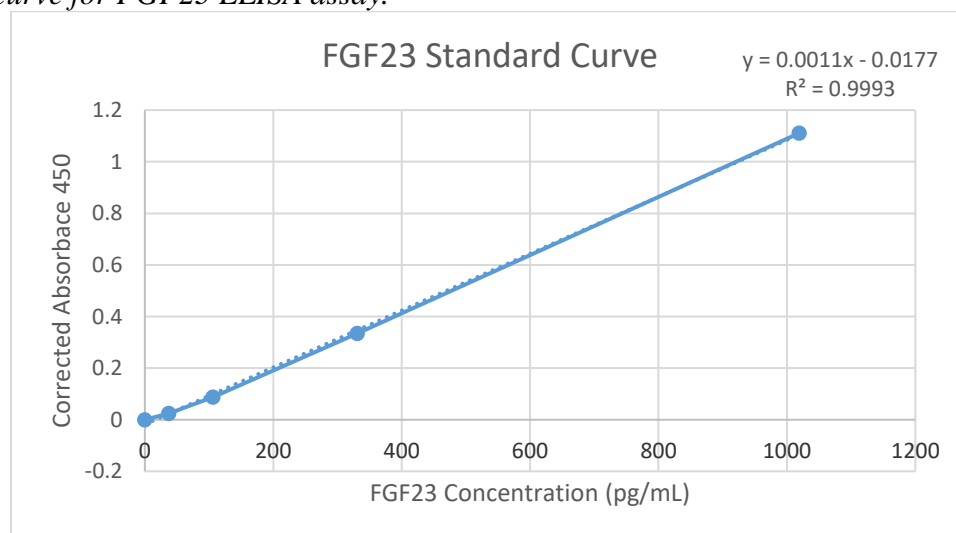
Fibroblast Growth Factor-23 ELISA Plate Format for CC-325 and NPS 2143 Interference Testing.

	Well 1 & 2	Well 3 & 4	Well 5 & 6
A	Blank	N-serum	*
B	Standard 1	N-serum + DMSO	*
C	Standard 2	N-serum 20 μ M CC-325	N-serum 20 μ M NPS 2143
D	Standard 3	N-serum 10 μ M CC-325	N-serum 10 μ M NPS 2143
E	Standard 4	N-serum 5 μ M CC-325	N-serum 5 μ M NPS 2143
F	standard 5	N-serum 2.5 μ M CC-325	N-serum 2.5 μ M NPS 2143
G	Control 1	N-serum 1.25 μ M CC-325	N-serum 1.25 μ M NPS 2143
H	Control 2	N-serum 0.6125 μ M CC-325	N-serum 0.6125 μ M NPS 2143

Note. *= Due to insufficient volume of naïve serum; data from A3-4 was used for A5-6 and data from B3-4 was used for B5-6. N- Serum is naïve serum.

Figure 12.

Standard curve for FGF23 ELISA assay.



Both control I and II were within the manufacturer established range. To measure the impact of DMSO on the FGF23 assay, data from naïve serum + DMS (B3-4) were compared with data from Naïve serum alone (A3-4). The addition of DMSO to naïve serum had a negative impact on the concentration of FGF23 in serum, which was measured at 1.5% (Table 25). To further measure the impact of test articles on FGF23 assay, the result from each well was compared with well with N-serum + DMSO. Percent changes for each concentration are listed in Table 25.

Table 25.

The FGF23 ELISA Results for CC-325 and NPS 2143 Interference Testing

	Mean Value Well 1 & 2	Mean Value Well 3 & 4	Mean Value Well 5 & 6
A	Blank	118	118*
B	Standard	116 (-1.5)1	116 (-1.5) *1
C	Standard	107 (-8.0)2	97 (-16.7)2
D	Standard	109(-6.0)2	110 (-4.9)2
E	Standard	114 (-1.5)2	111 (-4.3)2
F	Standard	115 (-0.9)2	114 (-1.9)2
G	77	112 (-3.4)2	112 (-3.7)2
H	199	105 (-9.4)2	103 (-11.5)2

Note. () indicates percent change; 1= percent change from N-serum; 2= percent change from N-serum + DMSO. Control I range: 46-76; Control range II: 140-234. * = Due to insufficient volume of naïve serum; data from A3-4 was used for A5-6 and data from B3-4 was used for B5-6.

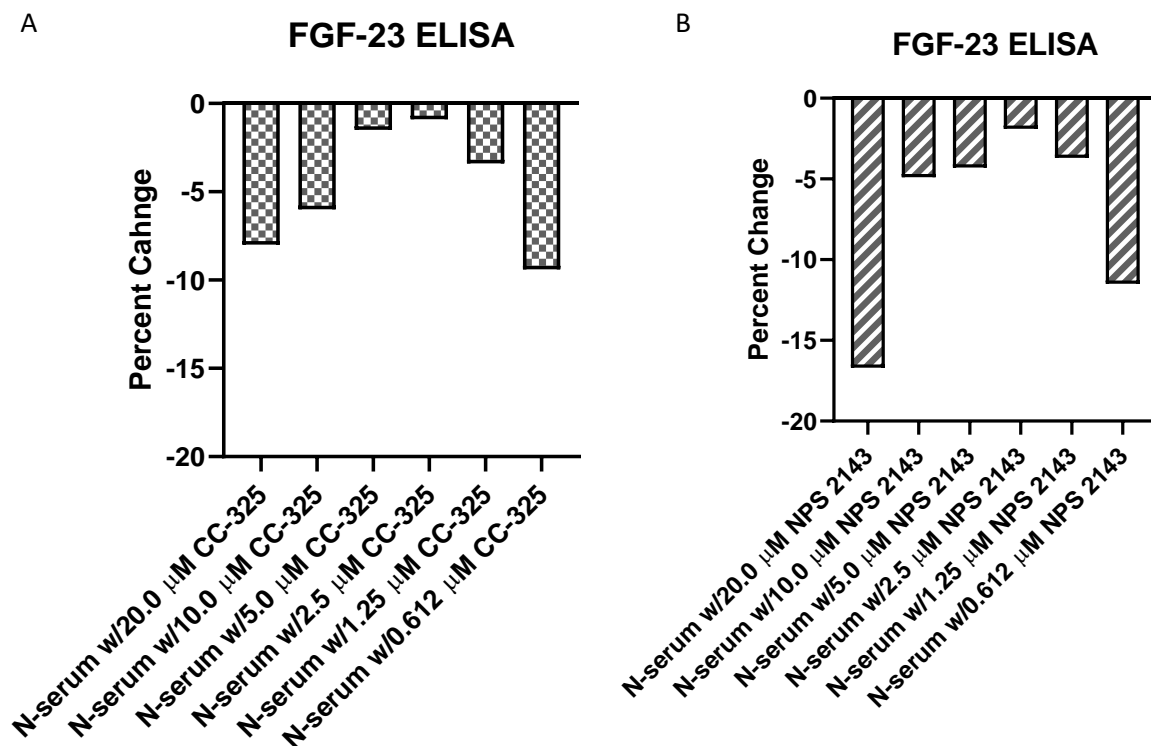
The effect of CC-325 on FGF23 assay was not dose dependent and the maximum decrease in FGF23 concentration was observed at the highest and lowest concentration of CC-325 (Table 25, Figure 13). CC-325 of 2.5 μ M caused the minimum decrease (0.9%) in FGF23 concentration. Overall, there is no conclusive evidence that presence of CC-325 in sample could affect the concentration of FGF23 in serum in a significant way. Based on the

information in package insert the inter-assay coefficient of variation is 4.0% for low (60 pg/mL) and high (167 pg/mL) concentrations.

The effect of NPS 2143 on FGF23 assay was not dose dependent either. The largest change was observed at the highest and lowest concentration of NPS 2143 in the samples. Since the data from wells A&B 3-4 were copied to wells A&B 5-6, respectively, it is possible that additional errors are introduced in column 5-6 calculations. These data show the largest negative change (-17%) at 20 μ M, and the least amount of change at 2.5 μ M (1.9%).

Figure 13.

Percent change in serum FGF23 measurement from target value (naïve serum) due to CC-325 (A) and NPS 2143 (B) concentrations in serum.



Main Study Results

Clinical Observations

All animals survived until scheduled necropsy. A statistically significant decrease in body weight was seen in CC-325 and C-325 + NPS 2143 treatment groups on Days 3-5, when compared with vehicle control group. Animals in Group 4, NPS 2143 alone, were weighed only on Day 5. The change in body weights is shown in Figure 14 and statistical analysis values are listed in Table 26. Raw body weight data is shown in Appendix F. Clinical sign of toxicity was observed in animals treated with CC-325. On Day 4, one animal from Group 2 had hunched posture and another animal from Group 2 and two animals from Group 4 had pilo-erection. On Day 5, one animal from Group 2 and two animals from Group 4 had hunched posture and one animal from each Group 2 and 4 had pilo-erection. Summary of the clinical signs are shown in Appendix G.

Figure 14.

Mean (\pm SD) body weight for all treatment group.

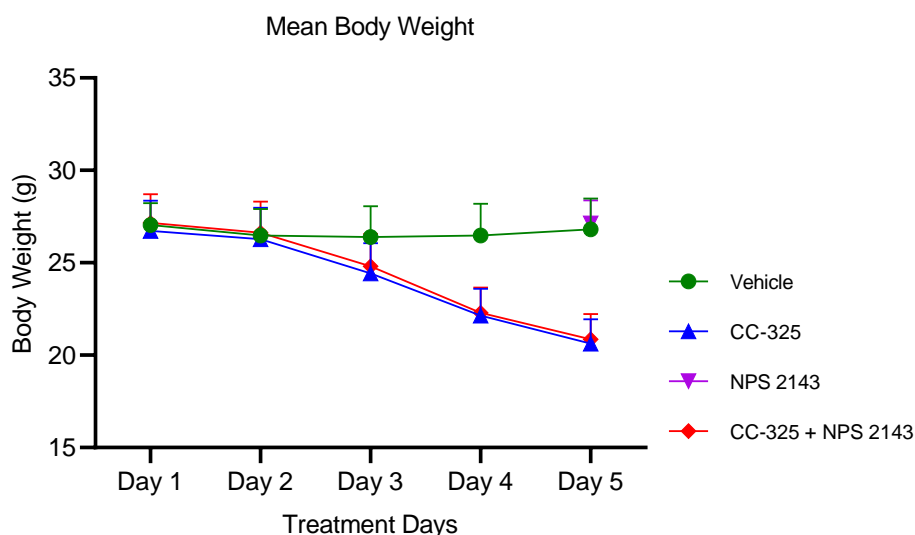


Table 26.

Mean Body Weight for All Treatment Groups.

Treatment	Day 1	Day 2	Day 3	Day 4	Day 5
Vehicle	27.04	26.48	26.39	26.48	26.80
CC-325	26.73	26.27	24.43***	22.14*****	20.62*****
NPS 2143	ND	ND	ND	ND	27.13
CC-325 + NPS 2143	27.16	26.62	24.81***	22.28*****	20.86*****

Note. *** = $p \leq 0.001$; ***** = $p \leq 0.0001$

Toxicokinetic Data

Toxicokinetic blood collection procedure and timepoints are described in detail in method section. A summary of TK dose concentrations and blood collection timepoints is shown in Table 27.

Table 27.

Dose Concentration and Blood Collection Timepoints for Toxicokinetic Treatment Groups.

Blood Collection Time Points (hr)							
Group	Treatment	0	1.5	3	5	9	24
5	CC-325 15 mg/kg BID	√	√	√	√	√	√
6	NPS 2143 120 mg/kg/day	√	√	√	√	√	√
7	CC-325 15 mg/kg BID NPS 2143 120 mg/kg/day	√	√	√	√	√	√

Plasma concentrations of CC-325 from single agent and combination treatment groups, Groups 5 and 7, are shown in Table 28. Test article CC-325 was administered one hour prior to NPS 2143 administration, therefore the collection timepoints for CC-325 were one hour longer than the collection timepoints for NPS 2143. Exposures (AUC) were calculated for 0-25 hours; the exposure of CC-325 was 10.1 and 14.7 μM for single agent and combination treatment, respectively. Based on the expert opinion from Drug Metabolism and Pharmacokinetic (DMPK)

department toxicokinetic scientist, these two values are roughly similar, meaning there is no evidence of drug-drug interaction. Because the exposures of CC-325 in treatment Groups 2 and 4 were similar, we would expect a similar change in iCa^{2+} and PTH in these treatment groups.

Table 28.

Mean Plasma Concentrations of CC-325 for Groups 5 and 7.

Mean Plasma Concentrations of CC-325		
Day 5	CC-325	CC-325 + NPS 2143
Time (hr)	Concentration (μ M)	Concentration (μ M)
0	0.340	0.370
1.5	1.480	1.250
3	0.827	1.810
5	0.513	0.443
9	0.223	0.567
25	0.295	0.293
AUC (0-25) (μ M.hr)	10.1	14.7
Cmax	1.48	1.81
Tmax	1.5	1.5

Plasma concentrations of NPS 2143 from single agent and combination treatment groups, Groups 6 and 7, are shown in Table 29. Test article NPS 2143 was administered one hour after the CC-325 administration, therefore the collection timepoints for NPS 2143 are one hour shorter than the collection timepoints for CC-325. Exposures were calculated for 0-24 hours, which were 6.2 and 16.6 μ M for single agent and combination group, respectively. The exposure of NPS 2143 in the combination groups was greater than the exposure as a single agent, which could result in increased pharmacological effects in the combination group. The exact reason for increased exposure of NPS 2143 in Group 4 is unknown, however drug-drug interaction between CC-325 and NPS 2143 could have caused this increase. Raw TK data is listed in Appendix F.

Table 29.

Mean Plasma Concentrations of NPS 2143 for Groups 6 and 7.

Mean Plasma Concentrations of NPS 2143		
Day 5	NPS-2143	NPS 2143 + CC-325
Time (hr)	Concentration (μM)	Concentration (μM)
0	?	0.00
0.5	0.495	1.36
2	0.582	2.01
4	0.765	0.918
8	0.224	0.82
24	0.0190	0.0866
AUC (0-24) (μM.hr)	6.2	16.6
C _{max}	0.765	2.01
T _{max}	4.0	2.0

Blood collection for endpoints measurements

Based on the reported efficacy of NPS 2143 in literature, and our own pilot data, the effects of orally administered NPS 2143 on PTH and iCa^{2+} is acute and C_{max} dependent. Based on the pilot study data, the dose of 200 mg/kg had the maximum effect on PTH at 2-hr postdose and iCa^{2+} at 4-hr postdose. Therefore, not only these timepoints were included in the blood collection timepoints, but also, they were collected precisely at each timepoint. To reduce the variability associated with the sample collection time, all samples were collected within two minute of target time. The blood collection schedule for all treatment groups is listed in Table 30.

Table 30.

Schedule of Sample Collection for All Tests.

		Group 1	Group 2	Group 3	Group 4
Treatment	Time*	Vehicle 2	CC-325	NPS 2143	CC-325 + NPS 2143
Sample collection on Day 5	Day 5 (0-hr)	Predose	1-hr Postdose	Predose	Prior to NPS 2143 dose and 1-hr post CC-325 dose
	Day 5 (2-hr)	2-hr Postdose	3-hr Postdose	2-hr Postdose	2-hr post 2143 dose and 3-hr post CC-325 dose
	Day 5 (4-hr)	4-hr Postdose	5-hr Postdose	4-hr Postdose	4-hr post 2143 dose and 5-hr post CC-325 dose
	Day 5 (6-hr)	6-hr Postdose	7-hr Postdose	6-hr Postdose	4-hr post 2143 dose and 7-hr post CC-325 dose
	Day 6 (24-hr)	24-hr Postdose	25-hr Postdose	24-hr Postdose	24-hr post 2143 dose and 25-hr post CC-325 dose

Note. * = Time is based on the NPS 2143 dose

Serum Chemistry (Axcel analyzer)

The individual results for serum chemistry are listed in Appendix H. The value of globulin was calculated by subtracting albumin value from total protein. Each time point was a terminal sacrifice; therefore, no serial samples were collection for serum chemistry. Statistical analysis was performed by comparing each treatment group with vehicle control group at each timepoint. However, in order to assess the effect of NPS 2143 on calcium concentration, as a single agent or combination treatment, the data from Group 2, CC-325 alone, was compared with Group 4, CC-325 + NPS 2143 treatment group.

Total serum calcium analysis was conducted using Axcel analyzer. The total serum calcium values were consistent with whole blood ionized calcium values measured by Stat Prime Profile analyzer at necropsy. The first measurement on Day 5 was at 0-hr, which was after 5 days of daily dosing including the morning of Day 5. Based on the in-house historical data, the drop in calcium at 0-hr was expected and based on the data from the pilot study the increase in calcium in NPS 2143 treated animals was also expected.

No changes in total calcium concentrations were seen in vehicle control group during the measurement period, 0-24 hours. Serum calcium in Group 2, CC-325 single agent treatment group, was 33-43% below vehicle control group level during the measurement period. The calcium concentration in NPS 2143 treatment group, Group 3, increased shortly after dosing and peaked at 4- to 6-hr timepoints (both similar values) before returning to predose values by 24-hr. The calcium in CC-325 + NPS 2143 treatment groups was initially low, however, it increased minimally at 2-hr (17%) and 4-hr (16%) timepoints when compared to CC-325 only treatment groups at the same timepoints, Figure 15. The total calcium in each treatment group was compared to vehicle control groups and is reported as percent difference in Figure 16 and Table 31.

Figure 15.

Mean (\pm SD) of total calcium in serum for all treatment groups.

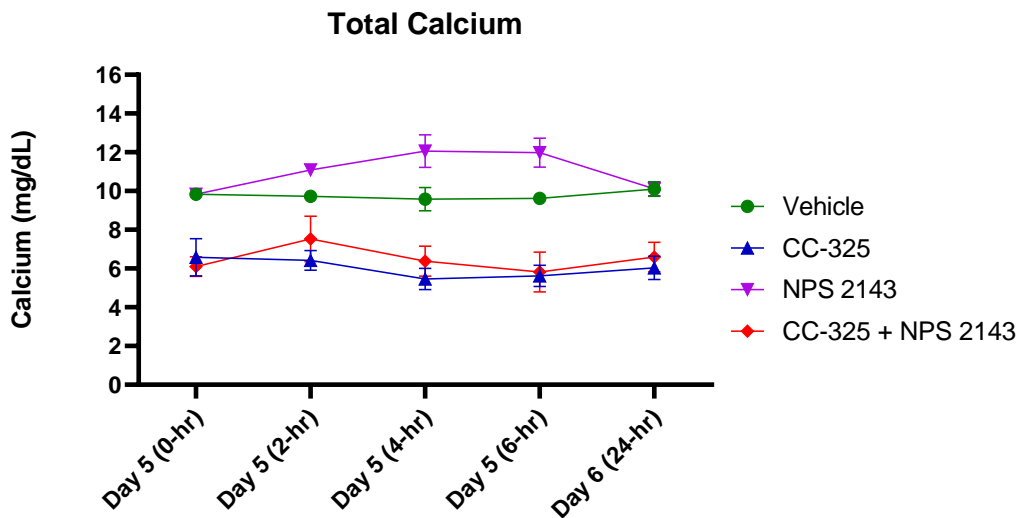
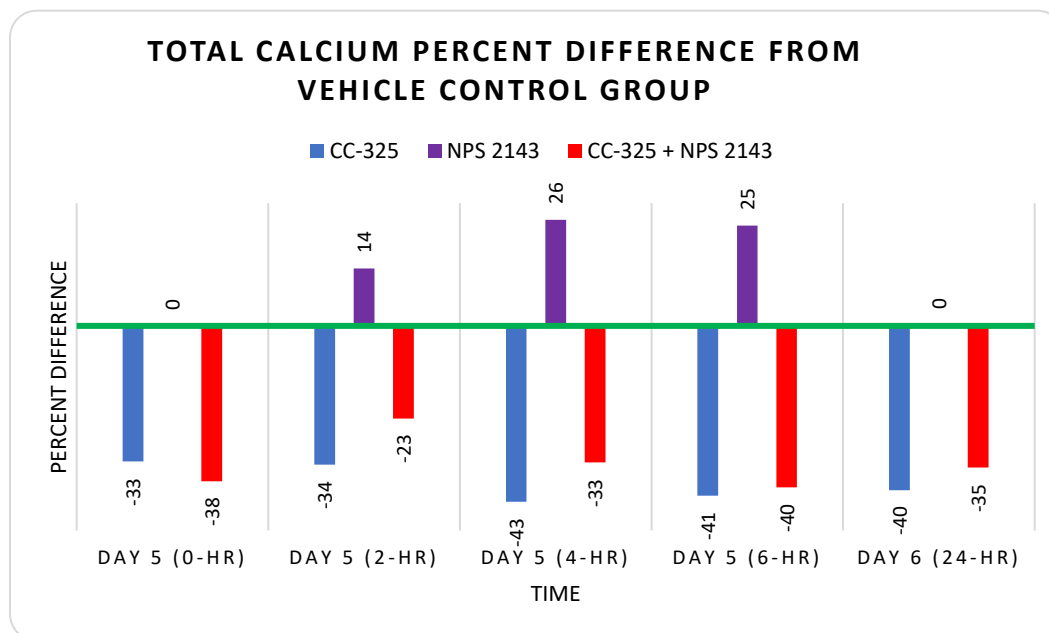


Figure 16.

Total calcium percent difference from vehicle control group.



Note. Serum total calcium percent difference from vehicle control group. The green horizontal line shows the vehicle control group calcium value that was used to calculate the percent difference from other treatment groups.

Table 31.

Mean Serum Chemistry for All Treatment Groups.

Analyte	Time	Group 1	Group 2	Group 3	Group 4
		Vehicle	CC-325	NPS 2143	CC-325 + NPS 2143
Calcium (mg/dL)	Baseline	9.84	6.58****	9.84	6.10****
	2-hr	9.72	6.42****	11.08**	7.52****
	4-hr	9.58	5.46****	12.06****	6.38****
	6-hr	9.62	5.63****	11.98****	5.82****
	24-hr	10.10	6.04****	10.12	6.60****

Note. ** = $p \leq 0.01$; **** = $p \leq 0.0001$

The change in serum magnesium, another divalent cation that effects CaSR, is less pronounced than calcium but had a similar trend to calcium (Figure 17, Table 32). There was a slight increase in magnesium in NPS 2143 treated mice at 2- and 4-hr timepoints, however, it

was smaller in both magnitude and duration when compared to calcium increase at the same group. The change in magnesium levels in the CC-325 and CC-325 + NPS 2143 treated mice were less pronounced and did not follow calcium trend.

Figure 17.

Mean (\pm SD) of serum magnesium for all treatment groups.

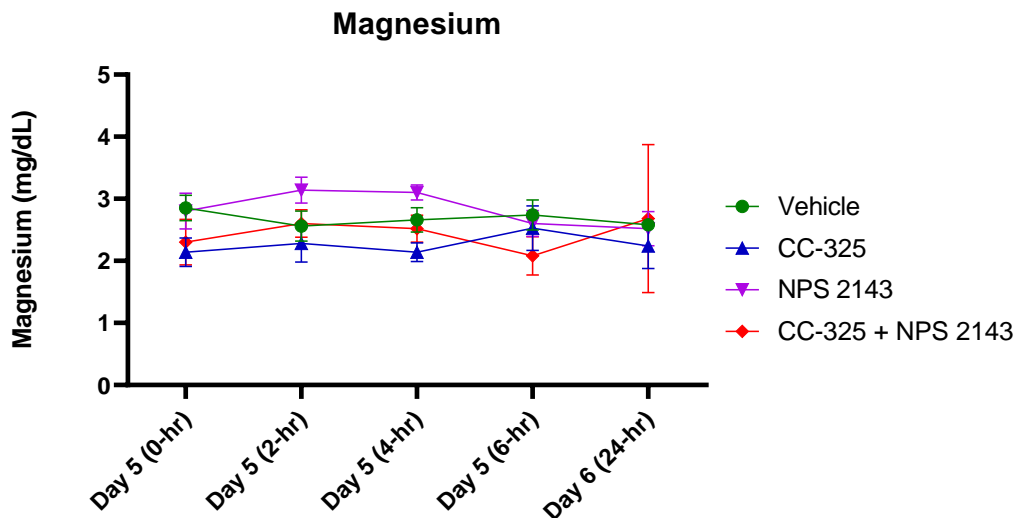


Table 32.

Mean Serum Chemistry for All Treatment Groups.

Analyte	Time	Group 1	Group 2	Group 3	Group 4
		Vehicle	CC-325	NPS 2143	CC-325 + NPS 2143
Magnesium (mg/dL)	Baseline	2.90	2.14**	2.80	2.30*
	2-hr	2.56	2.28	3.14*	2.60
	4-hr	2.66	2.14	3.10	2.52
	6-hr	2.74	2.52	2.60	2.08*
	24-hr	2.58	2.24	2.52	2.68

Note. * = $p \leq 0.05$; ** = $p \leq 0.01$

The results of serum phosphate for all treatment groups is shown in Figure 18 and Table 33. The phosphate levels in CC-325 and CC-325 + NPS 2143 treated mice was significantly increased in response to decrease in calcium at all timepoints, except 0-hr for

CC-325 single agent treatment group. There was no significant difference between NPS 2143 single agent treatment group and vehicle control group.

Figure 18.

Mean (\pm SD) of serum phosphate for all treatment groups.

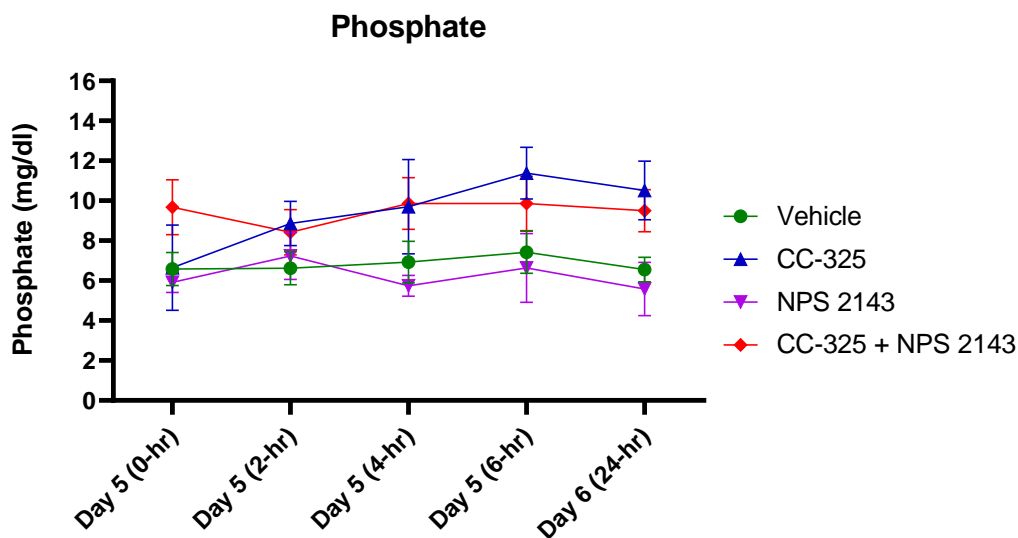


Table 33.

Mean Serum Chemistry for All Treatment Groups.

Analyte	Time	Group 1	Group 2	Group 3	Group 4
		Vehicle	CC-325	NPS 2143	CC-325 + NPS 2143
Phosphate (mg/dL)	0-hr	6.58	6.64	5.92	9.68***
	2-hr	6.62	8.86*	7.24	8.42
	4-hr	6.92	9.70**	5.74	9.86**
	6-hr	7.42	11.38****	6.64	9.86*
	24-hr	6.56	10.52****	5.58	9.50**
	24-hr	1.48	1.60	1.30	1.50

Note. * = $p \leq 0.05$; ** = $p \leq 0.01$; *** = $p \leq 0.001$; **** = $p \leq 0.0001$

The albumin concentrations are shown in Figure 19 and Table 34. Serum albumin level in CC-325 only treatment group was significantly lower than the vehicle control group at 4-hr postdose. In NPS 2143 only treatment group, albumin was significantly lower at 2-, 4-, and 6-hr

postdose. In combination group, albumin was significantly lower at 4- and 6-hr timepoints. Some of the changes were likely due to slight increase in serum albumin in control group and slight decrease in test article treatment groups.

Figure 19.

Mean (\pm SD) of serum albumin for all treatment groups.

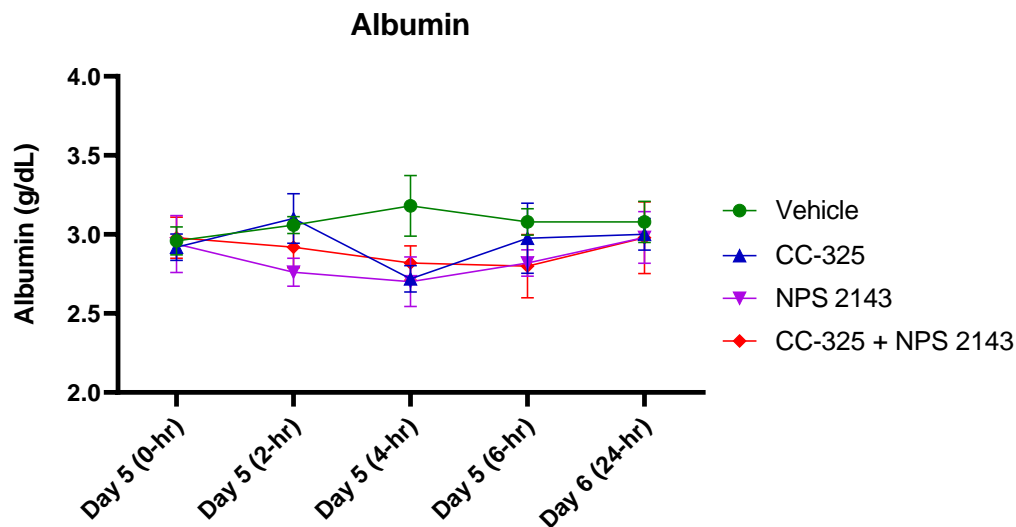


Table 34.

Mean Serum Chemistry for All Treatment Groups.

Analyte	Time	Group 1	Group 2	Group 3	Group 4
		Vehicle	CC-325	NPS 2143	CC-325 + NPS 2143
Albumin (g/dL)	0-hr	2.96	2.92	2.94	2.98
	2-hr	3.06	3.10	2.76**	2.92
	4-hr	3.18	2.72****	2.70****	2.82***
	6-hr	3.08	2.97	2.82*	2.80**
	24-hr	3.08	3.0	2.98	2.98

Note. * = $p \leq 0.05$; ** = $p \leq 0.01$; *** = $p \leq 0.001$; **** = $p \leq 0.0001$

The total protein concentrations are shown in Figure 20 and

Table 35. Total protein had similar changes to albumin, and although the changes were statistically significant, the actual magnitude of the change was small and had little biological impact. Globulin values are shown in Figure 21 and Table 36. There was a minimal but statistically significant decrease in globulin at 2-, 4-, and 6-hr postdose in test article treated groups, likely due to minimal decrease in total protein when compared with vehicle control group Table 36. The values for A/G calculation are shown in Figure 22, and the data shows significant increase at 6-hr timepoint in CC-325 and CC-325 + NPS 2143 treated mice, however, the change is minimal and has no pharmacological relevance.

Figure 20.

Mean \pm standard deviation of serum total protein for all treatment groups, (n=5/timepoint).

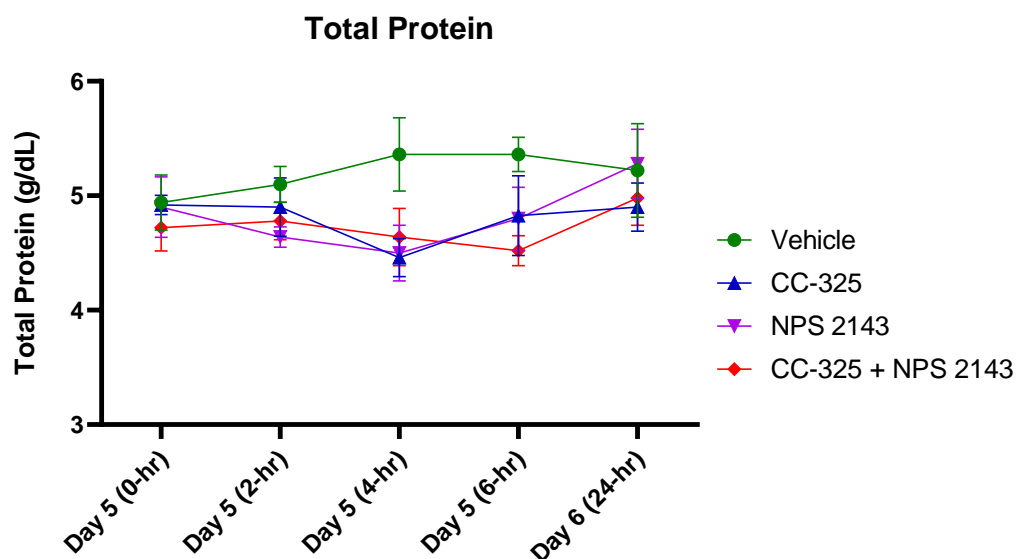


Table 35.

Mean Serum Chemistry for All Treatment Groups.

Analyte	Time	Group 1	Group 2	Group 3	Group 4
		Vehicle	CC-325	NPS 2143	CC-325 + NPS 2143
Total Protein (g/dL)	0-hr	4.94	4.92	4.90	4.72
	2-hr	5.10	4.90	4.64**	4.78
	4-hr	5.36	4.46****	4.50****	4.64****
	6-hr	5.36	4.82**	4.80**	4.52****
	24-hr	5.22	4.90	5.28	4.98

Note. * = $p \leq 0.05$; ** = $p \leq 0.01$; *** = $p \leq 0.001$; **** = $p \leq 0.0001$; ND = No Data

Figure 21.

Mean \pm standard deviation of serum globulin for all treatment groups.

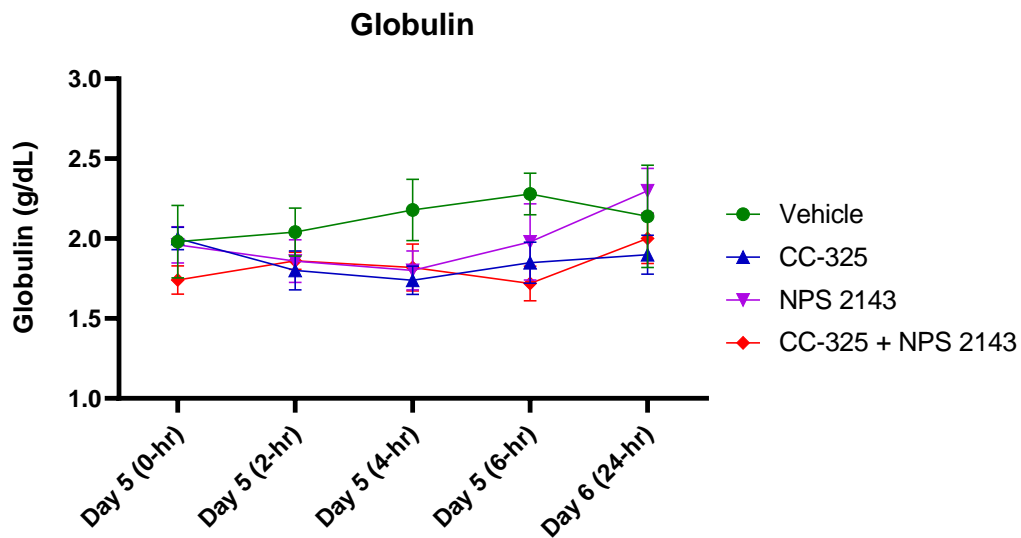


Figure 22.

Mean \pm standard deviation of albumin/globulin ratio for all treatment groups.

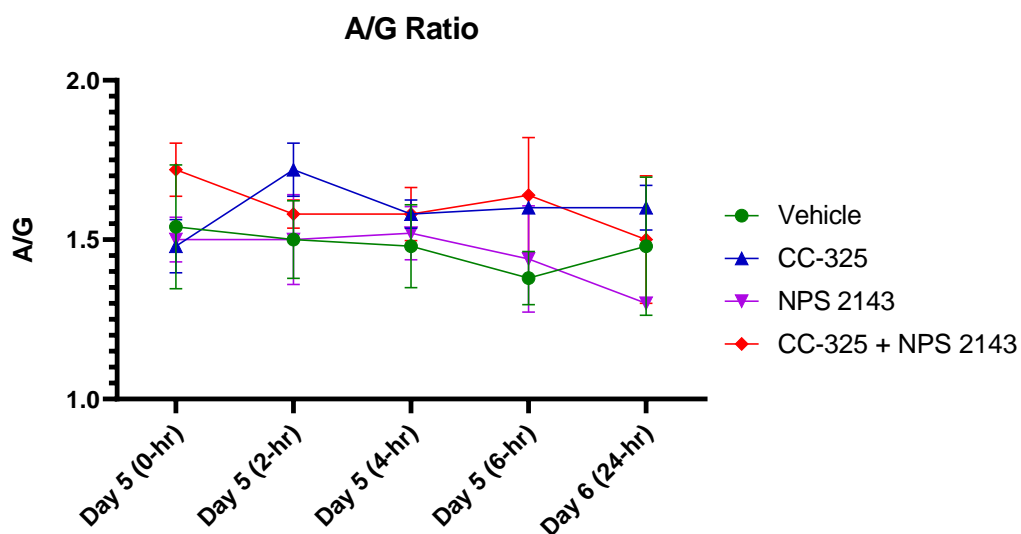


Table 36.

Mean Serum Chemistry for All Treatment Groups.

Analyte	Time	Group 1	Group 2	Group 3	Group 4
		Vehicle	CC-325	NPS 2143	CC-325 + NPS 2143
Globulin (g/dL)	0-hr	1.98	2.00	1.96	1.74*
	2-hr	2.04	1.80*	1.86	1.86
	4-hr	2.18	1.74*****	1.80***	1.82**
	6-hr	2.28	1.85***	1.98**	1.72*****
	24-hr	2.14	1.90*	2.30	2.0
Albumin/Globulin	0-hr	1.54	1.48	1.50	1.72
	2-hr	1.50	1.72*	1.50	1.58
	4-hr	1.48	1.58	1.52	1.58
	6-hr	1.38	1.60*	1.44	1.64**
	24-hr	1.48	1.60	1.30	1.50

Note. * = $p \leq 0.05$; ** = $p \leq 0.01$; *** = $p \leq 0.001$; ***** = $p \leq 0.0001$; ND = No Data

Serum Chemistry (Stat Profile Prime)

Prior to sacrifice of each mouse, 100 μ L of whole blood was collected in capillary tubes with lithium heparin preservative. Samples were immediately loaded into a Stat Profile Prime analyzer and Na^+ , K^+ , Cl^- , iCa^{2+} , and pH were measured. Raw data from Stat Profile Prime is tabulated in Appendix I. The level of iCa^{2+} in vehicle control group was consistent during the measurement period, 0 to 24 hours postdose. The mice treated with CC-325 either as a single agent or combination with NPS 2143 had decrease in iCa^{2+} level at 0-hr, compared to the vehicle control group, which was consistent with in-house historical data (Table 37). The level of iCa^{2+} in the CC-325 single agent treatment group, was low during the 0- to 24-hr measurement period, however, treatment group CC-325 + NPS 2143 had minimal increase at 2-hr (16%) and 4-hr (11%) post NPS 2143 dose. Mice treated with NPS 2143 alone had normal level of iCa^{2+} at 0-hr (prior to NPS 2143 dose) and significantly increased levels at 2-, 4-, and 6-hr timepoints. The level of iCa^{2+} returned to baseline by 24-hr postdose, which was consistent with the decrease in exposure of NPS 2143 in these mice.

Percent difference of iCa^{2+} was calculated by comparing each treatment group with vehicle control group, and data from these calculations are shown in

Figure 24. The maximum decrease in iCa^{2+} was observed at 4- and 6-hr postdose in CC-325 treated mice, which was 35% and 36% decrease, respectively. The maximum decrease in iCa^{2+} in CC-325 + NPS 2143 mice was observed at 0- and 6-hr postdose, which was about 35%. The maximum increase in iCa^{2+} was observed in NPS 2143 treatment group, which was measured at 4-hr postdose.

Figure 23.
Mean (\pm SD) of iCa^{2+} in whole blood for all treatment groups.

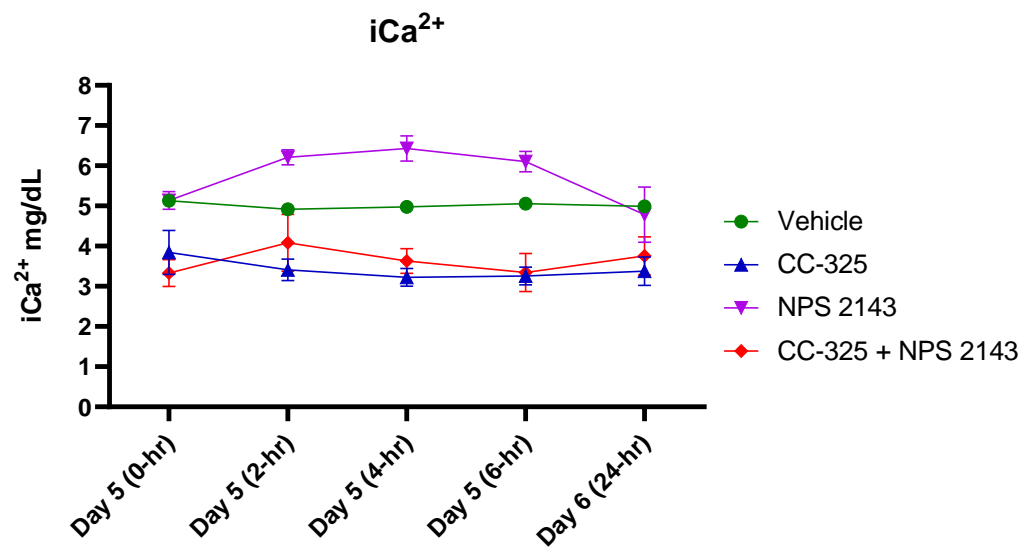
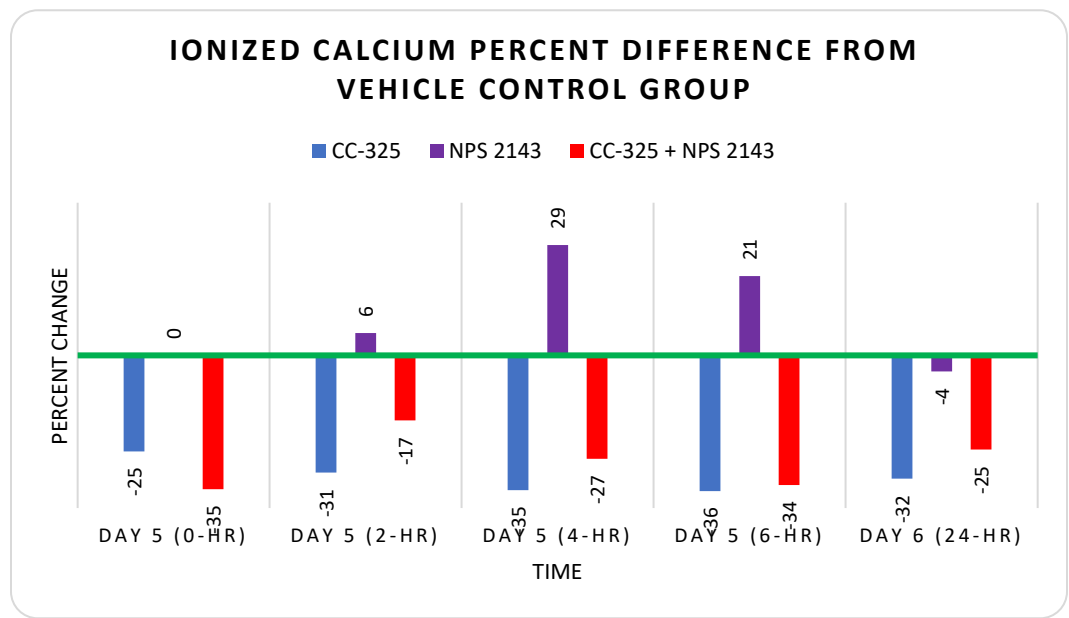


Figure 24.
Ionized calcium percent difference from vehicle control group.



Note. Percent iCa^{2+} difference from vehicle control group for all treatment groups. The green horizontal line shows the vehicle control ionized calcium value that was used to calculate the percent difference from other treatment groups.

Table 37.

Mean Serum Chemistry for All Treatment Groups.

Analyte	Time	Group 1	Group 2	Group 3	Group 4
		Vehicle	CC-325	NPS 2143	CC-325 + NPS 2143
iCa^{2+} (mg/dL)	0-hr	5.13	3.84*	5.14	3.33***
	2-hr	4.92	3.41***	5.21****	4.08
	4-hr	4.98	3.22****	6.42***	3.63***
	6-hr	5.06	3.26****	6.11**	3.34**
	24-hr	4.99	3.38**	4.78	3.76**

Note. * = $p \leq 0.05$; ** = $p \leq 0.01$; *** = $p \leq 0.001$; **** = $p \leq 0.0001$; ND = No Data

The effect of test article on the pH was also measure (Figure 25 and Table 38). There was no effect on pH by either test articles, suggesting that pH did not adversely affect iCa^{2+} measurement.

Figure 25.

Mean (\pm SD) of blood pH for all treatment groups.

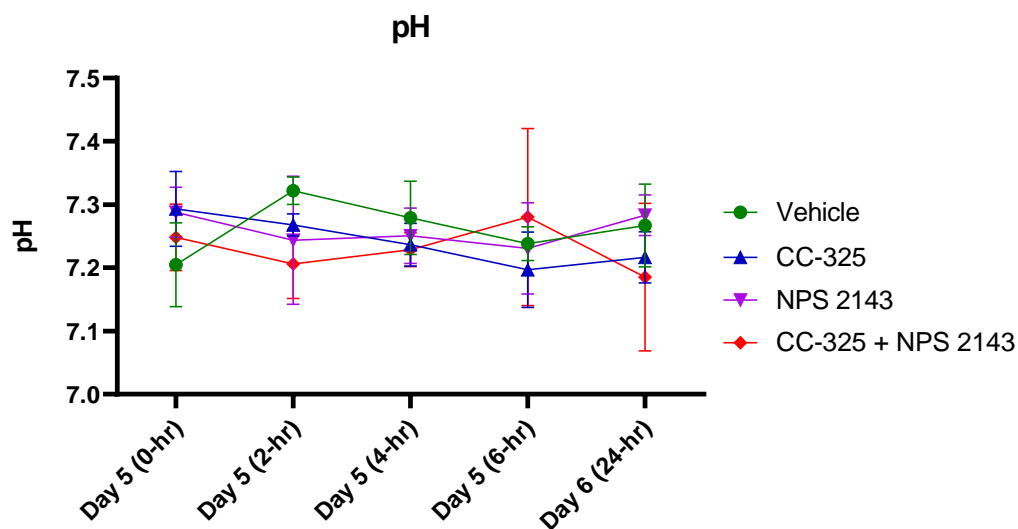


Table 38.

Mean Serum Chemistry for All Treatment Groups.

Analyte	Time	Group 1	Group 2	Group 3	Group 4
		Vehicle	CC-325	NPS 2143	CC-325 + NPS 2143
pH	0-hr	7.21	7.29	7.29	7.25
	2-hr	7.32	7.27**	7.24	7.21*
	4-hr	7.28	7.24	7.25	7.22
	6-hr	7.24	7.20	7.23	7.28
	24-hr	7.27	7.22	7.28	7.19
	6-hr	113.6	112.8	114.0	113.0
	24-hr	109.8	112.2	112.0**	114.0**

Note. * = $p \leq 0.05$; ** = $p \leq 0.01$; ND = No Data

The only significant change in Na^+ was observed in the CC-325 + NPS 2143 treatment group, which was an increase at 24-hr timepoint. There were no significant changes in K^+ , and changes in Cl^- at 24-hr timepoints were most likely due decrease in Cl^- in the vehicle treatment groups. The values for Na^+ , K^+ , and Cl^- are shown in Figure 26 through Figure 28, and

Table 39.

Figure 26.

Mean (\pm SD) of Na^+ for all treatment groups.

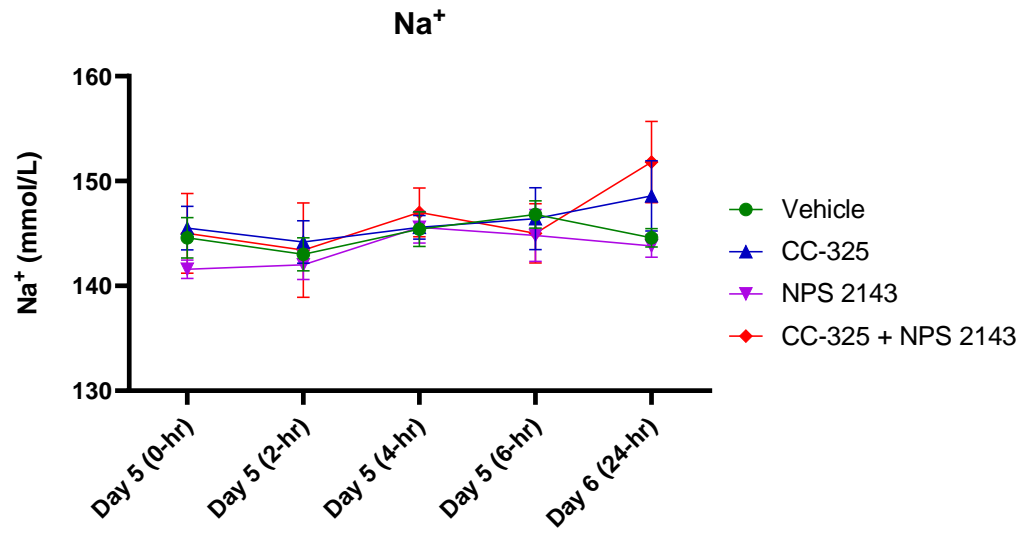


Figure 27.

Mean (\pm SD) of K^+ for all treatment groups.

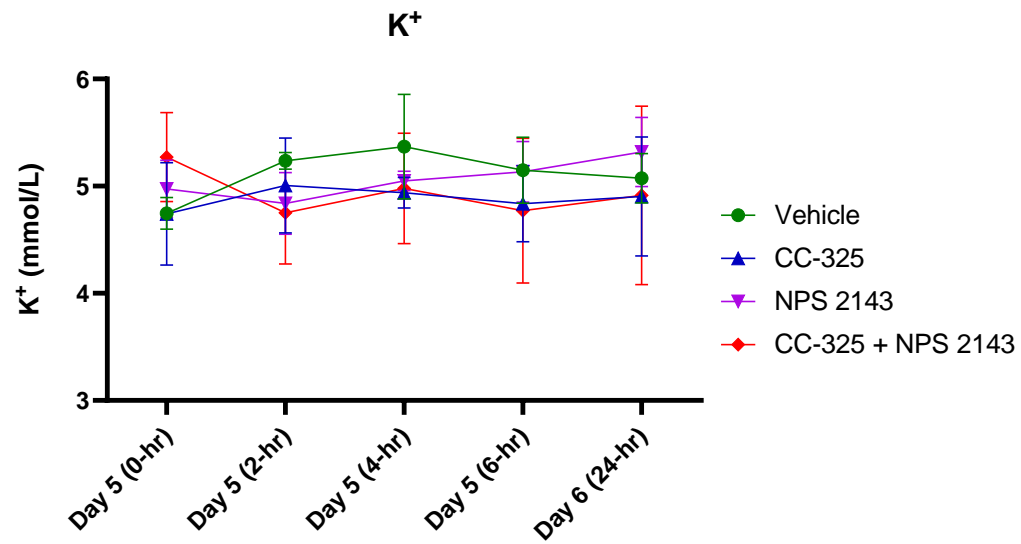


Figure 28.

Mean (\pm SD) of Cl^- for all treatment groups.

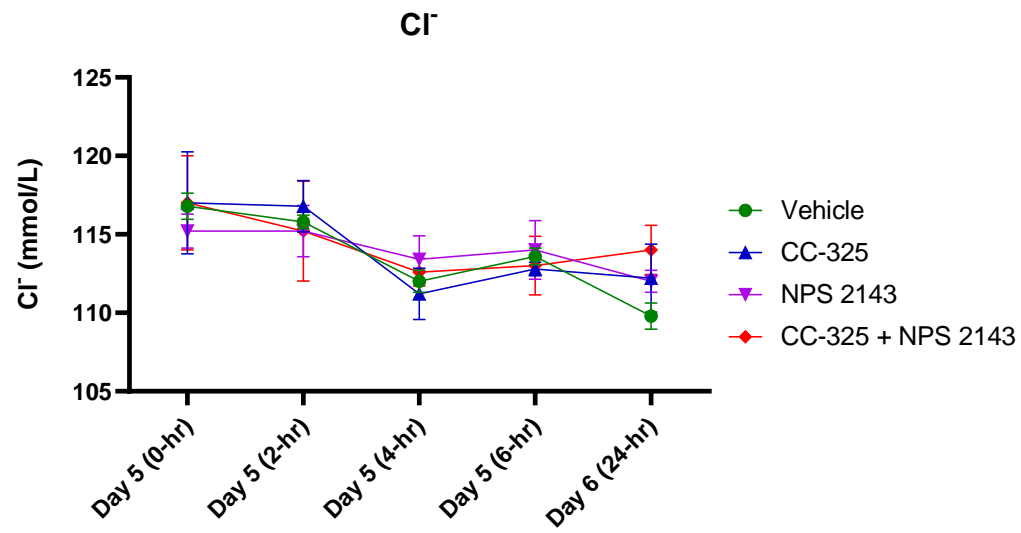


Table 39.

Mean Ionized Calcium, Electrolytes, and pH Values for All Treatment Groups.

Analyte	Time	Group 1	Group 2	Group 3	Group 4
		Vehicle	CC-325	NPS 2143	CC-325 + NPS 2143
Na ⁺ (mmol/L)	0-hr	144.6	145.5	141.6	145.0
	2-hr	143.0	144.2	142.0	143.4
	4-hr	145.4	145.6	145.6	147.0
	6-hr	146.8	146.4	144.8	145.0
	24-hr	144.6	148.6	143.8	151.8*
K ⁺ (mmol/L)	0-hr	4.746	4.742	4.974	5.270
	2-hr	5.236	5.006	4.838	4.750
	4-hr	5.370	4.940	5.050	4.980
	6-hr	5.148	4.836	5.134	4.770
	24-hr	5.074	4.904	5.134	4.914
Cl ⁻ (mmol/L)	0-hr	116.8	117.0	115.2	117.0
	2-hr	115.8	116.8	115.2	115.2
	4-hr	112.0	111.2	113.4	112.6
	6-hr	113.6	112.8	114.0	113.0
	24-hr	109.8	112.2	112.0**	114.0**

Note. * = $p \leq 0.05$; ** = $p \leq 0.01$

Serum PTH (ELISA Assay)

Serum samples were removed from the refrigerator and thawed on ice until processed for analysis. Samples were run in three different plates. In order to reduce the impact of plate to plate variation of data analysis, samples from each timepoint were run together. All the samples from 0- and 2-hr were ran on plate 1, samples from 4- and 6-hr were ran in plate 2 and samples from 24-hr were ran in plate 3. Based on the pilot study data, it was predicted that samples from Group 3 would have high PTH values, therefore samples from Group 3 (with the exception of

0-hr) were diluted 1 to 5 (1:5) and were loaded into plate 3 for analysis. Results from the diluted run were used for data analysis, and Table 40 shows the PTH results for all treatment groups.

The PTH data had similar trend as iCa^{2+} with slightly different time course. The serum PTH levels in vehicle control group were variable, with highest level of PTH observed at 4-hr timepoint. The serum PTH level in mice treated with CC-325, Group 2 and 4, was below levels compared to vehicle treated animals at every timepoint. The PTH level in mice treated with NPS 2143 as a single agent, Group 3, was significantly increased, with the peak of 675 pg/mL at 2-hr post dose. The increased level of serum PTH in these mice continued until 6-hr post dose and returned to baseline at 24-hr postdose, which is consistent with decrease in exposure to NPS 2143 in these mice. The mice in Group 4, CC-325 + NPS 2143 treatment group, did not have an increase in serum PTH even after administration of NPS 2143, Figure 29 and Table 40.

Figure 29.

Mean (\pm SD) of serum PTH for all treatment groups.

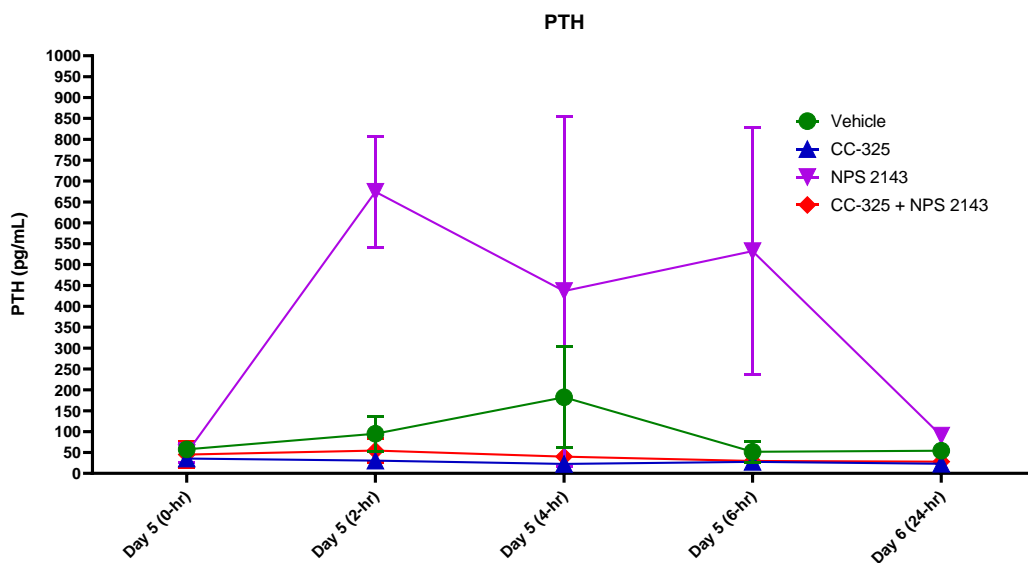


Table 40.

Mean PTH Values for All treatment Groups.

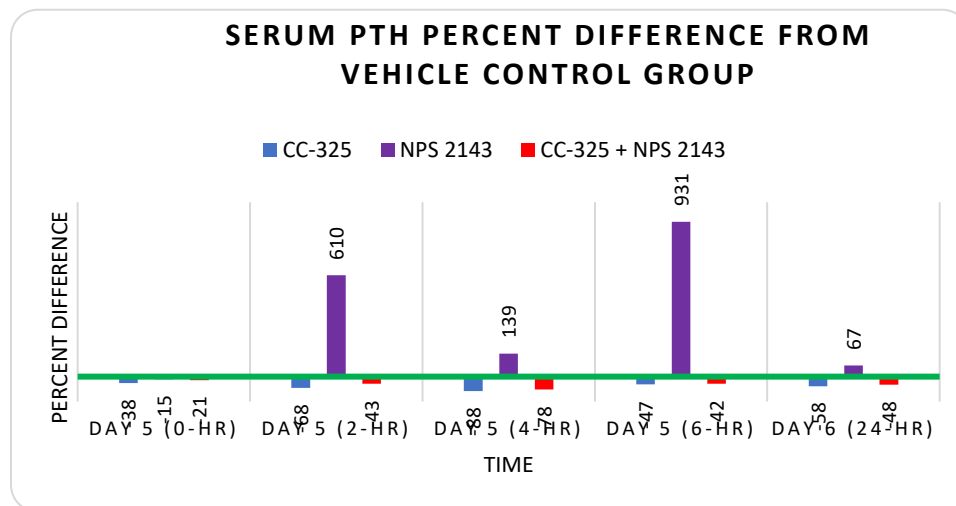
Analyte	Time	Group 1	Group 2	Group 3	Group 4
		Vehicle	CC-325	NPS 2143	CC-325 + NPS 2143
PTH1 (pg/mL)	0-hr	57.64	35.57*	48.72	45.28
	2-hr	95.04	30.42	674.4***	54.55
	4-hr	182.4	22.80	436.6	39.97
	6-hr	51.59	27.60	532.1*	29.78
	24-hr	54.34	22.93*	90.48*	28.13

Note. * = $p \leq 0.05$; *** = $p \leq 0.001$

The level of serum PTH in each treatment group was compared with vehicle control group and percent change from vehicle control groups was calculated, the result of this analysis is shown in Figure 31.

Figure 30.

Serum PTH percent difference from vehicle control group.



Note. Percent PTH difference from vehicle control group for all treatment groups. The green horizontal line shows the vehicle control ionized calcium value that was used to calculate the percent difference from other treatment groups.

Serum FGF23 (ELISA assay)

Serum samples were removed from the refrigerator and thawed on ice until processed for analysis. Samples were run in three different plates. Similar to the PTH sample analysis, samples from each timepoint were run together in one plate to reduce the impact of plate to plate variation on sample analysis. All the samples from 0- and 2-hr were ran on plate 1, samples from 4- and 6-hr were ran in plate 2 and samples from 24-hr were ran in plate 3. The FGF23 data is shown in Figure 31 and Table 41. Serum FGF23 levels in vehicle control group ranged from 131-211 pg/mL. Since there is no historical data for serum FGF23 concentration in huCRBN KI mice, the vehicle control values were used for comparison and statistical analysis. The serum FGF23 level in mice treated with CC-325, either as a single agent or combination with NPS 2143, was significantly lower than the vehicle control at all measured timepoints. The level of serum FGF23 in NPS 2143 animals did not change during any of the measured timepoints. The administration of NPS 2143 after CC-325 treatment, Group 4, did not appear to change the FGF23 in these mice. Further analysis of the data was performed by calculating the percent difference for each treatment group at each timepoint, Figure 32.

Figure 31.

Mean (\pm SD) of serum FGF23 for all treatment groups.

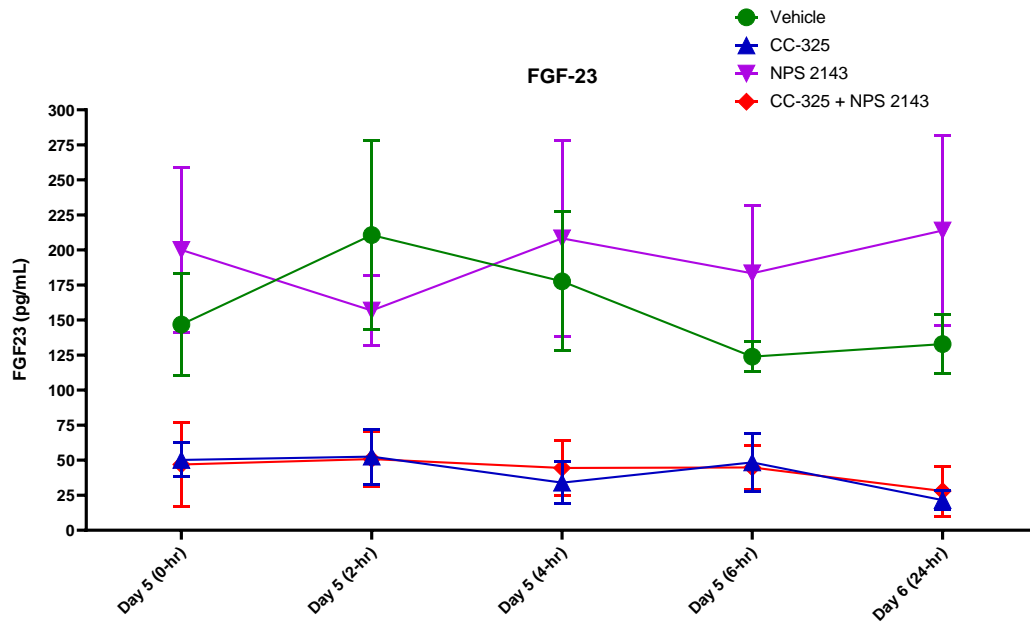


Table 41.

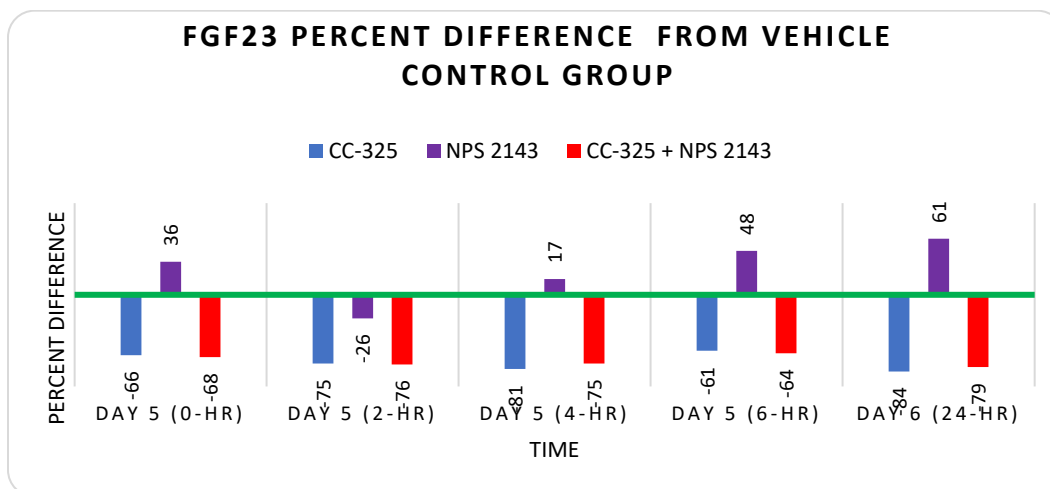
Mean FGF23 Values for All treatment Groups

Analyte	Time	Group 1	Group 2	Group 3	Group 4
		Vehicle	CC-325	NPS 2143	CC-325 + NPS 2143
FGF23 (pg/mL)	0-hr	146.9	50.16**	200.1	46.92**
	2-hr	210.7	52.55*	156.8	50.83*
	4-hr	177.6	33.95**	208.3	44.39**
	6-hr	123.9	48.38***	183.3	44.87****
	24-hr	132.8	21.51***	213.9	28.05***

Note. * = $p \leq 0.05$; ** = $p \leq 0.01$; *** = $p \leq 0.001$; **** = $p \leq 0.0001$

Figure 32.

FGF23 percent difference from vehicle control group.



Note. FGF23 percent difference from vehicle control group. The green horizontal line shows the vehicle control FGF23 value that was used to calculate the percent difference from other treatment groups.

Histopathology evaluation

Parathyroid glands from all treatment groups were collected at necropsy and stored in 10% neutral buffer formalin (NBF) for 48 hours and then transferred to 70% ethanol and held until processing. The mouse parathyroid is very small tissue that is sitting on top of the thyroid that is attached to each side of the mouse trachea. Due to its small size, it can be difficult to locate and section. The histology contract lab in charge of processing and sectioning the parathyroid glands had difficulty locating parathyroid for several mice. This resulted in missing parathyroid for several animals including 3 from Group 1, 7 from Group 2, 2 from Group 3, and 5 from Group 4.

The only histopathological finding in parathyroid was necrosis, which was observed in animals treated with CC-325 or CC-325 + NPS 2143. The summary of findings is listed below in Table 42.

Table 42.

Summary of Microscopic Findings for All Treatment Groups.

	Dosage Group	Control	2	3	4
	Number of Animals	25	25	25	25
	Number Examined	22	18	23	21
	Number Unremarkable	22	18	23	18
Gland, Thyroid/Gland, parathyroid	Number Examined	22	18	23	21
Necrosis	Animals number (severity)		2011(m) 2013(m) 2014(m) 2015(mi) 2021(m) 2022(m) 2024(mi) 2025(m)		4015(mi) 4019(mi) 4024(mi)
Total Findings Incidence		0	8	0	3

Note. m = Minimal; mi = Mild

Immunohistochemistry

Two unstained parathyroid slides from each animal were obtained and used for immunohistochemistry staining. One slide was used for PTH and another for GSPT1 staining. After staining, slides were loaded into an Aperio automatic slide scanner and scanned. The images were then loaded into HALO software and the intensity of the stains were scored. As described in method section, the scores for IHC range from 1-300, with 1 being no stain and 300 being the maximum stain. The higher the stain intensity, the higher the amount of the biomarker was present.

PTH

The summary of the IHC for PTH data is shown in Figure 32 and Table 43. The H-scores from vehicle control groups at each timepoint served as a baseline for PTH in parathyroid gland. The mice treated with CC-325 single agent or in combination with NPS 2143 had significantly lower levels of PTH in the parathyroid gland at all timepoints (0- to 24-hr), however, the mice treated with CC-325 + NPS 2143 had slightly lower PTH at 2-hr post treatment than CC-325 as a single agent. The mice treated with NPS 2143 as a single agent, had the same level of PTH at 0-hr (pre dose) and significantly lower level of PTH at 2- and 6-hr postdose when compared with the vehicle control group. The levels of PTH in all treatment groups were compared with vehicle control group, and a summary of the statistical analyses is shown in Table 43 below. A representative of IHC staining from selected animals is shown in Figure 35. The intensity of the staining from representative animals at each timepoint is consistent with the scores provided in Table 43.

Figure 32.
Mean \pm SEM of PTH H-Score for all treatment groups.

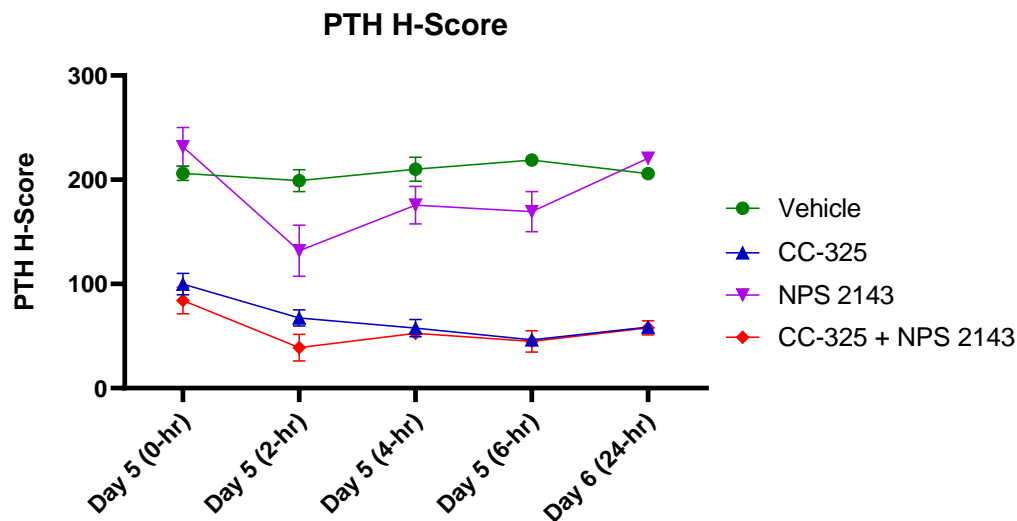


Table 43.
Mean PTH H-Score for IHC Stained Parathyroid Sections.

Analyte	Time	Group 1	Group 2	Group 3	Group 4
		Vehicle	CC-325	NPS 2143	CC-325 + NPS 2143
PTH (H-Score)	0-hr	206.0	99.93****	231.5	84.13****
	2-hr	199.0	67.33****	131.9***	38.82****
	4-hr	210.1	57.62****	175.6	52.50****
	6-hr	218.9	46.39****	169.5*	44.91****
	24-hr	205.9	58.70****	220.6	57.88****

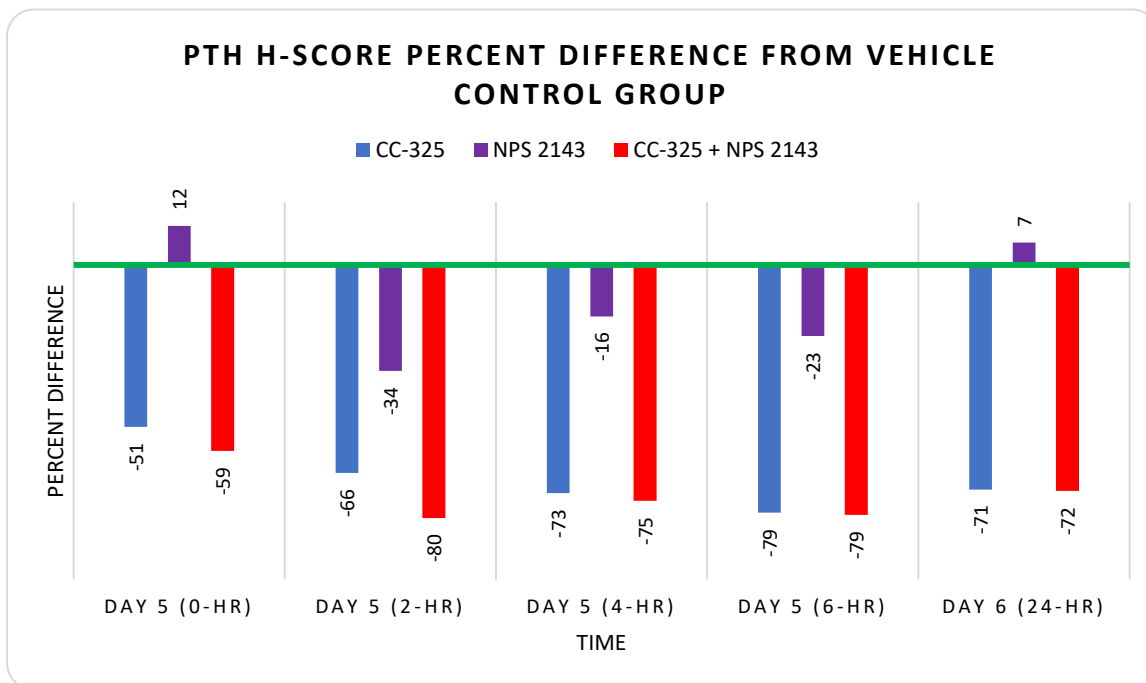
Note. * = $p \leq 0.05$; ** = $p \leq 0.01$; *** = $p \leq 0.001$; **** = $p \leq 0.0001$

The percent change in PTH for each treatment group was calculated by comparing the difference between the PTH in that group and vehicle control group. The decrease in PTH in CC-325 single agent treatment group was 51-80%, in CC-325 + NPS 2143 treatment groups it was 59-79%, and in NPS 2143 as a single agent treatment group it was 16-34%. There was a

minimal increase (7-12%) in PTH in NPS 2143 single agent treatment group at 0- and 24-hr timepoints. The result of this calculations is shown in Figure 34.

Figure 34.

PTH H-Score percent difference from vehicle control group.



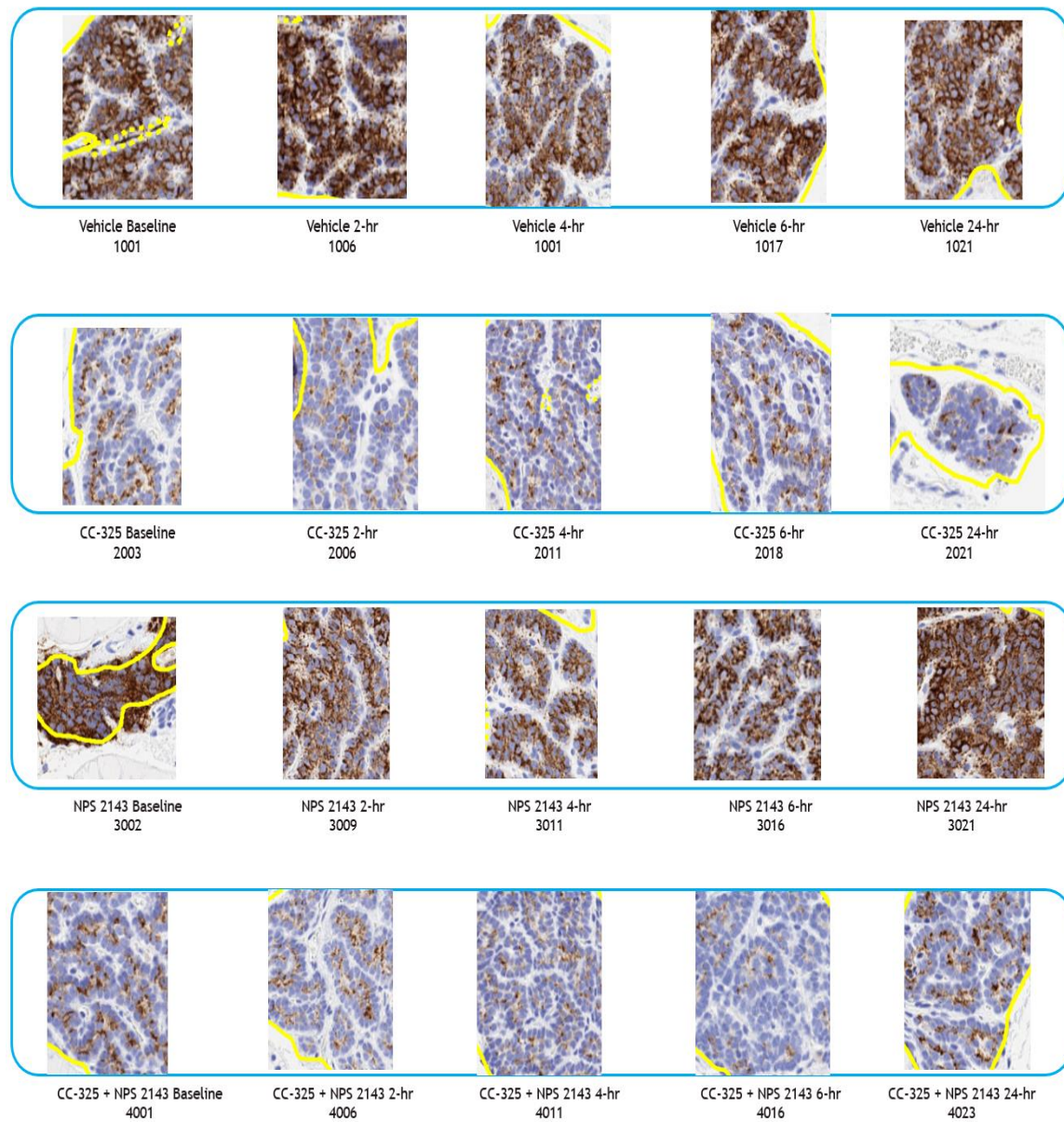
Note. Percent PTH H-Score difference from vehicle control group for all treatment groups. The green horizontal line shows the vehicle control PTH H-Score value that was used to calculate the percent difference from other treatment groups.

The IHC images below in **Error! Reference source not found.** are representative images of the PTH staining in parathyroid gland for each treatment group at different timepoints. The mice in vehicle control group had the highest staining representing the normal level of PTH in parathyroid. The mice in the CC-325 single agent treatment group (Group2) had decreased staining, which indicates decreased level of PTH in parathyroid at all timepoints. The mice treated with NPS 2143 as a single agent had similar staining to vehicle control group at 0-hr but decreased staining at 2- and 4-hr timepoints, which returned to baseline by 24-hr. The mice treated with CC-325 + NPS 2143 had similar staining intensity as CC-325 single agent treatment

group, however, the overall scoring of each timepoint shows that the PTH was slightly lower at 2-hr timepoint in the CC-325 + NPS 2143 treatment group when compared with the CC-325 single agent treatment group.

Figure 35.

Parathyroid hormone Immunohistochemistry staining images.



Note. Representative images of IHC staining for PTH in parathyroid gland from each treatment groups at different timepoints. Animal numbers are provided under each treatment group.

GSPT1

The summary of the IHC H-scores for GSPT1 staining is shown in Figure 33 and

Table 44. The H-Score from vehicle control group shows average GSPT1 in parathyroid gland during the 24-hour measurement period. The mice treated with CC-325 as a single agent or in combination with NPS 2143 had significantly lower level of GSPT1 H-Score in parathyroid gland at all timepoints (0- to 24-hr). The H-Score for mice treated with CC-325 as a single agent was slightly lower than the combination group at 0-, 4-, 6, and 24-hr timepoints. The GSPT1 H-score of the mice treated with NPS 2143 as a single agent did not differ from vehicle control group. The level of GSPT1 in all treatment groups were compared with vehicle control group, and a summary of statistical analysis is shown in

Table 44.

Figure 33.

Mean \pm SEM of PTH H-Score for all treatment groups.

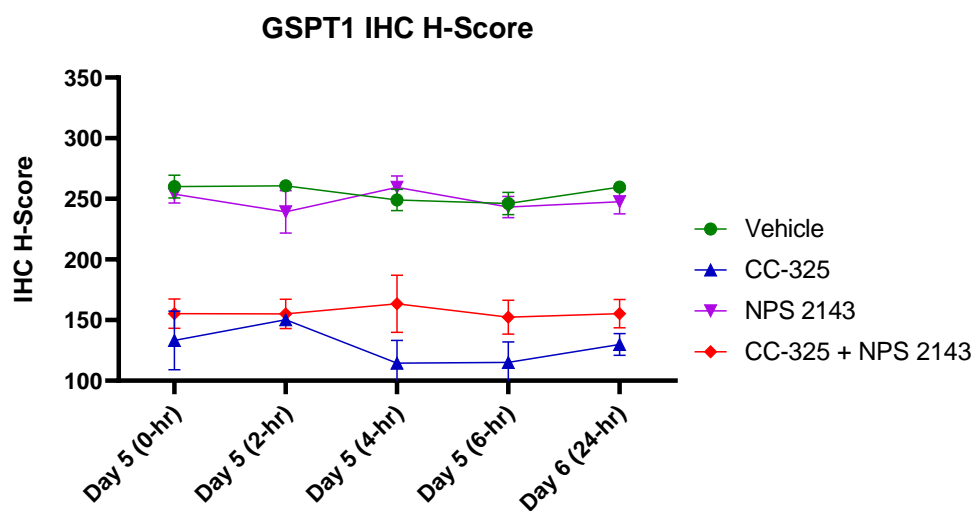


Table 44.

Mean GSPT1 H-Score for IHC Stained Parathyroid Gland Sections.

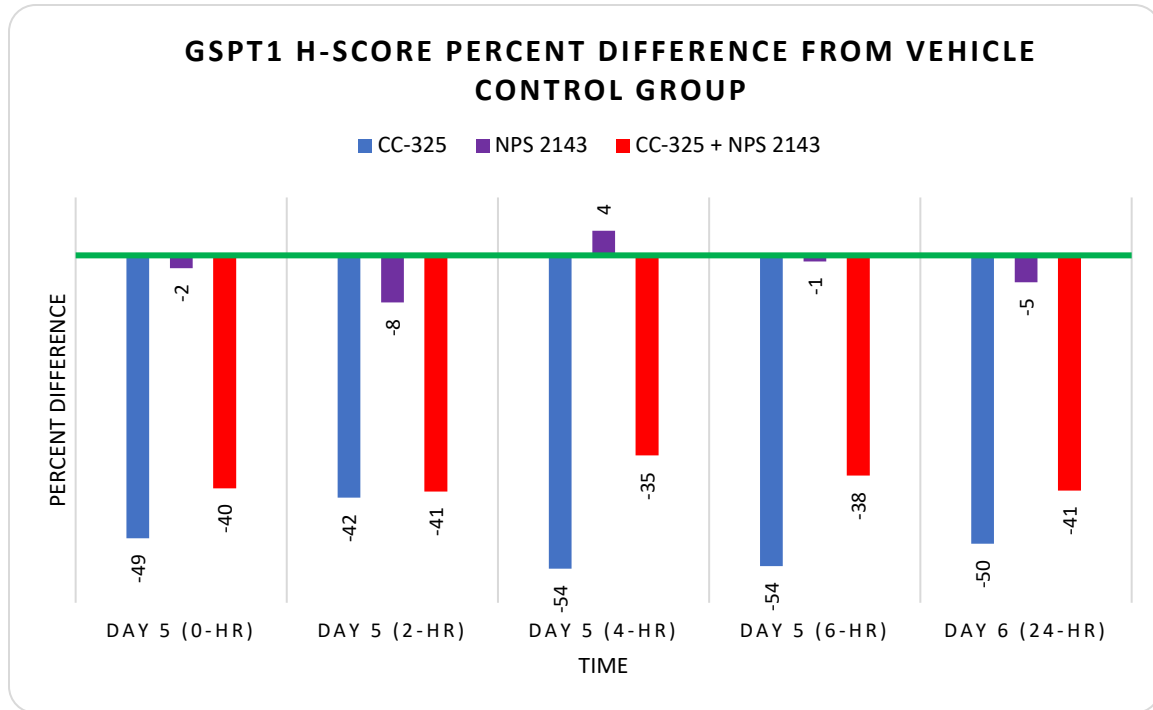
Analyte	Time	Group 1	Group 2	Group 3	Group 4
		Vehicle	CC-325	NPS 2143	CC-325 + NPS 2143
GSPT1 (H-Score)	0-hr	260.0	133.0****	254.2	155.4****
	2-hr	260.7	151.6****	239.5	154.4****
	4-hr	248.8	114.2****	259.4	162.8****
	6-hr	245.9	113.9****	243.3	152.4****
	24-hr	259.6	130.3****	247.5	154.2****

Note. *** = $p \leq 0.001$; **** = $p \leq 0.0001$

The percent difference in GSPT1 H-Scores between test article treated mice and vehicle control group was calculated, and data from this analysis is shown in Figure 34. The percent decrease in H-Scores in the CC-325 single agent treatment group was 42-54%, in CC-325 + NPS 2143 treatment group was 35-41%, and in NPS 2143 single agent treatment group was 2-8%. In NPS 2143 single agent treatment groups, there was a minimal (4%) increase in GSPT1 H-Score at 4-hr timepoint.

Figure 34.

GSPT1 H-Score percent difference from vehicle control group.

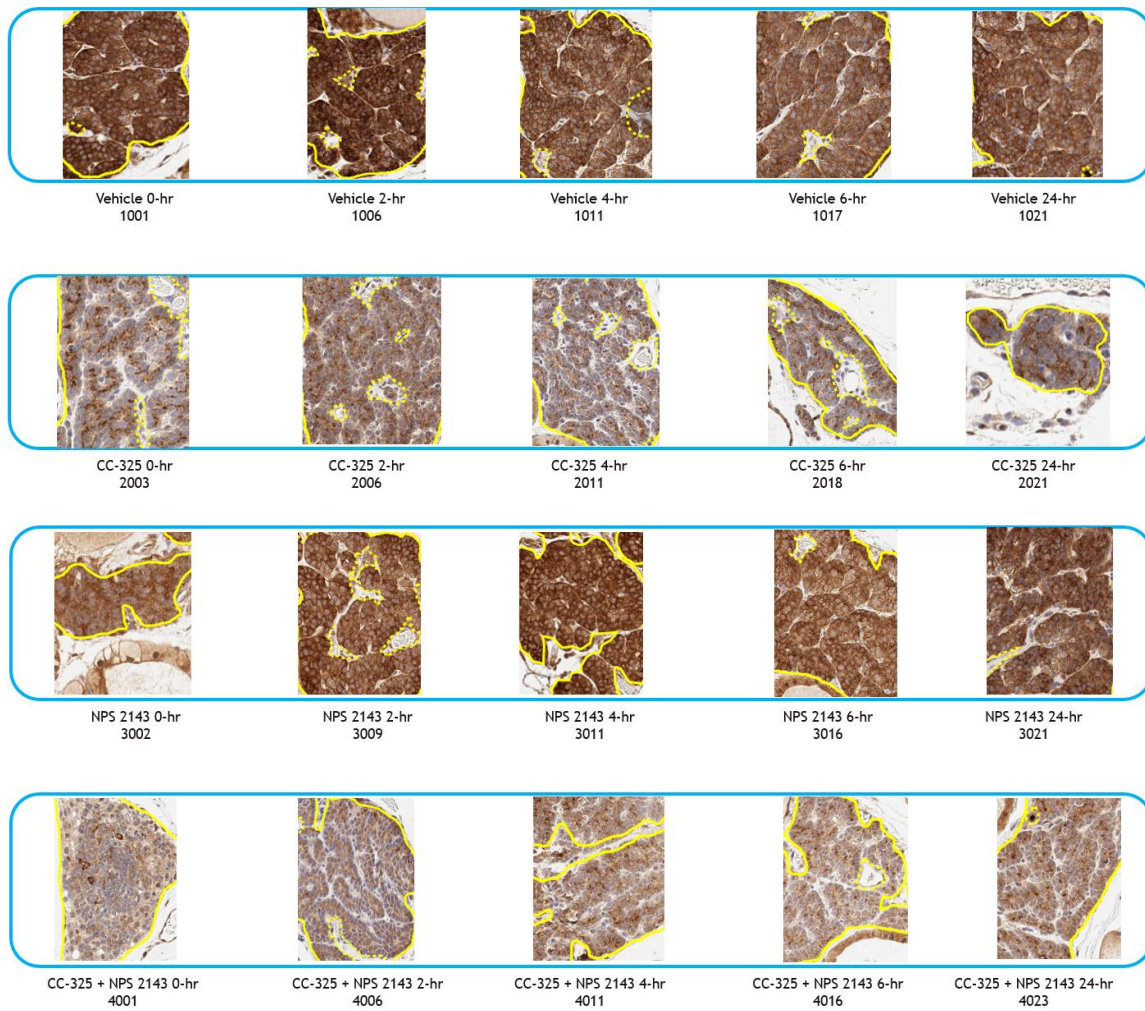


Note. Percent GSPT1 H-Score difference from vehicle control group. The green horizontal line shows the vehicle control GSPT1 IHC H-Score that was used to calculate the percent difference in other treatment groups.

A representative of IHC image for each timepoint is below, Figure 35, are the representation of the GSPT1 staining in parathyroid for each treatment group at different timepoints. The mice in vehicle control group had the highest staining representing the normal GSPT1 in parathyroid. The mice in the CC-325 single agent treatment group (Group2) had decreased staining, which indicates decreased level of GSPT1 in parathyroid at all timepoints. The mice treated with NPS 2143 as a single agent had similar staining to vehicle control group. The mice treated with CC-325 + NPS 2143 had similar staining intensity as CC-325 single agent treatment group, however, the overall scoring of each timepoint shows that GSPT1 in this treatment group is slightly higher than the CC-325 single agent treatment group.

Figure 35.

GSPT1 Immunohistochemistry staining images.



Note. Representation of IHC staining for GSPT1 in parathyroid gland from each treatment groups at different timepoints. Animal numbers are provided under each treatment group.

In Situ Hybridization:

The summary of the ISH H-Score for PTH mRNA is shown in Figure 36 and Table 45. The vehicle control group PTH mRNA H-Score represents the baseline level for huCRBN KI mice. The level of PTH mRNA in all treatment groups were compared with vehicle control group, and a summary of statistical analysis is shown in Table 45. The mice treated with CC-325 only had significantly decreased score at 2-, 4- and 6-hr timepoints. The mice in the CC-325 +

NPS 2143 treatment group had a significant decrease in PTH mRNA H-score at 0-, 2-, and 4-hr timepoints. The mice treated with NPS 2143 as a single agent had an increase in PTH mRNA H-Score at 2-, 4-, 6-, and 24-hr timepoints.

Figure 36.

Mean \pm SEM of PTH m-RNA H-Score for all treatment groups.

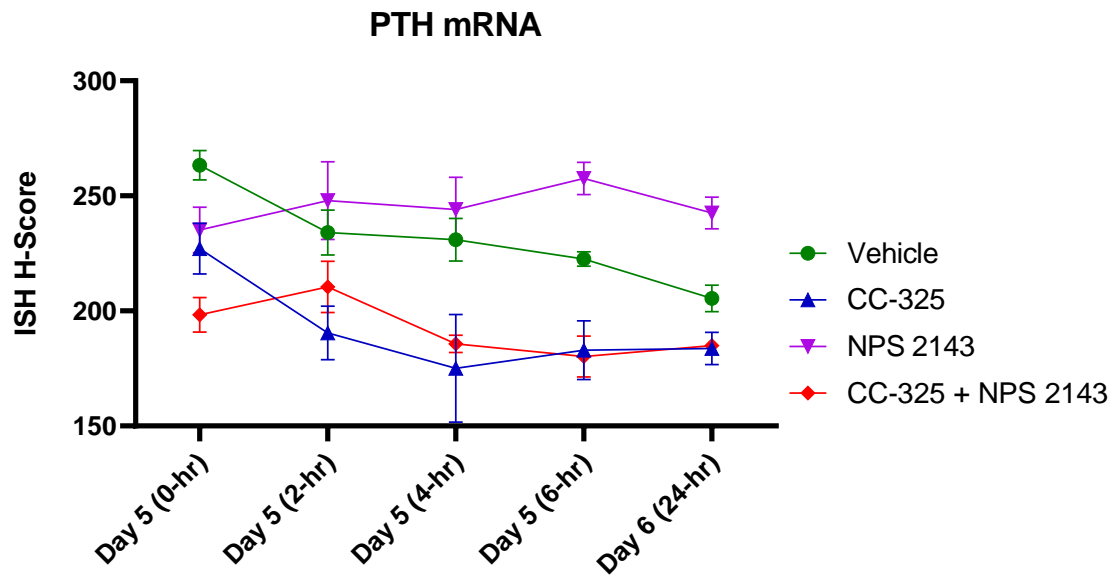


Table 45.

Mean PTH mRNA H-Score for ISH Stained Parathyroid Sections.

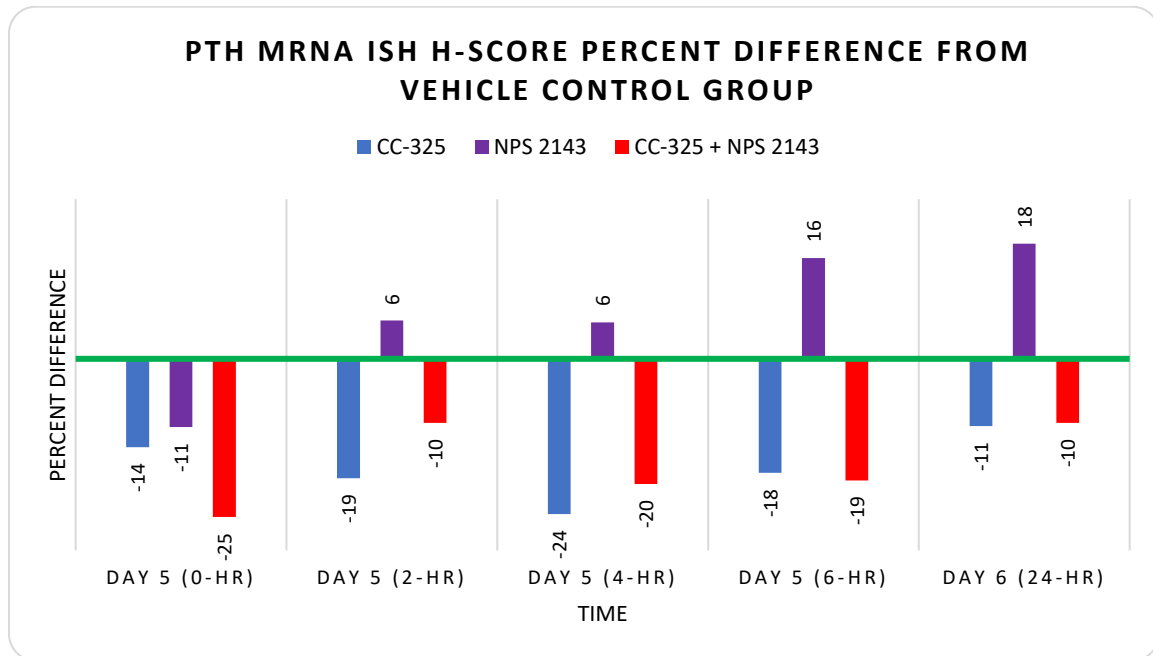
Analyte	Time	Group 1	Group 2	Group 3	Group 4
		Vehicle	CC-325	NPS 2143	CC-325 + NPS 2143
PTH mRNA (H-Score)	0-hr	263.4	226.9	235.3	198.2****
	2-hr	234.0	190.3*	248.0	210.5
	4-hr	230.9	174.8**	244.1	185.7*
	6-hr	222.4	182.7*	257.5	180.1*
	24-hr	205.5	183.9	242.5	184.9

Note. * = $p \leq 0.05$; ** = $p \leq 0.01$; *** = $p \leq 0.001$; **** = $p \leq 0.0001$

The percent change in PTH mRNA mean H-Score for each treatment group was calculated by comparing the difference between the mean H-Score in that group and vehicle control group Table 45. The decrease in mean H-Score in CC-325 single agent treatment group was 14-24%, in the CC-325 + NPS 2143 group the decrease was 10-25%, and in the NPS 2143 single agent treatment group it was decreased at baseline (11%) but that level increased after treatment with NPS 2143 and stayed higher until the 24-hr timepoint (increase of 6-18%), Figure 37.

Figure 37.

PTH mRNA ISH H-Score percent difference from vehicle control group.

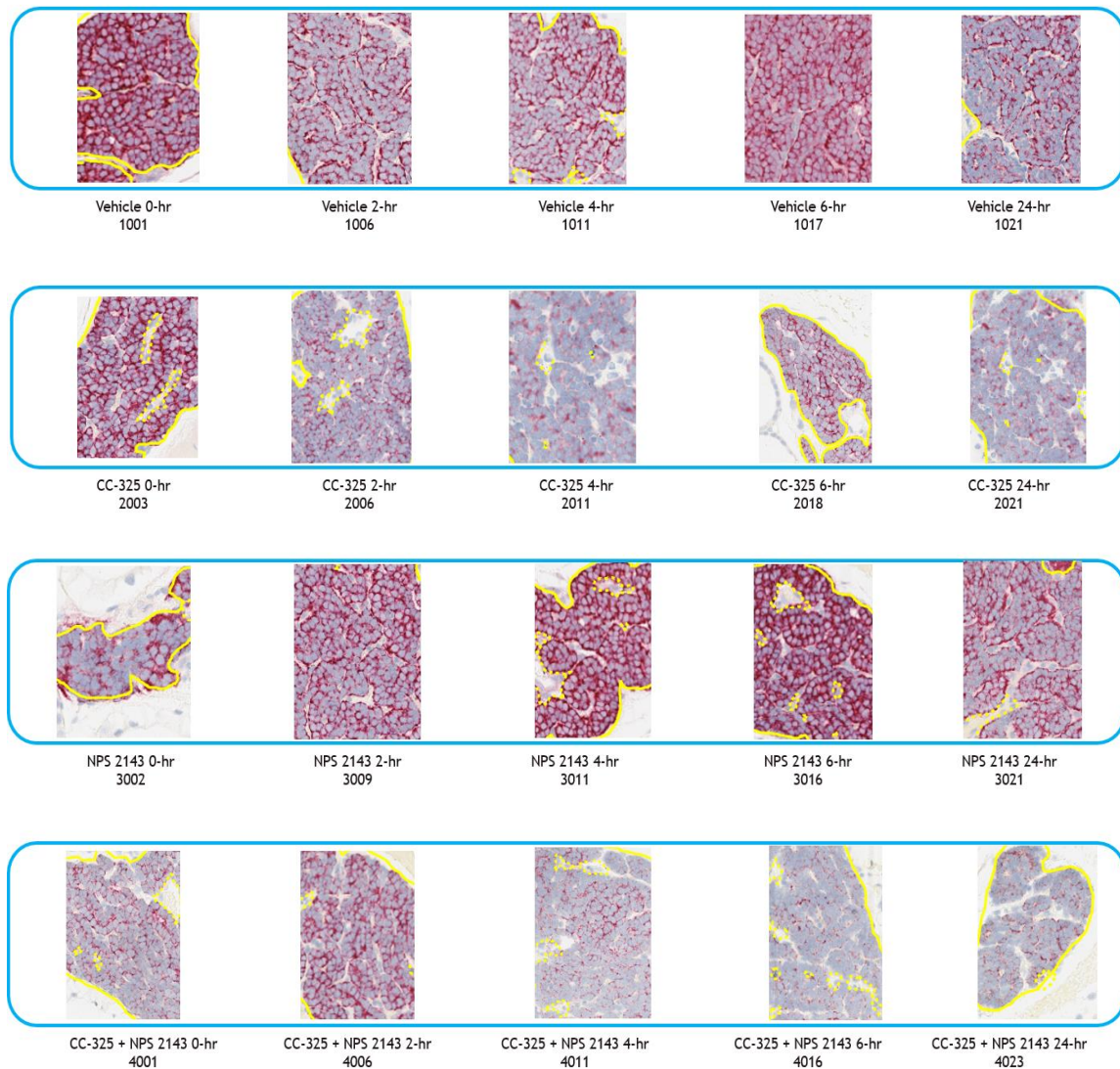


Note. Percent PTH mRNA ISH H-Score difference from vehicle control group. The green horizontal line shows the vehicle control H-scores that was used to calculate the percent difference in other treatment groups.

A representative of PTH mRNA ISH image for each timepoint is shown in Figure 38. These images are the representation of the PTH mRNA ISH staining in parathyroid for each treatment group at different timepoints. The mice in vehicle control group had the highest staining representing the normal level of PTH mRNA in parathyroid. The mice in the CC-325 single agent treatment group (Group2) had decreased staining, which indicated decreased levels of PTH mRNA in parathyroid at all timepoints. The mice treated with NPS 2143 as a single agent had moderately darker staining when compared to vehicle control group. The mice treated with CC-325 + NPS 2143 had similar staining intensity as CC-325 single agent treatment group, although the staining at 2-hr timepoint in CC-325 + NPS 2143 treatment group was slightly stronger than CC-325 single agent treatment group.

Figure 38.

PTH mRNA In Situ hybridization staining images.



Note. Representative of ISH stain for PTH mRNA from each treatment groups at all timepoints. Animals numbers are listed below each treatment group.

Hypothesis Testing

Hypothesis 1: Treatment of huCRBN KI mice with CC-325 will inhibit the synthesis of Parathyroid Hormone

H₀1: After 5 days of treatment with CC-325, a single dose administration of NPS 2143 will not increase the serum parathyroid hormone and serum iCa^{2+} .

H_A1: After 5 days of treatment with CC-325, a single dose administration of NPS 2143 will increase serum parathyroid hormone and iCa^{2+} .

To test this hypothesis, the change in iCa^{2+} and PTH in vehicle and CC-325 treated groups were measured. Treatment with CC-325 for 5 days as a single agent and in combination with NPS 2143, decreased the level of iCa^{2+} and serum PTH by the average of 30% at 0-hr timepoint when compared with vehicle control group, Figure 39 and Figure 40. It was also shown that treatment with a single dose of NPS 2143 increased PTH and subsequently iCa^{2+} , by as much as 910% and 29%, respectively. However, the mice treated with CC-325 and then treated with NPS 2143 did not show significant increase in PTH or iCa^{2+} when compared with either vehicle control group or CC-325 single agent treatment group, Figure 41.

The percent difference between serum PTH in CC-325 + NPS 2143 and CC-325 as a single agent is shown in Figure 41, and these data shows only a minimal increase in PTH at 2- and 4-hr post NPS 2143 treatment. Clearly, this minimal increase in PTH was not enough to restore normocalcemia. Statistical analysis was conducted to compare these two groups, and the results showed that there were no significant differences in PTH (Figure 39) and iCa^{2+} (Figure 40) between mice treated with CC-325 as a single agent or CC-325 + NPS 2143. These data support the null hypothesis that there were no differences in PTH and iCa^{2+} between treatment with CC-325 as a single agent or CC-325 + NPS 2143. Therefore, it can be concluded that the NPS 2143 is unable to increase PTH in mice treated with CC-325 to restore normocalcemia. In other words, CC-325 inhibits PTH production in mice treated with CC-325 for at least 5 days.

Figure 39.

Mean (\pm SD) of PTH for groups administered CC-325.

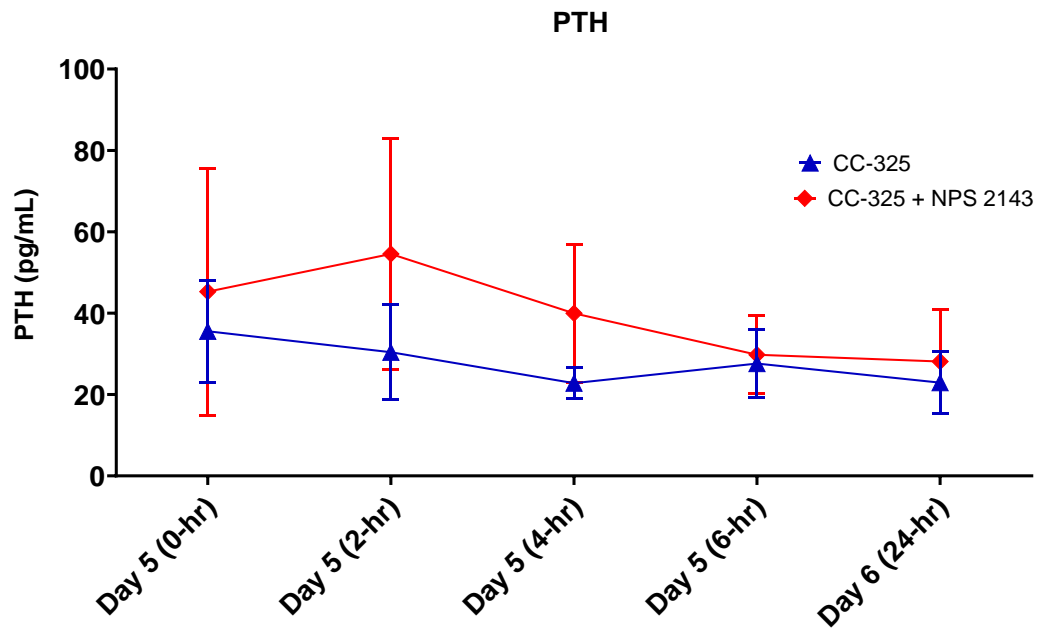


Figure 40.

Mean (\pm SD) of iCa^{2+} for groups administered CC-325.

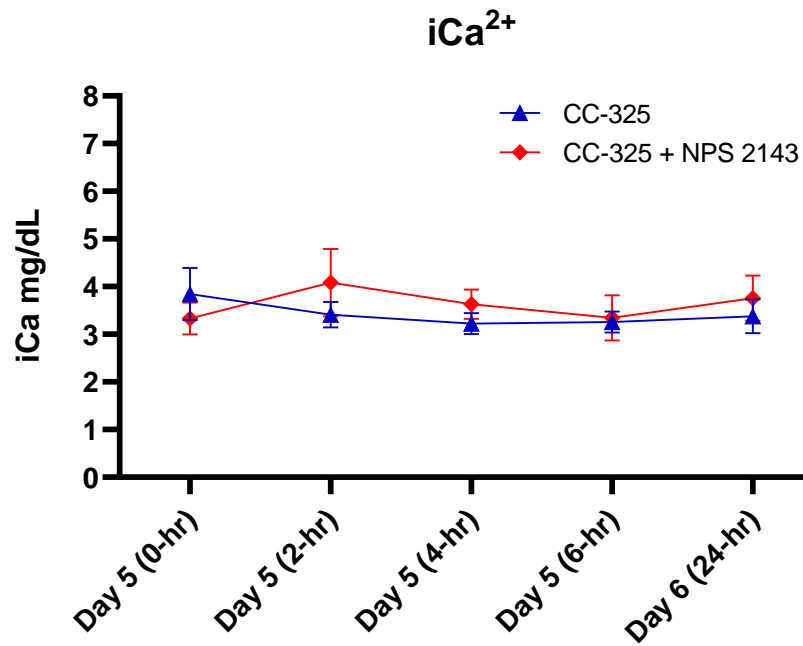
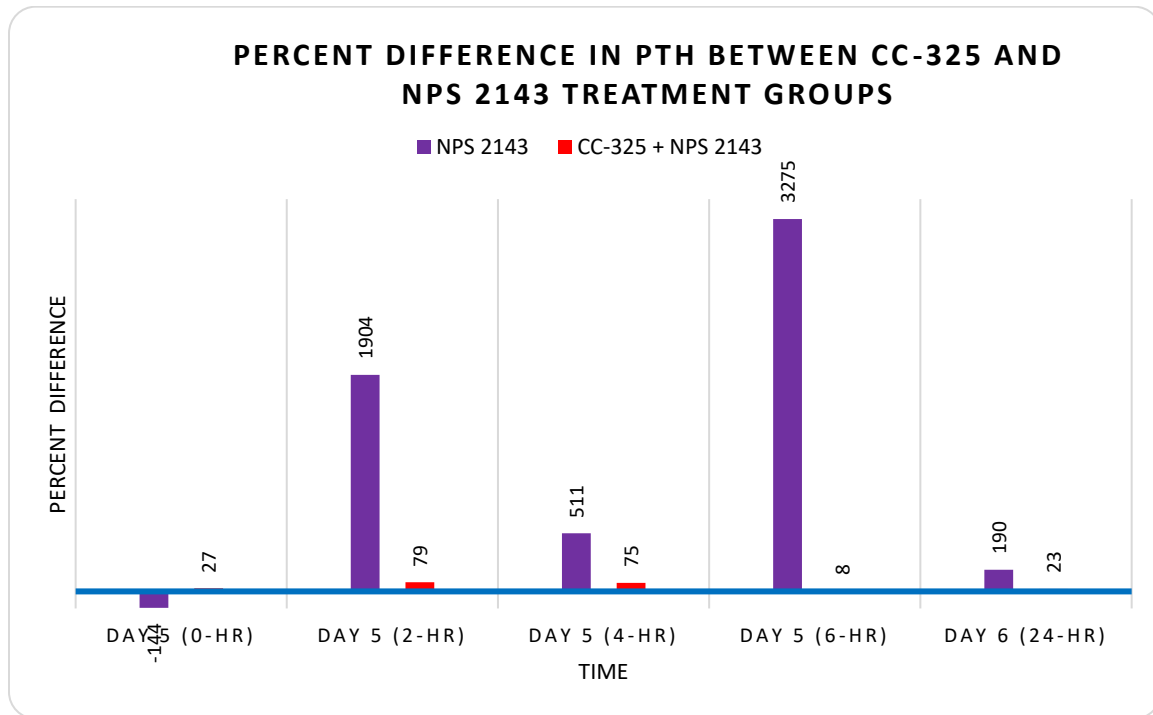


Figure 41.

Percent difference in PTH between CC-325 and NPS 2143 treatment groups.



Note. Percent PTH difference between CC-325 single agent, combination and NPS 2143 treatment groups. The blue horizontal line is the CC-325 single agent treatment group value set as baseline that is used to calculate the percent difference with other two treatment groups.

Hypothesis 2: Treatment of huCRBN KI mice with CC-325 does not affect the secretion of parathyroid hormone from the parathyroid gland.

H₀2: After 5 days of treatment with CC-325, with or without a single dose administration of NPS 2143, serum parathyroid hormone levels correlate with the intracellular parathyroid hormone levels.

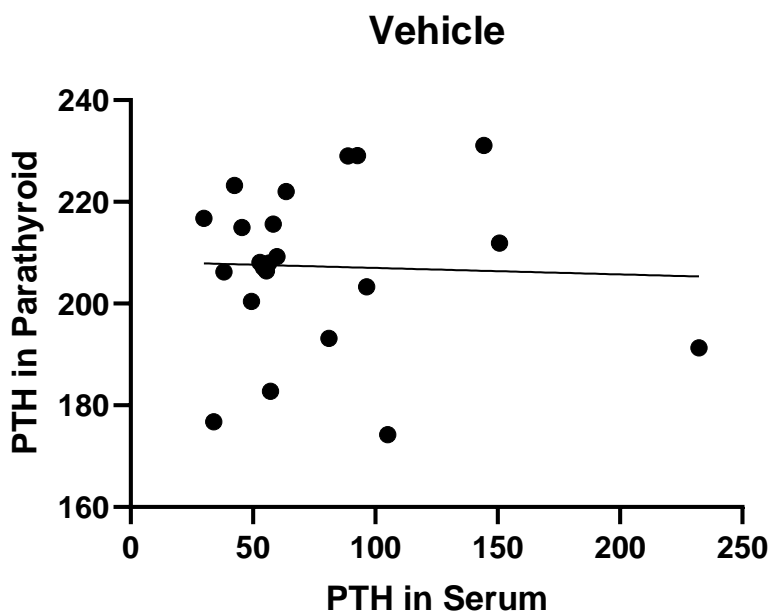
H_A2: After 5 days of treatment with CC-325, with or without a single dose administration of NPS 2143, there is no correlation between serum parathyroid hormone level and intracellular parathyroid hormone level.

To test our null hypothesis, a Pearson's correlation analysis was conducted. The correlation analysis was performed between serum concentration and PTH and IHC H-scores in parathyroid gland. The serum PTH concentration in each group was compared with H-score in that treatment group. The Pearson coefficient determined the correlation coefficient, relationship, and the strength of the association between serum and intracellular PTH concentrations. The correlation coefficient “r” and R^2 for all treatment groups are shown in Table 46.

Correlation score “r” for vehicle control group was -0.0376 ($R^2 = 0.0014$) and the p value was 0.8679, indicating that there is no strong correlation between the serum PTH concentration and the level of PTH in parathyroid gland. Figure 42 shows the correlation data for this treatment group.

Figure 42.

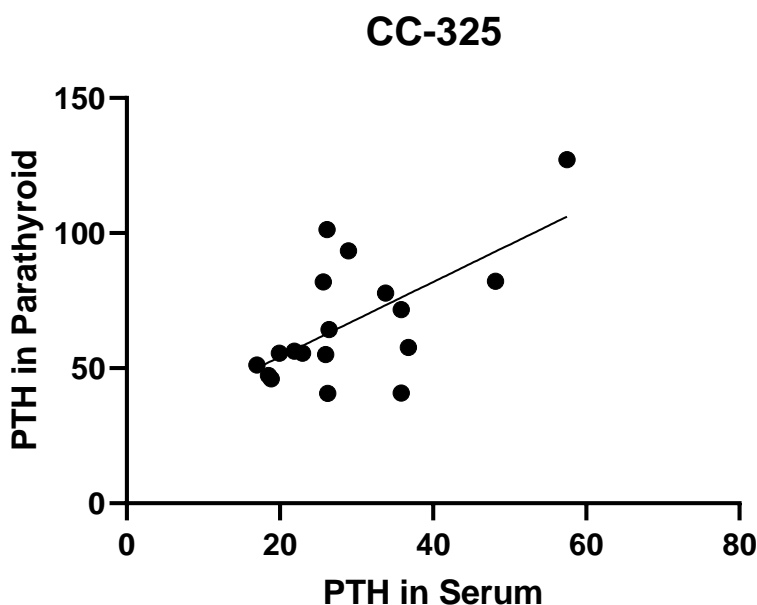
Correlation analysis of serum and intracellular PTH in vehicle treated mice.



The correlation score “r” for mice treated with CC-325 as a single agent was 0.6341 ($R^2 = 0.4021$) and the p value of 0.00047 indicating that there is a strong correlation between the serum and intracellular PTH. Figure 43 shows the correlation data for this treatment group. Since the level of serum and intracellular PTH have correlation and the p value indicates that “r” is significantly different from zero (0) (meaning the correlation is not by chance) we can conclude that null hypothesis is true.

Figure 43.

Correlation analysis of serum and intracellular PTH in CC-325 treated mice.

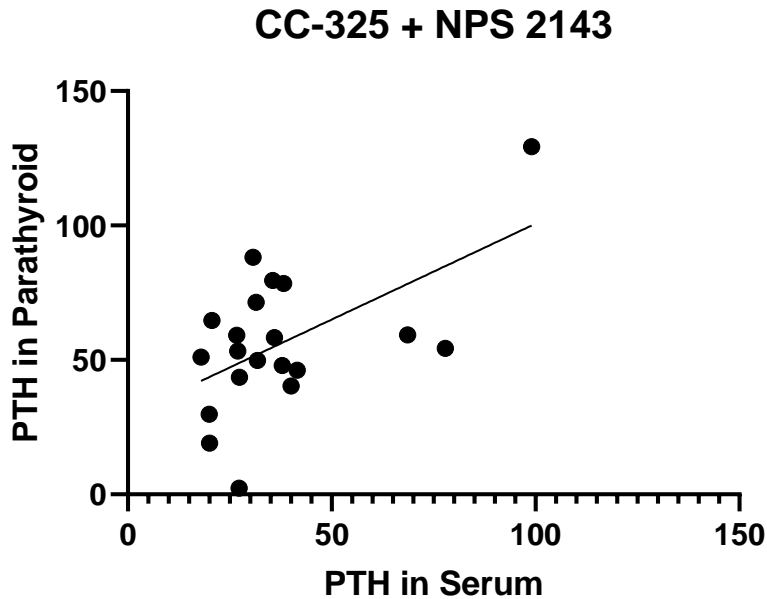


The data from other treatment groups also support the null hypothesis. The correlation between serum and intracellular PTH in mice treated with CC-325 + NPS 2143 was also measured, Figure 44. The “r” score for this group was 0.5597 ($R^2 = 0.3313$) with a p value of 0.0103 indicating that there is a moderate correlation between serum and intracellular PTH, Table 46. Despite administration of NPS 2143, which has been shown to increase serum PTH and iCa^{2+} , there is no increase in serum PTH and iCa^{2+} in these mice. This data further supports

the null hypothesis that there is no sequestration of PTH in parathyroid gland and parathyroid releases all the available PTH upon stimulation.

Figure 44.

Correlation analysis of serum PTH and intracellular PTH in CC-325 + NPS 2143 mice.



The “r” score for NPS 2143 only treatment group, was -0.5868 ($R^2 = 0.3443$) and the p value was 0.0026, indicating that there is a moderate inverse correlation between the serum and intracellular PTH following administration of NPS 2143, Table 48.

Figure 45.

Correlation analysis of serum and intracellular PTH in NPS 2143 treated mice.

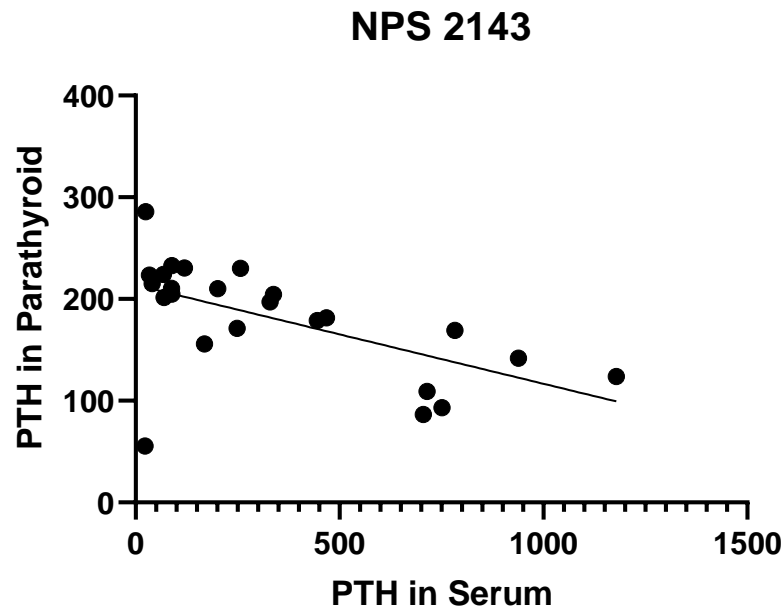


Table 46.

Correlation Coefficient Values for Comparing Serum PTH and IHC H-Score for amount of PTH in Parathyroid Gland.

	Group 1	Group 2	Group 3	Group 4
Value	Vehicle	CC-325	NPS 2143	CC-325 + NPS 2143
r^*	-0.0376	0.6341	-0.5868	0.5597
R^2	0.0014	0.4021	0.3443	0.3133
P (two-tailed)	0.8679	0.0047	0.0026	0.0103
Number of XY Pairs	22	18	24	20

Note. * = Pearson r

Hypothesis 3: Treatment of huCRBN KI mice with CC-325 regulates parathyroid hormone production at transcription level.

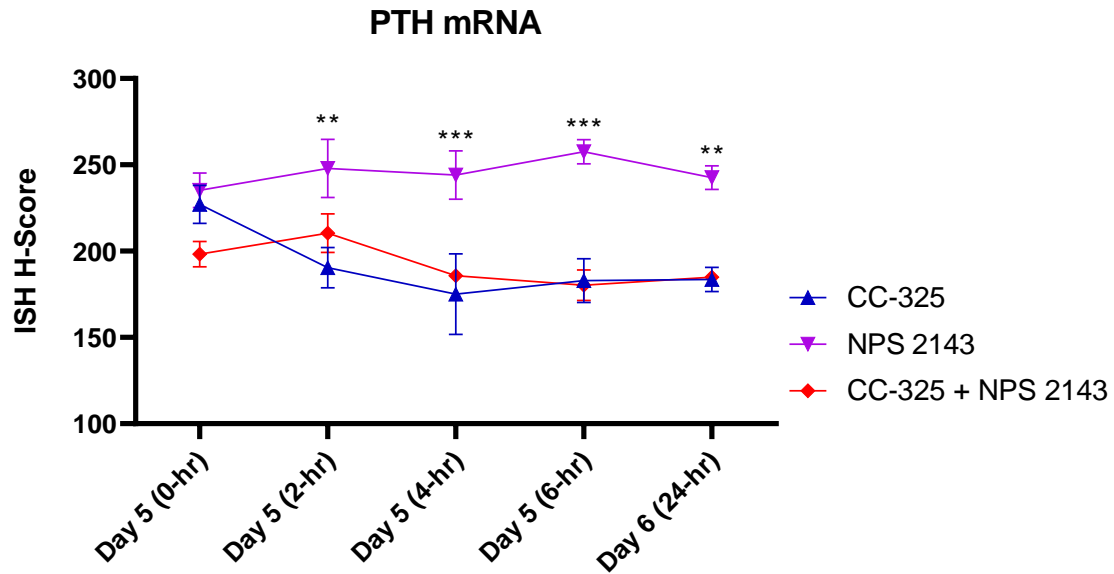
H₀3: Treatment with CC-325 has no effect on parathyroid hormone mRNA.

H_A3: Treatment with CC-325 decreases parathyroid hormone mRNA

The essence of this hypothesis is that the decrease in serum PTH is due to decrease in PTH synthesis or instability of PTH mRNA that could lead to decrease in PTH. To test this hypothesis, the level of PTH mRNA in the parathyroid Chief cells was measured. This test was performed by in situ hybridization staining. The data from this analysis is shown in Figure 36. The intensity of stain was scored using HALO software, the results of this analysis is show below in Table 47. Our assumption was that vehicle control group represents the normal level of PTH mRNA in parathyroid, Figure 36. The percent difference between CC-325 single agent treatment, CC-325 + NPS 2143, and NPS 2143 treatment groups is shown in Figure 47. At 0-hr timepoints (1- hour post CC-325 treatment) the PTH mRNA score in CC-325 single agent treatment group and CC-325 + NPS 2143 was 227, and 198, respectively. After treatment with NPS 2143, the level of PTH mRNA in NPS 2143 single agent treatment groups moderately increased, however, the increase in CC-325 + NPS 2143 was minimal. A statistical analysis was performed, indicating that the only difference in PTH mRNA is between CC-325 single agent and NPS 2143 single agent treatment groups. This further confirms that PTH mRNA production is not increasing in CC-325 + NPS treatment groups.

Figure 46.

Mean \pm SEM of PTH H-Scores for CC-325, CC-325 + NPS 2143, and NPS 2143 treatment groups.



Note. ** = $p \leq 0.01$; *** = $p \leq 0.001$

Values of NPS 2143 and CC-325 + NPS 2143 were compared with CC-325 single agent treatment group.

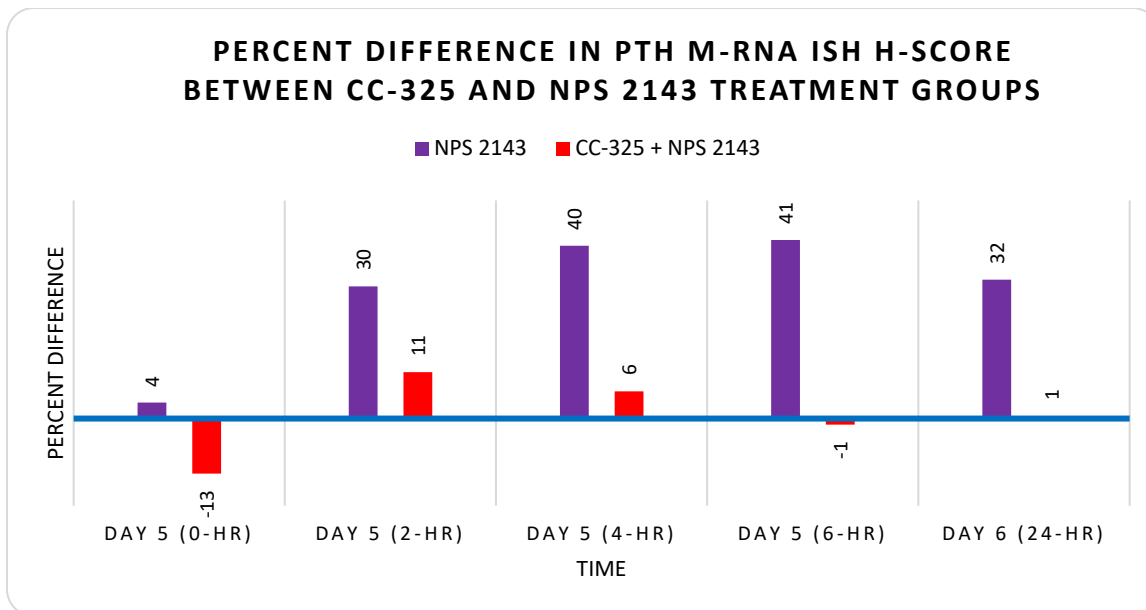
Table 47.

Mean PTH mRNA H-Score for ISH Stained Parathyroid Sections.

Analyte	Time	Group 1	Group 2	Group 3	Group 4
		Vehicle	CC-325	NPS 2143	CC-325 + NPS 2143
PTH mRNA (H-Score)	0-hr	263.4	227.1	235.2	198.3***
	2-hr	234.0	190.5*	247.9	210.5
	4-hr	230.9	175.0**	244.1	185.7*
	6-hr	222.6	182.9*	257.6	180.2*
	24-hr	205.4	183.6	242.6*	185.0

Figure 47.

Percent difference in PTH mRNA ISH H-Score between CC-325 and NPS 2143 treatment groups.



Note. Percent difference in PTH mRNA ISH H-Score between CC-325 and CC-325 + 2143 and NPS 2143 treatment Groups. The blue horizontal line is the CC-325 single agent treatment group value set as baseline that is used to calculate the percent difference with other two treatment groups.

Hypothesis 4: After treatment with CC-325, serum FGF23 decreases.

H₀4: After 5 days of treatment with CC-325, serum FGF23 concentration don't change.

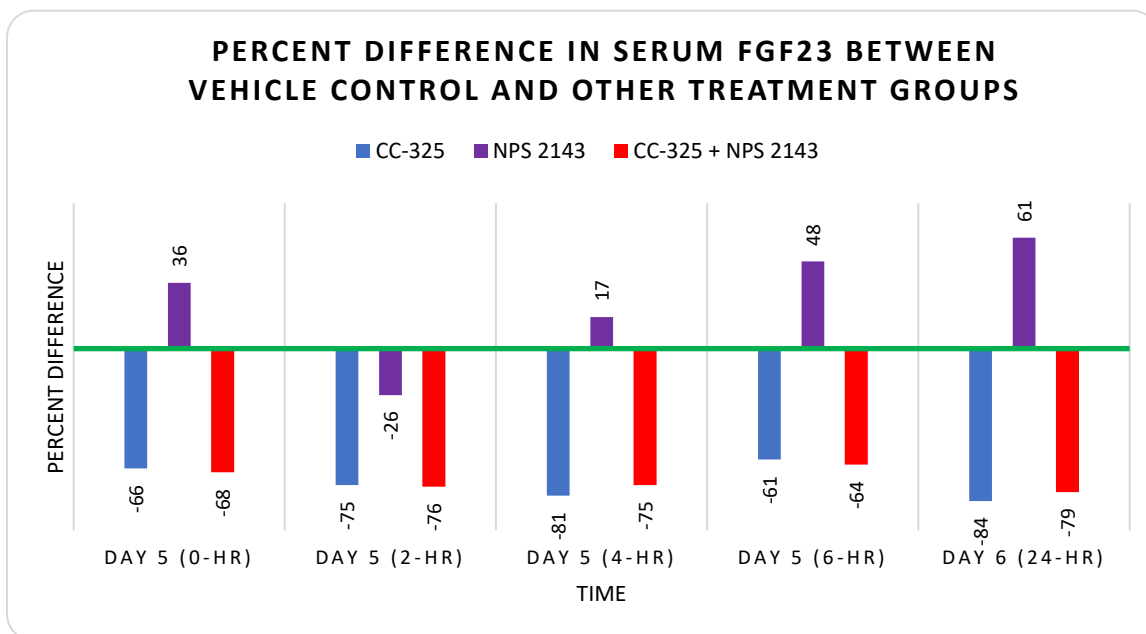
H_A4: After 5 days of treatment with CC-325, serum FGF23 concentration decreases.

To test this hypothesis, serum samples from all treatment Groups were analyzed for FGF23. The results are summarized and shown in Table 41 (page 113). To test the null hypothesis, we made an assumption that the values from vehicle control group provides the baseline for FGF23 in huCRBN KI mice. Animals treated with CC-325 and CC-325 + NPS 2143 both had decreases in FGF23 when compared with vehicle control group. The statistical analysis is summarized and shown in Table 41 (page 113); these data show FGF23 levels in CC-325 and CC-325 + NPS 2143 treatment groups were significantly different from vehicle control group at

all timepoints. The percent difference in FGF23 between vehicle and other treatment groups was calculated, these data are shown in Figure 48, which indicate an increase in FGF23 in NPS 2143 alone treatment group and a decrease in FGF23 in CC-325 treatment groups (CC-325 and CC-325 + NPS 2143). These results, collectively support the rejection of null hypothesis and acceptance of alternative hypothesis, meaning, after treatment with CC-325, the serum concentration of FGF23 decreases.

Figure 48.

Percent difference in serum FGF23 between vehicle control and other treatment groups.



Note. Percent difference in serum FGF23 between vehicle control and CC-325 and CC-325 + 2143 and NPS 2143 treatment Groups. The green horizontal line is the vehicle control treatment group value set as baseline that is used to calculate the percent difference with other two treatment groups.

Summary

This chapter presented the data and statistical analyses for each of the study objectives and hypotheses. In this study, we demonstrated that degradation of GSPT1 by CC-325 in huCRBN KI mice caused a decrease in serum PTH. This finding was further confirmed by administration of NPS 2143, a potent negative allosteric modulator of CaSR that, by itself,

increases PTH. Mice treated with CC-325 did not have an increase in serum PTH post administration of NPS 2143, confirming the first hypothesis. To investigate the cause of the decrease in PTH after administration of CC-325 and lack of increase in PTH after administration of NPS 2143, additional hypotheses were tested.

We hypothesized that the lack of increase in PTH is due to a decrease of PTH in parathyroid chief cells and not impaired PTH release from parathyroid. This hypothesis was tested by measuring and correlating extracellular (serum) and intracellular (in chief cells) PTH levels. Data supported our hypothesis that the level of serum and intracellular PTH have strong positive correlation.

Third, the lack of PTH production was investigated. We hypothesized that the decrease in PTH production was due to decline in PTH mRNA. To test this hypothesis, the level of PTH mRNA in Chief cells was measured by in-situ hybridization staining. The data supported the rejection of null hypothesis and supported the alternative hypothesis that there is a decrease in PTH mRNA in Chief cells.

These data collectively support the conclusion that treatment with CC-325 decrease PTH mRNA, which leads to decline parathyroid PTH and subsequently to decrease in serum PTH that eventually manifest as hypocalcemia. Treatment with NPS 2143 did not increase PTH mRNA, therefore was unable to restore normocalcemia in these mice.

Finally, the concentration of FGF23 in all treatment groups was measured, with the goal of this measurement to determine the change in FGF23 concentration in response to change in PTH under hypocalcemia condition. Decreases in serum FGF23 concentration, even during the hyperphosphatemic state with a nadir in PTH levels, is consistent with the notion that PTH plays a key role in maintaining the FGF23 serum concentration.

CHAPTER FIVE: DISUSSION

This chapter presents a review of the results presented in Chapter four. The results are presented in the context of the listed hypotheses, clinical implications and in comparison, to the literature and historical reviews where available. Limitations of the study and the recommendations or the future studies are also discussed in this chapter.

Overview of the Problem

Hypocalcemia is a potentially life-threatening condition that if not treated can be fatal. The causes of hypocalcemia have been discussed in detail in Chapter Two, among them is drug induced hypocalcemia. One of drugs that can cause hypocalcemia is CC-325, which is a potent degrader of GSPT1. The goal of this research was to investigate the mechanism of hypocalcemia induced by GSPT1 degradation in mice. Prior to conducting this experiment, several in vivo studies were conducted (in-house studies) to evaluate the sensitivity of the huCRBN KI mice to CC-325. As the result of these studies, the magnitude of hypocalcemia could be predicted based on the dose and duration of CC-325 treatment in huCRBN KI mice. The data from in-house investigative studies revealed that despite hypocalcemia in mice, PTH is not increased. Calcium homeostasis is normally maintained by the parathyroid gland, kidney, bone, and intestine, with multiple points of regulation. The parathyroid gland responds to changes in iCa^{2+} concentration in the extracellular space and alters the secretion of PTH (Hakami & Khan, 2019). The concentration of PTH in plasma regulates calcium resorption from bone, calcium reabsorption by the renal tubules, and vitamin D activation in the kidney, which promotes calcium and phosphate absorption in the intestines (M. Lee & Partridge, 2009). Therefore, the lack of increase in PTH in mice treated with CC-325 was a significant finding and triggered the investigation into the following questions:

1. Does GSPT1 degradation in huCRBN KI mice inhibits PTH increase even when stimulated with potent negative allosteric modulator of CaSR?
2. Does GSPT1 degradation in huCRBN KI mice cause sequestration of PTH in parathyroid?
3. Does GSPT1 degradation in huCRBN KI mice affect PTH mRNA level in parathyroid?
4. Does decrease in PTH affect the serum concentration of FGF23 in huCRBN KI mice?

Discussion of the Studies

Human CRBN KI mice are transgenic mice that were produced by Celgene Corporation in collaboration with a contract research organization. These mice are not available to researcher outside of the Celgene organization therefore there is little publication on the use of these mice in research. Internally, Celgene scientists have used these mice for several years and there are internal data on the characteristics and biology. Several studies have been conducted to investigate the utility of these mice for GSPT1 related hypocalcemia.

Pilot Study

The purpose of the pilot study was two-fold: first, to find the tolerable dose of NPS 2143 in huCRBN KI mice that can cause measurable increases in PTH and iCa^{2+} , and second, to determine the dynamic range for PTH and iCa^{2+} in these mice. To find the dynamic range, we also used NPS R-568 to induce hypocalcemia by decreasing PTH in these mice. Since there were no published data on use of these compounds in huCRBN KI mice, the pilot study was essential to obtaining this information. The selection of formulation and the initial dose of the NPS 2143 in mice was based on the published data (Gowen et al., 2000), however based on our initial pilot data, the dose of NPS 2143 for the main study was optimized. The magnitude of increase in PTH and iCa^{2+} concentrations in the pilot were consistent with the published data

(Hannan et al., 2015) however, the actual concentrations for PTH were different. This could be due to several factors including the source of NPS 2143, the strain of mice, the method of PTH measurement and the study design (i.e. blood collection timepoints in study). The source of NPS 2143 for this experiment was Millipore Sigma, whereas the source of NPS 2143 in the Gowen et al., 2000 study was NPS pharmaceuticals. The bleeding of mice in this experiment was not serial, whereas the data from the literature was from serial bleeding. Finally, and most important is that huCRBN KI mice were used in this experiment, which had no precedent prior to this pilot study.

Data from pilot study revealed an approximately 18-fold increase in PTH over vehicle control group at peak, which was 2-hr after the administration of NPS 2143. Ionized and total calcium were increased and peaked at 2-hour postdose. There were no changes in electrolytes in the NPS 2143 treatment group when compared with vehicle control group. These data showed that NPS 2143 at 200 mg/kg can cause an acute increase PTH and iCa^{2+} in huCRBN KI mice.

Interference studies

The purpose of the interference studies was to investigate the effects of test articles, CC-325 and NPS 2143, on PTH and FGF23 ELISA assays when they are present in high concentrations in serum. Data from the interference studies showed that low concentrations of test articles had minimal effects on the serum PTH and FGF23 measurement.

At the time of this interference study, no huCRBN KI mouse Pharmacokinetic (PK) data was available to guide the concentration selection for the interference study, therefore, a wide range of concentrations were selected. The selected range of 0.61 to 20 μ M was based on projected high and low concentration of each test article in huCRBN KI mice. Data from the PTH assay showed dose dependent negative effect on the serum PTH at all CC-325 concentrations except

1.25 μM , which has a positive effect of 7%. The highest and the lowest effects were the decrease of 8% and 2% in serum PTH measurement, which were observed at 20 and 0.61 μM respectively. These effects, particularly at lower concentration of CC-325, were close to the PTH inter-assay CV, which was 5.5%, and are not considered significant.

The effect of NPS 2143 on the PTH assay was limited to 5% decrease in serum PTH measurement at all NPS 2143 concentrations except 1.25 μM , which resulted in the increase of 5% in serum PTH. Overall, the effect of NPS 2143 on PTH measurement was $\pm 5\%$, which was within the assay CV.

The effects of test articles on the FGF23 assay was slightly different than the PTH assay. The CC-325 in the serum resulted in 1-9% decrease in serum FGF23 at the concentration of 0.61 to 20 μM . The effects were not dose dependent, since the highest negative effect was observed at 0.61 and 20 μM and the lowest effect at 2.5 μM . The average effect of the concentrations ≤ 2.5 μM was 4.8%. Considering that the inter-assay CV for FGF23 was 4.4%, the impact of the CC-325 on serum FGF23 measurement was considered minimal.

The effect of NPS 2143 on the serum FGF23 measurement was more pronounced and not dose proportional. NPS 2143 had negative effect of 2 to 17 % on serum FGF23 measurement between 0.61 to 20 μM concentrations. One potential contributing factor for this large negative effect was shortage of naïve serum for testing for this assay. Due to this shortage, the results for naïve serum and naïve serum + DMSO from the adjust wells (A&B 3 and 4) were used for A&B 5 and 6 wells. This duplication of data from one column to another might have contributed to large effect of NPS 2143 on serum FGF23 measurement. Overall, the average negative effect for the four concentrations between 1.25 to 10 μM was 3.7%, which was below the inter-assay

CV of 4.4%. Based on these data, it is reasonable to conclude that the lower concentrations of NPS 2143 had minimal effect of the serum FGF23 measurement.

Main Study

Clinical findings

The goal of this experiment was to investigate the mechanism of hypocalcemia observed in huCRBN KI mice after administration of CC-325, a potent GSPT1 degrader. To investigate this mechanism, an *in vivo* experiment was designed and conducted. Samples from this experiment were collected at endpoints listed in the method section. The dose of CC-325 for the experiment were selected based on the historical in-house data, which showed that the dose of 15 mg/kg BID for 5 days would be tolerated, but cause hypocalcemia. As expected, moderate body weight loss was observed in the CC-325 treatment groups, however all animals tolerated the treatment until schedule necropsy. The body weight in the CC-325 treatment groups, either as a single agent or combination with NPS 2143 was significantly decreased on Days 3 through 5. Since animals treated with NPS 2143 as a single agent were only treated on Day 5, they were weighed only on that day. Their body weight on Day 5 was consistent with vehicle control group.

Exposure of CC-325 and NPS 2143 in mice

The exposures of CC-325 and NPS 2143 in mice were consistent. The exposures of CC-325 and NPS 2143 were measured both as single agent and in combination group with each other. On Day 5, CC-325 was dose one hour prior to NPS 2143 administration, therefore the CC-325 TK timepoints were one hour longer than the NPS 2143 TK timepoints. The exposure (AUC_{0-25}) of CC-325 in the mice treated with CC-325 as a single agent was 10.1 $\mu\text{M}\cdot\text{hr}$, while CC-325 exposure in the combination groups was slightly higher at 14.7 $\mu\text{M}\cdot\text{hr}$. Although the

exposure in the combination group was 50% higher than the CC-325 as a single agent, this increase was not considered significant. Several factors might have contributed to the exposure difference between these two treatment groups. They include small n size for each timepoint, animal to animal variation, lack of serial bleeding in the TK groups, and the analytical variability. Although the effects of drug-drug interaction could not be ruled out, the magnitude of difference between these two exposures did not point to drug-drug interaction as a cause of increase in exposures in the combination group.

The exposure of NPS 2143 in huCRBN KI mice both as a single agent and combination with CC-325 was measured. The exposure (AUC_{0-24}) of NPS 2143 as a single agent was 6.2 $\mu\text{M}\cdot\text{hr}$ and 16.6 $\mu\text{M}\cdot\text{hr}$ in combination group. Similar factors that might have contributed to CC-325 exposure differences could have contributed to the NPS 2143 exposure differences as well. However, the NPS 2143 exposure in combination groups was roughly 3-fold higher than NPS 2143 as a single agent, therefore the drug-drug interaction could not be ruled out. In order to investigate the drug-drug interaction between these two molecules, additional in vitro assays must be conducted. These assays include cytochrome p450 inhibition assay, which could reveal if the NPS 2143 metabolism was affected. Additional assays such as transporters function assessment could be performed to investigate the absorption or the clearance of the NPS 2143 in the combination group. The increase in the NPS 2143 exposure in the combination group might have resulted in increased pharmacological effects of NPS 2143 in that group, however, we were not able to measure that increase in our experiment.

Accuracy of total calcium measurement

The albumin concentration had no effect of calcium concentration. The degree of change in ionized and total calcium was consistent during the study. There was no significant change in

albumin or total protein in any of the treatment groups, indicating that the change in calcium concentration was real and not affected by albumin concentration. The percent drop in calcium concentration in this experiment was consistent with the drop in the previous in-house studies with CC-325.

The impact of protocol deviation on study integrity

As noted earlier, there was a protocol deviation, which resulted in administration 120 mg/kg of NPS 2143 instead of 200 mg/kg as described in the protocol. However, since increase in PTH and iCa^{2+} in this experiment was similar to the pilot study, it can be concluded that the protocol deviation had no impact on the integrity of the study.

The impact of parathyroid necrosis on PTH production

Histologic evaluation of the parathyroid gland revealed minimal to mild necrosis in mice treated with CC-325. It is feasible that single cell necrosis in parathyroid had some impact on PTH production in these mice. However, the immunohistochemistry staining showed that there were still many viable cells in parathyroid.

Hypotheses

Effects on PTH

After testing hypotheses 1, 2, and 3, it was concluded that treatment with CC-325 caused decrease in serum PTH and subsequently iCa^{2+} because of reduction in PTH synthesis and not sequestration of PTH in parathyroid. Analysis of the data revealed that the treatment with CC-325 as a single agent or in combination with NPS 2143 resulted in decreased serum PTH and iCa^{2+} in mice; however, there was minimal differences in PTH and iCa^{2+} between these two treatment groups. The serum PTH and iCa^{2+} in the CC-325 only treatment group were

consistently lower than vehicle control group at all measured timepoints, however, mice treated with CC-325 + NPS 2143 had minimal increase in PTH and iCa^{2+} at the 2- and 4-hr timepoints when compared with the CC-325 only treatment group, Figure 23 (page 105) and Figure 29 (page 110). The increase in serum PTH in the CC-325 + NPS 2143 treatment group over the CC-325 only treatment group at 2-hr and 4-hr timepoints were 79% and 75%, respectively. Based on the TK data, Table 29 (page 94), the T_{max} for NPS 2143 in mice was at 2-hr postdose, which corresponded with the slight increase in serum PTH and iCa^{2+} in the combination group. However, at the same timepoint, 2-hr postdose, the level of serum PTH and iCa^{2+} in the NPS 2143 only treatment group was significantly higher than the vehicle control or CC-325 only treatment group. The increase of PTH in the NPS 2143 only treatment group was 1900% over the CC-325 only or 1800% over the CC-325 + NPS 2143 treatment groups. These data show that CC-325 inhibited the increase in PTH even when mice were treated with a potent negative allosteric modulator of CaSR. To investigate the cause of this inhibition, we performed further analysis to compare the level of serum with intracellular PTH.

The data from serum and intracellular PTH (IHC H-Scores) were analyzed. A correlation analysis was performed, and results are shown in Figure 43 and Figure 45. The Pearson correlation analysis for serum and intracellular PTH in CC-325 only treatment group showed that there was a strong positive correlation between the serum and intracellular PTH in this treatment group, meaning that the reason for decrease in serum PTH was decrease in PTH synthesis and not sequestration in parathyroid. Similar correlation analysis was performed for CC-325 + NPS 2143 treatment group, which showed that even after stimulation of parathyroid gland with NPS 2143, the level of serum and intracellular PTH had moderate positive correlation. These two analyses collectively, indicate that lack on increase in PTH in CC-325 treated mice was because

of decrease in PTH synthesis in both unstimulated and stimulated parathyroid and not sequestration of PTH in parathyroid. It is important to emphasize that when correlating a quantitative value, such as serum PTH, with semi-quantitative value, such as PTH H-scores, the accuracy of the correlation could be impacted, however, trend of correlation and the interpretation of the data would not change.

A correlation analysis for the vehicle and NPS 2143 only treatment groups was also performed, these data are shown in Figure 42 and Figure 45, respectively. The analysis of the vehicle control group showed very weak correlation between serum and intracellular PTH, which was likely due to the high variability in the serum PTH. Review of serum PTH concentrations, Figure 29 (page 110), and intracellular PTH H-Scores, Figure 32 (page 114), for the vehicle control group revealed that serum PTH had large variability in comparison with the intracellular PTH H-scores. Therefore, the lack of correlation in the vehicle control groups can be attributed, at least partially, to serum PTH variability.

The serum and intracellular PTH in the NPS 2143 only treatment group had negative correlation. This was due to significant increase in serum PTH in absence of change in intracellular PTH H-scores, except for minimal decrease at 2- and 4-hr post dose. This correlation data suggests that the parathyroid gland of these mice were generating and releasing significant amount of PTH, therefore serum PTH was high while intracellular PTH was roughly intact.

These data collectively indicate that NPS 2143 can stimulate the production of PTH and CC-325 can inhibit production. Animals treated with CC-325 followed by NPS 2143 were unable to synthesize PTH, therefore decrease in serum PTH in these animals is due to lack of PTH synthesis and not sequestration in parathyroid.

To further investigate the cause of decrease in PTH synthesis in CC-325 treated mice, the level of PTH mRNA in parathyroid was measured. The data from this analysis is shown in Figure 36 (page 120) and Figure 46 (page 132). Similar to IHC H-Scores, the values of ISH H-scores were semi-quantitative. As discussed earlier, this could certainly reduce the accuracy of the analysis. The Day 5 (0-hr) timepoint data, Figure 36 (page 120), shows the degree of variability in these mice. At 0-hr, the vehicle treated mice and NPS 2143 mice had different level of PTH mRNA H-score, although at 0-hr timepoint, the NPS 2143 mice were not dosed and they were sacrificed while naïve. Also, at 0-hr timepoint, the H-score for NPS 2143 mice was the same as CC-325 treated mice, which again, the NPS 2143 mice were naïve at 0-hr while the CC-325 mice were treated for 5 days. This level of variability from a newly developed semi-quantitative PTH mRNA ISH assays was not surprising. However, at the later timepoints, as the level of drug concentrations increased, the difference in the H-scores became more pronounced. The level of PTH mRNA in the NPS 2143 only treatment group was not significantly changed at 2- and 4-hr, but it was minimally increased at 6-hr. The lack of increase in PTH mRNA while there was significant synthesis and release of PTH from parathyroid during the first few hours after compound was onboard can be explained by possible PTH mRNA stabilization during the treatment period. In vitro studies have shown that calcium and phosphate determine PTH mRNA stability through the balance between stabilization and degradation of the factors that interact with PTH mRNA (T. Naveh-Many & Nechama, 2007). The R-568, a positive allosteric modulator of CaSR can significantly decrease in PTH, and this effect was shown to be contributed by two factors, acceleration of transcription degradation and reduction in gene transcription (Ritter et al., 2008). It is possible that NPS 2143, a negative allosteric modulator of

CaSR, increases PTH by stabilizing mRNA at 2- and 4-hr and also increases transcription of PTH mRNA at 6-hr timepoint.

Further analysis of the data, shown in Figure 46 (page 132), also revealed significant decrease in PTH mRNA in CC-325 treatment mice, with or without NPS 2143, when compared with NPS 2143 single agent treatment group. This data revealed that even stimulation by NPS 2143 cannot increase transcription of PTH in mice treated with CC-325. Therefore, the null hypothesis was rejected, and alternative hypothesis was accepted that CC-325 decreases PTH mRNA.

Effects on FGF23

In this experiment, we observed lower serum FGF23 concentration in the CC-325 treatment groups. The FGF23 secretion is driven by PTH, hyperphosphatemia and 1,25(OH)₂D. In this experiment the decrease in FGF23 in CC-325 treated mice is likely driven by decrease in decrease in PTH and likely decrease in 1,25 (OH)₂D, which was not measured in this experiment. The change of FGF23 during hyperphosphatemia and hyperparathyroidism has been extensively reported in the literature; however, its biological effects during hypocalcemia with decreased levels of PTH has yet to be elucidated. In this experiment, we measured the levels of FGF23 during hypocalcemia and hypoparathyroidism conditions. FGF23 plays an important role in phosphate homeostasis and it has positive correlation with calcium and negative correlation with PTH. The FGF23 increases the output and decreases the intake of phosphorus by directly increasing phosphaturia and indirectly decreasing intestinal phosphorus absorption by decreasing 1,25(OH)₂D levels. It has been well established that FGFR1 and α -Klotho are present on the surface of parathyroid, therefore binding of FGF23 to its binding site and α -Klotho suppresses both PTH secretion and PTH gene expression. Conversely, increase in PTH increases FGF23

transcription, although it would take several days to manifest (Ben-Dov et al., 2007). Injection of mice with PTH, increases FGF23 mRNA levels in mouse femurs, however, intact FGF23 was rapidly degraded within a few hour through an unidentified mechanism (Knab et al., 2017). In this experiment, the serum concentration of $1,25(\text{OH})_2\text{D}$ was not measured, however, it can be predicted that decreased in PTH would cause decrease in $1,25(\text{OH})_2\text{D}$ production. As described earlier, FGF23 levels directly correlate with calcium and indirectly with PTH, which under hypocalcemia condition (low calcium and high PTH) it hold true. Here, in this experiment, the question is what happens to levels of FGF23 if there is hypocalcemia and low PTH concentration. As shown in Figure 31 (page 113), the level of FGF23 decreases even under the hyperphosphatemia and hypoparathyroidism. In a study by (Rodriguez-Ortiz et al., 2012), injection of $1,25(\text{OH})_2\text{D}$ into parathyroidectomized rats with decreased serum calcium and FGF23 and increased phosphate normalized FGF23 levels, indicating that FGF23 concentrations are effected by other hormones. In an experimental model of primary hyperparathyroidism, FGF23 is increased, suggesting that PTH may directly increase FGF23 and may also increase FGF23 through stimulation of $1,25(\text{OH})_2\text{D}$ (Rodriguez-Ortiz et al., 2012). Based on this information, it is reasonable to predict that mice treated with CC-325 are likely $1,25(\text{OH})_2\text{D}$ deficient, although measurement of $1,25(\text{OH})_2\text{D}$ was not feasible in this experiment.

Conclusion

In this study, it was shown that degradation of GSPT1 causes hypocalcemia by decreasing PTH. The decrease in PTH was because of decreased PTH synthesis due to decreased PTH mRNA. Additionally, decreased PTH caused a decrease in FGF23, which had no impact on bone resorption and restoration of calcium homeostasis.

Limitation of the Study

This study was affected by design and analytical limitations. The most important design limitation was the number of animals in each treatment group. This was a large experiment with over 115 mice in 7 groups; however, the n size for each toxicological assessment timepoint was only 5, and the size of the groups for TK timepoints was even lower at 3. Although these n sizes were sufficient for the statistical analysis, larger n sizes could provide more robust data analysis, particularly for some of the semi-quantitative assays such as IHC and ISH H scores. Similarly, the larger n size for TK timepoints could provide tighter data and reduced SD.

Another design challenge was limitation of ISH probe for PTH mRNA due to limited availability of the probes, only n=3 (3 of 5) from each treatment group was analyzed, this type of sampling could introduce sampling bias in the data analysis. However, based on the small standard deviation in the results, it can be concluded the effect of sampling bias was very low on the data analysis and interpretation.

Additional limitation of this experiment was the small blood volume from mice. Although, all the endpoints of this experiment were measured successfully, the lack of spare serum or plasma samples made it impossible to repeat or confirm an analysis. Additionally, it has been reported that PTH has longer stability in EDTA plasma, however, due to blood volume limitation, only serum was collected for PTH analysis.

An analytical limitation was inability to measure 1,25(OH)₂D in serum. Currently there is no commercial assay for measuring mouse 1,25(OH)₂D; however, the LC/MS method could be an option for analysis, but it was not explored. Measuring the change in vitamin D in this experiment would provide important information in the role of vitamin D in restoring calcium homeostasis after treatment with GSPT1 degrader.

Another significant limitation was the histological processing of parathyroid gland. Mouse parathyroid glands are extremely small and difficult to identify and section. The histology laboratory in charge of processing of parathyroid glands was unable to identify and section 15 (15 out of 100) parathyroid. However, since these 15 parathyroid were missing from various treatment groups and timepoints, the impact on the data analysis was minimal.

Recommendation for Future Studies

Although this study answered several important questions, many more questions remain to be answered. Data from this study guide us toward several important research questions, including the role and the level of GSPT1 degradation in other tissues in the mice (i.e. kidney). In kidney, PTH stimulates calcium reabsorption in the distal tubule by activating specific ion channels and increases phosphate excretion in the proximal tubule mainly by regulating sodium-coupled cotransporters. It also enhances intestinal calcium and phosphate uptake by stimulating the conversion of 25-hydroxyvitamin D₃ to 1, 25-dihydroxyvitamin D₃. The PTH1R is expressed in proximal tubules, cortical ascending limbs, and distal convoluted tubules and it internalize the Na-Pi cotransporter and inhibits phosphate absorption. Therefore, it is important to investigate the role of GSPT1 degradation in the kidney. Additionally, assessing the effects of GSPT1 degradation on calcium and vitamin D receptors in parathyroid and kidney could provide more insight into mechanism of hypocalcemia.

It is also important to measure the serum calcitonin and assess the effects of GSPT1 degradation on thyroid function and calcium homeostasis. It is also critical to understand the impact of long-term FGF23 suppression on bone resorption and ossification.

Finally, further investigation into the mechanism of PTH mRNA decrease could provide insight into understanding the mechanism of hypocalcemia caused by GSPT1 degradation in huCRBN KI mice.

APPENDIX A.

ICa²⁺ And Electrolytes

Principles of Measurement Performed by Stat Profile Prime CCS Analyzer.

Measuring Technology: Ten Planar Sensors (Na, K, Cl, iCa, pH, PCO₂, PO₂, Glucose, Lactate, Hematocrit) in a Micro Sensor Card

Principle of Measurement (Sodium, Potassium, Chloride, and Ionized Calcium)

These parameters are measured by the Ion-Selective Electrode (ISE), which selectively measures the activity of ionic species. When the ISE is contacted with a sample, potential is developed. The potential is proportional to the logarithm of the ionic activity (a_i) and is measured versus a reference electrode. This relationship can be described by the Nernst equation.

Principle of pH Measurement

pH is measured using a hydrogen ion selective membrane. One side of the membrane is in contact with a solution of constant pH. The other side is in contact with a solution of unknown pH. A change in potential develops which is proportional to the pH difference of these solutions. This change in potential is measured against a reference electrode of constant potential. The magnitude of the potential difference is measured, and is used to calculate the pH of the unknown solution.

Ionized Calcium Normalized to pH 7.4

The activity and concentration of ionized calcium in whole blood is pH dependent. In vitro, a pH increase of 0.1 unit decreases the ionized calcium level by 4 to 5% (conversely, a pH decrease has an equal but opposite effect). The sample of choice for ionized calcium determination is anaerobically collected whole blood. If an anaerobic sample is not available, by measuring the actual pH of the sample at which the ionized calcium concentration was measured, then normalized ionized calcium can be calculated. Normalized ionized calcium represents what the ionized calcium concentration would have been if the initial pH was 7.40 (the midpoint of the pH reference range).

The equation used for this calculation is as follows:

$$\log [\text{iCa}]_{7.4} = \log [\text{Ca}^{++}]_X - 0.24 (7.4 - X)$$

where X = measured pH of the sample

[iCa]_X = ionized calcium concentration in the sample
at the measured pH

[iCa]_{7.4} = normalized concentration of ionized calcium
at pH 7.40

The equation assumes a normal concentration of total protein and may be used for measured values between pH 7.2 and 7.6. Between pH 6.9 and 7.2 and between pH 7.6 and 8.0, modified forms of the equation are used. Normalized ionized calcium values for samples with pH outside the range of pH 6.9 to pH 8.0 are not displayed.

Specimen Requirement

Lithium heparin whole blood samples from syringes, open tubes, small cups, and capillary tubes can be used on the Stat Profile Prime CCS Analyzer. The minimum sample size for analysis is 100 µL.

Quality Control

Healthcare facilities should follow federal, state, and local guidelines for testing quality control materials. At a minimum, Nova Biomedical recommends that each laboratory performs the following minimum QC procedures (Auto-Cartridge QC or External Ampule QC) on each analyzer:

- During each 8 hours of testing, analyze one level of Control.
- Analyze all 3 levels during each day of operation.
- After performing system maintenance, follow good laboratory practice guideline for performing quality control analysis.

Quality Control Within Run Precision Performance

The protocol consisted of 20 replicates per run for each of 3 different quality control materials on each of 3 Stat Profile Prime CCS Analyzers. The average, SD, CV%, and N for each analyzer for each QC level and parameter was calculated. The pooled average, SD, CV%, and N from all 3 analyzers for each QC level and parameter was calculated.

Precision

QC and linearity solution total imprecision performance estimates of the total imprecision were determined for the Stat Profile Prime CCS analyzers by analyzing the following solutions in duplicate over a period of 20 days; 2 runs per day for a total of 40 runs.

- Quality Control Material – 3 levels for each parameter in QC mode.
- Linearity Standards – 5 levels for each parameter in QC mode.

Whole Blood Run-to-Run Precision Performance Estimates of the whole blood run-to-run precision were determined in Syringe Mode and Capillary Mode. For each run, the whole blood was analyzed in triplicate on 3 Stat Profile Prime analyzers over 10 separate runs for a total of 30 results per analyzer. Statistical analysis for each analyzer for both Syringe Mode and Capillary Mode was calculated. Tables below show the precision data for each analyte.

Na Precision Data						
Sample	Pooled Mean (mmol/L)	N	Within run SD (Sr)	Within run % CV	Total imprecision SD (St)	Total Imprecision %CV
QC Level 1	158.3	240	0.56	0.35	0.68	0.43
QC Level 2	140.1	240	0.12	0.09	0.25	0.18
QC Level 3	120.2	240	0.08	0.07	0.18	0.15
Linearity Std 1	89.7	240	0.45	0.50	0.56	0.62
Linearity Std 2	116.1	240	0.25	0.21	0.52	0.45
Linearity Std 3	132.0	240	0.53	0.40	0.71	0.54
Linearity Std 4	154.5	240	0.40	0.26	0.63	0.41
Linearity Std 5	163.7	240	0.43	0.26	0.80	0.49

K Precision Data						
Sample	Pooled Mean (mmol/L)	N	Within run SD (Sr)	Within run % CV	Total imprecision SD (St)	Total Imprecision %CV
QC Level 1	5.81	240	0.020	0.34	0.03	0.48
QC Level 2	3.81	240	0.005	0.14	0.01	0.36
QC Level 3	1.87	240	0.002	0.13	0.02	0.97
Linearity Std 1	11.70	240	0.041	0.35	0.07	0.59
Linearity Std 2	1.91	240	0.006	0.32	0.02	0.92
Linearity Std 3	4.36	240	0.014	0.32	0.02	0.55
Linearity Std 4	6.38	240	0.024	0.38	0.04	0.63
Linearity Std 5	1.60	240	0.006	0.40	0.02	1.23

iCa Precision Data						
Sample	Pooled Mean (mmol/L)	N	Within run SD (Sr)	Within run % CV	Total imprecision SD (St)	Total Imprecision %CV
QC Level 1	1.51	240	0.007	0.45	0.02	1.13
QC Level 2	0.97	240	0.002	0.22	0.00	0.43
QC Level 3	0.53	240	0.001	0.23	0.01	1.85
Linearity Std 1	2.81	240	0.031	1.09	0.05	1.78
Linearity Std 2	1.44	240	0.004	0.26	0.01	0.53
Linearity Std 3	1.06	240	0.002	0.21	0.01	0.63
Linearity Std 4	0.51	240	0.001	0.14	0.01	1.31
Linearity Std 5	0.17	240	0.001	0.58	0.01	6.38

CI Precision Data						
Sample	Pooled Mean (mmol/L)	N	Within run SD (Sr)	Within run % CV	Total imprecision SD (St)	Total Imprecision %CV
QC Level 1	131.5	240	0.57	0.43	2.30	1.75
QC Level 2	103.0	240	0.72	0.70	1.52	1.48
QC Level 3	86.1	240	0.27	0.32	1.38	1.60
Linearity Std 1	73.5	240	0.15	0.21	1.26	1.71
Linearity Std 2	82.6	240	0.10	0.12	0.67	0.82
Linearity Std 3	100.5	240	0.11	0.11	0.67	0.66
Linearity Std 4	124.5	240	0.11	0.09	1.45	1.17
Linearity Std 5	133.5	240	0.13	0.10	2.04	1.53

APPENDIX B.

Albumin Principles of The Assay

For the quantitative determination of albumin concentration in serum and lithium heparin plasma using the ACE Axcel® Clinical Chemistry Systems.

The ACE Albumin Assay is based on the Doumas and Briggs modification of the bromcresol green (BCG) dye method:

albumin + BCG dye (yellow) BCG-albumin complex (green)

Reaction: An increase in absorbance of the green colored complex is directly proportional to the albumin concentration measured bichromatically at 629 nm/692 nm.

Specimen Requirement

- Use clear, unhemolyzed serum.
- Specimen stable at 4°C for up to 72 hours and frozen at -20°C for 6 months or indefinitely at -70°C.
-

Quality Control

- Alfa Wassermann Level 1 and Level 2 Chemistry Controls were used for QC check.
- Controls were run when a new reagent lot is loaded and/or recalibration of the test was performed.
- Control values outside of acceptable limits were troubleshoot prior to any sample analysis.
- The manufacturer mean values and expected ranges will be used for quality control. We recognize that our laboratory's mean for this analyte may not duplicate the mean value printed on the manufacture's insert, however, our control values must fall within the expected range.

Sensitivity

Analytical Sensitivity - determined on the clinical chemistry systems according to CLSI Protocol EP17-A provided by the manufacturer.

	ACE Axcel
LoD (g/dL)	0.09
LoQ (g/dL)	0.09

Precision

Precision - determined on the clinical chemistry systems according to CLSI Protocol EP5-A2 provided by the manufacturer.

System	Sample	Mean (g/dL)	Within Run		Total	
			SD	CV %	SD	CV %
ACE Axccl (n = 22 days)	1	2.3	0.04	1.7	0.05	2.0
	2	4.0	0.04	0.9	0.06	1.4
	3	5.6	0.05	1.0	0.07	1.2
	4	4.3	0.05	1.1	0.06	1.4

Limitation of The Assay

The performance of the Albumin Assay has been verified at 37°C using cuvettes and reagents manufactured exclusively for Alfa Wassermann Diagnostic Technologies, LLC.

- Do not use hemolyzed samples.
- A comprehensive list of drugs and other substances which can affect albumin concentration in serum is given by Young, et al.

Additional limitations on Specimen Collection, Storage and Handling and Performance Characteristics are listed in the package insert.

Total Protein

Principles of The Assay

For the quantitative determination of total protein concentration in serum and lithium heparin plasma using the ACE Axccl® Clinical Chemistry Systems.

The ACE Total Protein Assay is a modification of Weichselbaum's biuret reagent. Weichselbaum introduced the use of sodium potassium tartrate, as an alkaline stabilizer, and potassium iodide to prevent auto reduction of the copper sulfate.

protein + Cu²⁺ + Alkaline Medium → Cu-protein complex (violet)

Reaction: An increase in absorbance of the violet colored complex is directly proportional to the total protein concentration measured bichromati-cally at 544 nm/692 nm.

Specimen Requirement

- Use clear, unhemolyzed serum.
- Specimen stable at 4°C for up to 72 hours and frozen at -20°C for 6 months or indefinitely at -70°C.

Quality Control

- Alfa Wassermann Level 1 and Level 2 Chemistry Controls will be used for QC check.
- Controls were run when a new reagent lot was loaded and/or recalibration of the test is performed.

- Control values outside of acceptable limits were troubleshoot prior to any sample analysis.
- The manufacturer mean values and expected ranges were used for quality control. We recognize that our laboratory's mean for this analyte may not duplicate the mean value printed on the manufacture's insert, however, our control values fell within the expected range.

Sensitivity

Analytical Sensitivity - determined on the clinical chemistry systems according to CLSI Protocol EP17-A provided by the manufacturer.

	ACE Axcel
LoD (g/dL)	0.15
LoQ (g/dL)	0.31

Precision

Precision - determined on the clinical chemistry systems according to CLSI Protocol EP5-A2.⁸

System	Sample	Mean (g/dL)	Within Run		Total	
			SD	CV %	SD	CV %
ACE Axcel (n = 22 days)	1	3.5	0.08	2.4	0.10	2.9
	2	6.9	0.11	1.6	0.13	1.9
	3	10.0	0.08	0.8	0.10	1.0
	4	6.6	0.10	1.4	0.11	1.6

Limitation of The Assay

The performance of the Total Protein Assay has been verified at 37°C using cuvettes and reagents manufactured exclusively for Alfa Wassermann Diagnostic Technologies, LLC.

- Do not use hemolyzed samples.
- Extensive hemolysis should be avoided because the proteins released will react with ACE Total Protein Reagent.
- A comprehensive list of drugs and other substances which can affect total protein concentration in serum is given by Young, et al.

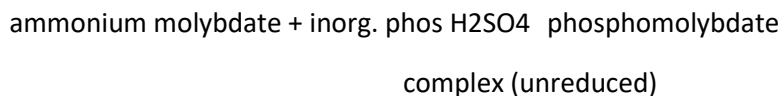
Additional limitations for Specimen Collection, Storage and Handling and Performance Characteristics are listed in package insert.

Phosphorus

Principles of The Assay

ACE Inorganic Phosphorus U.V. Reagent is intended for the quantitative determination of inorganic phosphorus concentration in serum and lithium heparin plasma using the ACE Axcel® Clinical Chemistry Systems

The ACE Inorganic Phosphorus Assay is based on the method of Daly and Ertingshausen with modifications by Amador and Urban that measures the unreduced phosphomolybdate complex in the ultra-violet (U.V.) range.



Reaction: An increase in absorbance is directly proportional to the phosphorus concentration measured bichromatically at 340 nm/378 nm.

Specimen Requirement

Serum/ Plasma Samples

- Separate serum/ plasma from red blood cells within 1 hour of collection because red blood cells contain organic phosphates, which can leak into serum as inorganic phosphorus.
- Use clear, unhemolyzed serum or lithium heparin plasma.
- Specimen stable for 4 days at 4-8°C and for 1 year at -20°C.

Quality Control

- Alfa Wassermann Level 1 and Level 2 Chemistry Controls will be used for QC check.
- Controls were run when a new reagent lot was loaded and/or recalibration of the test is performed.
- Control values outside of acceptable limits were troubleshoot prior to any sample analysis.
- The manufacturer mean values and expected ranges were used for quality control. We recognize that our laboratory's mean for this analyte may not duplicate the mean value printed on the manufacture's insert, however, our control values fell within the expected range.

Sensitivity

Analytical Sensitivity - determined on the clinical chemistry systems according to CLSI Protocol EP17-A provided by the manufacturer.

		ACE Axccl
Serum	LoD (mg/dL)	0.07
	LoQ (mg/dL)	0.22

Precision

Precision - determined on the clinical chemistry systems according to CLSI Protocol EP5-A2.¹¹

Serum Assay

System	Sample	Mean (g/dL)	Within Run		Total	
			SD	CV %	SD	CV %
ACE Axcel (n = 21)	1	3.8	0.06	1.6	0.07	1.7
	2	8.2	0.12	1.4	0.13	1.5
	3	12.6	0.24	1.9	0.24	1.9
	4	4.5	0.08	1.7	0.11	2.5

Limitation of The Assay

The performance of the Inorganic Phosphorus Assay has been verified at 37°C using cuvettes and reagents manufactured exclusively for Alfa Wassermann Diagnostic Technologies, LLC.

- Phosphorus contamination (usually from detergents) will adversely affect this assay. Disposable plasticware is highly recommended.
- Do not use icteric, lipemic or hemolyzed samples.
- A comprehensive list of drugs and other substances which can affect inorganic phosphorus concentration in serum/ plasma is given by Young, et al.

Additional limitations for Specimen Collection, Storage and Handling and Performance Characteristics are listed in package insert.

Calcium

Principles of The Assay

The ACE Calcium-Arsenazo Assay is a dye binding procedure in which calcium forms a blue-purple complex with Arsenazo III under acidic conditions.¹

For the quantitative determination of calcium concentration in serum and lithium heparin plasma using the ACE Axcel® Clinical Chemistry Systems. This test is intended for use in clinical laboratories and physician office laboratories.

Calcium + Arsenazo III Acidic Medium Calcium-Arsenazo III Complex

Reaction: An increase in absorbance is directly proportional to the calcium concentration measured bichromatically at 647 nm/692 nm.

Reagent Composition

Active Ingredients Concentration

Arsenazo III ≥ 0.15 mmol/L

Buffer and Surfactant

Specimen Requirement

- Blood collection tubes MUST be free of calcium.
- Obtain blood with minimum venous occlusion and without exercise or after restoring circulation for > 1 minute.

- Separate serum/ plasma from cells as soon as possible after collection because red cells can absorb calcium.
- Use clear, unhemolyzed serum or lithium heparin plasma.
- Specimen stable for 7 days at 20-25°C, 3 weeks at 4-8°C, and 8 months at -20°C.

Quality Control

- Alfa Wassermann Level 1 and Level 2 Chemistry Controls will be used for QC check.
- Controls were run when a new reagent lot was loaded and/or recalibration of the test is performed.
- Control values outside of acceptable limits were troubleshoot prior to any sample analysis.
- The manufacturer mean values and expected ranges were used for quality control. We recognize that our laboratory's mean for this analyte may not duplicate the mean value printed on the manufacture's insert, however, our control values fell within the expected range.

Sensitivity

Analytical Sensitivity - determined on the clinical chemistry systems according to CLSI Protocol EP17-A.¹⁰

		ACE	ACE Alera	ACE Axcel
Serum	LoD (mg/dL)	0.13	0.11	0.11
	LoQ (mg/dL)	0.20	0.23	0.20

Precision

Precision - determined on the clinical chemistry systems according to CLSI Protocol EP5-A2.⁹

Serum Assay

System	Sample	Mean (g/dL)	Within Run		Total	
			SD	CV %	SD	CV %
ACE Axcel (n = 21 days minimum)	1	6.5	0.15	2.3	0.15	2.3
	2	9.7	0.13	1.4	0.13	1.4
	3	12.5	0.19	1.5	0.21	1.7
	4	9.0	0.12	1.3	0.20	2.2

Limitation of The Assay

The performance of the Calcium-Arsenazo Assay has been verified at 37°C using cuvettes and reagents manufactured exclusively for Alfa Wassermann Diagnostic Technologies, LLC.

- Disposable plasticware is highly recommended. Contamination of glassware with calcium (usually from detergents) will adversely affect this assay. All glassware MUST be thoroughly acid-washed prior to use.
- Oxalate, citrate and EDTA anticoagulants interfere by binding calcium.

- Use clear, unhemolyzed serum.
- False elevations of serum/ plasma calcium are caused by venous stasis during collection and by prolonged storage of blood.
- Dust or other environmental contamination may increase the background of the reagent in the bottle and the reagent added to the cuvette.
- A comprehensive list of drugs and other substances which can affect calcium concentration in serum/ plasma is given by Young, et al.

Additional limitations for Specimen Collection, Storage and Handling and Performance Characteristics are listed in package insert.

Magnesium

Principles of The Assay

For the quantitative determination of magnesium concentration in serum and lithium heparin plasma using the ACE Axcel[®] Clinical Chemistry Systems.

The ACE Magnesium Assay is a colorimetric dye-complexing method that uses Xylidyl blue-1 for a rapid, easy and accurate determination of magnesium in serum/ plasma. EGTA prevents calcium interference by preferential chelation of calcium present in the sample. A surfactant system is included to remove protein interference.

Specimen Requirement

- Obtain blood with minimum venous occlusion.
- Separate specimen from the erythrocytes as soon as possible because the magnesium concentration in erythrocytes is substantially greater than in serum.¹
- Use clear, unhemolyzed serum or lithium heparin plasma.
- Store serum/plasma in stoppered tubes if analysis is delayed.
- Specimen stable for 7 days at 4-8°C and 1 year at -20°C if the serum/ plasma is separated from the erythrocytes.

Quality Control

- Alfa Wassermann Level 1 and Level 2 Chemistry Controls will be used for QC check.
- Controls were run when a new reagent lot was loaded and/or recalibration of the test is performed.
- Control values outside of acceptable limits will be troubleshoot prior to any sample analysis.
- The manufacturer mean values and expected ranges were used for quality control. We recognize that our laboratory's mean for this analyte may not duplicate the mean value printed on the manufacture's insert, however, our control values fell within the expected range.

Sensitivity

Analytical Sensitivity - determined on the clinical chemistry systems according to CLSI Protocol EP17-A. The results are as follows:

	ACE	ACE Alera	ACE Axcel
LoD (mg/dL)	0.39	0.37	0.34
LoQ (mg/dL)	0.43	0.37	0.34

Precision

Precision - determined on the clinical chemistry systems according to CLSI Protocol EP5-A2.⁸

System	Sample	Mean (g/dL)	Within Run		Total	
			SD	CV %	SD	CV %
ACE Axcel (n = 21 days minimum)	1	2.2	0.10	4.7	0.11	5.1
	2	4.0	0.11	2.8	0.12	2.9
	3	5.0	0.10	1.9	0.14	2.8
	4	1.7	0.12	6.7	0.13	7.5

Limitation of The Assay

The performance of the Magnesium Assay has been verified at 37°C using cuvettes and reagents manufactured exclusively for Alfa Wassermann Diagnostic Technologies, LLC.

- Do not use hemolyzed samples.
- A comprehensive list of drugs and other substances which can affect magnesium concentration in serum is given by Young, et al.

Additional limitations for **Specimen Collection, Storage and Handling and Performance Characteristics** are listed in the package insert.

APPENDIX C.

The Fibroblast Growth Factor 23

Principles of The Assay

This kit is intended for research use only in the quantitative determination of mouse FGF23 levels in plasma, serum* or cell culture media. This assay is also useful in the determination of rat FGF23 levels. This Mouse FGF23 (Intact) ELISA Kit is a homologous, two-site enzymelinked immunosorbent assay (ELISA) for the measurement of intact FGF23. Two affinity purified goat polyclonal antibodies have been selected to detect epitopes within the amino-terminal and carboxylterminal regions of mouse FGF23. The amino-terminal antibody is biotinylated for capture and the carboxyl-terminal antibody is conjugated with the enzyme horseradish peroxidase (HRP) for detection. In a two-step reaction a sample containing mouse FGF23 is first incubated with the biotinylated antibody in a streptavidin coated microtiter well. After washing the well to remove any unbound antibody and other components, the well is incubated with the HRP conjugated antibody. FGF23 contained in the sample is immunologically bound by the capture antibody and the detection antibody to form a “sandwich” complex:

Well/Avidin— Biotin Anti-mFGF23 — Mouse FGF23 — HRP Anti-mFGF23
(NH₂-terminal) (C-terminal)

Following another wash the enzyme antibody bound to the well is incubated with a substrate solution in a timed reaction and then measured in a spectrophotometric microtiter plate reader. The enzymatic activity of the antibody complex bound to the well is directly proportional to the amount of FGF23 in the sample. A standard curve is generated by plotting the absorbance versus the respective FGF23 concentration for each standard on linear or logarithmic scales. The concentration of mouse FGF23 in the samples is determined directly from this curve.

Specimen Requirement

The FGF23 molecule appears to be unstable resulting in decreased immunoreactivity over time. Sample collection and storage procedures should be carried out in an expeditious manner. Due to the lability of the molecule EDTA plasma is the preferred sample type. *In mice, serum values can be approximately 10% lower than EDTA plasma values. However, in rats, serum values can be approximately 30% lower than EDTA plasma values. Forty microliters of EDTA plasma, serum or culture media are required to assay the sample in duplicate. Centrifuge the sample and separate the plasma, serum or media from the cells. Samples should be assayed immediately or stored frozen at -20°C or below. Avoid repeated freezing and thawing of specimens.

Quality Control

To assure the validity of the results each assay should include adequate controls with known levels of mouse FGF23. Immotopics recommends that all assays include the laboratory's own mouse FGF23 controls in addition to those provided with this kit.

Sensitivity

The sensitivity of the Mouse FGF23 (Intact) ELISA as determined by the 95% confidence limit on 20 duplicate determinations of the 0 pg/mL Standard is 6 pg/mL.

Specificity

No data on specificity is available in package insert.

Precision

To assess intra-assay precision the mean and coefficient of variation were calculated from 20 duplicate determinations of two samples each performed in a single assay.

Mean Value (pg/mL)	Coefficient of Variation
65	4.4 %
170	2.3 %

To assess inter-assay precision the mean and coefficient of variation were calculated from duplicate determinations of two samples performed in 20 assays.

Mean Value (pg/mL)	Coefficient of Variation
60	4.0 %
167	4.0 %

Limitation of The Assay

The lowest concentration of mouse FGF23 measurable is 6 pg/mL (assay sensitivity) and the highest concentration of mouse FGF23 measurable without dilution is the value of the highest standard.

2. The reagents in this Mouse FGF23 (Intact) ELISA kit have been optimized so that together with the two-step reaction the high dose "hook effect" is not a problem for samples with elevated FGF23 values. Samples with levels between the highest standard and 1,000,000 pg/mL will read greater than the highest standard and should be diluted 1:10 or greater with the 0 pg/mL Standard or optional Sample Diluent reagent and reassayed for correct values.
3. Grossly lipemic samples may affect the immunological response and it is recommended that results obtained with such samples be scrutinized accordingly.
4. Differences in protein concentration and protein type between samples and standards in an immunoassay contribute to "protein effects" and dose biases. When measuring low protein concentration culture media samples against high protein concentration standards, it is recommended that like samples be assayed together in the same assay to minimize this bias.

APPENDIX D.

Parathyroid Hormone

Principles of The Assay

The Mouse PTH 1-84 ELISA Kit is a two-site enzyme-linked immunosorbent assay (ELISA) for the measurement of PTH in mouse plasma or cell culture media. Two different goat polyclonal antibodies have been affinity purified against mouse PTH to detect the biologically active intact form of mouse PTH. The antibody which recognizes epitopes within the midregion/C-terminal portion (39-84) of the peptide is biotinylated for capture. The other antibody, which recognizes epitopes within the N-terminal region (1-34), is conjugated with the enzyme horseradish peroxidase (HRP) for detection.

A sample containing mouse intact PTH is incubated simultaneously with the biotinylated capture antibody and the HRP conjugated antibody in a streptavidin coated microtiter well. Intact PTH (1-84) contained in the sample is immunologically bound by the capture antibody and the detection antibody to form a “sandwich” complex:

Well/Avidin-Biotin Anti-Mouse PTH — Mouse Intact PTH — HRP Anti-Mouse PTH

At the end of this incubation period, the well is washed to remove any unbound antibody and other components. The enzyme bound to the well is then incubated with a substrate solution in a timed reaction and then measured in a spectrophotometric microtiter plate reader. The enzymatic activity of the antibody complex bound to the well is directly proportional to the amount of PTH 1-84 in the sample. A standard curve is generated by plotting the absorbance versus the respective PTH 1-84 concentration for each standard on linear or logarithmic scales. The concentration of mouse intact PTH in the samples is determined directly from this curve. *(Standards are analytically prepared from synthetic Mouse Intact PTH 1-84.)*

Specimen Requirement

Store the kit at 2-8°C upon receipt. **Store the standards and controls at -20°C or below after reconstitution.** For the expiration date of the kit refer to the label on the kit box. All components are stable until this expiration date.

Prior to use allow all reagents to come to room temperature and mix by gentle swirling and inversion. Reagents from different kit lot numbers should not be combined or interchanged.

Quality Control

To assure the validity of the results each assay should include adequate controls with known levels of mouse intact PTH. Immutopics recommends that all assays include the laboratory's own mouse intact PTH controls in addition to those provided with this kit.

Sensitivity

The sensitivity of the mouse PTH 1-84 assay as determined by the 95% confidence limit on 20 duplicate determinations of the 0 pg/mL Standard is 4 pg/mL.

Precision

To assess intra-assay precision the mean and coefficient of variation were calculated from 20 duplicate determinations of two samples each performed in a single assay.

Mean Value	(pg/mL)	Coefficient of Variation
63		5.6 %
198		2.4 %

To assess inter-assay precision the mean and coefficient of variation were calculated from duplicate determinations of two samples performed in 20 assays.

Mean Value	(pg/mL)	Coefficient of Variation
60		5.7 %
209		5.4 %

Limitation of The Assay

1. The lowest concentration of mouse PTH 1-84 measurable is 4 pg/mL (assay sensitivity) and the highest concentration of mouse PTH 1-84 measurable without dilution is the value of the highest standard.
2. The reagents in this Mouse PTH 1-84 ELISA kit have been optimized so that the high dose “hook effect” is not a problem for samples with elevated intact PTH values. Samples with mouse intact PTH levels between the highest standard and 500,000 pg/mL will read greater than the highest standard and should be diluted 1:10 with the 0 pg/mL Standard or optional Sample Diluent and reassayed for correct values.
3. Grossly lipemic serum or plasma samples may affect the immunological response and it is recommended that results obtained with such samples be scrutinized accordingly.
4. Differences in protein concentration and protein type between samples and standards in an immunoassay contribute to "protein effects" and dose biases. When measuring low protein concentration culture media samples against high protein concentration standards, it is recommended that like samples be assayed together in the same assay to minimize this bias.

APPENDIX E.

Pilot Study Protocol

An Investigation into the Mechanism of Parathyroid Hormone Modulation in Mice Following Acute Exposure to Positive and Negative Allosteric Modulators of Calcium Sensing Receptor

1. OBJECTIVE

In order to further investigate the mechanism of hypocalcemia caused by oral GSPT-1 degrader, CC0781325, there is need to establish the dynamic range for parathyroid hormone (PTH), vitamin D, PTH mRNA as well as other factors known to regulate PTH production, such as transcription factors GATA3, Gcm2, and MafB. To do so, this pilot study will be conducted with two molecules, a positive allosteric modulator of calcium sensing receptor (CaSR) (NPS R-568) and negative allosteric modulator of CaSR (NPS 2143).

The objectives of this pilot study are as follow:

1. To establish the baseline for iCa^{2+} , Mg^{2+} , phosphorus, albumin, pH, vitamin D, and PTH in huCRBN KI and establish the magnitude of change in these parameters after treatment with NPS R-568 and NPS 2143.
2. To establish the correlation among circulating PTH level, intracellular PTH, and mRNA PTH in parathyroid.
3. Establish the baseline and assess the magnitude of change in CaSR, PTH transcription factors GATA3, Gcm2, and MafB, as well at PTH mRNA before and after treatment with NPS R-568 and NPS 2143.
4. Assess the utility of NPS R-568 or NPS 2143 for mechanistic study of GSPT-1 associated hypocalcemia.

2. MATERIALS AND METHODS

2.1. Experimental Animals

Male huCRBN KI homozygous knock-in (KI) mice will be obtained from Taconic and will be randomly assigned to toxicologic (Tox) assessment groups. Animals will be used for toxicological evaluation after single oral dose. Animals will be approximately 10-12 weeks old and weigh approximately 19 to 27 grams at the time of group assignment. Animals will be allowed to acclimate to the laboratory environment for a minimum of 5 days. Pristima will be used to randomize animals to treatment groups using strata-based method. Each group will be identified with a cage card bearing the study identification number and dosing group. Assigned animal numbers will be written on tails using an indelible marker.

2.2. Housing and Environment

HuCRBN KI mice assigned to each treatment groups will be group housed up to 5 animals per cage. Animal(s) might be housed individually if there is sign of fighting or injury. Animals will be fed with Harlan Teklad diet and water ad libitum and housed with a 12-hour light/dark cycle. Mice will not be fasted prior to necropsy.

2.3. Test Substances

Identity: NPS R-568 [HCl Salt]

Batch/Lot No.: 0000029590

Supplier or Source: Sigma-Aldrich INC.

Formulation: 15% 2-Hydroxypropyl- β -cyclodextrin (HP β CD)

Molecular Weight: 340.29

Formula Weight: 322.29

Correction Factor: 1.06

Purity (%): $\geq 95\%$ (HPLC)

Identity: NPS 2143 [HCl Salt]

Batch/Lot No.: 0000049663

Supplier or Source: Sigma-Aldrich INC.

Formulation: 15% HP β CD

Molecular Weight: 445.38

Formula Weight: 427.38

Correction Factor: 1.04

Purity (%): $\geq 95\%$ (HPLC)

Storage Conditions: The bulk powder will be stored refrigerated (2-8°C) protected from light. The formulated material will be used with 4 hours of preparation stored at room temperature.

Handling Precautions: Per standard laboratory precautions for biologically active compounds and according to SDS, if available.

Supplier/Manufacturer: Sigma-Aldrich INC.

Certificate of Analysis: A certificate of analysis or equivalent describing the test article characterization will be placed in the study file and information included in the study report.

Test Article:

2.4. Dose Preparation and Administration

The oral route of administration is chosen because in published studies (Fox et al., 1999; Gowen et al., 2000; Hannan et al., 2015; Nemeth et al., 2001), both NPS R-568 and NPS 2143 were orally dose up to 100 mg/kg; no clinical signs of toxicity was reported in these studies. Formulations of NPS R-568 and NPS 2143 will be prepared from the bulk powder by mixing with the vehicle according to the procedure below. Formulations will be prepared on each dosing day. The vehicle or test article formulation will be given orally a dose volume of 5 mL/kg. The required volume of vehicle or drug solution for each animal will be based on the most recent individual body weight.

The vehicle, NPS R-568, and NPS 2143 formulations will be prepared according to the instructions below.

Preparation of 100 mL of 15% HP β CD

1. Place 15 g of HP β CD in a glass screw cap bottle
2. Add 90 mL of HPLC grade water
3. Stir to mix thoroughly until final solution forms.
4. QS to 100 mL.

NPS R-568 in 15% HP β CD

1. Add the compound according to Table 1 to a small glass screw cap bottle.
2. Add required volume of 15% HP β CD vehicle to the bottle.
3. Vortex for 1 minutes.
4. Sonicate the formulations for 1 minute.
5. Vortex the formulations prior to dosing each animal.

NPS 2143 in 15% HP β CD

6. Add the compound according to Table 1 to a small glass screw cap bottle.
7. Add required volume of 15% HP β CD vehicle to the bottle.
8. Vortex for 1 minutes.
9. Sonicate the formulations for 1 minute.
10. Vortex the formulations prior to dosing each animal.

Dose levels and dose concentrations are listed in Table 1.

Table 1:**Dose Levels and Concentrations**

Group	Treatment	Dose Level (mg/kg)	Formulation Concentration (mg/mL) Free Base	Formulation Concentration (mg/mL) Salt
1	Vehicle	0	0	0
2	NPS R-568	50	10	10.6
3	NPS 2143	200	40	41.6

2.4.1. Formulation Analysis:

Before dosing the animals on Day 1, one (1) aliquot of 200 μ L will be taken from the middle portion of the formulations using positive displacement pipetting for accurate volume. Bubbles adhering to the side of the tip will be wiped off prior to dispensing to the tubes. The aliquots will be stored at -80° C. If formulation analysis becomes necessary, a protocol amendment will be issued to describe the detail of such analysis.

Dose Selection Criteria

There are no published or unpublished data on effects of NPS R-568 and NPS 2143 in huCRBN KI mice. This is the first study to establish the effects of NPS R-568 and NPS 2143 in huCRBN KI mice. As described above, the objective of this study is to further investigate the mechanism by which PTH decrease or increase in response to positive or negative allosteric modulation of CaSR.

Negative Allosteric Modulator of CaSR (Agonism) NPS R-568

NPS R-568 is a phenylalkylamine compound that acts as an agonist (calcimimetic) on parathyroid CaSR, making CaSR more sensitive to Ca^{2+} concentration. NPS R-568 potentiates the effects of circulating calcium on CaSR on parathyroid, leading to decreased parathyroid hormone levels. The hypocalcemia response to NPS R-568 is due to rapid decrease in serum PTH levels (Fox et al., 1999). In a study by (Fox et al., 1999), plasma PTH and Ca^{2+} levels after a single oral dose treatment with NPS R-568 (as the hydrochloride salt) at doses of 3.3, 10, 33, and 100 mg/kg were measured. Blood samples were collected for assay of plasma Ca^{2+} and PTH levels, immediately before and at 0.25, 0.5, 1, 1.5, 2, 4, 6, 24, and 48 h after the administration of NPS R-568 or vehicle. Plasma PTH levels were significantly reduced within 15 min of NPS R-568 administration and remained significantly lower up to 30 minutes. The length of time that PTH level stayed low was dose dependent; the rate of restoration toward the baseline level was faster at the lower doses. Plasma PTH levels in rats dosed with 33 and 100 mg/kg remained at trough level up to 1-hour postdose, while PTH levels in rats receiving the 3.3 or 10 mg/kg doses were not significantly different from vehicle treatment group at this timepoint. PTH levels in rats receiving the 33 and 100 mg/kg doses remained significantly lower than control group at 2-hour postdose. At ≥ 4 -hour post dose, there was no significant difference in PTH level in any of the treatment groups.

In order to investigate objectives 1 and 2, we are selecting a dose that can keep PTH low for up to 4 hours postdose, and based on the published data discussed above, we are selecting 50 mg/kg.

Positive Allosteric Modulator of CaSR (Antagonism) NPS 2143

In an experiment by (Nemeth et al., 2001), Sprague Dawley (SD) rats were subject to 2-hour infusion with NPS 2143 at the rate of 1 mg/kg/min, which resulted in a rapid increase in plasma PTH levels that peaked (4-5 fold over baseline) about 30 minutes post start of infusion and stayed high for the duration of infusion. The increase in PTH was associated with increase in plasma Ca^{2+} levels, which increased about 90 minutes after the start of the infusion and returned to baseline an hour after the end of infusion. Similar results were seen after intraperitoneal (ip) administration of 30 mg/kg NPS 2143 to mice. Oral administration of NPS 2143 prolonged the duration of PTH increase up to 4, and 24 hours after 30 and 100 mg/kg dose to mice and rats, respectively (Gowen et al., 2000; Hannan et al., 2015). (Gowen et al., 2000; Hannan et al., 2015)

In order to further investigate objectives 1 and 2, we are selecting a dose of NPS 2143 that can keep PTH high for at least 4 hours postdose, and based on the published data discussed above, we are selecting 200 mg/kg.

Experimental Groups

Male huCRBN KI mice will be assigned to experimental groups as indicated in Table 2 and will be treated once on Day 1.

Table 2:

Experimental Groups

	Animal Numbers	Treatment	Dose Level (mg /kg)	Dose Volume (mL/kg)
Group 1	2001-2030	Vehicle	0	5
Group 2	3001-3030	NPS R-568	50	5
Group 3	4001-4030	NPS 2143	200	5

Table 3 below provides the schedule of treatment and collection time; all collections are terminal.

Table 3:

Blood and Tissue Collection Schedule

Treatment Group	0.5-hr Blood & TP	1-hr Blood and Tissue	2-hr* Blood & TP	4-hr* Blood and Tissue
Group 2	2001-2005	2006-2010	2011-2015	2016-2020
Group 3	3001-3005	3006-3010	3011-3015	3016-3020
Group 4	4001-4005	4006-4010	4011-4015	4016-4020
n	15	15	15	15

* = Tissues to be collected are: Thyroid/parathyroid; TP = Thyroid/parathyroid gland

2.5. Experimental Procedures

2.5.1. Clinical Observations

All animals will be observed for clinical signs pre-dose and approximately 1 hour after the end of each oral administration on dosing day and prior to necropsy. All observations will be recorded into Pristima. Observations will include, but not limited to, grooming, stool consistency, central nervous system clinical signs and general activity. Moribund animals may be sacrificed before study termination at the discretion of the study director.

2.5.2. Body Weights

Body weights of all animals will be recorded once prior to dosing.

2.5.3.1. Clinical Laboratory Tests

Serum chemistry parameters will be evaluated in all surviving animals on scheduled and unscheduled necropsy. Clinical pathology tests will not be evaluated in animals found dead.

2.5.3.2. Serum Chemistry

At necropsy, 100 μL of whole blood will be collected via retro-orbital bleeding in capillary tube containing Li-heparin. iCa^{2+} , Na^+ , K^+ , pH and Cl^- will be measured on STAT Profile Prime analyzer (Nova Biomedical). Data from this analysis will be imported into Pristima, Table 4.

At necropsy, additional 600 μL of blood will be collected in a gold top tubes with serum separator. Serum will be separated within 60 minutes of collection and aliquoted as follow:

Aliquot 1: 75 μL of serum for PTH

Aliquot 2: 75 μL of serum for Vitamin D₂, D₃

Aliquot 3: 100 μL for serum chemistry panel (Table 5)

Aliquot 4: Backup sample

Electrolytes

Table 4:

Nova Stat Profile Prime Panel

iCa^{2+}	Na^+
K^+	Cl^-
pH	

Table 5:**Alfa Wassermann Serum Chemistry Panel**

Ca ²⁺	Phosphorus
Albumin	Albumin/Globulin Ratio (calculated)
Total Protein	Globulin (calculated)
Mg ²⁺	

Table 6:**ELISA Panels**

Parathyroid Hormone (PTH)
1,25(OH) ₂ D (Vitamin D ₂ and D ₃)

2.5.4. Pathology

Pathology evaluation consisting of gross findings and tissue collections will be performed at unscheduled and scheduled necropsy.

2.5.4.1. Euthanasia

All animals will be anesthetized with isoflurane then will be sacrificed via cervical dislocation.

2.5.4.2. Gross Pathology

The following tissues will be evaluated grossly from all Toxicologic Assessment animals euthanized early or terminated at study completion:

Adrenal	Liver/gall bladder	Small Intestine
Bone (sternebra, femur)	Kidneys	Spleen
Brain	Lung	Skin
Esophagus	Mandibular lymph node	Stomach
Eyes	Mesenteric lymph node	Thymus
Heart	Pancreas	Trachea
Large intestine	Skeletal muscle	Urinary bladder
Testes	Epididymis and seminal vesicle	Prostate
Thyroid/Parathyroid		

Additional tissues may be evaluated at the discretion of the pathologist or prosector.

2.5.4.4. Histopathology

The following tissues will be collected from unscheduled or at scheduled necropsy:

Thyroid/parathyroid	Small intestine	Gross lesions ^(b)
Kidneys	Femur ^(a)	

^(a) Decalcified in formic acid following formalin fixation

^(b) Processed and examined only if considered drug related

Tissues will be fixed in 10% buffered formalin. Thyroid/parathyroid gland and kidney will be sectioned and stained with hematoxylin and eosin and examined microscopically. Small intestine and femur will be kept in formalin for potential future analysis. If such analysis becomes necessary, a protocol amendment will be issued to detail the sample and data analysis.

2.5.4.5. Immunohistochemistry

Immunohistochemistry analysis of GSPT-1, GATA3, Gcm2, MafB, CaSR, and PTH in the parathyroid glands will be performed on the tissues collected at scheduled and unscheduled necropsy. Other markers and/or tissues may be evaluated at the discretion of the pathologist or study director.

2.5.4.6 In Situ Hybridization (ISH)

In situ hybridization will be performed for PTH mRNA in parathyroid.

2.6. Statistical Analysis

Statistical analysis of quantitative clinical laboratory data will be conducted by Pristima. A Dunnett LSD Test and Cochran and Cox Test will be performed for parametric and nonparametric analysis, respectively.

APPENDIX F.
Individual and Summary of Body Weight (g)

Page 1 of 6

Males						
Group #	Animal #	Treatment Day: 1 Session 1	Day: 2 Session 1	Day: 3 Session 1	Day: 4 Session 1	Day: 5 Session 1
Control	1001	24.7	22.9	21.2	21.7	22.9
	1002	25.7	23.4	24.3	25.0	24.7
	1003	25.4	25.2	24.5	23.4	24.3
	1004	25.4	24.6	24.0	24.2	25.2
	1005	25.2	25.0	25.2	25.1	25.8
	1006	26.8	26.1	26.3	26.2	26.1
	1007	26.6	26.7	26.4	26.2	27.2
	1008	26.2	25.8	25.5	25.7	26.0
	1009	26.3	26.2	26.8	26.9	26.6
	1010	28.2	26.1	26.9	26.9	27.4
	1011	27.3	27.4	27.2	27.9	27.2
	1012	28.1	27.0	27.6	28.6	29.9
	1013	27.5	27.9	28.3	28.4	28.2
	1014	26.5	27.4	27.4	27.6	27.2
	1015	26.6	26.5	25.5	25.4	25.1
	1016	27.3	27.2	26.4	26.7	26.3
	1017	28.3	27.5	27.4	27.7	27.4
	1018	27.0	26.6	26.8	27.0	27.1
	1019	27.2	26.6	26.8	26.8	27.0
	1020	27.6	26.9	26.9	26.7	26.5
	1021	28.2	26.2	26.2	26.1	26.2
	1022	28.5	27.2	27.2	26.5	27.5
	1023	29.4	28.8	29.1	28.2	29.1
	1024	27.9	27.9	27.0	27.7	29.5

+D = Dunnett LSD Test Significant at the 0.01 level

Individual and Summary of Body Weight (g)

Page 2 of 6

Males						
Group #	Animal #	Treatment Day: 1 Session 1	Day: 2 Session 1	Day: 3 Session 1	Day: 4 Session 1	Day: 5 Session 1
Control	1025	28.2	28.8	28.9	29.4	29.6
	(n)	25	25	25	25	25
	Means	27.04	26.48	26.39	26.48	26.80
	SDevs	1.189	1.439	1.673	1.713	1.683
2	2001	23.9	23.4	21.8	21.0	20.3
	2002	25.7	25.4	22.9	20.0	18.5
	2003	25.4	24.1	22.9	21.1	19.3
	2004	24.4	24.6	22.0	20.5	18.6
	2005	23.5	23.2	21.6	19.2	18.8
	2006	23.3	23.8	21.8	19.1	17.9
	2007	26.5	25.6	24.7	21.6	19.5
	2008	26.5	26.2	25.0	22.6	20.3
	2009	26.3	25.2	23.9	22.1	20.9
	2010	26.0	25.9	24.9	22.6	20.8
	2011	27.2	26.9	24.2	21.7	20.4
	2012	27.1	26.7	25.6	22.3	20.8
	2013	27.1	26.2	25.8	22.8	21.1
	2014	27.5	27.5	24.9	23.2	21.9
	2015	27.3	24.2	21.9	20.7	19.7
	2016	27.0	26.6	24.7	22.1	20.2
	2017	27.7	27.1	25.4	22.8	21.3
	2018	27.2	27.8	26.4	24.4	22.5
	2019	28.3	27.3	24.6	22.4	21.5
	2020	28.0	28.5	26.6	23.6	21.7

+D = Dunnett LSD Test Significant at the 0.01 level

Individual and Summary of Body Weight (g)

Page 3 of 6

Males						
Group #	Animal #	Treatment Day: 1 Session 1	Day: 2 Session 1	Day: 3 Session 1	Day: 4 Session 1	Day: 5 Session 1
2	2021	27.5	27.2	25.4	23.8	22.8
	2022	27.5	27.1	25.3	23.0	21.8
	2023	29.3	28.5	26.0	23.7	21.7
	2024	28.7	29.0	26.2	23.0	21.0
	2025	29.3	28.8	26.2	24.2	22.3
	(n)	25	25	25	25	25
	Means	26.73	26.27	24.43	22.14	20.62+D
	SDevs	1.637	1.704	1.624	1.454	1.319
3	3001	-	-	-	-	26.5
	3002	-	-	-	-	26.3
	3003	-	-	-	-	27.0
	3004	-	-	-	-	27.8
	3005	-	-	-	-	29.9
	3006	-	-	-	-	28.2
	3007	-	-	-	-	26.4
	3008	-	-	-	-	27.3
	3009	-	-	-	-	27.3
	3010	-	-	-	-	28.1
	3011	-	-	-	-	28.7
	3012	-	-	-	-	27.9
	3013	-	-	-	-	26.9
	3014	-	-	-	-	24.2
	3015	-	-	-	-	27.1
	3016	-	-	-	-	26.1

+D = Dunnett LSD Test Significant at the 0.01 level

Individual and Summary of Body Weight (g)

Page 4 of 6

Males						
Group #	Animal #	Treatment Day: 1 Session 1	Day: 2 Session 1	Day: 3 Session 1	Day: 4 Session 1	Day: 5 Session 1
3	3017	-	-	-	-	28.0
	3018	-	-	-	-	27.2
	3019	-	-	-	-	26.7
	3020	-	-	-	-	27.3
	3021	-	-	-	-	29.3
	3022	-	-	-	-	24.9
	3023	-	-	-	-	26.5
	3024	-	-	-	-	25.9
	3025	-	-	-	-	26.8
	(n)	0	0	0	0	25
	Means	-	-	-	-	27.13
	SDevs	-	-	-	-	1.247
4	4001	23.6	22.4	22.7	20.8	19.0
	4002	24.1	24.1	22.1	19.8	19.0
	4003	24.1	23.6	20.7	19.8	18.8
	4004	26.4	24.6	24.3	21.9	19.6
	4005	26.1	25.6	23.0	21.9	19.6
	4006	26.1	25.8	24.7	21.9	19.6
	4007	28.1	26.0	24.7	21.9	21.5
	4008	28.1	26.2	22.9	20.9	20.7
	4009	26.6	26.0	23.7	21.7	20.4
	4010	27.5	27.3	25.4	22.6	20.4
	4011	26.1	26.3	24.4	21.9	19.7
	4012	26.8	26.3	24.5	22.1	20.8

+D = Dunnett LSD Test Significant at the 0.01 level

Individual and Summary of Body Weight (g)

Page 5 of 6

Males						
Group #	Animal #	Treatment Day: 1 Session 1	Day: 2 Session 1	Day: 3 Session 1	Day: 4 Session 1	Day: 5 Session 1
4	4013	26.7	26.2	25.5	22.4	20.8
	4014	28.1	27.9	26.4	24.5	23.4
	4015	28.4	28.5	24.6	21.6	21.3
	4016	27.4	26.7	24.7	22.0	20.1
	4017	27.7	26.7	24.7	22.0	21.2
	4018	28.7	28.3	26.3	22.5	23.1
	4019	27.2	28.5	27.5	24.8	22.1
	4020	28.4	27.9	26.1	23.2	21.0
	4021	28.4	27.4	24.7	21.8	20.3
	4022	27.6	27.7	27.3	25.1	23.0
	4023	27.9	27.7	24.6	22.0	20.9
	4024	28.9	28.1	26.1	23.4	21.4
	4025	29.9	29.7	28.6	24.6	23.7
	(n)	25	25	25	25	25
	Means	27.16	26.62	24.81	22.28	20.86+D
	SDevs	1.546	1.691	1.759	1.374	1.374

+D = Dunnett LSD Test Significant at the 0.01 level

APPENDIX G.
Summary of Daily Clinical Signs

Page 1 of 7

Males
Treatment, Day 1

Category, Observations	Dosage Groups:	Control	2	4	5	7
	Number Examined:	25	25	25	6	6
	Number Normal:	25	25	25	6	6

Summary of Daily Clinical Signs

Page 2 of 7

Males Treatment, Day 2

Category, Observations	Dosage Groups:	Control	2	4	5	7
	Number Examined:	25	25	25	6	6
	Number Normal:	25	25	25	6	6

Summary of Daily Clinical Signs

Page 3 of 7

Males Treatment, Day 3

Category, Observations	Dosage Groups:	Control	2	4	5	7
	Number Examined:	25	25	25	6	6
	Number Normal:	25	25	25	6	6

Summary of Daily Clinical Signs

Page 4 of 7

Males						
Treatment, Day 4						
Category, Observations	Dosage Groups:	Control	2	4	5	7
	Number Examined:	25	25	25	6	6
	Number Normal:	25	24	23	6	6
Gait/Posture, hunched posture		0	1	0	0	0
Hair, pilo-erection		0	1	2	0	0

Summary of Daily Clinical Signs

Page 5 of 7

Males							
Treatment, Day 5							
Category, Observations	Dosage Groups:	Control	2	3	4	5	6
	Number Examined:	25	25	25	25	6	6
	Number Normal:	25	20	25	20	3	6
Gait/Posture, hunched posture		0	1	0	2	1	0
Hair, pilo-erection		0	5	0	5	3	0

Summary of Daily Clinical Signs

Page 6 of 7

Males Treatment, Day 5

Category, Observations	Dosage Groups:	7
	Number Examined:	6
	Number Normal:	4
Behavior, activity decreased		1
Hair, pilo-erection		2

APPENDIX H.

Serum Chemistry Calibration and Controls and Raw data

BRISTOL MYERS SQUIBB

CALIBRATION REPORT

TEST: ALB

STATE: CAL PASSED

CAL D/T: 07/16/20 12:51

CALIBRATOR	<----- RESPONSE ----->				CONCENTRATION	
	1	2	3	AVERAGE	SET PT	CALC
GEMCAL	0.4834	0.4782	0.4801	0.4806	4.2	4.2

CALIBRATOR	CAL FACTOR	CAL FACTOR RANGE
GEMCAL	8.7393	5.0000 - 11.0000

TEST: CA

STATE: CAL PASSED

CAL D/T: 07/16/20 12:55

CALIBRATOR	<----- RESPONSE ----->				CONCENTRATION	
	1	2	3	AVERAGE	SET PT	CALC
GEMCAL	0.2084	0.2052	0.2042	0.2059	9.9	9.9

CALIBRATOR	CAL FACTOR	CAL FACTOR RANGE
GEMCAL	48.0791	32.0000 - 56.0000

BRISTOL MYERS SQUIBB

CALIBRATION REPORT

TEST: PHOS

STATE: CAL PASSED

CAL D/T: 07/16/20 12:59

CALIBRATOR	<----- RESPONSE ----->				CONCENTRATION	
	1	2	3	AVERAGE	SET PT	CALC
GEMCAL	0.1567	0.1567	0.1571	0.1568	5.1	5.1

CALIBRATOR	CAL FACTOR	CAL FACTOR RANGE
GEMCAL	32.5176	27.0000 - 47.0000

TEST: MG

STATE: CAL PASSED

CAL D/T: 07/16/20 13:00

CALIBRATOR	<----- RESPONSE ----->				CONCENTRATION	
	1	2	3	AVERAGE	SET PT	CALC
GEMCAL	0.1609	0.1652	0.1659	0.1640	2.8	2.8

CALIBRATOR	CAL FACTOR	CAL FACTOR RANGE
GEMCAL	17.0740	13.0000 - 19.0000

BRISTOL MYERS SQUIBB

CALIBRATION REPORT

TEST: TP

STATE: CAL PASSED

CAL D/T: 07/16/20 13:02

CALIBRATOR	<----- RESPONSE ----->				CONCENTRATION	
	1	2	3	AVERAGE	SET PT	CALC
GEMCAL	0.1727	0.1711	0.1729	0.1722	6.6	6.6

CALIBRATOR	CAL FACTOR	CAL FACTOR RANGE
GEMCAL	38.3200	31.0000 - 49.0000

BRISTOL MYERS SQUIBB

CALIBRATION REPORT

TEST: CA

STATE: CAL PASSED

CAL D/T: 07/16/20 12:55

CALIBRATOR	<----- RESPONSE ----->				CONCENTRATION	
	1	2	3	AVERAGE	SET PT	CALC
GEMCAL	0.2084	0.2052	0.2042	0.2059	9.9	9.9

CALIBRATOR	CAL FACTOR	CAL FACTOR RANGE
GEMCAL	48.0791	32.0000 - 56.0000

GEMCAL

READING WAVELENGTH 647

DATA POINT	(SECS) TIME	<----- ABSORBANCE ----->		
		1	2	3
IB	N/A	0.1702	0.1552	0.1538
EARLY	3	0.3883	0.3783	0.3770
1	103	0.4026	0.3844	0.3829

BLANKING WAVELENGTH 692

DATA POINT	(SECS) TIME	<----- ABSORBANCE ----->		
		1	2	3
IB	N/A	0.0131	0.0107	0.0093
EARLY	3	0.0445	0.0419	0.0414
1	103	0.0459	0.0428	0.0424

BRISTOL MYERS SQUIBB

CALIBRATION REPORT

TEST: MG

STATE: CAL PASSED

CAL D/T: 07/16/20 13:00

CALIBRATOR	<----- RESPONSE ----->				CONCENTRATION	
	1	2	3	AVERAGE	SET PT	CALC
GEMCAL	0.1609	0.1652	0.1659	0.1640	2.8	2.8

CALIBRATOR	CAL FACTOR	CAL FACTOR RANGE
GEMCAL	17.0740	13.0000 - 19.0000

GEMCAL

READING WAVELENGTH 525

DATA POINT	(SECS) TIME	<----- ABSORBANCE ----->			<----- EB ----->	
		1	2	3	REAGENT	SAMPLE
EARLY	3	1.1500	1.1637	1.1575	1.0471	
1	243	1.1790	1.1903	1.1899	1.0695	

BLANKING WAVELENGTH 692

DATA POINT	(SECS) TIME	<----- ABSORBANCE ----->			<----- EB ----->	
		1	2	3	REAGENT	SAMPLE
EARLY	3	0.1976	0.2034	0.2020	0.2447	
1	243	0.1989	0.2059	0.2048	0.2503	

BRISTOL MYERS SQUIBB

QUALITY CONTROL REQUISITION REPORT

CONTROL: LEVEL 1

LOT: 1213UNCM

D/T: 07/16/20

12:46

TEST	RESULT	ACCEPTABLE RANGE	[ACCEPTABLE]	UNITS
ALB	3.0	2.9 - 3.5	[*]	g/dL
TP	4.6	4.4 - 5.0	[*]	g/dL
CA	9.3	8.9 - 10.3	[*]	mg/dL
PHOS	3.0	2.7 - 3.3	[*]	mg/dL
MG	2.2	1.8 - 2.4	[*]	mg/dL

CORRECTIVE ACTION:

BRISTOL MYERS SQUIBB

QUALITY CONTROL REQUISITION REPORT

CONTROL: LEVEL 2

LOT: 937UECM

D/T: 07/16/20
12:47

TEST	RESULT	ACCEPTABLE RANGE	[ACCEPTABLE]	UNITS
ALB	4.3	4.1 - 4.9	[*]	g/dL
TP	7.2	6.9 - 7.9	[*]	g/dL
CA	11.3	11.0 - 12.6	[*]	mg/dL
PHOS	6.6	6.3 - 7.7	[*]	mg/dL
MG	4.5	4.0 - 5.2	[*]	mg/dL

CORRECTIVE ACTION:

APPENDIX I.
Individual and Summary of Serum Chemistry Excel Values

Page 1 of 7

Treatment Day 5 (Scheduled Animal Room - Session 1)								
Males								
Group #	Animal #	ALB (g/dL)	CA (mg/dL)	PHOS (mg/dL)	GLOB (g/dL)	A/G	TP (g/dL)	MG (mg/dL)
Control	1001	2.8	9.5	7.9	2.0	1.4	4.8	-
	1002	3.0	9.9	6.7	1.7	1.8	4.7	3.1
	1003	3.0	9.8	6.1	1.8	1.7	4.8	2.8
	1004	3.0	10.1	5.7	2.2	1.4	5.2	2.9
	1005	3.0	9.9	6.5	2.2	1.4	5.2	2.6
	1006	3.1	9.8	8.0	2.1	1.5	5.2	2.9
	1007	3.0	9.5	6.3	2.1	1.4	5.1	2.5
	1008	3.1	9.9	6.5	2.2	1.4	5.3	2.7
	1009	3.0	9.4	5.8	2.0	1.5	5.0	2.3
	1010	3.1	10.0	6.5	1.8	1.7	4.9	2.4
	1011	3.1	8.6	6.8	2.1	1.5	5.2	2.6
	1012	3.3	9.9	5.3	2.1	1.6	5.4	2.6
	1013	3.2	9.7	6.9	2.0	1.6	5.2	2.6
	1014	3.4	10.2	8.1	2.5	1.4	5.9	3.0
	1015	2.9	9.5	7.5	2.2	1.3	5.1	2.5
	1016	3.0	9.5	5.7	2.4	1.3	5.4	2.6
	1017	3.0	9.5	8.4	2.2	1.4	5.2	3.0
	1018	3.2	9.8	7.3	2.3	1.4	5.5	2.4
	1019	3.1	9.7	7.6	2.4	1.3	5.5	2.9
	1020	3.1	9.6	8.1	2.1	1.5	5.2	2.8

#C = Cochran and Cox Test Significant at the 0.001 level

+C = Cochran and Cox Test Significant at the 0.01 level

Individual and Summary of Serum Chemistry Axcel Values

Page 2 of 7

Treatment Day 5 (Scheduled Animal Room - Session 1)

Males								
Group #	Animal #	ALB (g/dL)	CA (mg/dL)	PHOS (mg/dL)	GLOB (g/dL)	A/G	TP (g/dL)	MG (mg/dL)
Control	1021	3.0	9.6	7.0	2.4	1.3	5.4	2.6
	1022	3.1	9.9	6.8	2.0	1.6	5.1	2.6
	1023	3.0	10.2	6.0	2.1	1.4	5.1	2.5
	1024	3.0	10.6	7.2	1.7	1.8	4.7	2.6
	1025	3.3	10.2	5.8	2.5	1.3	5.8	2.6
	(n)	25	25	25	25	25	25	24
	Means	3.07	9.77	6.82	2.12	1.48	5.20	2.67
	SDevs	0.131	0.378	0.878	0.224	0.154	0.299	0.210
2	2001	2.8	8.0	4.6	2.0	1.4	4.8	2.3
	2002	2.9	5.3	9.9	2.0	1.5	4.9	2.3
	2003	3.0	6.6	5.8	2.0	1.5	5.0	2.0
	2004	2.9	6.6	5.3	2.1	1.4	5.0	1.8
	2005	3.0	6.4	7.6	1.9	1.6	4.9	2.3
	2006	2.9	6.4	9.3	1.6	1.8	4.5	2.5
	2007	3.0	5.7	10.1	1.8	1.7	4.8	1.9
	2008	4.5	6.8	7.3	0.4	11.3	4.9	2.5
	2009	4.3	6.2	8.2	0.4	10.8	4.7	2.0
	2010	4.4	7.0	9.4	0.5	8.8	4.9	2.5
	2011	2.7	4.8	10.8	1.7	1.6	4.4	2.3
	2012	2.8	5.3	10.2	1.8	1.6	4.6	2.0

#C = Cochran and Cox Test Significant at the 0.001 level

+C = Cochran and Cox Test Significant at the 0.01 level

Individual and Summary of Serum Chemistry Axcel Values

Page 3 of 7

Treatment Day 5 (Scheduled Animal Room - Session 1)

Males								
Group #	Animal #	ALB (g/dL)	CA (mg/dL)	PHOS (mg/dL)	GLOB (g/dL)	A/G	TP (g/dL)	MG (mg/dL)
2	2013	2.8	6.3	9.4	1.8	1.6	4.6	2.3
	2014	2.7	5.3	12.2	1.8	1.5	4.5	2.0
	2015	2.6	5.6	5.9	1.6	1.6	4.2	2.1
	2017	2.7	4.9	10.2	1.7	1.6	4.4	3.0
	2018	3.1	6.1	10.6	1.9	1.6	5.0	2.2
	2019	2.9	6.0	13.1	1.8	1.6	4.7	2.6
	2020	3.2	5.5	11.6	2.0	1.6	5.2	2.3
	2021	3.0	6.5	10.3	1.9	1.6	4.9	2.1
	2022	2.9	6.7	8.9	1.7	1.7	4.6	2.0
	2023	3.1	6.1	11.3	2.0	1.6	5.1	2.4
	2024	3.1	5.7	9.5	2.0	1.6	5.1	2.8
	2025	2.9	5.2	12.6	1.9	1.5	4.8	1.9
	(n)	24	24	24	24	24	24	24
	Means	3.09	6.04#C	9.34#C	1.68#C	2.67	4.77#C	2.25#C
	SDevs	0.527	0.748	2.292	0.500	2.973	0.254	0.296
3	3001	3.2	9.6	5.3	2.0	1.6	5.2	2.4
	3002	2.9	10.1	6.0	2.1	1.4	5.0	2.8
	3003	3.0	9.7	6.3	2.0	1.5	5.0	2.7
	3004	2.9	10.1	6.5	1.9	1.5	4.8	3.2
	3005	2.7	9.7	5.5	1.8	1.5	4.5	2.9

#C = Cochran and Cox Test Significant at the 0.001 level

+C = Cochran and Cox Test Significant at the 0.01 level

Individual and Summary of Serum Chemistry Axcel Values

Page 4 of 7

Treatment Day 5 (Scheduled Animal Room - Session 1)

Males								
Group #	Animal #	ALB (g/dL)	CA (mg/dL)	PHOS (mg/dL)	GLOB (g/dL)	A/G	TP (g/dL)	MG (mg/dL)
3	3006	2.7	10.7	7.3	-0.1	-27.0	2.6	3.0
	3007	2.7	10.8	5.6	-2.3	-1.2	0.4	2.9
	3008	2.6	11.4	8.8	2.0	1.3	4.6	3.4
	3009	2.8	11.3	7.7	2.0	1.4	4.8	3.1
	3010	2.8	11.2	6.8	1.7	1.6	4.5	3.3
	3011	2.8	12.4	5.6	1.9	1.5	4.7	3.1
	3012	2.6	12.0	6.0	1.9	1.4	4.5	3.2
	3013	2.7	12.0	6.4	1.8	1.5	4.5	3.2
	3014	2.5	10.8	5.7	1.6	1.6	4.1	2.9
	3015	2.9	13.1	5.0	1.8	1.6	4.7	3.1
	3016	2.7	13.3	9.7	1.8	1.5	4.5	2.9
	3017	2.8	11.6	6.2	2.0	1.4	4.8	2.4
	3018	2.9	11.5	6.0	2.3	1.3	5.2	2.4
	3019	2.8	11.6	5.7	2.1	1.3	4.9	2.6
	3020	2.9	11.9	5.6	1.7	1.7	4.6	2.7
	3021	2.8	9.6	6.8	2.2	1.3	5.0	2.4
	3022	3.1	10.4	4.9	2.4	1.3	5.5	3.0
	3023	2.9	9.9	6.0	2.2	1.3	5.1	2.3
	3024	2.9	10.2	6.6	2.2	1.3	5.1	2.4
	3025	3.2	10.5	3.6	2.5	1.3	5.7	2.5

#C = Cochran and Cox Test Significant at the 0.001 level

+C = Cochran and Cox Test Significant at the 0.01 level

Treatment Day 5 (Scheduled Animal Room - Session 1)

Males								
Group #	Animal #	ALB (g/dL)	CA (mg/dL)	PHOS (mg/dL)	GLOB (g/dL)	A/G	TP (g/dL)	MG (mg/dL)
3	(n)	25	25	25	25	25	25	25
	Means	2.83#C	11.02#C	6.22	1.74	0.20	4.57+C	2.83
	SDevs	0.173	1.066	1.232	0.966	5.692	1.038	0.333
4	4001	3.1	6.5	10.7	1.8	1.7	4.9	2.2
	4002	3.1	5.9	9.0	1.8	1.7	4.9	1.9
	4003	2.9	6.4	7.6	1.8	1.6	4.7	2.9
	4004	3.0	6.4	10.2	1.7	1.8	4.7	2.2
	4005	2.8	5.3	10.9	1.6	1.8	4.4	2.3
	4006	3.1	8.7	7.2	1.9	1.6	5.0	2.7
	4007	2.8	8.1	8.9	1.9	1.5	4.7	2.9
	4008	2.8	7.8	7.7	1.8	1.6	4.6	2.6
	4009	3.0	7.4	8.2	1.9	1.6	4.9	2.5
	4010	2.9	5.6	10.1	1.8	1.6	4.7	2.3
	4011	2.8	6.0	10.5	1.8	1.6	4.6	2.3
	4012	3.0	6.7	10.3	2.0	1.5	5.0	2.8
	4013	2.8	5.9	10.1	1.8	1.6	4.6	2.3
	4014	2.8	7.6	10.8	1.9	1.5	4.7	2.6
	4015	2.7	5.7	7.6	1.6	1.7	4.3	2.6
	4016	2.9	5.1	10.1	1.7	1.7	4.6	2.0
	4017	2.6	5.2	11.0	1.9	1.4	4.5	2.3

#C = Cochran and Cox Test Significant at the 0.001 level

+C = Cochran and Cox Test Significant at the 0.01 level

Treatment Day 5 (Scheduled Animal Room - Session 1)

Males								
Group #	Animal #	ALB (g/dL)	CA (mg/dL)	PHOS (mg/dL)	GLOB (g/dL)	A/G	TP (g/dL)	MG (mg/dL)
4	4018	2.7	7.6	7.8	1.7	1.6	4.4	2.5
	4019	3.1	5.8	11.1	1.6	1.9	4.7	1.8
	4020	2.7	5.4	9.3	1.7	1.6	4.4	1.8
	4021	3.2	7.5	10.3	2.0	1.6	5.2	4.8
	4022	3.0	7.1	8.3	2.1	1.4	5.1	1.9
	4023	3.2	6.1	10.1	1.9	1.7	5.1	2.2
	4024	2.8	5.6	8.4	1.8	1.6	4.6	2.2
	4025	2.7	6.7	10.4	2.2	1.2	4.9	2.3
	(n)	25	25	25	25	25	25	25
	Means	2.90#C	6.48#C	9.46#C	1.83#C	1.60	4.73#C	2.44
	SDevs	0.171	0.999	1.267	0.149	0.143	0.242	0.585

#C = Cochran and Cox Test Significant at the 0.001 level

+C = Cochran and Cox Test Significant at the 0.01 level

Individual and Summary of Electrolytes-iCa Values

Page 1 of 7

Treatment Day 5 (Scheduled Animal Room - Session 1)

Males						
Group #	Animal #	CL (mmol/L)	iCa (mg/dL)	K (mmol/L)	NA (mmol/L)	pH
Control	1001	118.0	5.16	4.87	148.0	7.008
	1002	117.0	5.13	4.70	144.0	7.245
	1003	116.0	5.03	4.56	144.0	7.242
	1004	117.0	5.23	4.68	143.0	7.215
	1005	116.0	5.10	4.92	144.0	7.234
	1006	116.0	4.93	5.34	145.0	7.341
	1007	116.0	5.01	5.19	142.0	7.295
	1008	116.0	4.99	5.18	144.0	7.347
	1009	116.0	4.81	5.30	141.0	7.318
	1010	115.0	4.84	5.17	143.0	7.309
	1011	112.0	4.98	5.58	144.0	7.238
	1012	111.0	5.12	4.80	146.0	7.300
	1013	112.0	4.86	5.04	145.0	7.300
	1014	113.0	4.95	6.06	148.0	7.256
	1015	112.0	4.98	5.37	144.0	7.219
	1016	114.0	5.11	5.64	146.0	7.266
	1017	113.0	5.02	5.13	146.0	7.198
	1018	114.0	5.01	5.16	146.0	7.253
	1019	114.0	5.15	5.00	149.0	7.226
	1020	113.0	4.99	4.81	147.0	7.248

#C = Cochran and Cox Test Significant at the 0.001 level

*C = Cochran and Cox Test Significant at the 0.05 level

Individual and Summary of Electrolytes-iCa Values

Page 2 of 7

Treatment Day 5 (Scheduled Animal Room - Session 1)

Males						
Group #	Animal #	CL (mmol/L)	iCa (mg/dL)	K (mmol/L)	NA (mmol/L)	pH
Control	1021	110.0	4.97	5.34	146.0	7.362
	1022	109.0	4.98	4.86	144.0	7.202
	1023	110.0	5.03	5.06	144.0	7.254
	1024	109.0	5.06	4.84	144.0	7.216
	1025	111.0	4.91	5.27	145.0	7.300
	(n)	25	25	25	25	25
	Means	113.60	5.014	5.115	144.88	7.2557
	SDevs	2.661	0.1030	0.3383	1.878	0.06933
2	2001	121.0	4.63	5.50	148.0	7.208
	2002	-	-	4.91	-	-
	2003	113.0	3.71	4.48	143.0	7.306
	2004	117.0	3.65	4.31	145.0	7.345
	2005	117.0	3.38	4.51	146.0	7.314
	2006	118.0	3.56	5.29	146.0	7.239
	2007	114.0	2.98	4.42	141.0	7.274
	2008	118.0	3.54	5.28	146.0	7.269
	2009	117.0	3.31	4.64	144.0	7.286
	2010	117.0	3.65	5.40	144.0	7.271
	2011	110.0	3.02	5.13	147.0	7.200
	2012	110.0	3.17	4.74	144.0	7.300

#C = Cochran and Cox Test Significant at the 0.001 level

*C = Cochran and Cox Test Significant at the 0.05 level

Individual and Summary of Electrolytes-iCa Values

Page 3 of 7

Treatment Day 5 (Scheduled Animal Room - Session 1)

Group #	Animal #	CL (mmol/L)	iCa (mg/dL)	K (mmol/L)	NA (mmol/L)	Males
						pH
2	2013	113.0	3.58	4.95	146.0	7.267
	2014	110.0	3.07	5.00	145.0	7.247
	2015	113.0	3.26	4.88	146.0	7.205
	2016	113.0	3.02	4.73	145.0	7.120
	2017	113.0	3.17	4.79	151.0	7.153
	2018	112.0	3.55	5.38	146.0	7.266
	2019	113.0	3.41	4.88	147.0	7.211
	2020	113.0	3.13	4.40	143.0	7.235
	2021	112.0	3.58	4.80	145.0	7.242
	2022	112.0	3.88	4.16	150.0	7.240
	2023	113.0	3.21	5.72	151.0	7.227
	2024	115.0	3.24	4.92	152.0	7.145
	2025	109.0	2.96	4.92	145.0	7.228
	(n)	24	24	25	24	24
	Means	113.88	3.403#C	4.886	146.08	7.2416
	SDevs	3.026	0.3691	0.3937	2.701	0.05395
3	3001	116.0	4.88	5.12	141.0	7.298
	3002	114.0	5.32	4.67	141.0	7.234
	3003	116.0	5.40	4.80	143.0	7.292
	3004	114.0	5.07	4.93	142.0	7.343

#C = Cochran and Cox Test Significant at the 0.001 level

*C = Cochran and Cox Test Significant at the 0.05 level

Individual and Summary of Electrolytes-iCa Values

Page 4 of 7

Treatment Day 5 (Scheduled Animal Room - Session 1)

Group #	Animal #	CL (mmol/L)	iCa (mg/dL)	K (mmol/L)	NA (mmol/L)	Males
						pH
3	3005	116.0	5.01	5.35	141.0	7.272
	3006	116.0	6.32	4.96	143.0	7.159
	3007	113.0	6.20	4.84	140.0	7.381
	3008	116.0	6.47	5.18	143.0	7.130
	3009	117.0	6.06	4.39	143.0	7.262
	3010	114.0	6.01	4.82	141.0	7.287
	3011	115.0	6.67	5.08	148.0	7.227
	3012	114.0	6.52	4.89	145.0	7.234
	3013	114.0	6.52	5.10	146.0	7.208
	3014	113.0	5.88	5.11	145.0	7.265
	3015	111.0	6.55	5.07	144.0	7.320
	3016	111.0	6.37	4.93	141.0	7.212
	3017	114.0	6.24	4.76	147.0	7.159
	3018	114.0	5.78	5.21	144.0	7.330
	3019	115.0	5.89	5.43	145.0	7.174
	3020	116.0	6.25	5.34	147.0	7.279
	3021	112.0	3.58	4.80	145.0	7.242
	3022	113.0	5.05	5.58	144.0	7.262
	3023	111.0	4.89	5.51	142.0	7.317
	3024	112.0	5.05	5.50	144.0	7.313

#C = Cochran and Cox Test Significant at the 0.001 level

*C = Cochran and Cox Test Significant at the 0.05 level

Individual and Summary of Electrolytes-iCa Values

Page 5 of 7

Treatment Day 5 (Scheduled Animal Room - Session 1)

Males						
Group #	Animal #	CL (mmol/L)	iCa (mg/dL)	K (mmol/L)	NA (mmol/L)	pH
3	3025	112.0	5.34	5.20	144.0	7.282
	(n)	25	25	25	25	25
	Means	113.96	5.733#C	5.063	143.56*C	7.2593
	SDevs	1.791	0.7488	0.2912	2.142	0.06217
4	4001	116.0	3.51	4.67	143.0	7.261
	4002	117.0	3.25	5.19	144.0	7.285
	4003	122.0	3.58	5.82	151.0	7.159
	4004	116.0	3.53	5.43	146.0	7.247
	4005	114.0	2.77	5.24	141.0	7.288
	4006	117.0	4.84	5.18	147.0	7.263
	4007	116.0	4.33	4.96	144.0	7.217
	4008	119.0	4.24	4.63	148.0	7.211
	4009	113.0	4.07	5.01	141.0	7.115
	4010	111.0	2.92	3.97	137.0	7.224
	4011	112.0	3.52	4.34	146.0	7.245
	4012	113.0	3.73	4.93	149.0	7.205
	4013	112.0	3.40	4.73	145.0	7.267
	4014	114.0	4.12	5.18	145.0	7.207
	4015	112.0	3.37	5.72	150.0	7.219
	4016	112.0	3.02	3.97	142.0	7.218

#C = Cochran and Cox Test Significant at the 0.001 level

*C = Cochran and Cox Test Significant at the 0.05 level

Treatment Day 5 (Scheduled Animal Room - Session 1)

Males						
Group #	Animal #	CL (mmol/L)	iCa (mg/dL)	K (mmol/L)	NA (mmol/L)	pH
4	4017	115.0	3.11	5.42	148.0	7.160
	4018	115.0	4.17	5.51	148.0	7.252
	4019	111.0	3.28	4.62	143.0	7.275
	4020	112.0	3.13	4.33	144.0	7.229
	4021	116.0	4.45	3.47	157.0	6.985
	4022	112.0	3.95	5.12	148.0	7.273
	4023	115.0	3.34	5.47	154.0	7.262
	4024	113.0	3.29	5.02	148.0	7.214
	4025	114.0	3.75	5.49	152.0	7.192
	(n)	25	25	25	25	25
	Means	114.36	3.627#C	4.937	146.44	7.2189
	SDevs	2.644	0.5249	0.5832	4.407	0.06439

#C = Cochran and Cox Test Significant at the 0.001 level

*C = Cochran and Cox Test Significant at the 0.05 level

REFERENCES

- Alimohammadi, M., Bjorklund, P., Hallgren, A., Pontynen, N., Szinnai, G., Shikama, N., . . . Kampe, O. (2008). Autoimmune polyendocrine syndrome type 1 and NALP5, a parathyroid autoantigen. *N Engl J Med*, 358(10), 1018-1028. doi:10.1056/NEJMoa0706487
- Angelopoulos, N. G., Goula, A., Rombopoulos, G., Kaltzidou, V., Katounda, E., Kaltsas, D., & Tolis, G. (2006). Hypoparathyroidism in transfusion-dependent patients with beta-thalassemia. *J Bone Miner Metab*, 24(2), 138-145. doi:10.1007/s00774-005-0660-1
- Arany, I., & Safirstein, R. L. (2003). Cisplatin nephrotoxicity. *Semin Nephrol*, 23(5), 460-464. doi:10.1016/s0270-9295(03)00089-5
- Arey, B. J., Seethala, R., Ma, Z., Fura, A., Morin, J., Swartz, J., . . . Feyen, J. H. (2005). A novel calcium-sensing receptor antagonist transiently stimulates parathyroid hormone secretion in vivo. *Endocrinology*, 146(4), 2015-2022. doi:10.1210/en.2004-1318
- Arnold, A., Horst, S. A., Gardella, T. J., Baba, H., Levine, M. A., & Kronenberg, H. M. (1990). Mutation of the signal peptide-encoding region of the preproparathyroid hormone gene in familial isolated hypoparathyroidism. *J Clin Invest*, 86(4), 1084-1087. doi:10.1172/JCI114811
- Bai, M. (2004). Structure-function relationship of the extracellular calcium-sensing receptor. *Cell Calcium*, 35(3), 197-207. doi:10.1016/j.ceca.2003.10.018
- Bandeira, L. C., Rubin, M. R., Cusano, N. E., & Bilezikian, J. P. (2018). Vitamin D and Hypoparathyroidism. In *Vitamin D in Clinical Medicine* (pp. 114-124).
- Ben-Dov, I. Z., Galitzer, H., Lavi-Moshayoff, V., Goetz, R., Kuro-o, M., Mohammadi, M., . . . Silver, J. (2007). The parathyroid is a target organ for FGF23 in rats. *J Clin Invest*, 117(12), 4003-4008. doi:10.1172/JCI32409
- Bikle, D. D. (2014). Vitamin D metabolism, mechanism of action, and clinical applications. *Chem Biol*, 21(3), 319-329. doi:10.1016/j.chembiol.2013.12.016
- Bikle, D. D. (2018). Vitamin D Assays. *Front Horm Res*, 50, 14-30. doi:10.1159/000486062
- Bikle, D. D., Patzek, S., & Wang, Y. (2018). Physiologic and pathophysiologic roles of extra renal CYP27b1: Case report and review. *Bone Rep*, 8, 255-267. doi:10.1016/j.bonr.2018.02.004
- Bourgeois, S., Capuano, P., Stange, G., Muhlemann, R., Murer, H., Biber, J., & Wagner, C. A. (2013). The phosphate transporter NaPi-IIa determines the rapid renal adaptation to dietary phosphate intake in mouse irrespective of persistently high FGF23 levels. *Pflugers Arch*, 465(11), 1557-1572. doi:10.1007/s00424-013-1298-9
- Bowl, M. R., Nesbit, M. A., Harding, B., Levy, E., Jefferson, A., Volpi, E., . . . Thakker, R. V. (2005). An interstitial deletion-insertion involving chromosomes 2p25.3 and Xq27.1, near SOX3, causes X-linked recessive hypoparathyroidism. *J Clin Invest*, 115(10), 2822-2831. doi:10.1172/JCI24156
- Breitwieser, G. E. (2012). Minireview: the intimate link between calcium sensing receptor trafficking and signaling: implications for disorders of calcium homeostasis. *Mol Endocrinol*, 26(9), 1482-1495. doi:10.1210/me.2011-1370

- Breitwieser, G. E. (2013). The calcium sensing receptor life cycle: trafficking, cell surface expression, and degradation. *Best Pract Res Clin Endocrinol Metab*, 27(3), 303-313. doi:10.1016/j.beem.2013.03.003
- Breitwieser, G. E. (2014). Pharmacoperones and the calcium sensing receptor: exogenous and endogenous regulators. *Pharmacol Res*, 83, 30-37. doi:10.1016/j.phrs.2013.11.006
- Brown, E. M. (2013). Role of the calcium-sensing receptor in extracellular calcium homeostasis. *Best Practice & Research Clinical Endocrinology & Metabolism*, 27(3), 333-343. doi:10.1016/j.beem.2013.02.006
- Brown, E. M., & Hebert, S. C. (1997). Calcium-receptor-regulated parathyroid and renal function. *Bone*, 20(4), 303-309. doi:10.1016/s8756-3282(97)00002-1
- Brown, E. M., & MacLeod, R. J. (2001). Extracellular calcium sensing and extracellular calcium signaling. *Physiol Rev*, 81(1), 239-297. doi:10.1152/physrev.2001.81.1.239
- Burtis, C. A., Ashwood, E. R., Bruns, D. E., & Tietz, N. W. (2013). *Tietz textbook of clinical chemistry and molecular diagnostics* (5th ed.). St. Louis, Mo.: Saunders.
- Cavanaugh, A., Huang, Y., & Breitwieser, G. E. (2012). Behind the curtain: cellular mechanisms for allosteric modulation of calcium-sensing receptors. *Br J Pharmacol*, 165(6), 1670-1677. doi:10.1111/j.1476-5381.2011.01403.x
- Cavanaugh, A., McKenna, J., Stepanchick, A., & Breitwieser, G. E. (2010). Calcium-sensing receptor biosynthesis includes a cotranslational conformational checkpoint and endoplasmic reticulum retention. *J Biol Chem*, 285(26), 19854-19864. doi:10.1074/jbc.M110.124792
- Chen, G., Liu, Y., Goetz, R., Fu, L., Jayaraman, S., Hu, M. C., . . . Mohammadi, M. (2018). alpha-Klotho is a non-enzymatic molecular scaffold for FGF23 hormone signalling. *Nature*, 553(7689), 461-466. doi:10.1038/nature25451
- Cheng, S. X., Geibel, J. P., & Hebert, S. C. (2004). Extracellular polyamines regulate fluid secretion in rat colonic crypts via the extracellular calcium-sensing receptor. *Gastroenterology*, 126(1), 148-158. doi:10.1053/j.gastro.2003.10.064
- Colloton, M., Shatz, E., Miller, G., Stehman-Breen, C., Wada, M., Lacey, D., & Martin, D. (2005). Cinacalcet HCl attenuates parathyroid hyperplasia in a rat model of secondary hyperparathyroidism. *Kidney Int*, 67(2), 467-476. doi:10.1111/j.1523-1755.2005.67103.x
- Conigrave, A. D. (2016). The Calcium-Sensing Receptor and the Parathyroid: Past, Present, Future. *Front Physiol*, 7, 563. doi:10.3389/fphys.2016.00563
- Conigrave, A. D., & Ward, D. T. (2013). Calcium-sensing receptor (CaSR): pharmacological properties and signaling pathways. *Best Pract Res Clin Endocrinol Metab*, 27(3), 315-331. doi:10.1016/j.beem.2013.05.010
- Cooper, M. S., & Gittoes, N. J. (2008). Diagnosis and management of hypocalcaemia. *BMJ*, 336(7656), 1298-1302. doi:10.1136/bmj.39582.589433.BE
- de Jesus Ferreira, M. C., Helies-Toussaint, C., Imbert-Teboul, M., Bailly, C., Verbavatz, J. M., Bellanger, A. C., & Chabardes, D. (1998). Co-expression of a Ca²⁺-inhibitable adenylyl cyclase and of a Ca²⁺-sensing receptor in the cortical thick ascending limb cell of the rat kidney.

- Inhibition of hormone-dependent cAMP accumulation by extracellular Ca^{2+} . *J Biol Chem*, 273(24), 15192-15202. doi:10.1074/jbc.273.24.15192
- de Rouffignac, C., & Quamme, G. (1994). Renal magnesium handling and its hormonal control. *Physiol Rev*, 74(2), 305-322. doi:10.1152/physrev.1994.74.2.305
- Diaz-Soto, G., Rocher, A., Garcia-Rodriguez, C., Nunez, L., & Villalobos, C. (2016). The Calcium-Sensing Receptor in Health and Disease. *Int Rev Cell Mol Biol*, 327, 321-369. doi:10.1016/bs.ircmb.2016.05.004
- Ding, C., Buckingham, B., & Levine, M. A. (2001). Familial isolated hypoparathyroidism caused by a mutation in the gene for the transcription factor GCMB. *J Clin Invest*, 108(8), 1215-1220. doi:10.1172/JCI13180
- Dong, B. J. (2005). Cinacalcet: An oral calcimimetic agent for the management of hyperparathyroidism. *Clin Ther*, 27(11), 1725-1751. doi:10.1016/j.clinthera.2005.11.015
- Elin, R. J. (2010). Assessment of magnesium status for diagnosis and therapy. *Magnes Res*, 23(4), S194-198. doi:10.1684/mrh.2010.0213
- Elli, F. M., deSanctis, L., Maffini, M. A., Bordogna, P., Tessaris, D., Pirelli, A., . . . Mantovani, G. (2019). Association of GNAS imprinting defects and deletions of chromosome 2 in two patients: clues explaining phenotypic heterogeneity in pseudohypoparathyroidism type 1B/iPPSD3. *Clin Epigenetics*, 11(1), 3. doi:10.1186/s13148-018-0607-8
- Estepa, J. C., Aguilera-Tejero, E., Lopez, I., Almaden, Y., Rodriguez, M., & Felsenfeld, A. J. (1999). Effect of phosphate on parathyroid hormone secretion in vivo. *J Bone Miner Res*, 14(11), 1848-1854. doi:10.1359/jbmr.1999.14.11.1848
- Fawcett, W. J., Haxby, E. J., & Male, D. A. (1999). Magnesium: physiology and pharmacology. *Br J Anaesth*, 83(2), 302-320. doi:10.1093/bja/83.2.302
- Ferry, S., Chatel, B., Dodd, R. H., Lair, C., Gully, D., Maffrand, J. P., & Ruat, M. (1997). Effects of divalent cations and of a calcimimetic on adrenocorticotrophic hormone release in pituitary tumor cells. *Biochem Biophys Res Commun*, 238(3), 866-873. doi:10.1006/bbrc.1997.7401
- Fogh-Andersen, N., Bjerrum, P. J., & Siggaard-Andersen, O. (1993). Ionic binding, net charge, and Donnan effect of human serum albumin as a function of pH. *Clin Chem*, 39(1), 48-52. Retrieved from <https://www.ncbi.nlm.nih.gov/pubmed/8419057>
- Fong, J., & Khan, A. (2012). Hypocalcemia: updates in diagnosis and management for primary care. *Can Fam Physician*, 58(2), 158-162. Retrieved from <https://www.ncbi.nlm.nih.gov/pubmed/22439169>
- Fox, J., Lowe, S. H., Petty, B. A., & Nemeth, E. F. (1999). NPS R-568: a type II calcimimetic compound that acts on parathyroid cell calcium receptor of rats to reduce plasma levels of parathyroid hormone and calcium. *J Pharmacol Exp Ther*, 290(2), 473-479. Retrieved from <https://www.ncbi.nlm.nih.gov/pubmed/10411552>
- Garrett, J. E., Tamir, H., Kifor, O., Simin, R. T., Rogers, K. V., Mithal, A., . . . Brown, E. M. (1995). Calcitonin-secreting cells of the thyroid express an extracellular calcium receptor gene. *Endocrinology*, 136(11), 5202-5211. doi:10.1210/endo.136.11.7588259

- Gattineni, J., & Baum, M. (2012). Genetic disorders of phosphate regulation. *Pediatr Nephrol*, 27(9), 1477-1487. doi:10.1007/s00467-012-2103-2
- Giusti, F., & Brandi, M. L. (2019). Clinical Presentation of Hypoparathyroidism. *Front Horm Res*, 51, 139-146. doi:10.1159/000491044
- Glendenning, P. (2013). It is time to start ordering ionized calcium more frequently: preanalytical factors can be controlled and postanalytical data justify measurement. *Ann Clin Biochem*, 50(Pt 3), 191-193. doi:10.1177/0004563213482892
- Goltzman, D., Hendy, G. N., Karaplis, A. C., Kremer, R., & Miao, D. (2018). Understanding Vitamin D From Mouse Knockout Models. In *Vitamin D* (pp. 613-631).
- Goltzman, D., Mannstadt, M., & Marcocci, C. (2018). Physiology of the Calcium-Parathyroid Hormone-Vitamin D Axis. *Front Horm Res*, 50, 1-13. doi:10.1159/000486060
- Gowen, M., Stroup, G. B., Dodds, R. A., James, I. E., Votta, B. J., Smith, B. R., . . . Fox, J. (2000). Antagonizing the parathyroid calcium receptor stimulates parathyroid hormone secretion and bone formation in osteopenic rats. *J Clin Invest*, 105(11), 1595-1604. doi:10.1172/JCI9038
- Grant, M. P., Stepanchick, A., Cavanaugh, A., & Breitwieser, G. E. (2011). Agonist-driven maturation and plasma membrane insertion of calcium-sensing receptors dynamically control signal amplitude. *Sci Signal*, 4(200), ra78. doi:10.1126/scisignal.2002208
- Grigorieva, I. V., Mirczuk, S., Gaynor, K. U., Nesbit, M. A., Grigorieva, E. F., Wei, Q., . . . Thakker, R. V. (2010). Gata3-deficient mice develop parathyroid abnormalities due to dysregulation of the parathyroid-specific transcription factor Gcm2. *J Clin Invest*, 120(6), 2144-2155. doi:10.1172/JCI42021
- Grigorieva, I. V., & Thakker, R. V. (2011). Transcription factors in parathyroid development: lessons from hypoparathyroid disorders. *Annals of the New York Academy of Sciences*, 1237(1), 24-38. doi:10.1111/j.1749-6632.2011.06221.x
- Hakami, Y., & Khan, A. (2019). Hypoparathyroidism. *Front Horm Res*, 51, 109-126. doi:10.1159/000491042
- Han, S. I., Tsunekage, Y., & Kataoka, K. (2015). Gata3 cooperates with Gcm2 and MafB to activate parathyroid hormone gene expression by interacting with SP1. *Mol Cell Endocrinol*, 411, 113-120. doi:10.1016/j.mce.2015.04.018
- Hannan, F. M., Walls, G. V., Babinsky, V. N., Nesbit, M. A., Kallay, E., Hough, T. A., . . . Thakker, R. V. (2015). The Calcilytic Agent NPS 2143 Rectifies Hypocalcemia in a Mouse Model With an Activating Calcium-Sensing Receptor (CaSR) Mutation: Relevance to Autosomal Dominant Hypocalcemia Type 1 (ADH1). *Endocrinology*, 156(9), 3114-3121. doi:10.1210/en.2015-1269
- Hendy, G. N., & Canaff, L. (2016). Calcium-Sensing Receptor Gene: Regulation of Expression. *Front Physiol*, 7, 394. doi:10.3389/fphys.2016.00394
- Hinson, J., Raven, P., & Chew, S. (2010). 12 - HORMONAL REGULATION OF PLASMA CALCIUM AND CALCIUM METABOLISM. In J. Hinson, P. Raven, & S. Chew (Eds.), *The Endocrine System (Second Edition)* (pp. 147-159): Churchill Livingstone.

- Hu, M. C., Shi, M., & Moe, O. W. (2019). Role of alphaKlotho and FGF23 in regulation of type II Na-dependent phosphate co-transporters. *Pflugers Arch*, 471(1), 99-108. doi:10.1007/s00424-018-2238-5
- Hu, M. C., Shi, M., Zhang, J., Pastor, J., Nakatani, T., Lanske, B., . . . Moe, O. W. (2010). Klotho: a novel phosphaturic substance acting as an autocrine enzyme in the renal proximal tubule. *FASEB J*, 24(9), 3438-3450. doi:10.1096/fj.10-154765
- Huang, Y., & Breitwieser, G. E. (2007). Rescue of calcium-sensing receptor mutants by allosteric modulators reveals a conformational checkpoint in receptor biogenesis. *J Biol Chem*, 282(13), 9517-9525. doi:10.1074/jbc.M609045200
- Huang, Y., Cavanaugh, A., & Breitwieser, G. E. (2011). Regulation of stability and trafficking of calcium-sensing receptors by pharmacologic chaperones. *Adv Pharmacol*, 62, 143-173. doi:10.1016/B978-0-12-385952-5.00007-5
- Imanishi, Y., Kawata, T., Kenko, T., Wada, M., Nagano, N., Miki, T., . . . Inaba, M. (2011). Cinacalcet HCl suppresses Cyclin D1 oncogene-derived parathyroid cell proliferation in a murine model for primary hyperparathyroidism. *Calcif Tissue Int*, 89(1), 29-35. doi:10.1007/s00223-011-9490-4
- Isono, H., Shoumura, S., Ishizaki, N., Emura, S., Hayashi, K., Iwasaki, Y., . . . Kitamura, Y. (1983). Effects of glucocorticoid on the ultrastructure of the mouse parathyroid gland. *Arch Histol Jpn*, 46(3), 293-305. doi:10.1679/aohc.46.293
- Isono, H., Shoumura, S., Ishizaki, N., Emura, S., Iwasaki, Y., Yamahira, T., & Kitamura, Y. (1985). Effects of starvation on the ultrastructure of the mouse parathyroid gland. *Acta Anat (Basel)*, 121(1), 46-52. doi:10.1159/000145941
- Jahnen-Dechent, W., & Ketteler, M. (2012). Magnesium basics. *Clin Kidney J*, 5(Suppl 1), i3-i14. doi:10.1093/ndtplus/sfr163
- Janicic, N., Soliman, E., Pausova, Z., Seldin, M. F., Riviere, M., Szpirer, J., . . . Hendy, G. N. (1995). Mapping of the calcium-sensing receptor gene (CASR) to human chromosome 3q13.3-21 by fluorescence in situ hybridization, and localization to rat chromosome 11 and mouse chromosome 16. *Mamm Genome*, 6(11), 798-801. doi:10.1007/bf00539007
- Kamitani-Kawamoto, A., Hamada, M., Moriguchi, T., Miyai, M., Saji, F., Hatamura, I., . . . Kataoka, K. (2011). MafB interacts with Gcm2 and regulates parathyroid hormone expression and parathyroid development. *J Bone Miner Res*, 26(10), 2463-2472. doi:10.1002/jbmr.458
- Kawakami, K., Takeshita, A., Furushima, K., Miyajima, M., Hatamura, I., Kuro-o, M., . . . Sakaguchi, K. (2017). Persistent fibroblast growth factor 23 signalling in the parathyroid glands for secondary hyperparathyroidism in mice with chronic kidney disease. *Scientific Reports*, 7(1). doi:10.1038/srep40534
- Kifor, O., Diaz, R., Butters, R., & Brown, E. M. (1997). The Ca²⁺-sensing receptor (CaR) activates phospholipases C, A2, and D in bovine parathyroid and CaR-transfected, human embryonic kidney (HEK293) cells. *J Bone Miner Res*, 12(5), 715-725. doi:10.1359/jbmr.1997.12.5.715

- Kittel B., Ernst H., Kamino K. (1996) Anatomy, Histology, and Ultrastructure, Parathyroid, Mouse. In: Jones T.C., Capen C.C., Mohr U. (eds) Endocrine System. Monographs on Pathology of Laboratory Animals. Springer, Berlin, Heidelberg
- Knab, V. M., Corbin, B., Andrukhova, O., Hum, J. M., Ni, P., Rabadi, S., . . . Christov, M. (2017). Acute Parathyroid Hormone Injection Increases C-Terminal but Not Intact Fibroblast Growth Factor 23 Levels. *Endocrinology*, 158(5), 1130-1139. doi:10.1210/en.2016-1451
- Kobrynski, L. J., & Sullivan, K. E. (2007). Velocardiofacial syndrome, DiGeorge syndrome: the chromosome 22q11.2 deletion syndromes. *Lancet*, 370(9596), 1443-1452. doi:10.1016/S0140-6736(07)61601-8
- Kragh-Hansen, U., & Vorum, H. (1993). Quantitative analyses of the interaction between calcium ions and human serum albumin. *Clin Chem*, 39(2), 202-208. Retrieved from <https://www.ncbi.nlm.nih.gov/pubmed/8432006>
- Kumar, R., & Thompson, J. R. (2011). The regulation of parathyroid hormone secretion and synthesis. *J Am Soc Nephrol*, 22(2), 216-224. doi:10.1681/ASN.2010020186
- Lee, M., & Partridge, N. C. (2009). Parathyroid hormone signaling in bone and kidney. *Curr Opin Nephrol Hypertens*, 18(4), 298-302. doi:10.1097/MNH.0b013e32832c2264
- Lee, S., Mannstadt, M., Guo, J., Kim, S. M., Yi, H. S., Khatri, A., . . . Juppner, H. (2015). A Homozygous [Cys25]PTH(1-84) Mutation That Impairs PTH/PTHrP Receptor Activation Defines a Novel Form of Hypoparathyroidism. *J Bone Miner Res*, 30(10), 1803-1813. doi:10.1002/jbmr.2532
- Letz, S., Rus, R., Haag, C., Dorr, H. G., Schnabel, D., Mohlig, M., . . . Schofl, C. (2010). Novel activating mutations of the calcium-sensing receptor: the calcilytic NPS-2143 mitigates excessive signal transduction of mutant receptors. *J Clin Endocrinol Metab*, 95(10), E229-233. doi:10.1210/jc.2010-0651
- Levi, R., Ben-Dov, I. Z., Lavi-Moshayoff, V., Dinur, M., Martin, D., Naveh-Many, T., & Silver, J. (2006). Increased parathyroid hormone gene expression in secondary hyperparathyroidism of experimental uremia is reversed by calcimimetics: correlation with posttranslational modification of the trans acting factor AUF1. *J Am Soc Nephrol*, 17(1), 107-112. doi:10.1681/ASN.2005070679
- Li, Y., Song, Y. H., Rais, N., Connor, E., Schatz, D., Muir, A., & Maclaren, N. (1996). Autoantibodies to the extracellular domain of the calcium sensing receptor in patients with acquired hypoparathyroidism. *J Clin Invest*, 97(4), 910-914. doi:10.1172/JCII18513
- Liamis, G., Milionis, H. J., & Elisaf, M. (2009). A review of drug-induced hypocalcemia. *J Bone Miner Metab*, 27(6), 635-642. doi:10.1007/s00774-009-0119-x
- Lienhardt, A., Bai, M., Lagarde, J. P., Rigaud, M., Zhang, Z., Jiang, Y., . . . Garabedian, M. (2001). Activating mutations of the calcium-sensing receptor: management of hypocalcemia. *J Clin Endocrinol Metab*, 86(11), 5313-5323. doi:10.1210/jcem.86.11.8016
- Lindberg, J. S. (2005). Calcimimetics: a new tool for management of hyperparathyroidism and renal osteodystrophy in patients with chronic kidney disease. *Kidney Int Suppl*(95), S33-36. doi:10.1111/j.1523-1755.2005.09505.x

- Liu, Z., Yu, S., & Manley, N. R. (2007). Gcm2 is required for the differentiation and survival of parathyroid precursor cells in the parathyroid/thymus primordia. *Dev Biol*, 305(1), 333-346. doi:10.1016/j.ydbio.2007.02.014
- Lopez-Girona, A., Mendy, D., Ito, T., Miller, K., Gandhi, A. K., Kang, J., . . . Chopra, R. (2012). Cereblon is a direct protein target for immunomodulatory and antiproliferative activities of lenalidomide and pomalidomide. *Leukemia*, 26(11), 2326-2335. doi:10.1038/leu.2012.119
- Ma, J. N., Owens, M., Gustafsson, M., Jensen, J., Tabatabaei, A., Schmelzer, K., . . . Burstein, E. S. (2011). Characterization of highly efficacious allosteric agonists of the human calcium-sensing receptor. *J Pharmacol Exp Ther*, 337(1), 275-284. doi:10.1124/jpet.110.178194
- Mace, M. L., Gravesen, E., Nordholm, A., Olgaard, K., & Lewin, E. (2018). Fibroblast Growth Factor (FGF) 23 Regulates the Plasma Levels of Parathyroid Hormone In Vivo Through the FGF Receptor in Normocalcemia, But Not in Hypocalcemia. *Calcif Tissue Int*, 102(1), 85-92. doi:10.1007/s00223-017-0333-9
- Mantovani, G. (2011). Clinical review: Pseudohypoparathyroidism: diagnosis and treatment. *J Clin Endocrinol Metab*, 96(10), 3020-3030. doi:10.1210/jc.2011-1048
- Mantovani, G., & Elli, F. M. (2019). Inactivating PTH/PTHrP Signaling Disorders. *Front Horm Res*, 51, 147-159. doi:10.1159/000491045
- Marcucci, G., & Brandi, M. L. (2019). A New Era for Chronic Management of Hypoparathyroidism: Parathyroid Hormone Peptides. *Front Horm Res*, 51, 165-171. doi:10.1159/000491047
- Matyskiela, M. E., Couto, S., Zheng, X., Lu, G., Hui, J., Stamp, K., . . . Chamberlain, P. P. (2018). SALL4 mediates teratogenicity as a thalidomide-dependent cereblon substrate. *Nat Chem Biol*, 14(10), 981-987. doi:10.1038/s41589-018-0129-x
- Matyskiela, M. E., Lu, G., Ito, T., Pagarigan, B., Lu, C. C., Miller, K., . . . Chamberlain, P. P. (2016). A novel cereblon modulator recruits GSPT1 to the CRL4(CRBN) ubiquitin ligase. *Nature*, 535(7611), 252-257. doi:10.1038/nature18611
- McGehee, D. S., Aldersberg, M., Liu, K. P., Hsuing, S., Heath, M. J., & Tamir, H. (1997). Mechanism of extracellular Ca²⁺ receptor-stimulated hormone release from sheep thyroid parafollicular cells. *J Physiol*, 502 (Pt 1), 31-44. doi:10.1111/j.1469-7793.1997.031bl.x
- Michels, T. C., & Kelly, K. M. (2013). Parathyroid disorders. *Am Fam Physician*, 88(4), 249-257. Retrieved from <https://www.ncbi.nlm.nih.gov/pubmed/23944728>
- Mizobuchi, M., Ritter, C. S., Krits, I., Slatopolsky, E., Sicard, G., & Brown, A. J. (2009). Calcium-sensing receptor expression is regulated by glial cells missing-2 in human parathyroid cells. *J Bone Miner Res*, 24(7), 1173-1179. doi:10.1359/jbmr.090211
- Moallem, E., Kilav, R., Silver, J., & Naveh-Many, T. (1998). RNA-Protein binding and post-transcriptional regulation of parathyroid hormone gene expression by calcium and phosphate. *J Biol Chem*, 273(9), 5253-5259. doi:10.1074/jbc.273.9.5253
- Moe, S. M. (2016). Calcium Homeostasis in Health and in Kidney Disease. *Compr Physiol*, 6(4), 1781-1800. doi:10.1002/cphy.c150052

- Morel, F. (1981). Sites of hormone action in the mammalian nephron. *Am J Physiol*, 240(3), F159-164. doi:10.1152/ajprenal.1981.240.3.F159
- Morito, N., Yoh, K., Usui, T., Oishi, H., Ojima, M., Fujita, A., . . . Takahashi, S. (2018). Transcription factor MafB may play an important role in secondary hyperparathyroidism. *Kidney Int*, 93(1), 54-68. doi:10.1016/j.kint.2017.06.023
- Morrissey, J. J., Hamilton, J. W., MacGregor, R. R., & Cohn, D. V. (1980). The secretion of parathormone fragments 34-84 and 37-84 by dispersed porcine parathyroid cells. *Endocrinology*, 107(1), 164-171. doi:10.1210/endo-107-1-164
- Muroya, K., Hasegawa, T., Ito, Y., Nagai, T., Isotani, H., Iwata, Y., . . . Ogata, T. (2001). GATA3 abnormalities and the phenotypic spectrum of HDR syndrome. *J Med Genet*, 38(6), 374-380. doi:10.1136/jmg.38.6.374
- Nakamoto, J. M., Sandstrom, A. T., Brickman, A. S., Christenson, R. A., & Van Dop, C. (1998). Pseudohypoparathyroidism type Ia from maternal but not paternal transmission of a Gsalpha gene mutation. *Am J Med Genet*, 77(4), 261-267. Retrieved from <https://www.ncbi.nlm.nih.gov/pubmed/9600732>
- Naveh-Many, T., Marx, R., Keshet, E., Pike, J. W., & Silver, J. (1990). Regulation of 1,25-dihydroxyvitamin D3 receptor gene expression by 1,25-dihydroxyvitamin D3 in the parathyroid in vivo. *J Clin Invest*, 86(6), 1968-1975. doi:10.1172/JCI114931
- Naveh-Many, T., & Nechama, M. (2007). Regulation of parathyroid hormone mRNA stability by calcium, phosphate and uremia. *Curr Opin Nephrol Hypertens*, 16(4), 305-310. doi:10.1097/MNH.0b013e3281c55ede
- Naveh-Many, T., & Silver, J. (2018). Transcription factors that determine parathyroid development power PTH expression. *Kidney Int*, 93(1), 7-9. doi:10.1016/j.kint.2017.08.026
- Naveh-Many, T., Silver, J., & Kronenberg, H. M. (2020). Parathyroid hormone molecular biology. In *Principles of Bone Biology* (pp. 575-594).
- Nechama, M., Ben-Dov, I. Z., Silver, J., & Naveh-Many, T. (2009). Regulation of PTH mRNA stability by the calcimimetic R568 and the phosphorus binder lanthanum carbonate in CKD. *Am J Physiol Renal Physiol*, 296(4), F795-800. doi:10.1152/ajprenal.90625.2008
- Nemeth, E. F., Delmar, E. G., Heaton, W. L., Miller, M. A., Lambert, L. D., Conklin, R. L., . . . Fox, J. (2001). Calcilytic compounds: potent and selective Ca²⁺ receptor antagonists that stimulate secretion of parathyroid hormone. *J Pharmacol Exp Ther*, 299(1), 323-331. Retrieved from <https://www.ncbi.nlm.nih.gov/pubmed/11561095>
- Nemeth, E. F., Steffey, M. E., Hammerland, L. G., Hung, B. C., Van Wagenen, B. C., DelMar, E. G., & Balandrin, M. F. (1998). Calcimimetics with potent and selective activity on the parathyroid calcium receptor. *Proc Natl Acad Sci U S A*, 95(7), 4040-4045. doi:10.1073/pnas.95.7.4040
- Nesbit, M. A., Hannan, F. M., Howles, S. A., Babinsky, V. N., Head, R. A., Cranston, T., . . . Thakker, R. V. (2013). Mutations affecting G-protein subunit alpha11 in hypercalcemia and hypocalcemia. *N Engl J Med*, 368(26), 2476-2486. doi:10.1056/NEJMoa1300253

- Powers, J., Joy, K., Ruscio, A., & Lagast, H. (2013). Prevalence and incidence of hypoparathyroidism in the United States using a large claims database. *J Bone Miner Res*, 28(12), 2570-2576. doi:10.1002/jbmr.2004
- Pozzan, T., Rizzuto, R., Volpe, P., & Meldolesi, J. (1994). Molecular and cellular physiology of intracellular calcium stores. *Physiol Rev*, 74(3), 595-636. doi:10.1152/physrev.1994.74.3.595
- Quarles, L. D. (2012). Skeletal secretion of FGF23 regulates phosphate and vitamin D metabolism. *Nat Rev Endocrinol*, 8(5), 276-286. doi:10.1038/nrendo.2011.218
- Quinn, S. J., Kifor, O., Kifor, I., Butters, R. R., Jr., & Brown, E. M. (2007). Role of the cytoskeleton in extracellular calcium-regulated PTH release. *Biochem Biophys Res Commun*, 354(1), 8-13. doi:10.1016/j.bbrc.2006.12.160
- Riccardi, D., Lee, W. S., Lee, K., Segre, G. V., Brown, E. M., & Hebert, S. C. (1996). Localization of the extracellular Ca(2+)-sensing receptor and PTH/PTHrP receptor in rat kidney. *Am J Physiol*, 271(4 Pt 2), F951-956. doi:10.1152/ajprenal.1996.271.4.F951
- Risco, F., Traba, M. L., & de la Piedra, C. (1995). Possible alterations of the in vivo 1,25(OH)2D3 synthesis and its tissue distribution in magnesium-deficient rats. *Magnes Res*, 8(1), 27-35. Retrieved from <https://www.ncbi.nlm.nih.gov/pubmed/7669505>
- Ritter, C. S., Pande, S., Krits, I., Slatopolsky, E., & Brown, A. J. (2008). Destabilization of parathyroid hormone mRNA by extracellular Ca2+ and the calcimimetic R-568 in parathyroid cells: role of cytosolic Ca and requirement for gene transcription. *J Mol Endocrinol*, 40(1), 13-21. doi:10.1677/JME-07-0085
- Rodriguez-Ortiz, M. E., Lopez, I., Munoz-Castaneda, J. R., Martinez-Moreno, J. M., Ramirez, A. P., Pineda, C., . . . Almaden, Y. (2012). Calcium deficiency reduces circulating levels of FGF23. *J Am Soc Nephrol*, 23(7), 1190-1197. doi:10.1681/ASN.2011101006
- Rodriguez, M. E., Almaden, Y., Canadillas, S., Canalejo, A., Siendones, E., Lopez, I., . . . Rodriguez, M. (2007). The calcimimetic R-568 increases vitamin D receptor expression in rat parathyroid glands. *Am J Physiol Renal Physiol*, 292(5), F1390-1395. doi:10.1152/ajprenal.00262.2006
- Rude, R. K., & Singer, F. R. (1981). Magnesium deficiency and excess. *Annu Rev Med*, 32, 245-259. doi:10.1146/annurev.me.32.020181.001333
- Saidak, Z., Brazier, M., Kamel, S., & Mentaverri, R. (2009). Agonists and allosteric modulators of the calcium-sensing receptor and their therapeutic applications. *Mol Pharmacol*, 76(6), 1131-1144. doi:10.1124/mol.109.058784
- Sanjad, S. A., Sakati, N. A., Abu-Osba, Y. K., Kaddoura, R., & Milner, R. D. (1991). A new syndrome of congenital hypoparathyroidism, severe growth failure, and dysmorphic features. *Arch Dis Child*, 66(2), 193-196. doi:10.1136/ad.66.2.193
- Saris, N. E., Mervaala, E., Karppanen, H., Khawaja, J. A., & Lewenstam, A. (2000). Magnesium. An update on physiological, clinical and analytical aspects. *Clin Chim Acta*, 294(1-2), 1-26. doi:10.1016/s0009-8981(99)00258-2
- Silver, J., & Naveh-Many, T. (2010). FGF23 and the parathyroid glands. *Pediatr Nephrol*, 25(11), 2241-2245. doi:10.1007/s00467-010-1565-3

- Silver, J., & Naveh-Many, T. (2018). Vitamin D and the Parathyroids. In *Vitamin D* (pp. 461-475).
- Silver, J., Naveh-Many, T., Mayer, H., Schmelzer, H. J., & Popovtzer, M. M. (1986). Regulation by vitamin D metabolites of parathyroid hormone gene transcription in vivo in the rat. *J Clin Invest*, 78(5), 1296-1301. doi:10.1172/JCI112714
- Silver, J., Russell, J., & Sherwood, L. M. (1985). Regulation by vitamin D metabolites of messenger ribonucleic acid for preproparathyroid hormone in isolated bovine parathyroid cells. *Proc Natl Acad Sci U S A*, 82(12), 4270-4273. doi:10.1073/pnas.82.12.4270
- Swaminathan, R. (2003). Magnesium metabolism and its disorders. *Clin Biochem Rev*, 24(2), 47-66. Retrieved from <https://www.ncbi.nlm.nih.gov/pubmed/18568054>
- Tebben, P. J., & Kumar, R. (2018). Vitamin D and the Kidney. In *Vitamin D* (pp. 437-459).
- Van Esch, H., Groenen, P., Nesbit, M. A., Schuffenhauer, S., Lichtner, P., Vanderlinden, G., . . . Devriendt, K. (2000). GATA3 haplo-insufficiency causes human HDR syndrome. *Nature*, 406(6794), 419-422. doi:10.1038/35019088
- Vetter, T., & Lohse, M. J. (2002). Magnesium and the parathyroid. *Curr Opin Nephrol Hypertens*, 11(4), 403-410. doi:10.1097/00041552-200207000-00006
- Wada, M., Furuya, Y., Sakiyama, J., Kobayashi, N., Miyata, S., Ishii, H., & Nagano, N. (1997). The calcimimetic compound NPS R-568 suppresses parathyroid cell proliferation in rats with renal insufficiency. Control of parathyroid cell growth via a calcium receptor. *J Clin Invest*, 100(12), 2977-2983. doi:10.1172/JCI119851
- Ward, D. T., McLarnon, S. J., & Riccardi, D. (2002). Aminoglycosides increase intracellular calcium levels and ERK activity in proximal tubular OK cells expressing the extracellular calcium-sensing receptor. *J Am Soc Nephrol*, 13(6), 1481-1489. doi:10.1097/01.asn.0000015623.73739.b8
- Yamada, T., Tatsumi, N., Anraku, A., Suzuki, H., Kamejima, S., Uchiyama, T., . . . Okabe, M. (2019). Gcm2 regulates the maintenance of parathyroid cells in adult mice. *PLoS One*, 14(1), e0210662. doi:10.1371/journal.pone.0210662
- Yu, G. C., & Lee, D. B. (1987). Clinical disorders of phosphorus metabolism. *West J Med*, 147(5), 569-576. Retrieved from <https://www.ncbi.nlm.nih.gov/pubmed/3321712>
- Yuan, Z., Opas, E. E., Vrikshajanani, C., Libutti, S. K., & Levine, M. A. (2014). Generation of mice encoding a conditional null allele of Gcm2. *Transgenic Research*, 23(4), 631-641. doi:10.1007/s11248-014-9799-7

VITA

Kamran Ghoreishi migrated to United States from Iran in 1989. He obtained his Bachelor of Science in microbiology and medical technology in 1995 from San Diego State University. After working as a clinical toxicologist at PosionLab for several years, he obtained his Master of Science in Public health toxicology in 2003. In 2001, he joined Celgene Corporation as a research scientist in drug discovery and development department. In 2013, Kamran obtained his Master of Science in regulatory affairs while working at Celgene Corporation. He is currently working at Bristol Myers Squibb Pharmaceuticals as a Sr. Scientist in Discovery Toxicology department.